UPPER JURASSIC (PORTLANDIAN) SEDIMENTOLOGY AND PALYNOFACIES OF CABO ESPICHEL, PORTUGAL

CENTRE FOR NEWFOUNDLAND STUDIES

TOTAL OF 10 PAGES ONLY
MAY BE XEROXED

(Without Author's Permission)

DAVID CRAIG BOLAND

National Library of Canada
Bibliothèque nationale du Canada

Canadian Theses Service
Services des thèses canadiennes

Ottawa, Canada
K1A 0N4

CANADIAN THESES
THÈSES CANADIENNES

NOTICE

The quality of this microfiche is heavily dependent upon the quality of the original thesis submitted for microfilming. Every effort has been made to ensure the highest quality of reproduction possible.

If pages are missing, contact the university which granted the degree.

Some pages may have indistinct print especially if the original pages were typed with a poor typewriter ribbon or if the university sent us an inferior photocopy.

Previously copyrighted materials (journal articles, published tests, etc.) are not filmed.

Reproduction in full or in part of this film is governed by the Canadian Copyright Act, R.S.C. 1970, c. C-30.

AVIS

La qualité de cette microfiche dépend grandement de la qualité de la thèse soumise au microfilmage. Nous avons tout fait pour assurer une qualité supérieure de reproduction.

S'il manque des pages, veuillez communiquer avec l'université qui a conféré le grade.

La qualité d'impression de certaines pages peut laisser à désirer, surtout si les pages originales ont été dactylographiées à l'aide d'un ruban usé ou si l'université nous a fait parvenir une photocopie de qualité inférieure.

Les documents qui font déjà l'objet d'un droit d'auteur (articles de revue, examens publiés, etc.) ne sont pas microfilmés.

La reproduction, même partielle, de ce microfilm est soumise à la Loi canadienne sur le droit d'auteur, SRC 1970, c. C-30.

THIS DISSERTATION
HAS BEEN MICROFILMED
EXACTLY AS RECEIVED

LA THÈSE A ÉTÉ
MICROFILMÉE TELLE QUE
NOUS L'AVONS REÇUE

NL-339 (r. 86/06)

Canada

UPPER JURASSIC (PORTLANDIAN) SEDIMENTOLOGY AND PALYNOFACIES OF CABO ESPICHEL, PORTUGAL

by

David Craig Boland, B.Sc. (Honours)

©

A THESIS SUBMITTED TO THE SCHOOL OF GRADUATE STUDIES IN PARTIAL FULFILLMENT OF THE REQUIREMENTS FOR THE DEGREE OF MASTER OF SCIENCE

DEPARTMENT OF EARTH SCIENCES
MEMORIAL UNIVERSITY OF NEWFOUNDLAND

JUNE 1986

ST.JOHN'S NEWFOUNDLAND

Permission has been granted to the National Library of Canada to microfilm this thesis and to lend or sell copies of the film.

The author (copyright owner) has reserved other publication rights, and neither the thesis nor extensive extracts from it may be printed or otherwise reproduced without his/her written permission.

L'autorisation a été accordée à la Bibliothèque nationale du Canada de microfilmer cette thèse et de prêter ou de vendre des exemplaires du film.

L'auteur (titulaire du droit d'auteur) se réserve les autres droits de publication; ni la thèse ni de longs extraits de celle-ci ne doivent être imprimés ou autrement reproduits sans son autorisation écrite.

ISBN 0-315-33647-1

ABSTRACT

Upper Jurassic (Portlandian) strata on the southeastern margin of the Lusitanian Basin at Praia do Cavalo, near Cabo Espichel, Portugal contain mixed carbonate and clastic sediments. From this section ten facies were identified to produce a model of Upper Jurassic shelf development on a passive Atlantic-type margin.

The model consists of carbonate shelf and clastic deltaic sediments linked by erosional and non-erosional contacts. The shallow marginal marine carbonate sequence consists of intertidal and low energy and high energy subtidal environments. The clastic sequence consists of interdistributary bay fill, crevasse splay, levee, channel, distributary mouth bar and delta front environments. Non-erosional boundaries occur where levees, crevasse splays and bay fill prograde over shallow subtidal nodular limestones and calcareous shales. Erosional boundaries occur where distributary channels scour through distributary mouth bars and prodelta strata to sharply rest upon lithified massive subtidal limestones.

The miospore assemblage consists of 49 terrestrial and 4 marine species in samples dominated by Corollina (Classopollis), Exesipollenites and Spheripollenites. Three palynofacies are identifed; the C.simplex palynofacies is associated with siliciclastic lithologies; C.itunensis

palynofacies is restricted to the carbonates and; the marine palynomorph facies is characteristic of some carbonates and delta front siliciclastics.

The C.simplex - sediment association indicates that this pollen was derived from a plant which occupied an inland marsh or levee environment. The C.itunensis - sediment association implies a plant living on or near a marginal marine carbonate coast resembling a "mangrove" or saltmarsh environment.

ACKNOWLEDGEMENTS

This thesis would not have been possible if it were not for the continuous guidance, advise and critical review from my supervisor and friend Dr. E.T. Burden. Dr. A. Aksu, co-supervisor is acknowledged for his review of the thesis and his scientific advise. Dr.R.N. Hiscott is thanked for his consultation on sedimentological aspects of this manuscript.

H. Gillespie is thanked for her laboratory expertise with regards to palynological processing. Thanks are expressed towards S. Loupe and W. Marsh for their superb photographic preparations.

The knowledgeable discussions with my office mate S. Solomon made many concepts of geology more understandable. My colleague A. Langille is also thanked for his continuing informative discussions. Support from my university peers R. Choaka, C. Ryley, D. Furey, D. Mosher and friends B. Morrey, K. Winters, L. Newman, C. Anstey, R. Reid and C. Churchill made my graduate years at Memorial interesting and memorable.

A special thank-you is expressed to the staff, especially A. Reid, and faculty of the Department of Earth Sciences.

The financial support from Mobil Oil of Canada is appreciated, for without their support this endeavour could not have been undertaken.

DEDICATION

This thesis is dedicated to my parents, Lorraine and Norman Boland, whose unsurpassable encouragement, assistance and moral support made all this possible.

Table of Contents

Page

Abstract..... ii

Acknowledgements..... iv

Dedication..... v

Table of Contents..... vi

List of Figures..... ix

List of Tables..... xii

Chapter 1 Introduction

1.1 General Statement..... 1

1.2 Purpose..... 4

1.3 Basin Development..... 7

1.4 Previous Work..... 11

1.5 Age of Section..... 15

1.6 Techniques..... 17

1.6.1 Field..... 17

1.6.2 Palynomorph Processing..... 18

1.6.3 Rock Classifications..... 21

1.6.4 Markov Chain Analysis..... 22

1.6.5 Palynomorph Analysis and Statistics. 27

Chapter 2 Sedimentology

2.1 Introduction..... 30

2.2 Facies Descriptions and Interpretations.... 31

2.2.1 Carbonates..... 33
2.2.2 Siliciclastics..... 51
2.3 A Model for Portlandian Siliciclastic Carbonate Successions..... 70
2.3.1 Carbonate Succession..... 72
2.3.2 Siliciclastic Succession..... 75
2.3.3 Boundary Conditions..... 77
2.4 Regional Depositional Setting..... 84

Chapter 3 Palynology
3.1 Systematics..... 89
3.1.1 Spores..... 91
3.1.1.1 Trilete..... 91
3.1.1.2 Monolete.....134
3.1.1.3 Alete.....137
3.1.2 Pollen.....139
3.1.2.1 Monoporate.....139
3.1.2.2 Bisaccate.....156
3.1.2.3 Monosulcate.....165
3.1.2.4 Perinous.....168
3.1.2.5 Inaperturate.....175
3.1.3 Marine Microplankton.....179
3.1.3.1 Acritarchs.....179
3.1.3.2 Dinoflagellates.....181
3.2 Palynofacies Analysis.....185
3.2.1 Introduction to Palynofacies.....185

3.2.2 Palynofacies.....187

3.2.2.1 *Corollina simplex* Facies.....187

3.2.2.2 *Corollina ituensis* Facies...188

3.2.2.3 Marine Palynomorph Facies....189

Chapter 4 Discussion.....190

4.1 Palynomorph Biostratigraphy.....190

4.2 Palynofacies and Depositional Environments.....194

4.3 Distribution Significance of *Corollina*.....201

Chapter 5 Conclusions.....206

Cited References.....209

Plates.....240

Appendix I Sampling and Processing Data.....253

Appendix II Markov Chain Analysis Results.....258

Appendix III Palynomorph Counts from Cabo Espichel.....(in pocket)

List of Figures:

Figure: 1.1 Location map..... 2
Figure: 1.2 Upper Jurassic sedimentary basins..... 3
Figure: 1.3 Shoreline at Praia do Cavalo..... 5
Figure: 1.4 Comparative lithostratigraphy..... 9
Figure: 1.5 History of stratigraphic correlation..... 12
Figure: 2.1 Summary of facies descriptions..... 32
Figure: 2.2 Photomicrograph of algal laminite..... 34
Figure: 2.3 Outcrop of algal laminite..... 34
Figure: 2.4 Mud cracks on algal laminite..... 35
Figure: 2.5 Photomicrograph of bioclastic packstone.. 39
Figure: 2.6 Oolite grainstone in massive limestone.. 39
Figure: 2.7 Outcrop of facies B..... 41
Figure: 2.8 Packstone with aligned shell fragments... 41
Figure: 2.9 Diplocraterion paralleum in facies B..... 42
Figure: 2.10 Photomicrograph of facies C..... 45
Figure: 2.11 Outcrop of nodular limestone..... 45
Figure: 2.12 Trace fossils in nodular limestone..... 47
Figure: 2.13 Vaginella sp. in facies C..... 47
Figure: 2.14 Photomicrograph of facies D..... 49
Figure: 2.15 Outcrop of facies D..... 49
Figure: 2.16 Mineral percentages of facies (E - I).... 52
Figure: 2.17 Photomicrograph of facies E..... 53
Figure: 2.18 Outcrop of facies E..... 55
Figure: 2.19 Woody debris in facies E..... 55

Figure: 2.20 Photomicrograph of facies..... 57
Figure: 2.21 Outcrop of facies F..... 57
Figure: 2.22 Photomicrograph of facies G..... 59
Figure: 2.23 Outcrop of facies G..... 59
Figure: 2.24 Photomicrograph of facies H..... 61
Figure: 2.25 Outcrop of facies H..... 63
Figure: 2.26 Trough cross-bedding in facies H..... 63
Figure: 2.27 Photomicrograph of facies I..... 65
Figure: 2.28 Outcrop of facies I..... 65
Figure: 2.29 Sedimentary structures in facies I..... 67
Figure: 2.30 Photomicrograph of facies J..... 69
Figure: 2.31 Outcrop of facies J..... 69
Figure: 2.32 Stratigraphic section..... (in pocket)
Figure: 2.33 Markov chain facies transitions..... 71
Figure: 2.34 Carbonate succession depositional model.. 73
Figure: 2.35 Siliciclastic succession depositional model..... 76
Figure: 2.36 Outcrop of the erosional boundary condition..... 78
Figure: 2.37 Model for the erosional boundary condition..... 79
Figure: 2.38 Outcrop of the non-erosioanl boundary condition..... 81
Figure: 2.39 Model for the non-erosional boundary condition..... 82
Figure: 2.40 Outcrop of cyclic package of siliciclastic

and carbonate facies..... 83

Figure: 2.41 Depositional model for Cabo Espichel..... 87

Figure: 3.1 Size frequency for Corollina.....150

Figure: 3.2 Pollen analysis diagram..... (in pocket)

Figure: 3.3 Pollen analysis diagram..... (in pocket)

Figure: 3.4 Pollen analysis diagram..... (in pocket)

Figure: 3.5 Pollen analysis diagram..... (in pocket)

Figure: 3.6 Pollen analysis diagram.....(in pocket)

Figure: 4.1 Comparison of palynozonations.....191

Figure: 4.2 Corollina pollen content in the Jurassic.....195

Figure: 4.3 Corollina distribution.....205

List of Tables:

Table 1 (Appendix II) Observed data.....259

Table 2 (Appendix II) Transition probability matrix...259

Table 3 (Appendix II) Independant trials matrix.....260

Table 4 (Appendix II) Difference matrix.....260

Table 5 (Appendix II) Normalized difference matrix....261

Table 1 (Appendix III) Palynomorph counts.....(in pocket)

CHAPTER 1 INTRODUCTION

1.1 General Statement

Praia do Cavalo at Cabo Espichel, Portugal, about 25 km south of Lisbon at the western end of the Serra da Arrabida (Figura 1.1), is on the northern limb of an east-west trending anticline about 30 km in length.

During the Mesozoic and Cenozoic this area was part of the tectonically active eastern margin of the Lusitanian Basin (Figures 1.1 and 1.2), a marginal basin bordering the Proto-Atlantic and positioned north of the Algarve Basin and east of the Grand Banks basins (R.C.L. Wilson 1975a, 1979; Fursich 1981). The geology of the Lusitanian Basin can be related to plume-generated uplift, rifting and sea-floor spreading which took place west of Portugal soon after the Hercynian orogeny (Wilson 1975a). Up to 5000 m of marine and continental sediments were deposited on Paleozoic strata or crystalline basement (Reyment 1973).

During the Late Jurassic, the Serra da Arrabida and Cabo Espichel regions were situated near the eastern hinge of this basin. At this time predominantly terrestrial sediments were deposited in the eastern part of the basin, whereas, in the west, marginal marine sediments were deposited.

During the Early Portlandian this eastern part of the

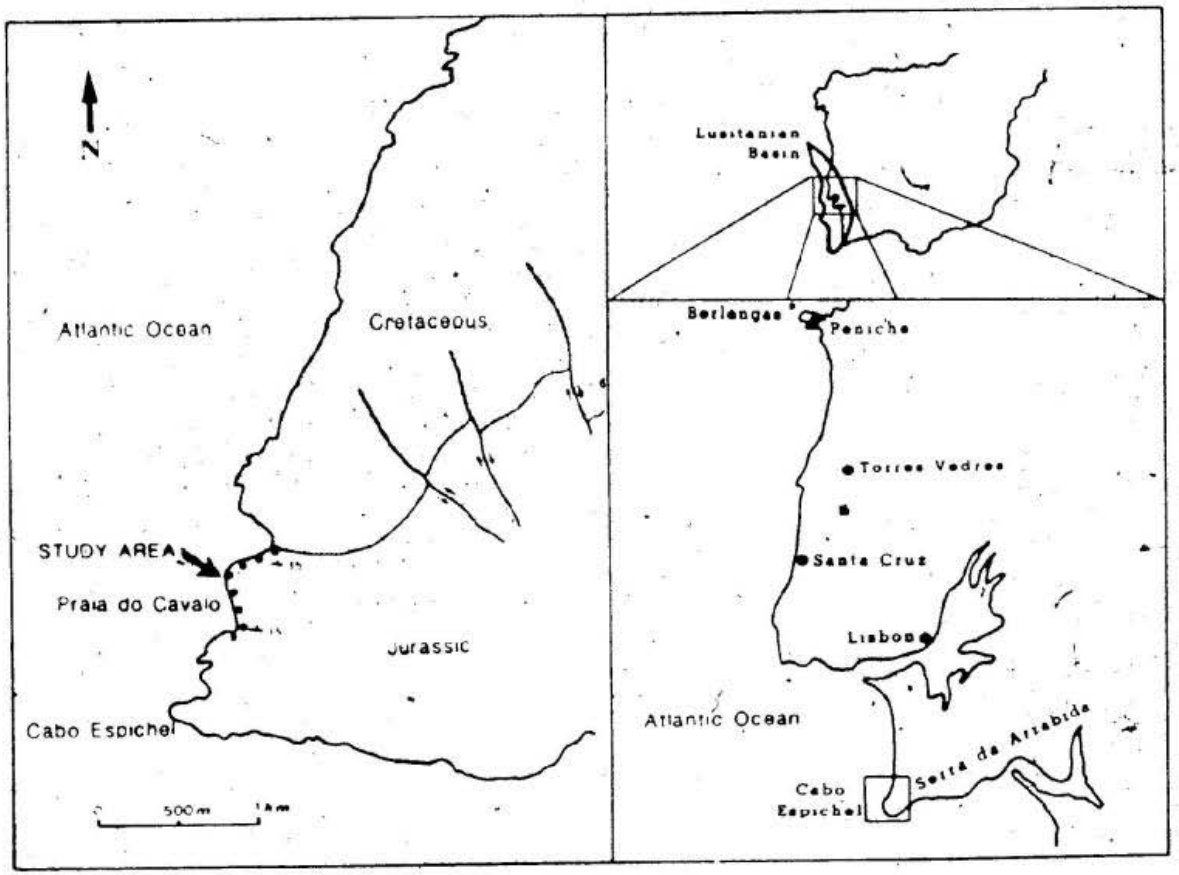


Figure 1.1 Location map of study area.

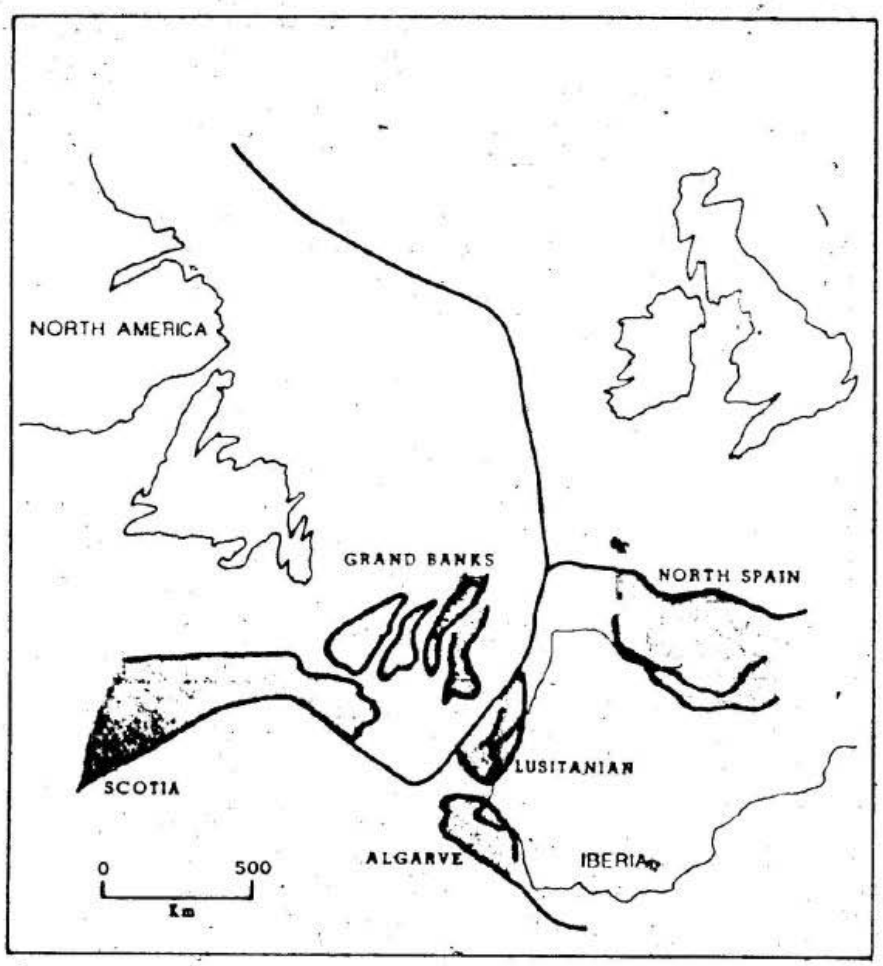


Figure 1.2 Sketch map outlining Upper Jurassic basins formerly adjacent to Iberia (modified after Wilson 1975a).

Lusitanian Basin experienced a transgressive event related to the decoupling of Europe and North America (Wilson 1975a; Hallam 1975, 1981). Periodic uplift of the Hercynian basement in the east during this Portlandian transgression caused increased erosion of the land mass and progadation of the terrestrial facies towards the west into a marginal marine environment (Wilson 1975a).

The sea cliffs at Praia do Cavalo contain a nearly complete sequence of Portlandian sediments dipping about 35° NW. The section is approximately 332 m thick and consists of several apparently repetitive cycles of carbonates and siliciclastics (Figure 1.3). Such cycles provide an ideal prerequisite for an investigation of the strata using Markov chain analysis. The boundaries between the carbonates and siliciclastics are both erosional and conformable and so well defined that they allow for the development of a model describing their boundary conditions.

1.2 Purpose

The purpose of this investigation is to describe the facies at Cabo Espichel and interpret the environments in which they were deposited. Markov chain analysis is used to aid the development of a statistically significant facies model and eventually a depositional model for the region. Palynology is used in conjunction with the sedimentology to



Figure 1.3 The shoreline at Praia do Cavalo, Cabo Espichel. At the base of a 125 m cliff containing a sequence of Portlandian sediments dipping 35° NW. This panorama illustrates the lower 200 m, of the 332 m section of shallow marine carbonate and deltaic siliciclastics "cyclothems". The larger boulders on the shore are near 2 m in height. Arrow indicates the base of the succession.



describe palynofacies and show their environmental relationships.

This information will prove useful in understanding the geological history of the Eastern Canadian continental margin. The East Coast of Canada is, in a general way, a mirror reflection of Lusitanian Basin stratigraphy; Grand Banks basins show lithologies revealing similar depositional environments, structural control and salt tectonics. In addition, the palynomorphs extracted from cores off Canada's east coast (Williams 1975; Bujak and Williams 1977) contain palynomorph assemblages similar to those found at Cabo Espichel. By preparing a comprehensive facies model of sediments and palynomorphs from outcrop in Portugal the chances for successful hydrocarbon plays will be enhanced and additional evidence on rifting and ocean development at the Jurassic-Cretaceous boundary will be presented.

1.3 Basin Development

The separation of North America from Africa along a north-easterly trending Triassic rift parallel to the Hercynian orogeny resulted in the development of the central Proto-Atlantic (Lancelot 1980). Graben faulting throughout the Late Triassic and Early Jurassic was accompanied by deposition of continentally-derived siliciclastics of the Eurydice Formation on the Grand Banks and the Silves

Formation in the Lusitanian Basin (Figure 1.4).

During the Early Jurassic the Lusitanian Basin recorded the first marine transgression from the north (Hallam 1981); since this transgression does not come from the east, it should not be considered an incursion of the Tethys through the Gibraltar strait (Lancelot 1980).

The Late Early Jurassic records for the first time a connection between the Tethys and the Proto-Atlantic; corresponding to the deposition of the Dagorda and Coimbra Formations in the Lusitanian Basin, and the Argo and Iroquois Formations on the Grand Banks (Figure 1.4). This connection is followed by a regressive event in the Middle Jurassic and a marine transgression during the Early Middle Jurassic (Lancelot 1980), which is represented by the Whale Formation on the Grand Banks and the Brenha Formation in the Lusitanian Basin (Figure 1.4).

The most important factor in the evolution of the Central Proto-Atlantic occurred during the Late Middle and Early Late Jurassic (Lancelot 1980). At this time the Lusitanian Basin became an elongate marginal marine basin which was subsiding at a relatively rapid rate; in places this exceeded 100 m per million years (Wilson 1979; Fursich 1981). In the north, east and south, the basin was bordered by Pre-Triassic basement rocks of the Iberian Meseta; in the west was an uplift of Hercynian rocks which today is the Berlengas Islands (Fursich 1981). A permanent connection

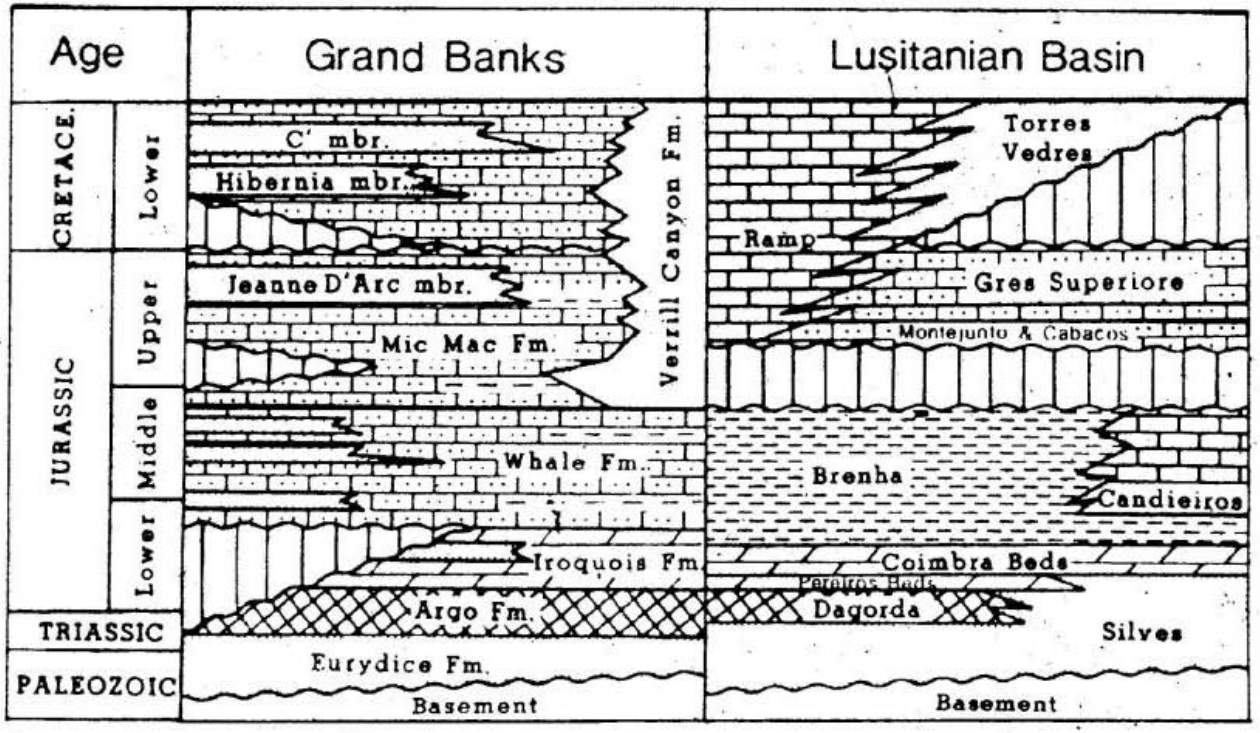


Figure 1.4 Generalized comparative lithostratigraphic chart for the Grand Banks and the Lusitanian Basin (after Arthur et.al. 1982; Wright and Wilson 1984).

to the Proto-Atlantic existed in the southwest, in the Lisbon-Sintra area (Ribeiro et al. 1972 in P. Wright 1984a).

The Lusitanian Basin shows no record of deposition during the early Late Jurassic; in places, a similar hiatus is recorded on the Grand Banks. Wilson (1979) suggests that during this time the area was probably subject to general uplift, plus localized uplift over diapiric structures as on the Grand Banks. Following this tectonic activity the area was reduced to sea level by a combination of erosion and subsidence (Wilson 1979). This event is subsequently marked by a widespread algal mat facies, and algal marsh-marginal marine facies (Wilson 1979).

The middle Late Jurassic is marked by pulses of increased subsidence accompanied by rapid uplift of the Hercynian basement. This probably indicates regional block faulting, with the horst areas supplying terrigeneous clastics to basins developing in grabens (Wilson 1979). A subsequent late Late Jurassic transgression, where shallow and marginal marine carbonates replace terrigeneous clastics, a kilometer of sediment in basin center and southern basin margin associated with the transgression (Wilson 1979). During the latest Jurassic, terrigeneous clastics from raised eastern source areas accumulated and interfingered southwards to Cabo Espichel (Wilson 1979). At Cabo Espichel, the uppermost Jurassic shows alterations of terrigeneous deltaic sandstones and sub-tidal to intertidal shelf or platform

limestones of the Gres Superoire Formation. This formation may be compared with the Mic Mac Formation on the Grand Banks.

1.4 Previous Work

In previous investigations the correlation of Portuguese strata has been confusing. Such confusion probably results from the combination of both biostratigraphy and lithostratigraphy in determining the age and names for strata; where maps are based on age rather than formations.

The Upper Jurassic sediments along the shore of Praia do Cavalo (Figure 1.1) were first examined in detail by Choffat (1901, 1906, 1908). He divided the Upper Jurassic into Pterocerian and Freixialian stages (Figure 1.5) and determined that within the Serra da Arrabida region, the terrestrial facies advanced gradually towards the west during the Upper Jurassic. Seifert (1963) raised the boundary of the Pterocerian stage to include the lowermost portion of Choffat's Freixialian stage (Figure 1.5). He also noted that in the Arrabida region, the Portlandian showed an alteration of terrigeneous sandstones and sub-tidal limestones indicating conditions fluctuating from shallow marine to deltaic.

More regional geological studies began to appear in 1965 when Zbyszewski et al. of the Portuguese Geological

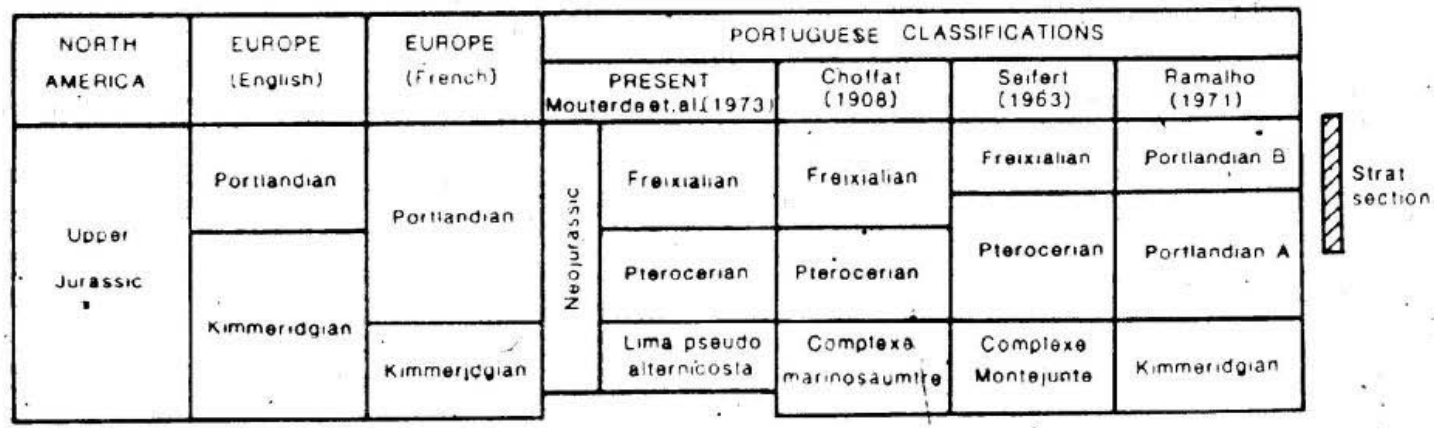


Figure 1.5 Chart showing the history of stratigraphic correlation.

Survey compiled a 1:50 000 map of the Arrabida region. This map broadly described the geology of rocks ranging in age from Jurassic to Pleistocene.

Ramalho (1971), also with the Portuguese Geological Survey, was the first to publish a detailed stratigraphical and paleontological study of the Upper Jurassic part of the Cabo Espichel section. He described both the macro- and microfauna and established a biostratigraphical subdivision for the Upper Jurassic. Earlier terminology was scrapped and strata were redefined as Portlandian A and Portlandian B (Figure 1.5). The boundary between the Portlandian A and B was defined on the basis of the first appearance of the Foraminifera Anchispirocyclina lusitanica (Egger) and Pseudocyclammina litus (Yokoyama). Lithologically, the boundary is placed roughly where the siliciclastics decrease and the carbonates begin to dominate.

Mouterde et al. (1973) revised the classification scheme of Ramalho (1971) by adopting the original classification presented by Choffat (1908). They did, however, substitute Complexe marinosaumtre with Lima pseudo alternicosta and placed all three stages under one name, Neojurassic (Figure 1.5).

Riley (1974) attempted the first palynological investigation of the Cabo Espichel section. Based upon the virtual absence of organic-walled microplankton (dinoflagellates and acritarchs), he postulated the Cabo

Espichel strata as restricted nearshore marine environment.

This investigation was subsequently dropped as a possible doctoral thesis, because of the lack of palynomorphs (pers. com. Sarjeant 1985).

At the other end of the size spectrum for fossils there are spectacular sauropod and theropod tracks exposed along limestone bedding surfaces of Praia do Cavalo (Telles Antunes 1976). These dinosaur tracks are of Portlandian age and have seldom been found in Europe. According to Antunes, the presence of dinosaurs points towards a moist and warm, coastal shallow marine environment, rich in vegetation.

More recently, Fursich and Schmidt-Kittler (1980) published an investigation of the Cabo Espichel locality. They based their stratigraphy on Ramalho's (1971) study, focusing on paleoecological and sedimentological aspects to retrace the environmental evolution of the southern part of the basin. Fursich and Schmidt-Kittler (1980) concluded that the sedimentary rocks at Cabo Espichel were deposited on a very protected shallow inner shelf which was separated from the open sea by a series of salt diapiric ridges in the form of swells or island chains. This extensive lagoon was generally subject to minor salinity fluctuations due to, either freshwater influx from the land, or heavy seasonal rainfall.

Felber et al. (1982) published a biofacies analysis

of Upper Jurassic marginal marine environments of Portugal, which included the paleogeography and facies distribution of the Serra da Arrabida region. They identified 11 facies types ranging from "terrestrial clastics, caliche crusts, brackish lagoons to tidal deposits and shallow marine biomicrites, nodular limestones, coral biostromes, intraclastic limestones and oolites. The spatial and temporal facies pattern indicates transgressions and regressions, which can be linked to the opening of the northern Atlantic" (Felber et al. 1982, p.21).

Recently, regional investigations of western Portugal, which includes the Cabo Espichel region have acquired importance as researchers attempt to understand the opening of the North Atlantic and its petroleum potential. Investigations of sedimentology and biostratigraphy by R.C.L. Wilson (1975a,b, 1979), P. Wright (1984a,b) and Gradstein (1979, 1983) have generated considerable interest from major oil companies.

In all of the previous studies from the Cabo Espichel region no one has attempted to describe in detail the siliciclastics, and in particular the boundary conditions between the carbonates and siliciclastics.

1.5 Age of Section

The strata at Praia do Cavalo, Cabo Espichel are

Portlandian in age. This is based upon ammonites, microfauna (Ramalho 1971) and dinosaur tracks (Telles Antunes 1976).

From biostratigraphy Ramalho (1971) was able to identify the Portlandian using the definitive occurrence of the ammonites Virgatosphinctes freguens (Quenst) and Lithacoceras siliceum (Oppel). He further subdivided the Portlandian into Portlandian A and B, with local subzones E_1, E_2, E_3 (Portlandian A) and F (Portlandian B). The Portlandian subzone E_1 was defined on the presence of the Foraminifera Everticyclammina virguliana (Koechlin), Freixialina planispiralis (Ramalho) and the relative increase in Vaginella and decrease in the algal species Clypeina jurassica (Favre). Subzones E_2 and E_3 were respectively defined by the appearance of Thaumatoporella parvovesiculifera (Raineri) and Permocalculus sp.. Portlandian B (subzone F) was defined on the first appearance of the Foraminifera Anchispirocyclina lusitanica (Egger) in conjunction with the algal species Zergatella sp.1. Recently, Kent and Gradstein (1985) used the top range of the Foraminifera Anchispirocyclina lusitanica as a means for regional identification of the Tithonian/ Berriasian boundary. The end of Portlandian B can be defined using the range tops of the ostracods Fabanella polita ornata (Steghaus), Cytherella suprajurassica (Oertli) and Cytherelloidea wekeri (Steghaus).

The base of the section examined in this thesis study begins near the top of subzone E_2. This point corresponds with an increase in the abundance of Rectocyclammina arrabidensis (Hottinger) in the first significant thick beds of siliciclastics in the Cabo Espichel section (Ramalho 1971).

A fossil identified by Ramalho (1971) as Vaginella sp. is common in the Kimmeridgian and Portlandian carbonates at Cabo Espichel.

Some bedding surfaces at Cabo Espichel contain spectacular dinosaur tracks which have been studied in some detail by Telles Antunes (1976). The presence of Neosauropus lagosteirensis (Telles Antunes) and Megalosauropus (?Eutynichnium) gomesi (Telles Antunes) implies a Portlandian age for the section. These tracks are similar to those described in other Portlandian strata of Western Europe and Russia (Telles Antunes 1976).

1.6 Techniques

1.6.1 Field

Exposures of Upper Jurassic sedimentary rocks along a steep cliff at Praia do Cavalo, Cabo Espichel were examined in May 1984. Access to the section was by foot; measurement was completed with a 2 m Jacob's staff. From the section,

cross-bedding was measured to determine paleocurrent direction, and boundary conditions between carbonates and siliciclastics were described as either erosional or non-erosional. Fifty samples were collected from calcareous and non-calcareous shales and sandstones for examination for palynomorphs and other organic debris (Appendix I). Most of these samples were collected from the lower part of the section where facies variations are best illustrated. In order to avoid recent contamination from wind and seaspray, samples were extracted from fresh rock chipped from the cliff face and packaged in sterile plastic bags. Twenty-one hand samples of carbonates and siliciclastics were collected for thin-section examination from beds representing the facies types.

1.6.2. Palynomorph Processing

For palynomorph analysis, the following processing procedure was used. Most of the following procedures are modified from Barss and Williams (1973).

Before preparation, all samples received a five digit number (Appendix I) identifying the sample and year of processing. Samples were then washed thoroughly with a wire brush in distilled water, and air dried for twelve hours. Samples were wrapped in aluminum foil, crushed to millimeter size, placed in labelled 250 ml beakers and

weighed (30-35 gms for shales and siltstones and 40-50 gms for sandstones and limestones). In order to avoid contamination, the crushing area was cleaned after each sample was crushed. Before chemical treatment four tablets each containing 12,100 ± 400 Eucalyptus grains (Stockmarr 1971) were added to each crushed sample.

To remove carbonates 100-150 ml of 20% hydrochloric acid was added to each sample. Methanol was used to control any excessive fizzing which may have occurred at this time. The sample was left for 8-10 hours until the reaction stopped, this was usually overnight. Samples were centrifuged for 4 minutes, and the acid decanted. Distilled water was then added, centrifuged and decanted to remove all remaining hydrochloric acid. Three or more washings were necessary to neutralize the sample. For large residues the procedure was speeded up by placing samples in labelled 50 ml test tubes and then centrifuging for about 4 minutes.

If test tubes were used, the sample was returned to beakers and 150 ml of concentrated hydrofluoric (HF) acid added to the sample. Initially a small amount of HF was added and slowly stirred to minimize hot, violent chemical reactions. Samples were checked for heat of reaction. And if cool, more HF was added. The samples were left for 8 to 12 hours (usually overnight) to dissolve silicates, then washed in distilled water, centrifuged and decanted three times. Residues were then examined with a microscope to

determine the quantity of residual minerals and precipitates. If too much mineral was present, the sample was placed in a hot HF bath. This procedure involved adding 50 ml of HF acid to a test tube containing the sample, and then placing it in a 250 ml beaker filled with hot (60°C) water. Samples were left for about 20 minutes, and again washed and centrifuged three times. Prior to sieving, a slide (1 of 5) of this unoxidized, unsieved sample was prepared according to the slide mounting method described elsewhere in this section.

Samples were then sieved through a 10 μm screen using a technique described by Cwynar et al. (1979). Prior to oxidizing, a slide (2 of 5) was mounted using this sieved, but unoxidized, sample. In addition, about 5 ml of the residue was placed in a labelled vial with 2 drops of phenol. Wet mounts of samples were examined under a microscope to determine the amount of time required for oxidation in Schultz solution. The time limitations were based upon the color and quantity of the organics present in each sample. If organics were black the sample was placed in Schultz solution for 5 minutes, brown for 3 minutes, and if yellow only 1 minute.

About 20 ml of Schultz solution was added to samples in a 50 ml test tube and then stirred. Samples were washed and centrifuged three times. While washing and sieving for the final time, 10% potassium carbonate was added to the

oxidized samples. The sample was then re-examined under a microscope. If too sandy, HF treatment was repeated and if coagulated, then Calgon solution was added to break up lumps before re-sieving. Samples (3, 4 and 5 of 5) were now ready for mounting.

To mount slides one drop of sample was placed upon a glass coverslip with three drops of polyvinyl alcohol and spread evenly with a sterile toothpick. The sample was left to dry for up to 2 hours. Once dry, two drops of Elvacite (Dupont) were placed upon the residue on the coverslip and then turned over onto the glass slide. The coverslip was allowed to settle on the slide where it was left to dry for up to 8 hours. Slides were then labelled to identify the sample, processing technique date, collector, and locality. To preserve residues, 2 drops of phenol were placed in a labelled vial with remaining sample.

1.6.3 Rock Classification

Dunham's (1962) classification of carbonates, expanded by Embry and Klovan (1972), is used because its applications cover field, hand specimen and thin section examinations. Rapid "spot" identification in the field proves to be one of it's many advantages, and, according to Flugel (1982), has no real disadvantages.

Folk's (1980) system is used for clastic rock

identification. It is based upon a simple ternary diagram, where the Q-pole contains all types of quartz including meta-quartzite (but not chert), the F-pole contains all single feldspar, plus granite and gneiss fragments and the RF-pole contains all other fine-grained rock fragments (eg. chert, slate, schist, volcanics, limestones, shale etc.).

1.6.4 Markov Chain Analysis

Siliciclastic and carbonate strata at Cabo Espichel appear to display some degree of vertical order and repetition of beds. A modified Markov chain analysis using the iterative proportional fitting technique proposed by Carr (1982) and Powers and Easterling (1982) was used to evaluate quantitatively the presence and extent of any repetitive or "cyclic" components. This method allows analysis of the probability of transition from one facies to another, and hence the detection of repetition of process and cyclicity in sedimentary packages.

Descriptions and applications of Markov processes in geology, and the historical development of these analyses are given in: Gingerich (1969); Selley (1969); Dacey and Krumbein (1970); Allen (1970); Miall (1973); Ethier (1975); Carr (1982); Powers and Easterling (1982); Johnson (1984) and Driese and Dott (1984) and texts: Davis (1973); Agterberg (1974) and Schwarzacher (1975). A concise

discussion of the use of Markov chain analysis in sedimentary facies studies appears in Miall (1973) and Hiscott (1981).

A computer program, for Markov chain analysis, developed by R.N. Hiscott of Memorial University and later modified by S. Solomon also of Memorial University was used to determine if the facies at Cabo Espichel possess Markov properties. However, as noted by Carr (1982), the presence of Markov properties in a facies succession only indicates the possibility of cyclicity.

The program developed by Hiscott calculates from the transition matrix (observed or raw data) a transition probability matrix, independent trials probability matrix (random or expected frequency), difference matrix (observed - expected frequency) and normalized difference matrix ((observed - expected)/ √ (expected)).

The procedure for determining Markov properties begins with the raw data (R) observed in the field being compiled in the form of 2-way (NxN) frequency tables, in which the frequency of occurrence of one facies overlain by another is recorded over all possible facies transitions. Here, N represents the number of facies recognized. For the present study a total of 11 facies (A through J) and a scour surface (SS) accounted for a grand total of 294 facies transitions (Appendix II, Table 1). Structural zeros are present in the diagonal of the matrix because, by definition, transitions

from a bed of one lithology to another bed of the same lithology are not recognized, even in those situations in which they are observable. These zeros refer to embedded Markov chains, and will be considered in these analyses. All other recognized zeros besides those in the diagonal are referred to as sampling zeros. These zeros occur as the result of sampling variation, the relative small size of the sample, or simply the lack of transitions between specified facies.

The upward vertical transition probability matrix is calculated as (Appendix II, Table 2):

$$P_{xy} = F_{xy} / \Sigma Rt_x$$

where, F_{xy} is the number of upward vertical transitions from facies x to facies y. Row totals, (Rt), column totals, (Ct) and the grand total (T), are defined as follows:

$$Rt_x = \sum_{y=1}^{k} F_{xy}$$

$$Ct_y = \sum_{x=1}^{k} F_{xy}$$

$$T = \sum_{x=1}^{k} \sum_{y=1}^{k} F_{xy}$$

From the transition probability matrix one can define the independent trials matrix; which is the random or expected frequency of transitions. The independent trials matrix, I, is defined as (Appendix II, Table 3):

$$I_{x,y} = Ct_y \; / \; (T - Ct_x)$$

From the derived results a simple difference matrix table was calculated (Appendix II, Table 4), where DM equals the observed data minus the expected data, so that Ct and Rt equal zero.

It is now possible to define the normalized difference matrix as (Appendix II, Table 5):

$$ND = R_{x,y} - I_{x,y} \; // I_{x,y} = \text{observed} - \text{expected} \; // \text{expected}$$

From the normalized difference matrix calculations all significant values were compiled in the construction of a Markov chain analysis flow diagram. Significance levels were based upon the normal distribution function, where z was greater than or equal to the value of 1.28. This value implies a statistically significant probability of 0.8997, approximately 90% for transitions between any two facies.

$$F(z) = 1//2\pi \int_{-\infty}^{z} e^{-1/2t^2} \; . \; dt$$

Data compiled from the independant trials matrix was used to test the observed transitions for the presence of a first order Markov property. A first order Markov chain is where the occurrence of a state depends only on a preceding state. This test was done by using one of two Chi-square tests (X^2), as outlined by Miall (1973) and Hiscott (1981)

with the null hypothesis being that there is no difference between the independent trials probability matrix and the observed transition probability matrix.

Test 1 (from Hiscott 1981)

$$X^2\ 1 = \sum_{x=1}^{N} \sum_{y=1}^{N} (F_{xy} - Rt_x * I_{xy})^2 / Rt_x * I_{xy}$$

This test statistic can be compared with the distribution of values for a X^2 distribution with $(N^2 - 2N)$ degrees of freedom.

Test 2 (from Hiscott 1981)

$$X^2\ 2 = 2 \sum_{x=1}^{N} \sum_{y=1}^{N} F_{xy} * \ln (P_{xy} * T / Ct_y)$$

This test can be compared with the distribution of values for a X^2 distribution with $(N - 1)^2 - N$ degrees of freedom.

For the present study both X^2 tests were used, with results of each test well exceeding the X^2 limit of 137.2 at a 99.99% confidence level for 89 degrees of freedom (Appendix II, Table 5).

1.6.5 Palynomorph Analysis and Statistics

Slides were scanned at 400X magnification using a Reichert Zetopan research microscope. Where possible all palynomorphs on a slide were counted and compiled in tabular form. Coarse grained sandstones yielded few palynomorphs, whereas some shale samples yielded in excess of 9,000 grains. In total, nearly 55,000 palynomorphs were encountered. From these data five palynomorph (saw-tooth) diagrams were constructed for 30-50 m sections of the Praia do Cavalo section and statistics were calculated to determine the diversity and evenness of species contained in each sample.

"Diversity or number of equally common taxa", according to Beerbower and Jordan (1969), "reflects both the number of species present and their proportional abundances. For example, a few, equally common species will yield as high a diversity as many, unequally common species". Diversity is defined by Pielou (1966) as "the degree of uncertainity attached to the specific identity of any randomly selected individual. The greater the number of species and the more nearly equal their proportions, the greater the uncertainity and hence the diversity".

Diversity, H', is given by the formula:

$$H' = - \sum_{i=1}^{s} p_i \ln(p_i)$$

and the diversity variance is

$$\sigma^2_H = (1/N)\left(\sum_{i=1}^{s'} p_i (\ln(p_i))^2 - (H')^2 \right)$$

where n_i is the number of individuals in taxon i and s' is the number of species counted in a count of N grains and $p_i = n_i/N$ (Pielou 1966).

Evenness, a statistic dependent upon diversity, is a measure of the equitability of probabilities for palynomorphs in a particular sample (Burden 1982). Evenness may be expressed as a ratio between the previously calculated diversity H' and the number of species in a sample. Evenness is

$$E = H'/\ln s$$

and the diversity variance is

$$\sigma^2_e = \sigma^2_H / (\ln s)^2$$

where s is the number of species in the assemblage.

Confidence limits (at 0.95 confidence level) for relative frequency abundance are calculated from equation:

$$p(0.95_{limit}) = \frac{(z + (K^2/2N) \pm K \sqrt{((Z(1-Z)/N + (K^2/4N^2))}}{1 + (K^2/N)}$$

where Z is the relative percent abundance of a taxon and K is a constant equal to 1.96 (Maher 1972). These limits are error bars on the palynomorph diagrams.

Such statistical information can be used as a tool in paleoecologic analysis for defining environmental boundaries. However, it should be noted that these statistics need not directly relate to the sites where plants grow. Transportation and selective preservation can change diversity values.

CHAPTER 2 SEDIMENTOLOGY

2.1 Introduction

The modern usage of the term facies has been reviewed by Teichert (1958) and Krumbein and Sloss (1963). The concept has been used since 1838 when Amand Gressly recognized that features observed in a particular lithology were useful for correlation and for predicting the occurrence of economic resources (Reading 1978). Facies are also important because their recognition and analysis provide the basis for an environmental interpretation of the stratigraphic units.

Unfortunately, the term has been used in many different ways since its first usage. Several recent authors such as Middleton (1978), Reading (1978), Walker (1984), Carr (1982) and Driese and Dott (1984) have used facies in different, though generally related, senses. In general, a facies is a body of rock with specified characteristics, defined on the basis of color, bedding, composition, texture, fossils and sedimentary structures (Reading 1978).

In this work the term 'facies' is used in two senses: (1) in the strictly observational sense of a rock product, (eg. algal laminite facies) and; (2) in a genetic sense for the products of a process by which a rock is thought to have formed, (eg. bioturbated sandstone and siltstone facies).

The environmental sense (eg.distributary channel facies) will be ignored in the facies description section, since all environmental interpretations will be discussed separately.

2.2 Facies Description and Interpretation

In this section, the ten main facies types ((A) Algal laminite, (B) Massive limestone, (C) Nodular limestone, (D) Calcareous shale, (E) Mudstone and fine grained sandstone with calcrete nodules, (F) Cross-bedded siltstone and sandstone, (G) Bioturbated sandstone and siltstone, (H) Coarse grained to conglomeratic trough cross-bedded sandstones, (I) Fine to medium grained sandstone, and (J) Non-calcareous silty shales), are described by giving an outline of the overall petrology, lithology, fauna and sedimentary structures, and the environments which they most likely represent are described and summarized (Figure 2.1). The Markov chain transitions between facies are also included to better understand the facies associations.

A considerable amount of work has already been undertaken by Fursich and Schmidt-Kittler (1980) in the Cabo Espichel area. This section summarizes and adds to their previous work. Additions include new title designations (Fursich and Schmidt-Kittler facies names are in brackets) revisions to facies descriptions, the addition of two new facies, modified environmental interpretations and an analysis of

	FACIES	LITHOLOGY	ENVIRONMENT
CARBONATES	A	Algal laminite	Intertidal
	B	Massive limestone	Higher energy subtidal
	C	Nodular limestone	Lower energy subtidal
	D	Calcareous shale	Lower energy subtidal
SILICICLASTICS	E	Mudstone and fine grained sandstone with calcareous nodules	Distributary bay fill
	F	Cross-bedded siltstone and sandstone	Crevasse splay
	G	Bioturbated sandstone and siltstone	Levee
	H	Coarse grained to conglomeratic trough cross-bedded sandstone	Channel
	I	Fine to medium grained sandstone	Distributary mouth bar
	J	Non-calcareous silty shale	Delta front

Figure 2.1 Facies descriptions.

facies transitions based on both field observations and Markov chain analysis, a procedure not undertaken by Fursich and Schmidt-Kittler.

2.2.1. Carbonates

Facies A: Algal laminite (Birds-eye micrites and laminated fenestral micrites)

Petrology: Laminated boundstone consists of alternating layers of micrite (2 mm thick), microsparic micrite (2 mm thick) and peloids (mostly faecal pellets) (0.5 mm thick) (Figure 2.2). Thin vertical tubes of microspar (10-15 μm in width and several mm long) are common throughout these beds. These tubes are similar to those described earlier by Davies (1970), Fursich and Schmidt-Kittler (1980) and Fischer (1981). According to these references they were probably produced by algal filaments.

Lithology and Fauna: Algal laminites, often measuring less than 1m thick, are commonly observed with alternating massive and nodular biomicrites in the upper part of the measured section. The algal laminites are structurally well laminated (Figure 2.3), or wavy with distinct polygonal mudcracks (Figure 2.4) possessing curled up margins. Rill marks and small crater-like imprints (raindrop impressions)



(Figure 2.2) Photomicrograph of algal laminite showing spar-filled burrows and faint lamination. Thin-section X40.



(Figure 2.3) Section of well laminated layers of algal laminites (facies A).



(Figure 2.4) Bedding plane of an algal laminite showing mud cracks and vertical burrows.

were also observed at some bedding planes. Bioturbation in this facies is rare, although the algal laminates are occasionally seen to be burrowed by Skolithos verticalis (Hall). Some laminated beds are ripped up and redeposited as poorly sorted angular lithoclasts with voids between them filled by sparry calcite.

Markov chain analysis shows significant transitions from massive biomicrite (facies B) to algal laminites, which are, in turn, frequently overlain by nodular biomicrite (facies C). Statistically insignificant observations for facies A grading into facies B, and facies C into facies A were also recorded.

Interpretation: The algal laminites facies at Cabo Espichel were formed on a low energy tidal flat (middle and upper intertidal). The algal laminates were affected by: 1) storm activity indicated by the poorly sorted angular ripped up lithoclasts, 2) subaerial exposure as indicated by the occurrence of mudcracks, and 3) rainfall as implied by the raindrop imprints similar to those illustated in Reineck and Singh (1980).

Algal laminites in the Cabo Espichel section can be compared with modern carbonate tidal flats such as Andros Island, Bahamas; Abu Dhabi, Persian Gulf; and Shark Bay, Western Australia (James 1984). Most recent examples occur in protected coastal environments (protected, that is, from the open ocean waves and swells, yet still affected by tides

and severe storms) or lying on the leeward side of a land mass (i.e. in an embayment), barrier island or associated with an extensive open marine platform.

A scanty geologic record of ancient algal mats is probably the result of low preservation potential in all but the most protected areas algal mats are removed during transgression (Wright 1984b). Futhermore, Wright notes that in a study undertaken by Perkins (1977), Pleistocene algal mats in Florida are preserved during the late phases of regression and not at the beginning of a transgression. Under these circumstances early lithification by subaerial exposure may be a necessary factor in preserving algal laminites (Wright 1984b). Such a condition appears to be responsible for the preservation of the algal laminites at Cabo Espichel. This condition becomes apparent in the Markov transitions where the facies sequence is massive limestone (facies B) grading into algal laminite (facies A); such a transition implies a regressive phase. Likewise, the statistically insignificant transitions from nodular limestone of facies B into facies A can be interpreted in a similar manner. Thus, it is reasonable to consider the algal laminites as the end of a stratigraphic sequence and a suitable marker for alphabetic labelling facies successions.

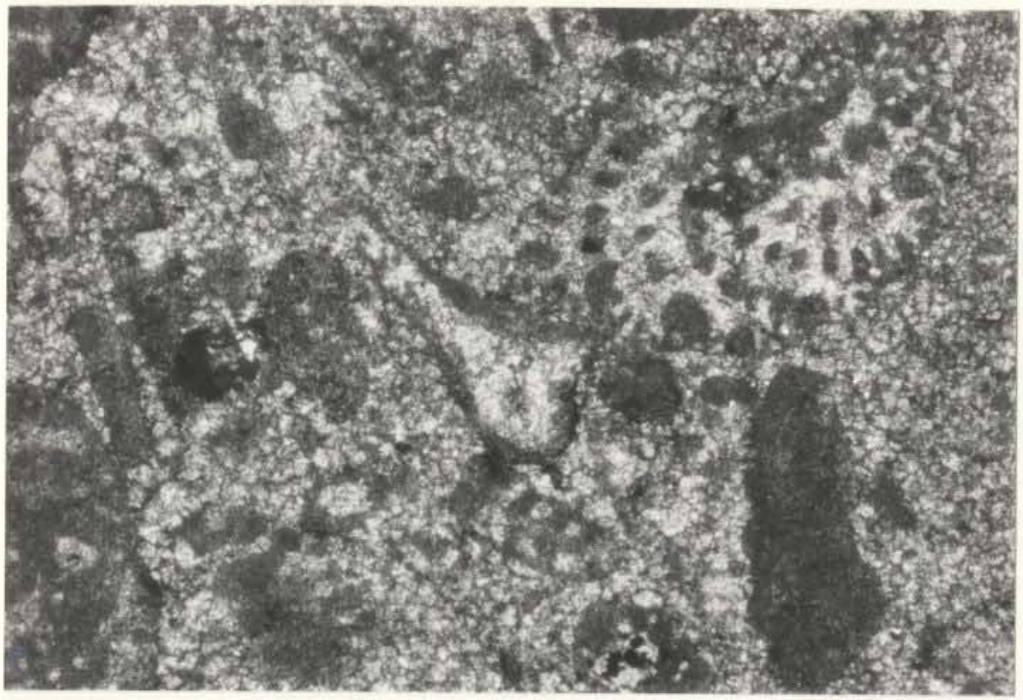
From sedimentology, the Portlandian section at Cabo Espichel, resembles the Upper Oxfordian Vale Verde Beds of the Lusitanian Basin (Wright 1984b). Wright interpreted the

Vale Verde Beds as a prograding delta-plain sequence where the algal mats developed at the final stages of the filling of interdistributary bays, including bays filled by crevasse sands. The facies succession at Cabo Espichel has some similarities with Wright's model; however, it differs in that the observed facies transitions suggest a shoreline setting for a carbonate platform away from deltas.

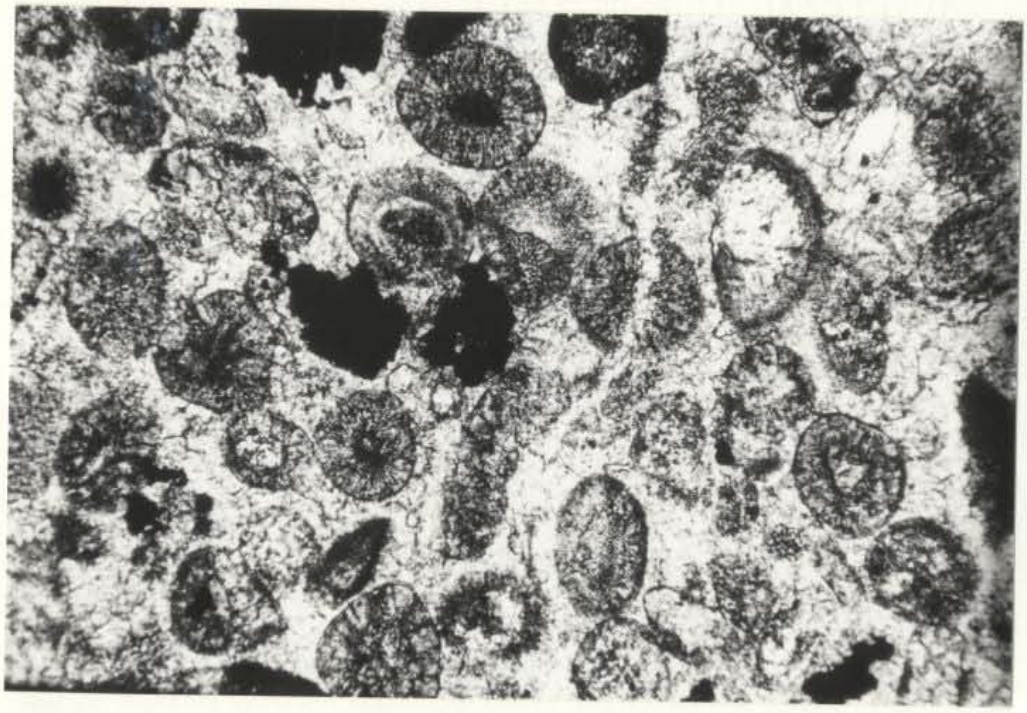
Facies B: Massive limestone (Biomicrites and micrites without extensive bioturbation)

Petrology: This facies contains two intimately associated rock types of equal importance. Firstly, it contains a bioclastic packstone (Figure 2.5). Clasts show considerable mechanical reworking as indicated by the presence of rounded bioclasts, quartz clasts and lithoclasts consisting of mudstone grains. Secondly, this facies contains a bioclastic oolite grainstone (Figure 2.6), resembling Upper Jurassic oolite grainstone described by Friedman (1961 in Reading 1978) from central Europe.

Lithology and Fauna: Massive limestones of facies B are dominantly gray, but may show a buff color from post-depositional oxidation (Figure 2.7). For the most part these beds are 1-3 m thick; some beds in the upper part of the section can reach 10 m in thickness. These limestones lack extensive bioturbation. Beds containing abundant



(Figure 2.5) Bioclastic packstone of facies B showing fragments of Foraminifera and bivalves. Thin-section 40X



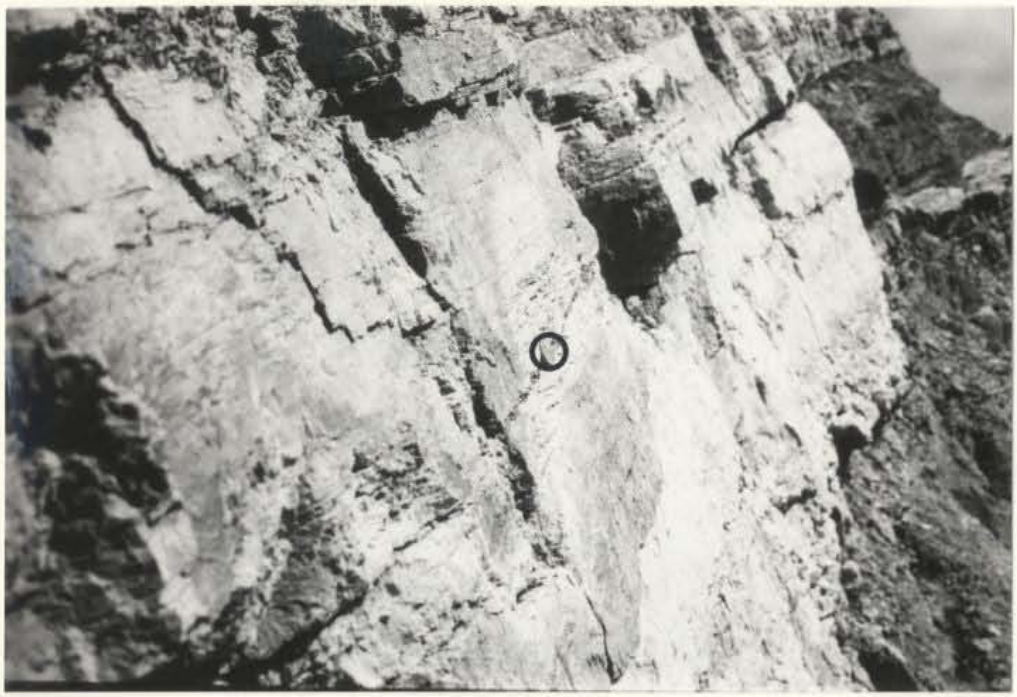
(Figure 2.6) Radial and concentric fibrous ooids from an oolite grainstone in the massive limestone. Thin-section X100.

reworked shell debris (Figure 2.8) indicate paleocurrents trending southwest. Small scale troughs (15 cm wide) and ripples with crude lamination are distinct in some beds (Figure 2.7). Beds of this facies may contain pebbles of quartz and feldspar. From Markov analysis they are associated with the nodular bioturbated limestone (facies C) and non-calcareous shale (facies J). Frequently, this facies is capped by algal laminite. A scour surface (SS) separates this facies from overlying siliciclastics.

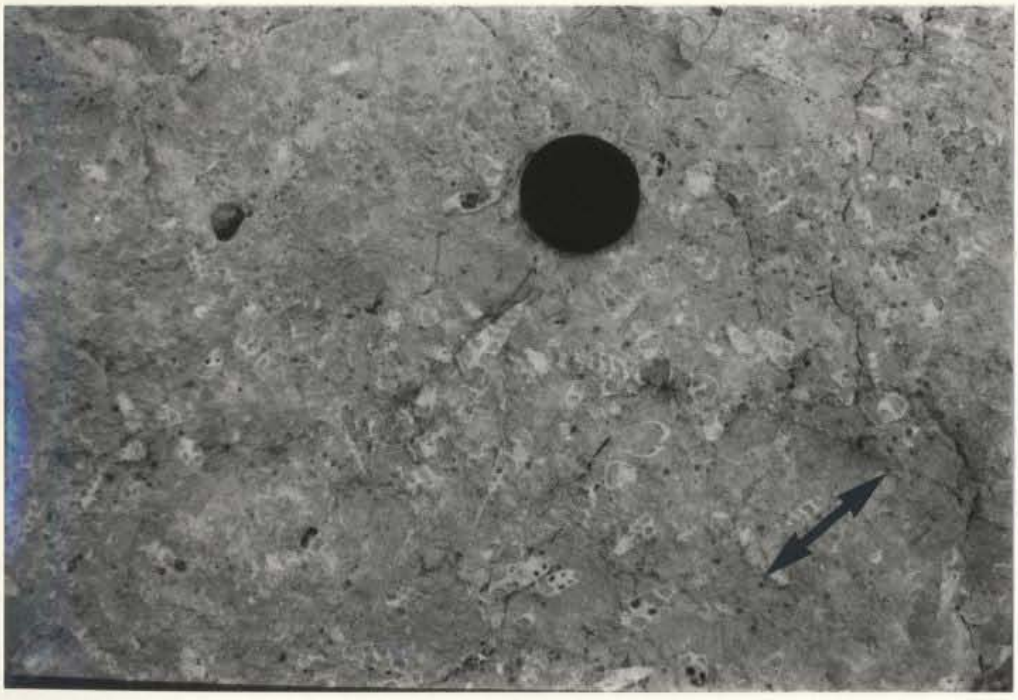
Though bioturbation is not common, there are beds which contain some trace fossils resembling those in the nodular limestone facies. For example Planolites sp. and Thalassinoides sp. were observed; however, Diplocraterion paralleum (Torell), a vertical U-shaped burrow, appears to be the most common (Figure 2.9).

The benthic fauna, mostly bivalves (Fursich and Schmidt-Kittler 1980), resembles assemblages observed in the nodular limestone facies. Some well exposed beds show bipedal and quadrupedal dinosaur tracks described by Telles Antunes (1976).

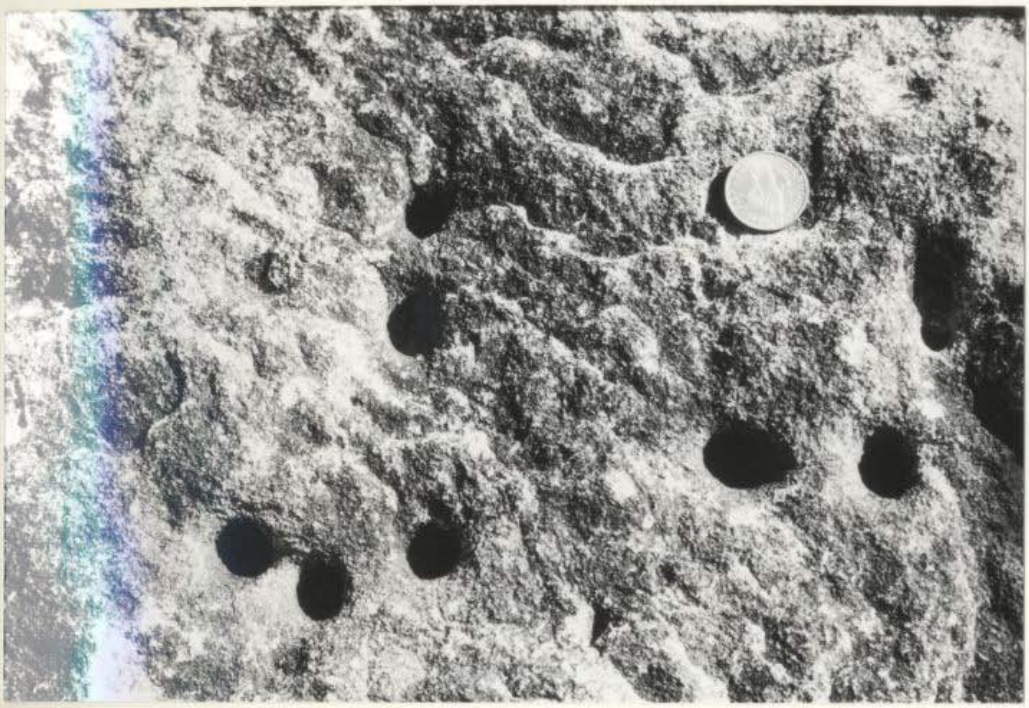
Interpretation: In general, the sedimentary structures, rounded clasts and lack of bioturbation suggests a relatively higher energy environment. Specific paleontological evidence suggesting more turbulent water is indicated where shells and burrows are aligned in a preferred direction (Figure 2.8). In addition, the presence



(Figure 2.7) Laterally continuous bed of buff brown to gray packstone (facies B) (coin for scale).



(Figure 2.8) Bed of packstone containing shell debris and clastic pebbles. Fossils indicate a preferred orientation in direction of arrow.



(Figure 2.9) Paired vertical burrows of Diplocraterion paralleum (Torell) is among the more common trace fossil in facies B.

of *Diplocraterion parallem* (Figure 2.9) is typical of sediments deposited from high energy conditions (Fursich 1975).

The presence of sauropod and theropod tracks on some well exposed beds of packstone indicates a relatively shallow marine environment. Dr. Dale Russell (pers. comm. 1986) suggested that on a muddy carbonate shelf the water depth is equal to four times the diameter of an adult dinosaur footprint. In the massive limestone facies at Cabo Espichel the footprints are up to 0.5 m in diameter (Telles Antunes 1976), implying a water depth of 2 m. Other evidence to substantiate this finding may be found in Bird (1944), Coombs (1980) and Lockley (1986).

Lithological evidence for higher energy is found in the oolite grainstones and quartz clasts found in this facies. Current transport is necessary for movement of these large particles from other localities.

These observations lead to the conclusion that this facies was formed seawards of the algal laminite in a more agitated environment (Reading 1978), at times relatively close to a terrestrial sediment source. This facies likely corresponds to a variety of higher energy shallow, probably subtidal environments (i.e. tidal channels and sublittoral shelf) in close proximity to a clastic source.

Facies C: Nodular limestone (Nodular biomicrite)

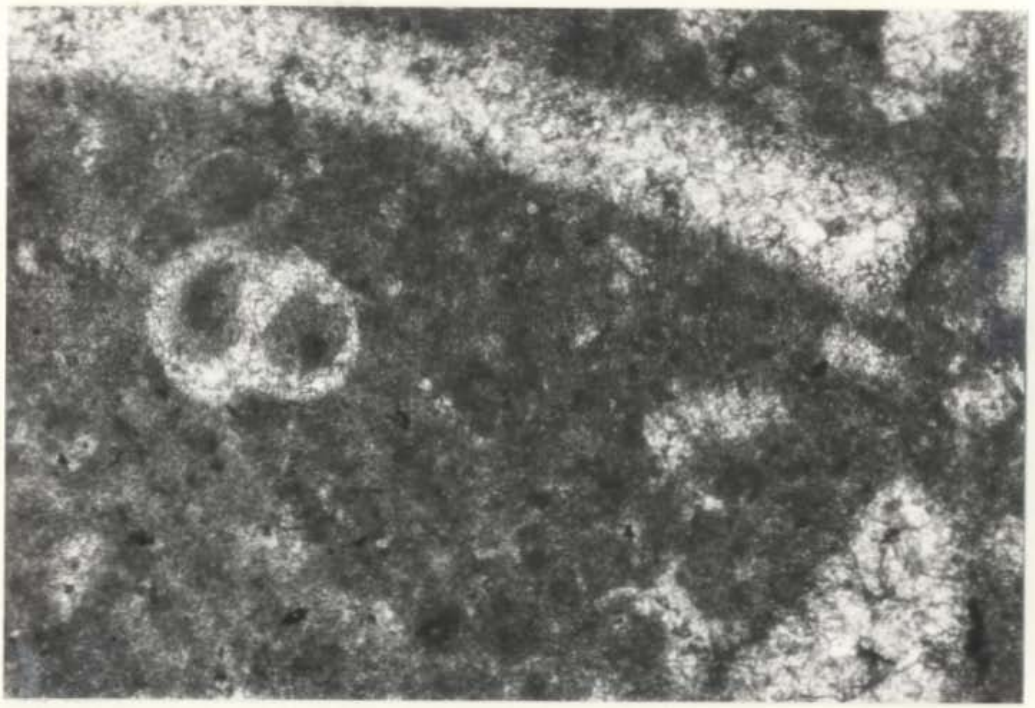
Petrology: This facies is predominantly a bioclastic wackestone. Rarely, bioclastic packstones and grainstones occur in some horizons.

The matrix of the bioclastic wackestone consists of 65% micrite (Figure 2.10). The macrofaunal debris is, likewise, quite high (35%) and consists of bivalves, gastropods and occasionally echinoderms. Larger, usually poorly sorted and sub-angular shell debris shows micritization. Peloids, subangular in shape, ranging from 50-200 μm in diameter, are common in some horizons. Ooids are not abundant; they tend to occur near the contact with the overlying massive biomicrite facies.

Terrigeneous quartz grains are common (10% of the rock) in nodular limestone beds near the massive biomicrite facies. Lower in the same bed quartz is virtually absent. The microfauna consists of Foraminifera, and Vaginella; the microflora is mainly debris of dasycladaceans and cyanophyceans (Fursich and Schmidt-Kittler 1980).

The bioclastic packstones and grainstones appear near the contact with the overlying massive limestone facies. At this contact peloids can be abundant.

Lithology and Fauna: Facies C is the most common facies in the section. The fossiliferous limestones are usually gray in color; they may show a buff color from



(Figure 2.10) Bioclastic wackestone of facies C consists of predominantly micrite with debris of gastropods and bivalves. Thin-section 40X.



(Figure 2.11) Laterally continuous bed of nodular limestone (facies C), showing extensive bioturbation and mixing of silts and fine sands amongst muddy carbonate.

post-depositional oxidation. Beds reaching 15 m thick, are commonly separated by centimeter-decimeter thick beds of calcareous shales (facies D) (Figure 2.11). For the most part beds of facies C are 1-2 m thick. Commonly nodular limestone grade into massive limestone (facies B). Fifty transitions from the nodular limestone into the massive limestone were observed in the section. In addition, nodular limestone commonly overlies the algal laminite (facies A).

The nodular appearance of the sediment is the result of bioturbation, mixing and burrowing by a Rhizocorallium irregulare (Mayer) and Thassinoides suevica (Rieth) fauna (Fursich and Schmidt-Kittler 1980) (Figures 2.11 and 2.12). The benthic fauna consists of more than 50 species of invertebrates, half of them are low energy, shallow burrowing, suspension-feeding bivalves (Fursich and Schmidt-Kittler 1980). Fursich and Schmidt-Kittler (1980) observed that these bivalves were much larger and more diverse than those found in the fine-grained clastics.

Interpretation: The relatively high degree of bioturbation is suggestive of, at times, low depositional rates and an environment protected from extensive mechanical reworking (Fursich and Schmidt-Kittler 1980). The trace fossils in the nodular limestone are known to be particularly abundant in protected shallow water environments such as lagoons or embayments (Fursich 1981).



(Figure 2.12) Well exposed bedding surface of facies C shows abundant Thalassinoides networks and Rhizocorallium.



(Figure 2.13) Abundant Vaginella striata are characteristic of some beds of the nodular limestones facies. 2X.

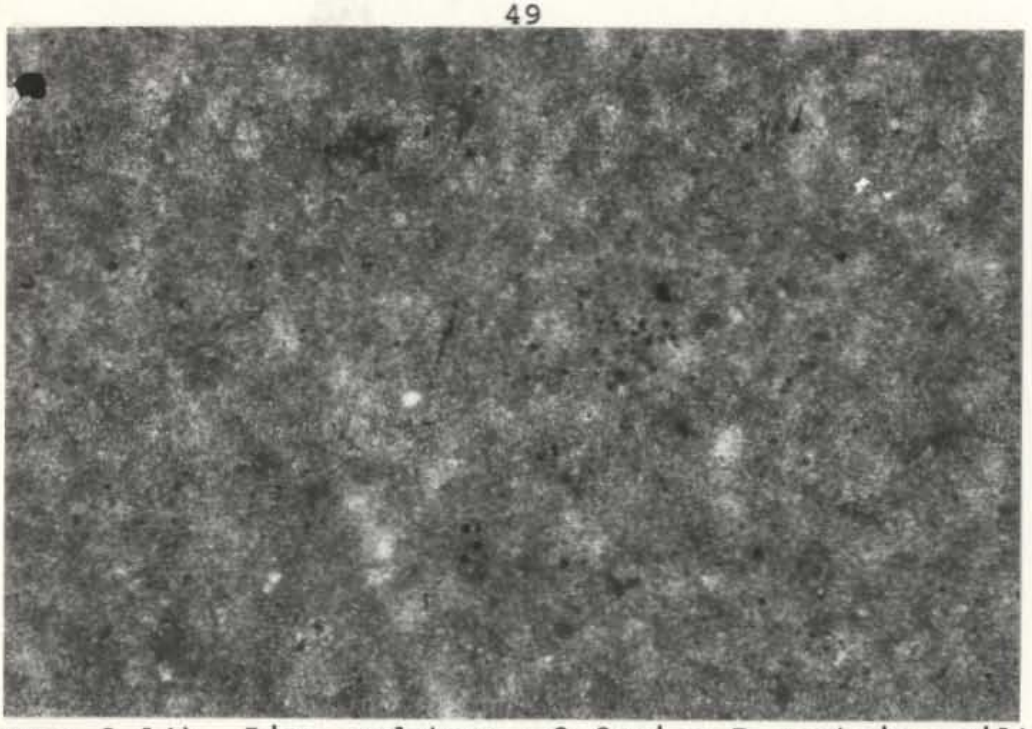
Specifically, the appearance of Rhizocorallium irregulare (Figure 2.12), a typical trace fossil of other low energy environments in the Jurassic, probably reflects periods of minimum disturbance and a relatively high content of organic matter in the sediment (Fursich 1981).

The benthic fauna described by Fursich and Schmidt-Kittler (1980) implies that the nodular limestone facies was deposited below fairweather wave base. The change in benthic fauna towards genera adaptable to a slightly reduced salinity may best be explained by "shallow, but protected, very extensive open marine platform or bays without significant amounts of terrigeneous influx" (Fursich and Schmidt-Kittler 1980, p.956). Water depths ranged from very shallow, as implied by transitions into the massive biomicrite facies and algal laminite facies, up to depths near 20 m as suggested from the benthic fauna (Fursich and Schmidt-Kittler 1980).

Facies D: Calcareous shale (Marls and marly silts)

Petrology: This facies is classified as a lime mudstone and contains more than 10% (silt size) grains in a mud-supported (micrite) matrix (Figure 2.14).

Lithology and Fauna: The black to gray calcareous shale facies occurs as interbeds of the nodular limestone facies C (Figure 2.15), and frequently occurs associated



(Figure 2.14) Lime mudstone of facies D contains silt size grains in a mud-supported micrite matrix. Thin-section X40.



(Figure 2.15) Beds of gray calcareous shale (facies D) occurring as interbeds of the nodular limestone facies C.

with the siliciclastics of facies E. Beds varying from a few centimeters to 3 m occasionally show small scale horizontal laminations; more frequently, these laminations are destroyed by bioturbation.

This facies contains the highest abundance of benthic fauna of the Cabo Espichel section. The fauna are represented by aligned shell debris occurring as continuous thin single shell "mats". Fursich and Schmidt-Kittler (1980) made similar observations and have identified these bivalves as "shallow marine infaunal suspension feeding bivalves".

Interpretation: The fact that most of the fauna in this facies are represented by aligned single-valved bivalve (1.5-2.0 cm wide) mats indicates a certain amount of reworking by gentle currents.

The calcareous shale facies is in such close association with the nodular biomicrite facies, that it implies a similar depositional environment. Exceptions to this pattern provide clues to one of the linkages between carbonates and clastics. Here, calcareous shales (facies D) are significantly associated with the siliciclastics of the distributary bay fill (facies E).

This facies may represent a low energy subtidal marine environment which is usually below wavebase. Additional evidence to suggest such an environment is implied by the marine fauna described by Fursich and Schmidt-Kittler

(1980). In addition, they observed that the fauna was composed of euryhaline species; that is species which tolerate a wide range of salinities. This implies that the environment was probably subject to fluctuations in salinity; fluctuations which may have resulted from the influx of freshwater from distributary channels.

2.2.2 Siliciclastics

Facies E: Mudstone and fine grained sandstone with calcareous nodules (In part alterations of poorly sorted silts and fine- to medium-grained sandstones)

Petrology: This rock is a feldspathic litharenite (Figure 2.16); with mica fragments. Glauconite was present in minor amounts. Plant debris was aligned in parallel laminations (Figure 2.17). Calcite cement permeates many sandstone beds. Fractures in the calcareous nodules are filled with sparry and blocky calcite.

Visually estimated porosity values of 30% in some horizons may be voids created from decayed plant roots. Elsewhere, wood debris and plant rootlets replaced by pyrite are common.

Lithology and Fauna: Laterally continuous beds of platey and mottled calcareous green and red laminated mudstone and red and gray fine grained sandstone occur as

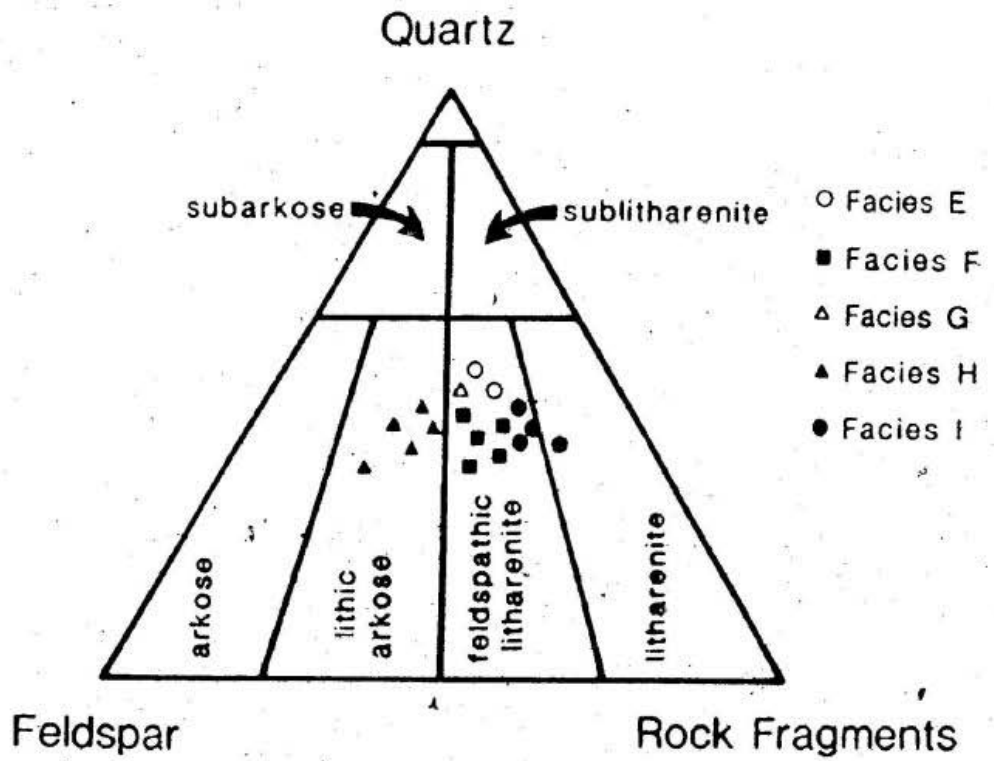
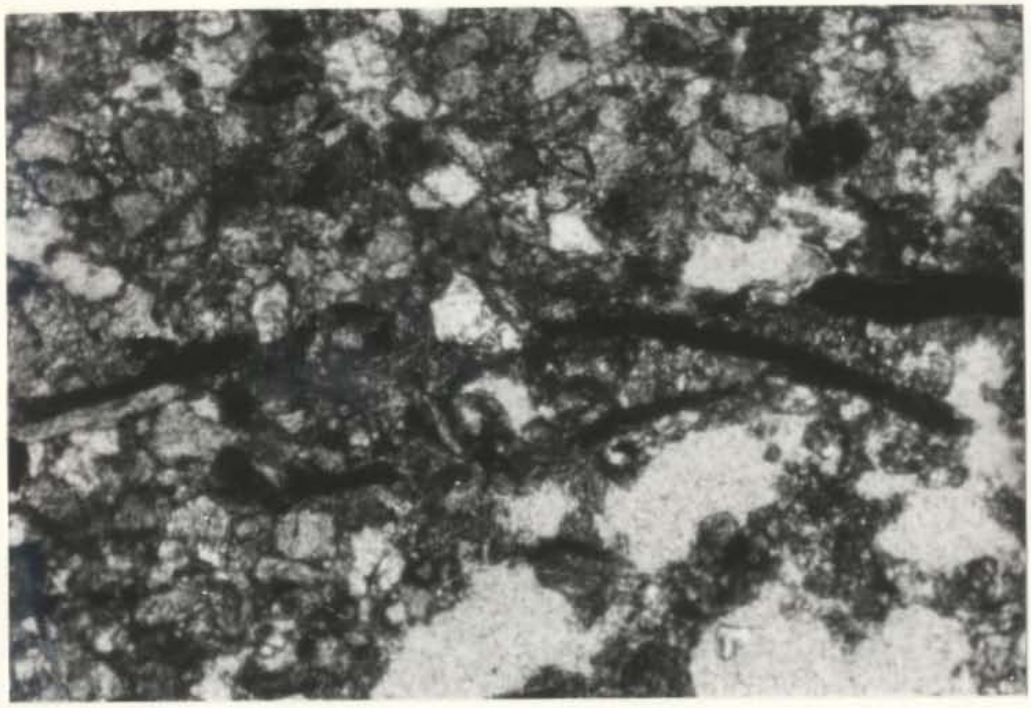


Figure 2.16 Average framework grain composition of facies E, F, G, H and I siliciclastics.

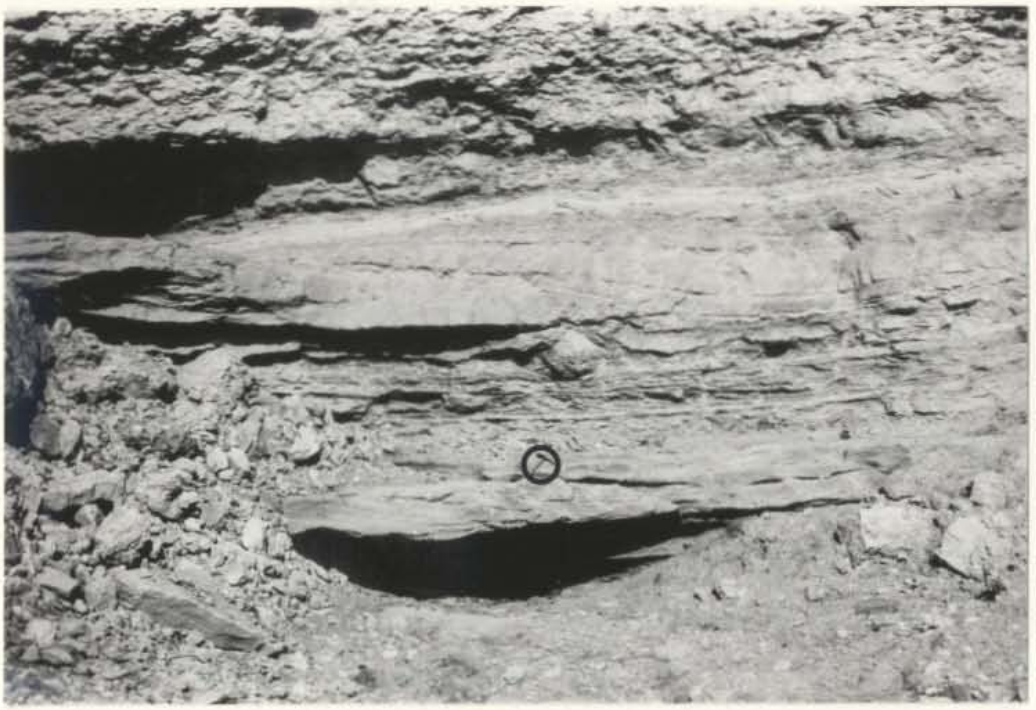


(Figure 2.17) Plant debris aligned with sandstones as parallel laminations in facies E. Thin-section X40.

beds which rarely exceed 2 m thickness. Beige calcareous nodules (between 3-8 cm in diameter) are the most distinctive feature of this facies (Figure 2.18). These nodules resemble those described by Fursich (1981) from Upper Jurassic strata, farther north, near Santa Cruz, Portugal. Markov transitions reveal that this facies is associated with siliciclastic facies F and G, and frequently overlies and underlies the calcareous shale facies D.

Bioturbation is common in the sandstones; invertebrate body fossils of the bivalve Eomiodon securiformis (Sharpe) and the oyster Liostrea are rare (Fursich and Schmidt-Kittler 1980).

Interpretation: The presence of laterally continuous red mudstone beds with irregular calcareous nodules suggest formation in an interdistributary bay of semi-arid climate (Allen 1964; Horne et al. 1978; Elliott 1981; Fursich 1981). The abundance of wood debris (Figure 2.19) and plant rootlets suggest periods of sub-aerial exposure, or a shallow water setting where some plants may grow. In addition to sub-aerial indicators, glauconite and marine bioturbation, with rare body fossils implies a marginal marine setting where sediments of what may be an interdistributary bay fill are deposited.



(Figure 2.18) Facies E, a green and red laminated mudstone and a red and gray fine grained sandstone with laterally continuous beds of platey and mottled beige calcareous nodules (hammer for scale).



(Figure 2.19) Woody debris in facies E.

Facies F: Cross-bedded sandstone and siltstone

Petrology: This facies is a feldspathic litharenite (Figure 2.16); the rock fragments are predominantly aggregate mica. Grains of quartz and feldspar are subangular and well sorted (Figure 2.20). Calcite cement is evident throughout, although primary interparticle porosity may be as high as 20% in some horizons.

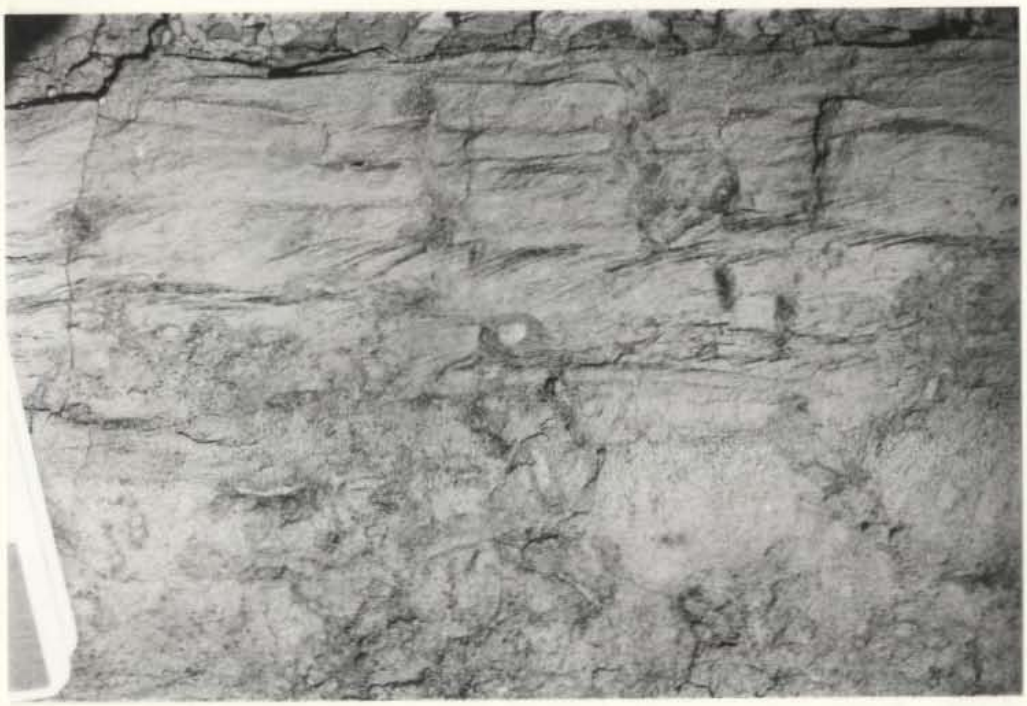
Lithology and Fauna: Gray-blue to red, often calcareous fine grained sandstone and siltstone occur as beds less than 1 m thick. Little bioturbation is evident. Nevertheless, burrows by Skolithos linearis are frequently observed. The general lack of bioturbation has allowed preservation of small-scale cross-beds, ripple drift laminae (Figure 2.21), and graded beds of coarsening upward cycles. Plant debris and pieces of lignite are frequently observed. This debris is not as common as that found in facies E. No invertebrate body fossils were found.

Markov chains reveal this facies to be almost exclusively intercalated between facies E and G. Occasionally it overlies facies J.

Interpretation: Facies F consists of coarsening upward cycles of cross-bedded and ripple laminated silts and sands which frequently overlie the possible bay fill facies E. Plant debris is common, but invertebrate body fossils are absent. Escape burrows from Skolithos linearis and the



(Figure 2.20) Photomicrograph of facies F show subangular and well sorted grains of quartz and feldspar. Thin-section X40.



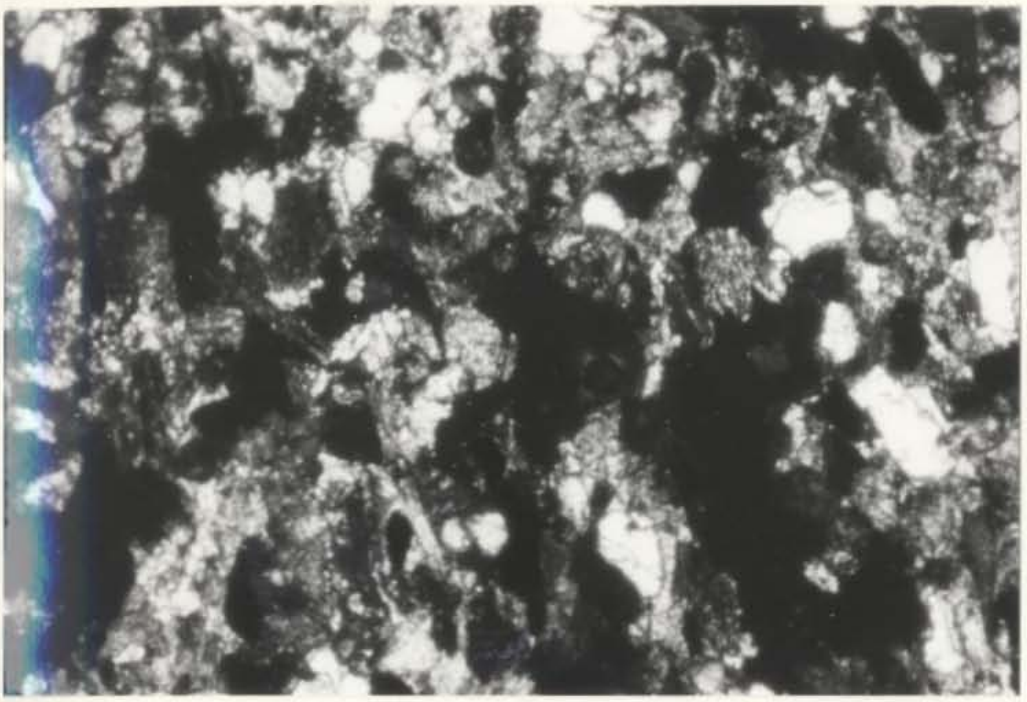
(Figure 2.21) Facies F, a gray-blue to red fine grained sandstones and siltstones showing small scale cross-bedding and ripple drift lamination.

ripple drift lamination indicate periods of rapid sedimentation. Such observations, together with the close association with bay fill deposits, suggests that this facies represents crevasse deposits in a marine/brackish environment similar to those described in Horne et al. (1978) and Reineck and Singh (1980).

Facies G: Bioturbated sandstone and siltstone with laminated mud (Not described in Fursich and Schmidt-Kittler)

Petrology: This facies is a feldspathic litharenite (Figure 2.16) with an abundance of organic debris and mica (Figure 2.22).

Lithology and Fauna: The poorly sorted, irregularly bedded bioturbated sandstone and siltstone with laminated mud facies is intercalated between coarser sands of facies H and the muds, silts and sands of facies F and E (Figure 2.23). This intercalation is identified as a significant feature by Markov analysis. Bed thicknesses generally do not exceed 1-2 m; in addition, the beds tend to thin laterally. These micaceous, gray, ocassionally red fine grained sandstones, exhibit distinct wavy bedding. Extensive bioturbation in some horizons, has obliterated primary sedimentary structures; elsewhere, mudstones exhibit parallel millimetre lamination, mudcracks, convolute bedding and load casts. Rare, unidentified species of bivalves and



(Figure 2.22) Facies G consists of fine grains of quartz, feldspar and abundant organic debris. Thin-section X40.



(Figure 2.23) The gray, at times red, fine grained bioturbated sandstones of facies G may contain penecontemporaneous deformation, mud-cracks and plant debris.

gastropods were observed in some beds. Plant debris and rootlets are very common.

Interpretation: The extensively bioturbated sandstone and siltstone with mud facies is associated with coarser sands of facies H and the muds, silts and sands of the crevasse splay and distributary bay fill deposits (facies F and E).

These deposits of fine to medium grained, red micaceous sands and calcareous silts with wavy lamination, plant debris, rootlets and mudcracks are interpretated to indicate a subaerial levee environment. Nevertheless, some strata within this facies exhibit convolute bedding, and burrows similar to those described by Fursich (1981) from a brackish marine fauna. Reineck and Singh (1980) described a similar sedimentary sequence which they interpreted as a natural levee complex.

Facies H: Coarse-grained to conglomeratic trough gross-bedded sandstones (Medium to coarse-grained, partly conglomeratic or pebbly sandstones)

Petrology: Sandstones in facies H are lithic arkose (Figure 2.16). The abundant feldspars, (orthoclase and microcline), are angular, coarse grained and vary from fresh to heavily weathered grains (Figure 2.24). The quartz grains show authigenic overgrowths; some quartz is



(Figure 2.24) Angular, coarse grained feldspar and quartz occur in facies H. Thin-section X40.

polycrystalline. In some strata the sandstone is cemented with small patches of poikilotopic calcite, occurring as small rhombs within pores of the detrital grains; whereas the remaining strata appears not to be cemented.

Lithology and Fauna: Dominantly red, or occasionally gray sandstones occur as fining upward lenticular bodies reaching thicknesses of 7 m. Grain size ranges from that of coarse sand to very large pebbles. Pebbles of quartz, feldspar and fine-grained sandstone were observed to accumulate predominantly within troughs (Figure 2.25). Intraformational sandstone pebbles, up to 6 cm diameter, are commonly subangular, whereas smaller pebbles, near 2 cm diameter, are sub-rounded to round. No imbrication of the pebbles was evident.

The contact with underlying sediment is always a scoured surface (SS). Near the contact the pebbles are associated with mudflakes derived from underlying shale and limestone beds. Facies H is frequently overlain by facies G and E, and is also associated with facies J.

The predominant sedimentary structure is large-scale trough-cross bedding (Figure 2.26); troughs have a mean orientation of 230° and a range of 195° to 250° (75 measurements). Often the trough-cross bedding is overlain by planar beds.

Lignite debris occurs within plane bedded sands. Trace fossils are extremely rare; there are only a few occurrences



(Figure 2.25) Pebbles of quartz, feldspar and fine-grained sandstone often accumulate in the troughs of facies H.



(Figure 2.26) Red, trough cross-bedded, coarse to granule conglomerate sandstone of facies H.

of Skolithos sp. near the contact with overlying facies. Body fossils are completely absent.

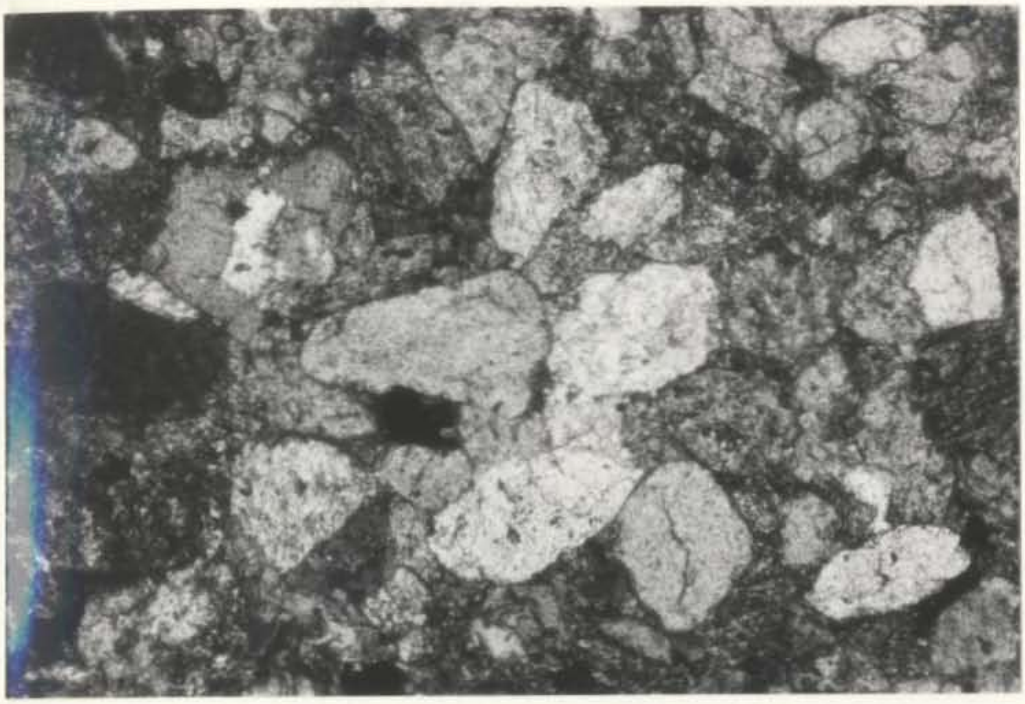
Interpretation: The coarse grain size of the feldspars and quartz imply close proximity to their source, likely uplifted blocks of Hercynian basement.

This facies is interpreted as a channel fill. Similar facies described by Horne et al. (1978), Coleman and Prior (1980), Elliott (1981) and Hopkins (1985) have been interpreted as fluvial channels. From facies association this deposit is probably representative of distributary channels advancing into a shallow marine environment. These channel sandstones are frequently overlain by levee and distributary bay fill deposits (facies G and E). In two particularly well exposed intervals, at 82 m and 102 m of the section the channel becomes plugged with non-calcareous silty shales of facies J.

Facies I: Fine to medium grained sandstone

Petrology: This sandstone is predominantly a feldspathic litharenite; one sample is a litharenite (Figure 2.16). The detrital grains of quartz and feldspar are clean (fresh), rounded and well sorted (Figure 2.27).

The sandstones are cemented with calcite cement. Nevertheless, 15-20% of primary interparticle porosity was observed in four thin sections.



(Figure 2.27) The grains of facies I are clean, rounded and well sorted sands. Thin-section X40.



(Figure 2.28) Facies I occurs as lenticular bodies of well sorted fine to medium grained red sandstone adjacent to facies H.

Lithology and Fauna: These fine to medium grained sandstones (Figure 2.28) often occurs as a lenticular body up to 4 m thick. These bodies occur at the base of, or adjacent to, trough cross-bedded pebbly sandstone (facies H); here, the contact between the two facies is scoured. In a typical sandstone of this facies, the upper 25% exhibits ripple and parallel laminated beds (1 cm thick), whereas the lower 75% shows occasional small-scale cross-bedding, fining-upward graded bedding and soft sediment deformation (Figure 2.29). Plant debris, while common throughout, is preferentially concentrated in thin laminations near the top of the facies.

Interpretation: The absence of lamination in the lower 75% of the facies suggests the lack of a tractional phase during deposition of these sands. It has been suggested by Middleton (1965) that beds lacking any lamination are formed either by very rapid deposition from suspension or by deposition from highly concentrated sediment dispersion. In some cases, original lamination may have been destroyed by liquefaction soon after deposition (Middleton and Southard 1977).

Clean and well sorted sand lacking detrital clay implies the presence of reworking of the sediment in a turbulent environment. The trend in figure 2.16 illustrates a decrease in the feldspar content from facies H to facies I. Such a trend would be expected where chemical weathering



(Figure 2.29) The sandstone of facies I with parallel laminated beds near the top of the facies, and soft sediment deformation resulting from liquefaction near the bottom.

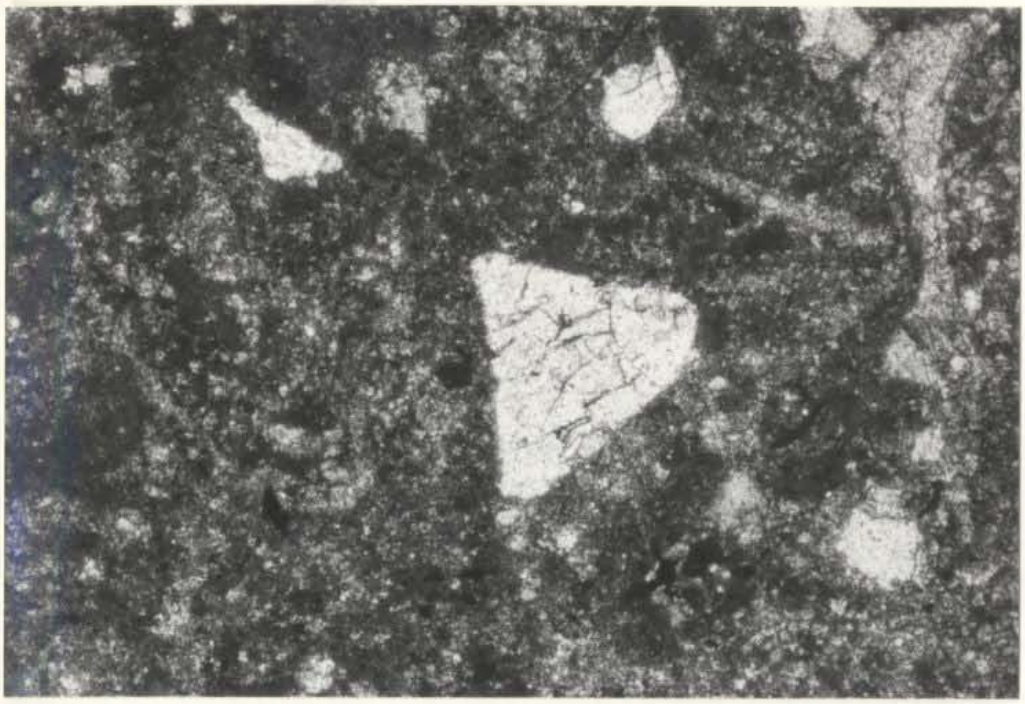
and dilution by addition of other minerals would decrease the amount of feldspar as it was transportd by the channel, so that eventually the sediment deposited as a distributary mouth bar is of a low feldspar content (facies I).

Lenticular sandstone bodies resembling this facies are known to form near the seaward limit of distributary channels as distributary mouth bar deposits (Horne et al. 1978; Reineck and Singh 1980; Coleman and Prior 1982). Such sandstones are often overlain unconformably by distributary channel deposits. In addition, mouth bar sands usually overlie silts and shales of a delta front environment. Such is the case with sandstones of facies I at Cabo Espichel, and a distributary mouth bar deposit in a delta-front environment is suggested.

Facies J: Non-calcareous silty shale

Petrology: Occasionally in some horizons detrital grains of quartz, feldspar and mica were distinguished from the matrix; however, mineral percentages could not be calculated because of minute grain sizes (Figure 2.30).

Lithology and Fauna: This black to gray silty shale facies (Figure 2.31) occurs at the base of coarsening-upward sequences. It is usually associated with the coarser sands of facies H and I; commonly it occurs above the massive limestone (facies B). In some beds parallel millimetre



(Figure 2.30) Detrital grains of quartz and feldspar occur in a clay matrix within facies J. Thin-section X40.



(Figure 2.31) Laminated black to gray silty shales of facies J occur at the base of coarsening-upward sequences and frequently overlay massive limestones of facies B.

scale lamination and ripple marks were observed; at other horizons these structures have been completely destroyed by bioturbation. The thickness of beds in this facies ranges from a few decimeters to 5 m. In some beds lignite debris is present. Trace fossils consist of Thalassinoides and Planolites species.

Interpretation: This facies represents the nearshore deposits formed during times of increased influx of terrigeneous material, possibly in a delta-front setting. Where facies J associates with the channel sands of facies H, it is more likely representative of a channel plug (eg. at the 82 m and 102 m intervals of the section).

The brackish marine fauna described in this non-calcareous shale by Fursich and Schmidt-Kittler (1980) indicates a quiet, shallow marine environment which was influenced by increasing fluviatile/deltaic processes, such as freshwater and terrigeneous sediments.

2.3 A Model for Portlandian Siliciclastic-Carbonate Successions

The Portlandian section at Cabo Espichel (Figure 2.32 in pocket) contains a sequence of alternating carbonate and siliciclastic sediments well suited for Markov analysis. The Markov analysis demonstrates the likelihood of individual siliciclastic and carbonate successions

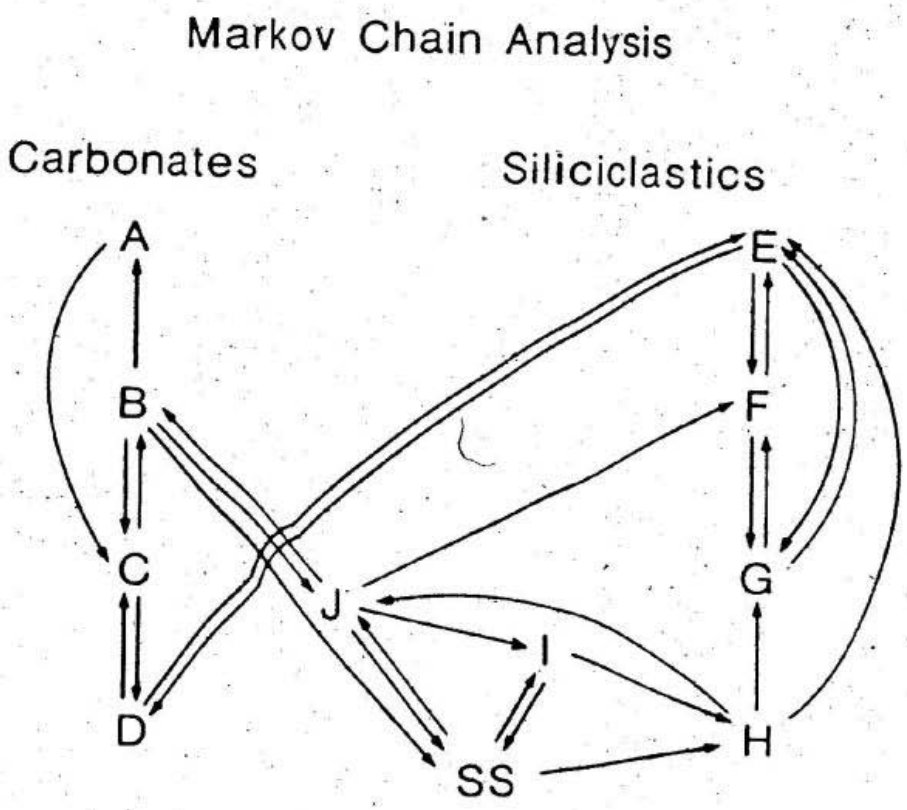


Figure 2.33 Facies transitions determined from Markov chain analysis; transitions based upon probabilities > 0.90 (see figure 2.1 for explaination of symbols).

(Figure 2.33). Examination of the boundary conditions from Markov analysis provides an opportunity to develop a model which may explain some of the geological conditions responsible for such contacts.

The following model will be discussed in three segments, the carbonate succession, the clastic succession and the boundary conditions. Each part demonstrates a different aspect of the complex geology of this basin.

2.3.1 Carbonate Succession

A general model for the carbonate succession at Cabo Espichel indicates that calcareous shale (facies D) is intercalated with subtidal nodular limestone (facies C). This is succeeded by subtidal massive limestone (facies B) and then capped by algal laminites (facies A) (Figure 2.34).

In general, this succession is rarely observed fully developed; other environmental parameters (i.e. tectonic) control the completeness of a single facies succession. In the lower 140 meters of the section (Figure 2.32 and Figure 2.34) massive limestones (facies B) are associated with nodular limestones, whereas in the upper 140 to 250 meters of the section, algal laminites (facies A) tend to be associated with the massive limestones, as the nodular limestones become less common. Here, a common facies

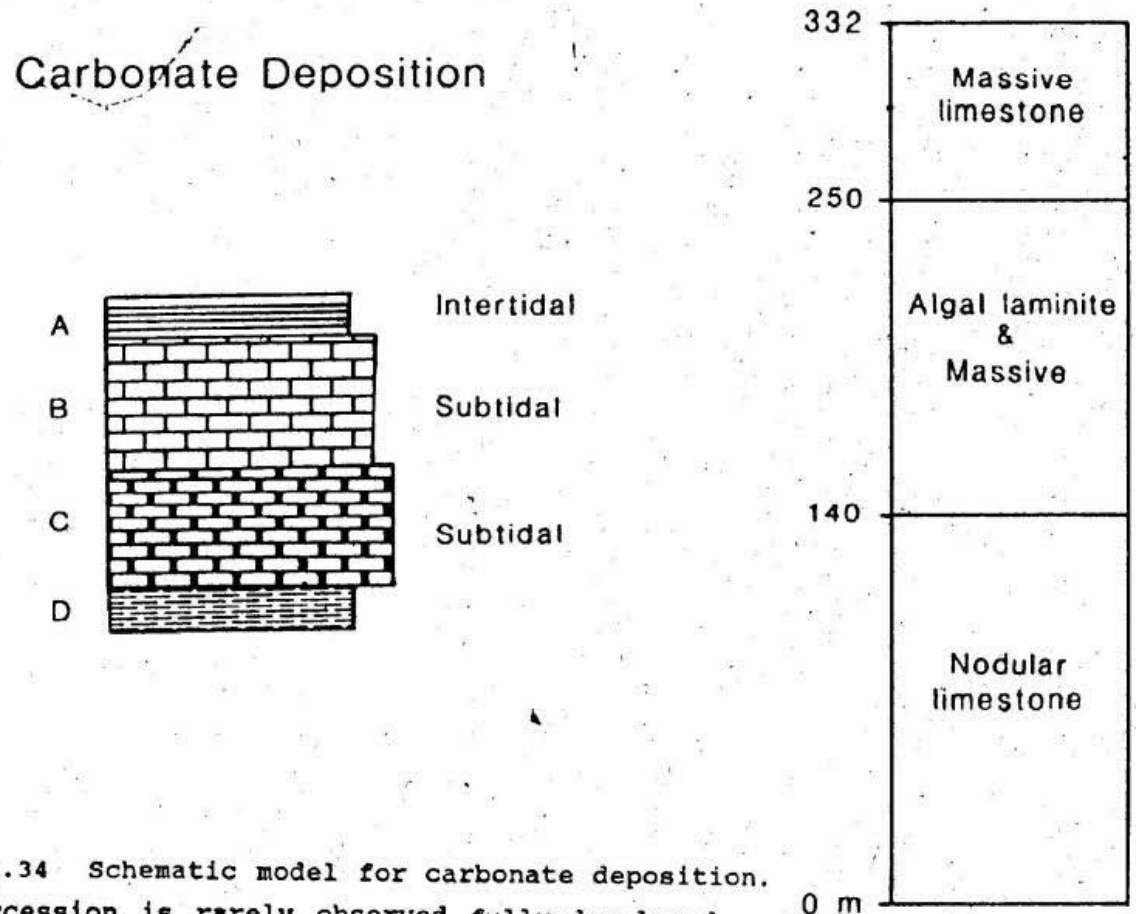


Figure 2.34 Schematic model for carbonate deposition. This succession is rarely observed fully developed because of environmental parameters such as tectonics.

transition is from massive limestone to laminated algal mats and back into massive limestone or, less frequently nodular limestone. The remainder of the section is dominated by massive limestone lacking mud (Figure 2.34). Fursich and Schmidt-Kittler (1980) did not recognize these transitions; from their text they have described a somewhat different facies transition of nodular limestone to algal laminite. This transition was not evident in this study. Here, Markov analysis may have allowed this transition to become more distinct.

Subtidal nodular limestones intercalated with calcareous shales are succeeded by subtidal massive limestones with silty debris, occasional terrigeneous clasts of quartz and feldspar. The presence of these clasts are the result of an increased influx of siliciclastic material from an advancing shoreline. In the lower 130 meters of the section the nodular and massive limestone sequence may continue into a channel facies, or a bay fill deposit. In the upper part of the section it tends to be overlain by nodular limestone, and occasionally algal laminites. The preservation of the algal laminites probably occurred during the regressive phase (Wright 1984b).

Overall, the siliciclastic mud decreases through the section from bottom to top. The lower 150 meters contains an abundance of non-calcareous and calcareous shale, whereas, the remaining 175 meters tends to lack mud. Such a

trend may imply an increase in wave energy or an absence of terrestrial sediments as the Cabo Espichel region underwent a local transgression.

2.3.2 Siliciclastic Successions

Generally, the model for the coarsening-upward siliciclastic succession consists of coarse pebbly sands of a distributary channel (facies H), adjacent to massive sands of a distributary mouth bar (facies I), which overlie delta front shales (facies J). This is overlain by levee (facies G), crevasse (facies F) and bay fill deposits (facies E) (Figure 2.35). The entire succession is sandwiched between carbonates of massive limestone (facies B) below and calcareous shale (facies D) above. There are, however, inconsistencies in the succession. At times, the non-calcareous silty shale (facies J) is associated with the channel sands (facies H); this is likely a channel plug and not a delta front deposit.

From a larger perspective the section illustrates that the siliciclastics become less common near the 140 meter level; one exception may be the bay fill deposits between the 215 and 229 m (Figure 2.35). This may imply a regressive cycle in a protected shallow marine environment in the lower part of the section.

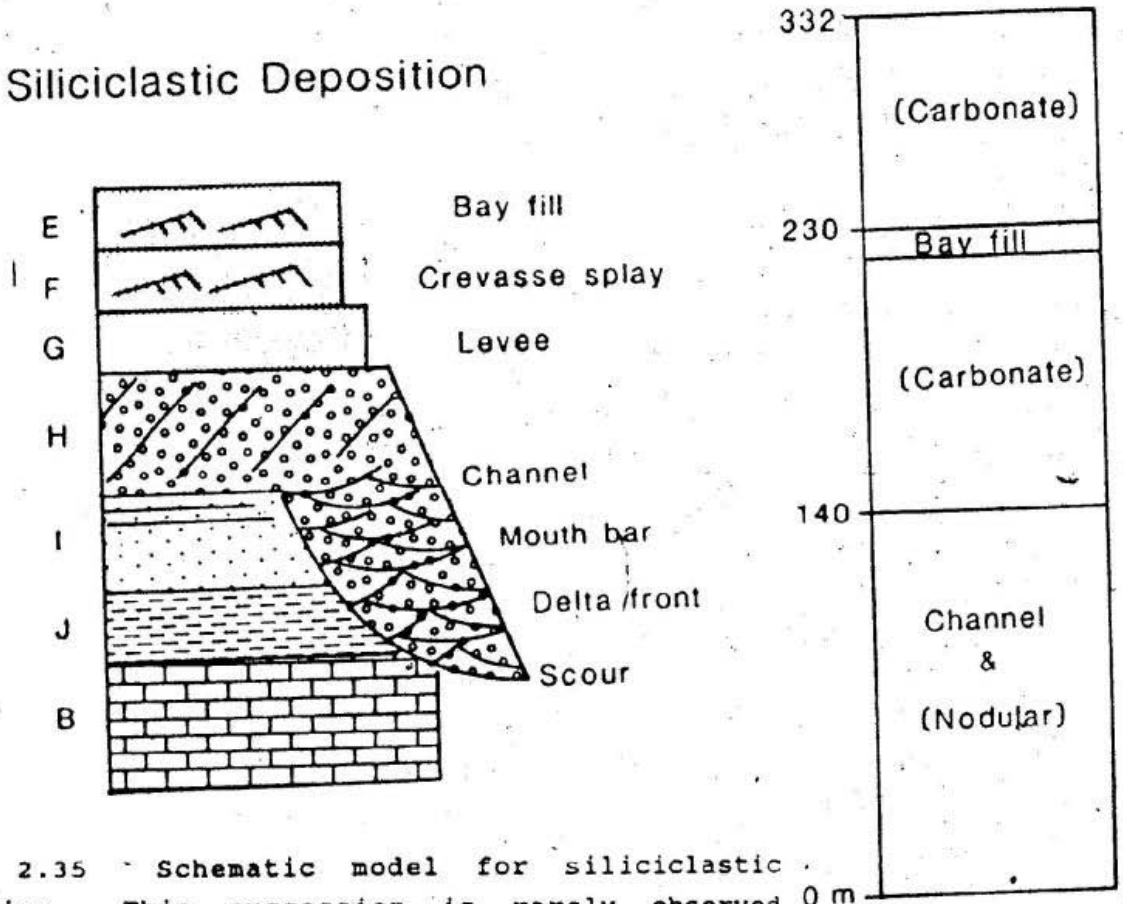
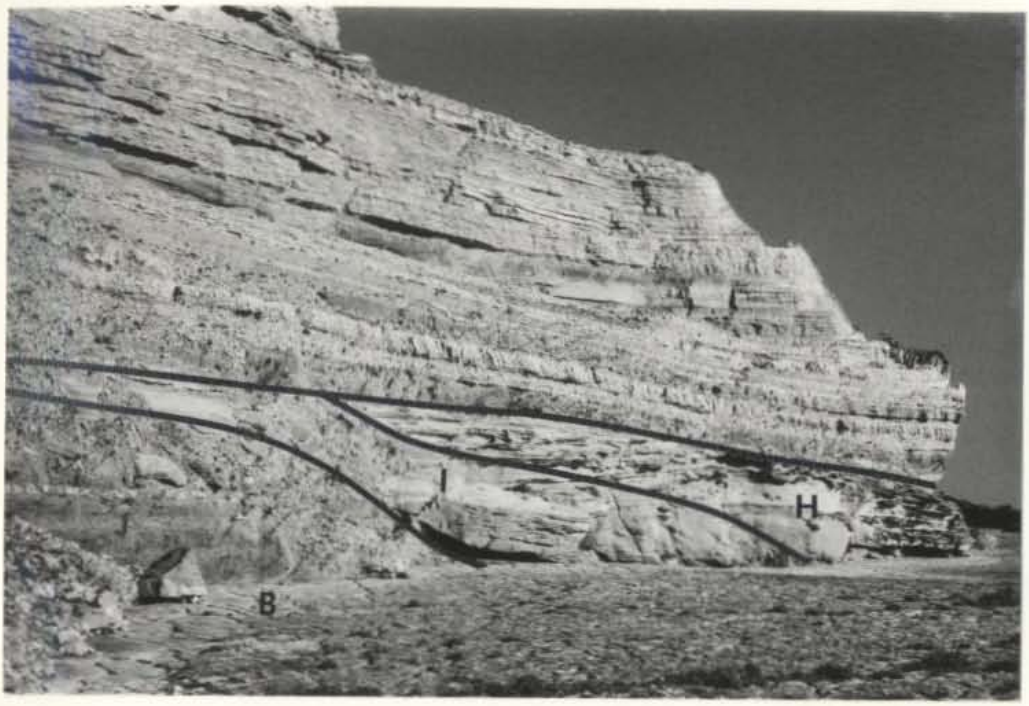


Figure 2.35 Schematic model for siliciclastic deposition. This succession is rarely observed fully developed because of environmental parameters.

2.3.3 Boundary Conditions

The transitions between the carbonate and siliciclastic facies occur in two ways 1) erosional, scoured contacts and 2) non-erosional, transgressive and regressive contacts. From these facies transition a model describing Portlandian siliciclastic-carbonate successions is developed.

The erosional boundary develops where distributary channels (facies H) scour (facies SS) through massive medium grained sandstone (facies I) of a distributary mouth bar, underlying delta front silts (facies J) and end in subtidal massive carbonates (facies B) (Figure 2.36 and 2.37). Scours in the underlying carbonate (facies B) may measure 7-8 m across and up to 40 cm in depth. These channels, whose overall dimensions exceed 30 m width and 6 m depth, usually form the base of fining-upward clastic successions. Above this scour surface lies lenticular bodies of trough and planar cross-bedded sands of the distributary channels (facies H). The fine to medium grained massive lenticular sandstone body of the distributary mouth bar (facies I) may occur either at the base of, or adjacent to, the distributary channel. The distributary mouth bar, a sandy shoal formed at the seaward limit of the distributary channel, is typically a coarsening upward cycle (Coleman and Prior 1980) in which the proximal deposits to the distributary are channeled. Subsequent to the formation of



(Figure 2.36) An erosional boundary where a distributary channel (H) scours through a distributary mouth bar (I) and delta front (J) into the subtidal massive limestones (B).

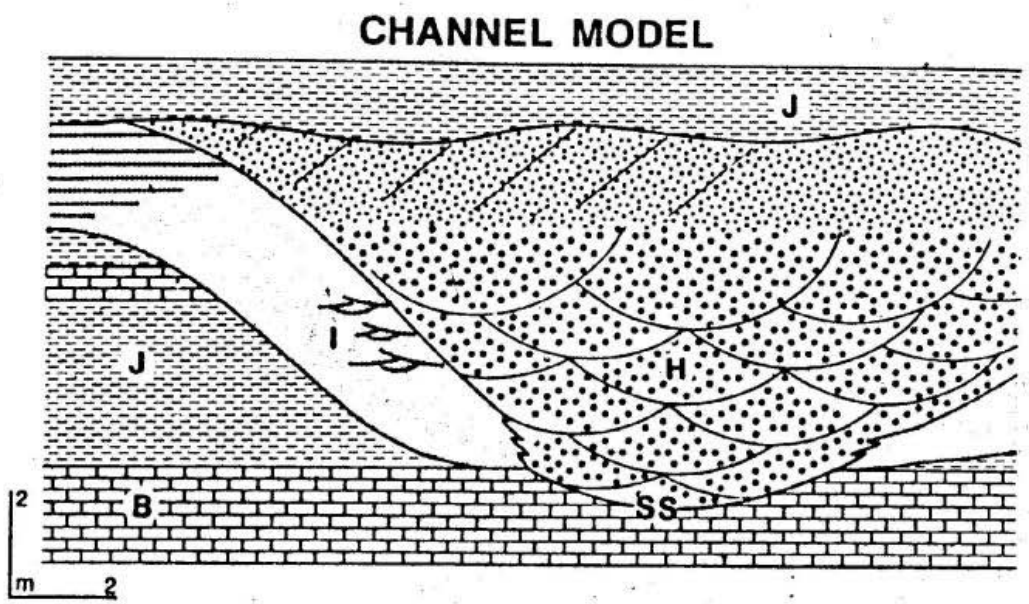


Figure 2.37 This model demonstrates an erosional contact condition between the siliciclastic and carbonate. This occurs where distributary elements advance through the distributary mouth bar and delta front deposits.

the mouth bar the channel advanced. This resulted in erosion of all facies (I, J and B) in it's path. The non-erosional boundary is a clastic fining-upward cycle consisting of reddish to greenish fine-sands and calcareous mudstone exhibiting parallel millimetre lamination and penecontemporaneous deformation (facies E) underlying a fine-sand silt (facies F) showing small-scale cross-bedding and ripple lamination. This clastic fining-upward cycle is then terminated by an extensively bioturbated medium-grained sandstone and siltstone (facies G) which is overlain by facies E (Figure 2.38). This facies association, respectively represents a variety of overbank deposits, distributary bay fill, crevasse splays and levees, which prograde into an interdistributary bay consisting of calcareous shales (facies D) and, further offshore, nodular limestones (facies C) (Figure 2.39 and Figure 2.40). It is between these facies associations that non-erosional contacts result from the progradation of the clastics into interdistributary bay carbonates or marine carbonates overstepping deltas. The siliciclastic sequence consisting of facies E through G represent a regressive phase infilling interdistributary bays. This regressive phase may be terminated as a transgression resulting in deposition of marine carbonates of facies C and D.

In general, the kinds of boundary conditions change through the section. In the lower 140 meters of the section



(Figure 2.38) A non-erosional regressive boundary where siliciclastics of distributary bay fill and crevasse splay prograde over subtidal nodular limestones and calcareous shale of an interdistributary bay or shallow shelf (book for scale).

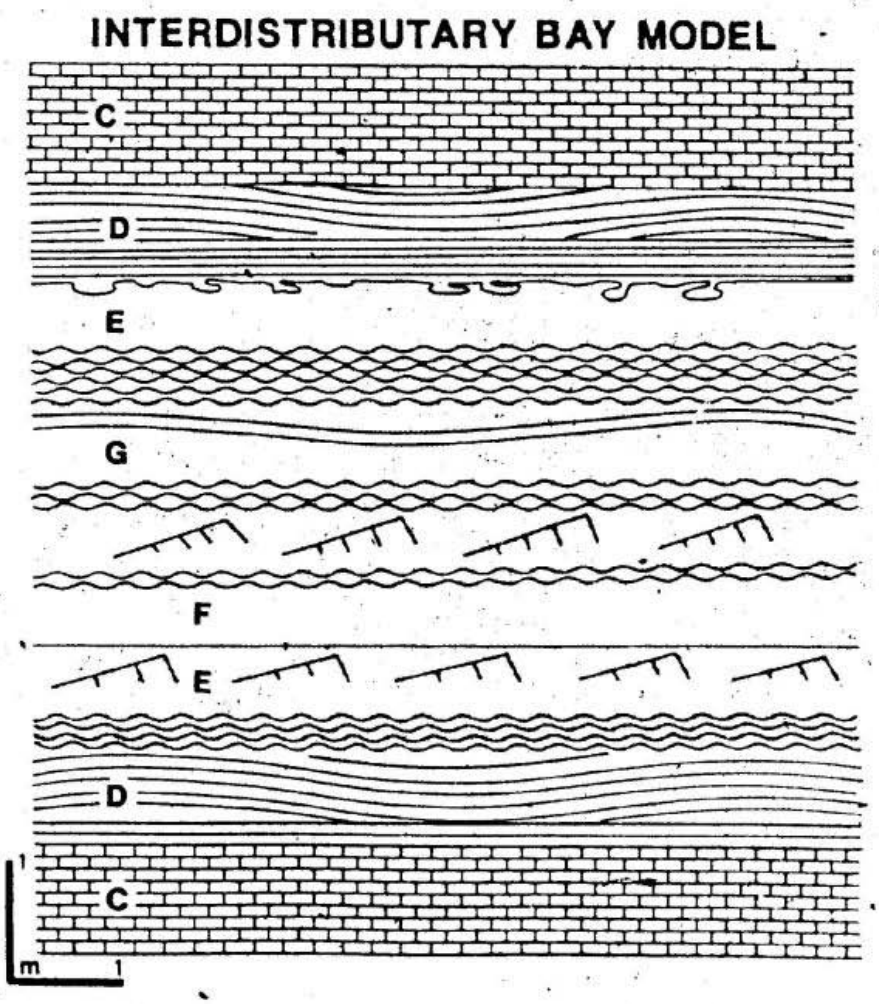
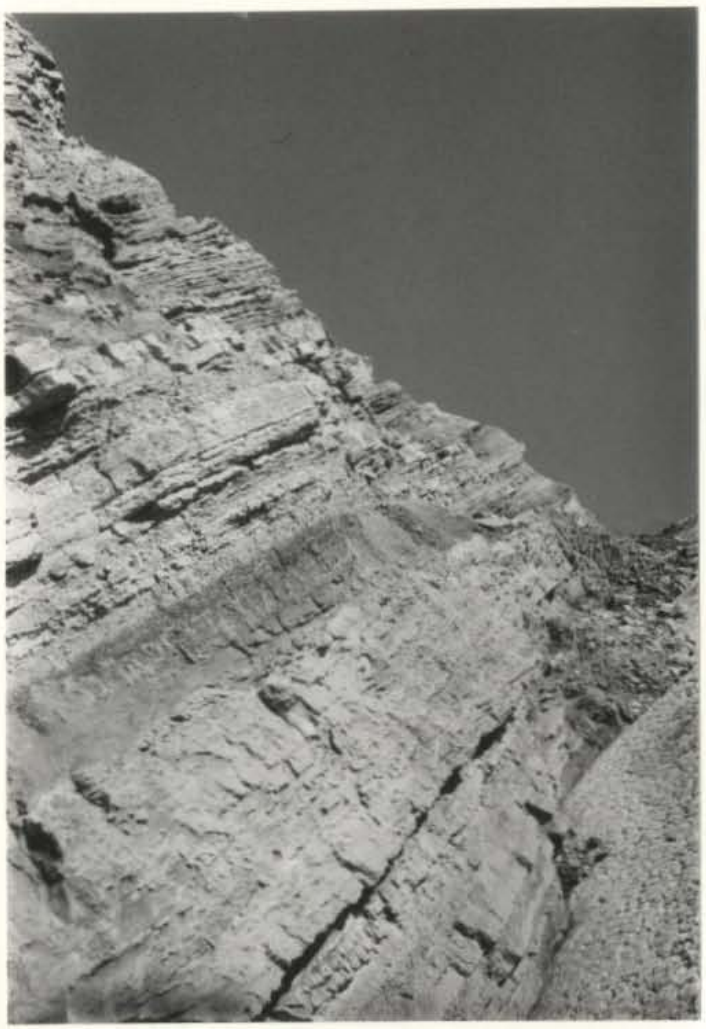


Figure 2.39 This model demonstrates a non-erosional contact condition between the siliciclastic and carbonate facies. This occurs where crevasse splay and bayfill deposits prograde into an interdistributary bay.



(Figure 2.40) Large scale cyclic package of interdistributary bay fill and crevasse splay siliciclastics conformably sandwiched between transgressive nodular limestones.

scouring by channel and distributary mouth bar sands are significant. Above 140 m, scouring evidently disappears. Conformable boundaries are also significant in the lower part of the section where the muddy deposits are common. With the exception of the interval from 215 to 229 m, where bay fill deposits overlie calcareous shales (facies D), mud becomes less common in the upper part of the section. As the mud content of the sediments drop so does the linkages between the siliciclastic and carbonate facies. This provides significant, albeit indirect evidence to show the evolution of a carbonate-clastic relationship during a gradual transgression of the Cabo Espichel area during the Portlandian.

2.4 Regional Depositional Setting

In concurrence with Fursich and Schmidt-Kittler (1980) the author agrees that the facies of the carbonate-siliciclastic section at Cabo Espichel implies continuous cycles of shallow marginal marine and terrestrial environments. Within this setting the water depth at any one time generally seems to have been quite shallow, and probably did not exceed 20 m (Fursich and Schmidt-Kittler 1980).

The majority of the facies, especially the nodular biomicrites, algal laminites and finer-grained delta front,

levee and bay fill clastics were deposited in a quiet, low energy setting. The remaining coarser-grained material, from the channel and distributary mouth bar were deposited from higher energy. This is also true for the massive limestone.

Paleogeographic investigations by Baldy et al. (1977 in Fursich and Schmidt-Kittler 1980) of the shelf to the west of central Portugal showed deposition of neritic limestones resembling those at Cabo Espichel. According to Fursich and Schmidt-Kittler (1980) this implies open shelf conditions to the west of central Portugal. They also hypothesized that beneath this shelf environment were NNE-SSW striking diapirs which may have generated island ridges or linear submarine highs. These structures acted as a system of barriers creating a protected lagoonal environment from the open shelf. It is agreed that a protected environment is necessary for the deposition of the lithologies observed at Cabo Espichel. There is, however, no concrete evidence for such barrier islands (R.C. Wilson pers.com. 1985) and Fursich (1981).

One alternative explanation may lie in a recent study from the Quaternary of Florida. Here, Harrison and Coniglio (1985) have found that an offshore barrier complex is not necessary for the creation of lagoonal type deposits. High wave energy diminishes over an extensive open marine platform.

During much of the Portlandian Cabo Espichel was likely a broad carbonate platform. From the modern record it is clear that such a setting could generate well protected muddy embayments. However, in this study the fine calcareous sediments are consistently associated with deltas. The coastline may well have been modified by deltas. According to Wilson (1975a) it is unlikely that the regressive periods at Cabo Espichel were the result of a global sea level fall, since they are relatively brief and only recognised locally. Elsewhere in Western Europe the Portlandian is represented by a transgression (Hallam 1981). Therefore in concurrence with Fursich and Schmidt-Kittler (1980) the carbonate facies may be viewed as a transgressive event with short tectonically controlled regressions illustrated at Cabo Espichel by westward prograding deltas in the lower part of the measured section.

For this regional model, the Portlandian at Cabo Espichel was an extensive inner shelf marginal marine carbonate platform, where rapidly prograding deltas emanating from tectonically active highlands farther east provided protection for the deposition of lagoonal type sediments (Figure 2.41).

The abundance of coarse, angular feldspar grains within the sandstone at Cabo Espichel, and the decreasing thickness of the clastic sequence from east to west have been related to a relatively steep rugged morpholgical gradient (Fursich

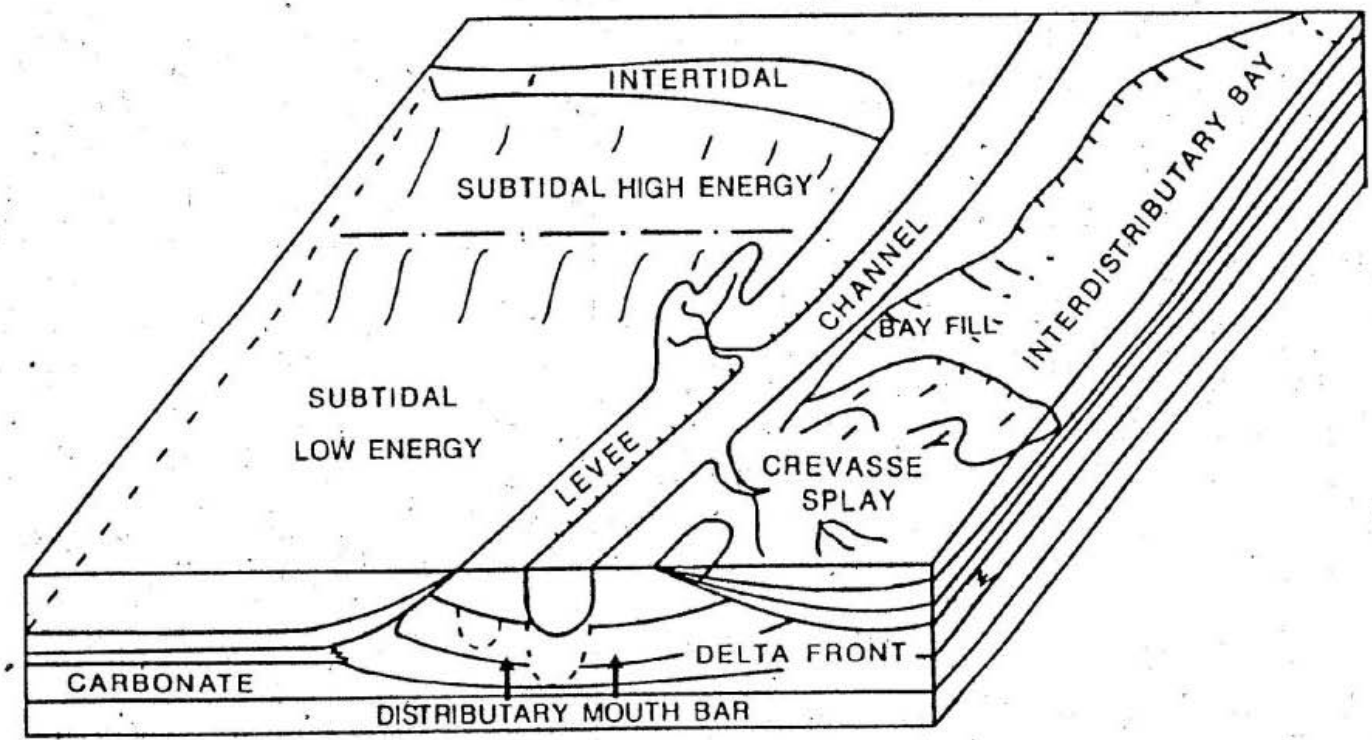


Figure 2.41 Depositional model for the Cabo Espichel showing environment distribution (modified after Coleman and Prior 1980).

and Schmidt-Kittler 1980). This gradient could have been the Hercynian basement bordering the Lusitanian Basin in the east, which was uplifted periodically during the Upper Jurassic along fault lines that ran North-South to the margin of the basin (Wilson 1975a). This uplift caused erosion and an influx of clastic material into the channels and eventually into marginal marine inner shelf environment.

Mixing of siliciclastic and carbonate facies in shallow shelf environments were studied in some detail by Mount (1984). The mixing which occurs at Cabo Espichel resembles three mixing types as described by Mount (1984). The "source mixing" process, the result of erosion and deposition of an uplifted source terrane, may be compared to the tectonic event causing uplift of the Hercynian basement at Cabo Espichel. The "facies mixing", a process of mixing of sediments along the diffuse borders between contrasting facies, may be compared to Cabo Espichel where there is mixing of interdistributary bay fill deposits and carbonates in a bay or lagoon. Facies mixing result in conformable boundaries. Mount's final mixing type, "punctuated mixing", is caused by the transfer of sediment between contrasting depositional environments during rare, high intensity sedimentation events. This can be compared to avulsions at Cabo Espichel, where deltaic channels prograde over lagoonal or bay carbonates. This mixing at Cabo Espichel results in an unconformable boundary condition.

CHAPTER 3 PALYNOLOGY

3.1 Systematics

Various classification systems are used to describe fossil palynomorphs. One such system based on the Linnean binomial system for classification is a "Natural Classification"; this classifies genera to supra-generic status by relating possible phyletic relationships as implied from similarities relationships with recent genera. This classification scheme has been used by Couper (1958), Filatoff (1975), Singh (1964, 1971) and Fensome (1983). One other system, known as the "Turma System" of Potonie and Kremp (1954, 1956) has been adopted by other authors, for example, Dettmann (1963) and Doring (1965). This system is based upon morphological features; phyletic relationships are not implied. A simplified version of the Turma System is used in this study. Palynomorphs identified in this study are classified alphabetically into one of the following categories:

3.1.1 SPORES

3.1.1.1 Trilete

3.1.1.2 Monolete

3.1.1.3 Alete

3.1.2 POLLEN

3.1.2.1 Monoporate

3.1.2.2 Bisaccate

3.1.2.3 Monosulcate

3.1.2.4 Perinous

3.1.2.5 Inaperturate

3.1.3 MARINE MICROPLANKTON

3.1.3.1 Acritarchs

3.1.3.2 Dinoflagellates

The entry for each species includes an illustration, selected synonymy derived from the Genera Card File of Jansonius and Hills (1976-1983) and references examined in this study (see refences cited), original or emended diagnosis where available, morphological description, dimensions of specimens, occurrence, relative abundance and comments on the stratigraphic range, distribution, comparisons with similar species and any additional specialized characteristics. Extensive synonymies for many of the species described in this chapter can be found in Fensome (1983). The species from Cabo Espichel are illustrated as palynomorph counts in Table 1 Appendix III.

3.1.1 SPORES

3.1.1.1 Trilete

Calamospora tener (Leschik) de Jersey

Cibotiumspora jurienensis (Balme) Filatoff

Cicatricosisporites striatus Rouse

Cicatricosisporites sp.

Concavissimisporites variverrucatus (Couper) Brenner

Contignisporites cooksonii (Balme) Dettmann

Contignisporites sp.

Converrucosisporites exquisitus Singh

Cyathidites minor Couper

Deltoidospora hallii Miner

Dictytophyllidites harrisii Couper

Impardecispora apiverrucata (Couper) Venkatchala et.al.

Klukisporites foveolatus Pocock

Leptolepidites plurituberosus (Doring) Dorhofer

Leptolepidites proxigranulatus (Brenner) Dorhofer

Neoraistrickia sp.

Osmundacidites wellmanii Couper

Pilosisporites trichopapillosus (Theirgart) Delcourt and Sprumont; Doring

Polycingulatisporites reduncus (Bolkhovitina) Playford and Dettmann

Polycingulatisporites sp.

Reticulisporites semireticulatus (Burger) Norris

Retitriletes singhii Srivastava

Stereisporites antiquasporites (Wilson and Webster) Dettmann

Todisporites major Couper

Tuberositriletes montuosus Doring

Undulatisporites undulapolus Brenner

Genus: Calamospora Schopf, Wilson and Bentall 1944

Type species: Calamospora hartungiana Schopf et.al. 1944

Calamospora tener (Leschik) de Jersey 1962

Plate: 1 Figure: 1

Selected Synonymy

1955 Laevigatosporites tener Leschik, pl.13; pl.1, fig.20

1958 Calamospora mesozoica Couper, p.132; pl.15, figs.3,4

1960 Calamospora nathorstii Halle; Klaus, p.116-118; pl.28, fig.1

1962 Calamospora tener Leschik; de Jersey, p.3; pl.1, figs.9,10

1964 Calamospora tener Leschik; Madler, p.92

1975 Calamospora mesozoica Couper; Filatoff, p.56; pl.8, figs.11,12

1984 Calamospora tener Leschik; Suneby, p.93; pl.3, figs.5,6

Original Diagnosis: See Leschik 1955, p.13.

Description: Trilete spore with laesurae measuring 15 μm in length. Trilete mark may not always be distinct; a circular contact area of exinal thickening with scabrate sculpture is occasionally present. Exine is very thin (0.5 μm), psilate and frequently folded.

Dimensions: 30(36)45 μm (5 specimens measured)

Occurrence: 25 specimens encountered, most abundant in the upper half of the section.

Comments: De Jersey (1962) placed C.mesozoica in synonomy with C. tener. Lund (1977) considers C.tener senior to C. mesozoica.

Calamospora is a Paleozoic genus, in which in spores of probable calamarian affinity are placed (Schopf et.al. 1944). The Mesozoic spores are placed in the genus because they are comparable in every respect (Couper 1958).

C.mesozoica and similar, if not identical, forms have been reported throughout Western Europe, Russia, and Arctic and Western Canada. Stratigraphic range is from Upper Triassic to Lower Cretaceous.

Genus: Cibotiumspora Chang 1965

Type species: Cibotiumspora paradoxa Malyavkina 1949; emend. Chang 1965

Cibotiumspora jurienensis (Balme 1957) Filatoff 1975

Plate: 1 Figure: 2 and 3

Selected Synonymy

1949 Tripartina paradoxa Malyvakina, p.50; pl.17, fig.21

1957 Concavisporites jurienensis Balme, p.20-21; pl.2, figs.30,31

1959 Concavisporites sinuatus Couper; Krutzsch, p.122

1964 Concavisporites jurienensis Balme; Balme, pl.6, fig.2

1965 Cibotiumspora paradoxa Malyavkina; Chang, p.165

1966 Concavisporites jurienensis Balme; Burger, p.237; pl.4, fig.6

1975 Cibotiumspora jurienensis Balme; Filatoff, p.60, pl.10, figs.8-13

Description (comb.nov.): "Amb, sides concave, rarely straight to slighty convex, apices rounded to somewhat pointed. Trilete, laesurae sinuous, 1 μm wide, extend to spore margin, and may be bordered by strong arcuate folds (kyrtome). Exine 1-2 μm thick, scabrate to punctate.

Distal face with a straight fold across at least one, generally all, apices" (Filatoff 1975, p.61).

Description: Trilete spore with triangular amb, sides concave, occasionally straight or convex with rounded apices. The trilete laesurae is straight. The exine is usually 1 to 2 μm thick and covered with psilate to scabrate ornamentation. Folding occurs along all the apices to create a dark region, which may be caused by the thicking of the exine.

Dimensions: 20(30)40 μm (5 specimens measured)

Occurrence: 9 specimens encountered in samples of the upper 200 m of the section.

Comments: Spores originally placed in Tripartina (Malyavkina 1949) do not agree with Tripartina as emended by Potonie (1960), since Tripartina have radiating sculpture. Therefore, Chang (1965) placed these forms under Cibotiumspora (Filatoff 1975).

C.jurienensis is a widespread Jurassic and Cretaceous miospore.

Genus: Cicatricosisporites Potonie and Gelletich 1933

Type species: Cicatricosisporites dorogensis Potonie and Gelletich 1933

Cicatricosisporites striatus Rouse 1962

Plate: 1 Figure: 4

Selected Synonymy

1962 Cicatricosisporites striatus Rouse, p.197; pl.4, figs.1,2

1966 Cicatricosisporites striatus Rouse; Burger, p.244; pl.6, fig.2

Original Diagnosis: "Subtriangular trilete spores, with parallel ribbing on the spore wall. The distal ribs run in one direction and are continuous with the proximal ribs. The latter, however, are oriented in parallel between the angles of the trilete arm, indicating the change of direction as the ribs encircle the equator. Width of ribs ca. 4.5 microns. Thickness of spore wall ca. 3.5 microns. Size range 43-48 microns" (Rouse 1962, p.197).

Description: Trilete spore, triangular amb, with straight to slightly convex to concave sides and rounded apices.

Straight laesurae extends for 3/4 or more of the spore radius. Exine is 1-2 μm thick, smooth at contact areas. Mural series consisting of ten muri are 1.5 to 2.5 μm wide, lumina 1.0 to 2.5 μm wide, four adjacent muri and lumina total 9 to 12 μm in width.

Dimensions: 33(52)68 μm equatorial diameter (5 specimens measured)

Occurrence: 70 specimens encountered, randomly distributed throughout the section.

Comments: This species was recorded in the Lower Berriasian of the Eastern Netherlands (Burger 1966).

This species of Cicatricosisporites observed occasionally in Portlandian strata at Cabo Espichel.

Cicatricosisporites sp.

Plate: 1 Figure: 5

Description: Trilete spore with circular amb. Straight laesurae extends 3/4 the spore radius in length. Exine is 1-2.0 μm thick. Distal muri extends to the equator of the spore. Muri 3 μm wide, lumina 1-2 μm wide; 9-11 ribs visible on distal exine.

Dimensions: 40 μm (1 specimen measured)

Occurrence: 2 specimens encountered; observed in sample P85212 5/5 at 314.0 m in a subtidal calcareous shale.

Comments: This specimen resembles C.myrtellii (Burger) except that the species observed at Cabo Espichel lacks the transverse distal rib, which is so characteristic of C.myrtellii. Similarity also exists with C.annulatus (Archangelsky and Gamerro) except for the arrangement of the distal ribs on C.annulatus which curve towards the equator; on the specimen at Cabo Espichel the distal ribs are straight.

Rare in the Portugeuse material.

Genus: Concavissimisporites Delcourt and Sprumont 1955

Type species: Concavissimisporites verrucosus Delcourt and Sprumont 1955

Concavissimisporites variverrucatus (Couper) Brenner

Plate: 1 Figure: 6

Original Diagnosis: "Trilete, laesurae about 3/4 radius of

spore, a weakly developed margo present in some specimens; equatorial contour triangular, sides concave, distal surface convex, proximal rather flattened; both proximal and distal surfaces sculptured with rounded verrucae, varying from 1.5 to 4 μm across in different specimens and projecting up to 2 μm above general surface; exine 2.5 to 4 μm thick, not thickening at apices. Size range 48(55)68 μm in equatorial diameter" (Couper 1958, p.142).

Description: Trilete spore with triangular amb, sides concave, apices rounded. Laesurae is straight and extends 2/3 to 3/4 the radius of the spore in length. The exine (1-2 μm thick) is both proximally and distally covered with rounded elongated verrucate towards the apices 1-2 μm in height and 2-4 μm in diameter. Verrucae are evenly spaced, with a 1 μm space between the sculpture. Near the laesurae the ornamentation is finely scabrate.

Dimensions: 68-70 μm (2 specimens measured)

Occurrences: 4 specimens encountered, restricted to sample P85171 5/5 at 22.0 m in a calcareous shale (facies D).

Comments: This specimen is known to occur in Upper Jurassic and Lower Cretaceous strata throughout the world.

Genus: Contignisporites Dettmann 1963

Type species: Contignisporites glebulentus Dettmann 1963

Contignisporites cooksonii (Balme 1957) Dettmann 1963

Plate: 1 Figure: 7

Selected Synonymy

1957 Cicatricosisporites cooksonii Balme, p.19; pl.1, figs.23,24; pl.2, figs.25,26

1963 Contignisporites cooksonii (Balme) Dettmann p.75; pl.XV,figs.11-16

1975 Contignisporites cooksonii (Balme) Dettmann; Filatoff p.65; pl.12,fig.8

Description (comb.nov.): "Microspores trilete, symmetrical about one plane, biconvex; amb roundly triangular, sometimes elongated along one median. Exine one layered, 3-4 μm thick in polar regions (inclusive of sculpture), thicker equatorially; cingulum 4-7 μm wide, cavate in corroded specimens. Distal exine with bilaterally symmetrical, cicatricose sculpture; sculptural elevations include six to nine, parallel, rarely bifurcating, low (2-3 μm high), rounded muri which coalese with cingulum towards equator. Muri wider (3.5-4.5 μm) than intervening lumina (1.5-2.5

μm); four adjacent muri and lumina total 20-25 μm in width. Proximal exine shows radial symmetry; smooth about pole, and with one, low, tangentially oriented murus (3.5-4.5 μm in width) on each interradial area near margin of cingulum. Laesurae straight, extending to cingulum, and with thin lips c. 1 μm high " (Dettmann 1963, p.75).

Description: see Dettmann (1963, p.75).

Dimensions: 33(42)51 μm in diameter (3 specimens measured)

Occurrence: 5 specimens encountered, observed in samples P85169 4/5 and P85170 5/5 at 14 and 16 m respectively; both samples were collected from facies D of subtidal calcareous shale.

Comments: Dettmann's species C. cooksonii compares well with the species observed at Cabo Espichel. This species has a wideworld distribution in material from Oxfordian to Aptian.

Contignisporites sp.

Plate: 1 Figure: 8

Description: Trilete spore with convex triangular amb. Laesurae are straight to slightly sinuous extending 3/4 of

the spore radius in length. Exine is about 2 μm thick and thicker equatorially. Proximal exine is psilate, the distal exine is sculptured with broad muri.

Dimensions: 48 μm (2 specimens measured)

Occurrences: 2 specimens observed in sample P85177 5/5 from a delta front shale at 45.5 m.

Comments: Rare in Portugeuse material. These specimens resemble C.problematicus (Couper), described by Doring (1965, pl.10, figs.6-8) except these species lack the distal muri arrangement and verrucate about the pole. C.problematicus has a Middle Jurassic to Lower Cretaceous distribution in Western European strata. Doring described C.problematicus as being associated with Exesipollenites tumulus, this is also the case in this sample.

Genus: Converrucosisporites Potonie and Kremp 1954

Type species: Converrucosisporites triquetrus Potonie and Kremp 1954

Converrucosisporites exquisitus Singh 1971

Plate: 1 Figure: 9

Selected Synonymy

1971 Converrucosisporites exquisitus Singh, p.116; pl.16, figs.4,5

1979 Converrucosisporites exquisitus Singh; Habib, pl.3, fig.6

Original Diagnosis: "Trilete; laesurae about 2/3 of the spore radius; commissures inconspicuous simple slits; amb triangular; sides straight to slightly convex; apices broadly rounded; proximal and distal surfaces oramented by large, evenly distributed, and closely spaced verrucae of uniform size; verrucae hemispherical, 6 to 10 microns in diameter, 4 to 7 microns high, and spaced 1 to 4 microns apart; exine thick" (Singh 1971, p.116).

Description: Triangular amb with slightly convex sides and rounded apices. Exine is 2-3 μm thick and ornamented by large semi-circular verrucae; 4 to 8 μm in diameter, and 3 to 6 μm in height. The trilete laesurae extends about 1/2 the radius of the spore.

Dimensions: 68(72)74 μm (10 specimens measured)

Occurrence: 36 specimens encountered, randomly distributed throughout the section.

Comments: The specimens observed in the present study are identifiable as C.exquisitus because of the large, bulbous verrucae.

This species has been previously described by Singh (1971) as occurring in the Albian. Habib (1979) encountered C.exquisitus in the lowermost Cretaceous of Spain. This species was found in Portlandian strata at Cabo Espichel.

Genus: Cyathidites Couper 1953

Type species: Cyathidites australis Couper 1953

Cyathidites minor Couper 1953

Plate: 1 Figure: 10

Selected Synonymy

1953 Cyathidites minor Couper, p.28, fig.13

1959 Cyathidites minor Couper; Delcourt and Sprumont, p.33; pl.6,fig.26

1962 Cyathidites minor Couper; Pocock, p.43; pl.4, figs.57,58

1964 Cyathidites minor Couper; Singh, p.71; pl.8, fig.13

1966 Cyathidites minor Couper; Burger, p.237; pl.4, fig.1

1975 Cyathidites minor Couper; Filatoff, p.60; pl.10, fig.7

1977 Cyathidites minor Couper; Srivastava, p.130; pl.1, figs.6,7

1982 Cyathidites minor Couper; Norris, pl.1, fig.7

Original Diagnosis: "Trilete, laesurae long, reaching almost to equator, consisting of simple commissures, no definite margo; equatorial contour triangular, sides concave, apices rather rounded; both proximal and distal surfaces convex, the distal markedly so; exine smooth, from 1.5 to 2.5 μm thick" (Couper 1953, p.28).

Description: Trilete; laesurae simple, over 3/4 radius of spore, equatorial outline triangular with distal concave sides; apices broadly rounded, distal face slightly convex, exine psilate, 0.75 to 1.5 μm thick.

Dimensions: 28(32)38 μm (10 specimens measured)

Occurrence: 43 specimens encountered; randomly distributed throughout the section.

Comments: C.minor with a worldwide distribution is frequently reported from the Cretaceous; it is only occasionally found in Jurassic strata.

C.minor is distinguished from C.australis by being smaller in diameter; C.minor averages 32 μm, whereas C.australis (Couper 1953) on average is 52 μm in diameter.

Genus: Deltoidospora Miner 1935

Type species: Deltoidospora hallii Miner 1935

Deltoidospora hallii Miner 1935

Plate: 1 Figure: 11

Selected Synonymy

1935 Deltoidospora hallii Miner p.618; pl.24, fig.7

1956 Deltoidospora hallii Miner; Potonie, p.13; pl.1,fig.1 (type species)

Diagnosis: "Small unassigned deltoid or sub-deltoid spores of the type that is commonly found associated with many Mesozoic ferns; such as Gleichenites, Gleicheniopsis, Laccopteris and others" (Miner 1935, p.618)..

Description: Trilete spore with a triangular amb, convex sides and rounded apices. The trilete laesurae extends for 3/4 or more the spore radius. The psilate exine is thin and generally less than 1.0 µm in thickness.

Dimensions: 30(39)60 µm (45 grains measured)

Occurrence: over 100 specimens encountered, distributed

throughout the section.

Comments: Deltoidospora with straight to moderately convex sides is distinguished from Cyathidites which has concave sides.

D.hallii is abundant and widespread in Jurassic and Cretaceous sediments.

Genus: Dictytophyllidites Couper 1958

Type species: Dictytophyllidites harrisii Couper 1958

Dictytophyllidites harrisii Couper 1958

Plate: 1 Figure: 12

Selected Synonymy

1958 Dictytophyllidites harrisii Couper, p.140; pl.21, figs. 5,6

1975 Dictytophyllidites harrisii Couper; Filatoff, p.61-62; pl.11, figs.1-7

1981 Dictytophyllidites harrisii Couper; Srivastava, pl.5, fig.10

Original Diagnosis: "Trilete, laesurae long reaching to the equator, commissures clearly raised, bordered by a

margo; equatorial contour triangular, sides usually concave but some 20% of the specimens have a straight to convex sides; distal surface markedly convex, proximal surface is rather flattened but because of the clearly raised commissures it comes to a sharp point at the middle of the triradiate scar giving a very characteristic appearance in equatorial (side) view; exine smooth, usually 1 to 1.5 μm but occasionally 2 μm thick" (Couper 1958, p.140).

Description: Trilete spore with triangular amb, slightly concave to convex sides with rounded apices. The laesurae which almost extend to the equator, are simple and may contain a margo. The exine is psilate and 1.0 to 2.0 μm thick. The essential distinct feature of this species is the raised laesurae and an adjacent margo (2-4 μm wide) separated from the laesurae by a small canal; the margo may continue directly to the apices appearing as secondary folds of the exine at the apices.

Dimensions: 20(28)40 μm (4 specimens measured)

Occurrence: 11 specimens encountered; occurs in the upper 200 m of the section.

Comments: This species has a worldwide distribution in Jurassic and Lower Cretaceous strata.

Genus: Impardecispora Venkatachala, Kar and Raza 1968

Type species: Impardecispora apiverrucata (Couper 1958) Venkatchala et.al. 1968

Impardecispora apiverrucata (Couper 1958) Venkatachala et.al. 1968

Plate: 2 Figure: 1

Selected Synonymy

1958 Trilobosporites apiverrucatus Couper, p.142; pl.21, figs.11,12

1962 Trilobosporites apiverrucatus Couper; Groot and Groot, p.150; pl.4, figs.2,4

1965 Concavissimisporites apiverrucatus (Couper) Doring, p.33-34;pl.13, figs.3,4

1968 Impardecispora apiverrucata (Couper) Venkatachala et.al.,p.124; pl.1, figs.1,2

1971 Trilobosporites apiverrucatus Couper; Singh, p.142; pl.19,figs.7,8

1982 Impardecispora apiverrucata (Couper) Venkatchala et.al.; Burden, p.213; pl.6,figs.2,3

Original Diagnosis: " Trilete, laesurae comparatively short, from 2/3 to 3/4 of the spore, most specimens showing a margo; equatorial contour triangular, with concave sides, distal surface convex, proximal rather flattened; polar regions of proximal and distal surfaces usually sculptured with granules or verrucae (up to 2.5 μm) some specimens have only a scabrate sculpture in the polar regions; in region of the apices, sculpture is clearly verrucate, verrucae from 3 to 6 μm across; larger verrucae sometimes developed as a single row bordered and occasionally encroaching on the margo; exine around 2 μm but up to 3 μm at apices in some specimens " (Couper 1958, p.142).

Description: Triangular amb with concave sides and rounded apices. The simple trilete laesurae are 2/3 or greater than the spore radius in length. The exine is of uniform thickness (1-2 μm). The exine is covered with circular, to slightly ellipsoidal verrucate ornamentation, the elements being 2 μm in height and up to 6 μm across. These verrucae increase in size towards the apices so that a clear distinction can be made between the verrucae on the apices and those near the center of the spore. The polar regions surrounding the laesurae are finely to coarsely granulate.

Dimensions: 74 to 76 μm (12 specimens measured)

Occurrence: near 30 specimens encountered; randomly distributed throughout the section.

Comments: This species is widespread in Oxfordian to Albian strata. In the Portugeuse material they were rare.

Genus: Klukisporites Couper 1958

Type species: Klukisporites variegatus Couper 1958

Klukisporites foveolatus Pocock 1964

Plate: 2 Figure: 2

Selected Synonymy

1964 Klukisporites foveolatus Pocock, p.194; pl.7, figs.5,6

1971 Klukisporites foveolatus Pocock; Singh, p.95; pl.13, fig.8

1976 Klukisporites sp.II Scott, p.577; pl.3, figs.4-6

1982 Klukisporites foveolatus Pocock; Burden, p.255; figs.1,2

Original Diagnosis: "Commissures somewhat gaping simple slits extending almost to its equator; on the sexinal surface commissures flanked by raised lips which form flap-like projections above them about 2.0 μm high at the

proximal pole. Amb triangular, sides slightly convex, apical angles slightly rounded. Nexine thin (less than 0.5 μm), tightly appreased to sexine. Sexine 2.5 μm thick at proximal pole and also at equator; proximal sexine smooth, distal sexine foveolate; foveolae rounded polygonal to more or less circular in outline, 2.5-5.0 μm in diameter, spaced 2.0-6.0 μm apart; foveolae extend onto the equatorial margins of the proximal face as shallow depressions in the smooth sexine; they do not extend onto the proximal contact area. Colour, orange-yellow. Equatorial diameter 36 (40) 42 μm in length of commissures ± 15 μm" (Pocock 1964, p.194).

Description: Trilete spore with triangular amb. Laesurae almost extends to the equatorial region. Sides slightly convex and psilate, with apices slightly rounded. Proximal sexine smooth, distal sexine (lumina) foevalate (rounded polygonal to circular) to foevo-reticulate.

Dimensions: 34(40)48 μm (10 specimens measured)

Occurrence: over 40 specimens randomly distributed throughout the section.

Comments: Ischyosporites and Klukisporites have been used to describe spores of similar morphology, the only

difference being that Klukisporites has been used for forms without apical exinal thickenings, whereas Ischyosporites has been used for taxa with these features (Fensome 1983).

Klukisporites foveolatus is almost identical to K.pseudoreticulatus Couper (1958); K.foveolatus has smaller, rounder, more densely distributed lumina than K.pseudoreticulatus.

K.foveolatus has been previously reported from Lower Cretaceous strata; with the discovery of K.foveolatus in strata from Cabo Espichel, the range should be extended to include the Upper Jurassic (Portlandian).

Genus: Leptolepidites Couper 1953; emend. Norris 1968

Type species: Leptolepidites verrucatus Couper 1953

Leptolepidites plurituberosus (Doring 1964a) Dorhofer 1979 [nomen nudum]

Plate: 2 Figure: 3

Selected Synonymy

1964a Mattesisporites plurituberosus Doring, p.38-39; pl.2, figs.9,10

1975 Leptolepidites rotundus Tralau; Vigran and Thusu, pl.3,

fig.18

1978 Leptolepidites rotundus Tralau; Birkelund et.al., pl.6, fig.4

1979 Leptolepidites plurituberosus (Doring) Dorhofer, pl.1, figs.41-42 [nomen nudum]

Original Diagnosis: See Doring 1964a, p.38-39 (in German).

Description: Trilete; laesurae extends for 2/3 of the spore radius (although rarely observed), equatorial outline rounded triangular to circular. The distal exine is covered by large verrucae ornamentation; the verrucae elements are 3-12 μm in diameter and 4 μm high.

Dimensions: 30(55)59 μm (15 specimens measured)

Occurrence: near 40 grains randomly distributed throughout the section; apparently more concentrated in the top 150 m of the section.

Comments: L.plurituberous occurs in the Northern hemisphere in Middle Jurassic to Early Cretaceous strata. In the present study it was observed in Upper Portlandian sediments of Cabo Espichel.

Leptolepidites proxigranulatus (Brenner 1963) Dorhofer 1979

Plate: 2 Figure: 4 and 5

Selected Synonymy

1963 Converrucosisporites proxigranulatus Brenner, p.60; pl.15,figs.1,3

1977 Leptolepidites psarosus Norris; Dorhofer, p.28; pl.4, fig.6

1979 Leptolepidites proxigranulatus (Brenner) Dorhofer, p.110;pl.1, figs.33,39,40

1982 Leptolepidites proxigranulatus (Brenner) Dorhofer; Burden, pl.20,figs.11-14

1983 Leptolepidites proxigranulatus (Brenner) Dorhofer; Fensome, p.154; pl.4, fig.7

Original Diagnosis: "Trilete spore; laesurae simple, reaching the margin; outline in polar view triangular with convex sides.

Exine, excluding sculptural elements, 1 μm thick, ornamented on the distal side by large, more or less circular tubercles 3-12 μm across and 5 μm high. The tubercles are closely spaced, occasionally having polygonal outlines; proximal surface covered with densely spaced grana, 1 μm in diameter and becoming verrucate to finely tuberculate in a few specimens" (Brenner 1963, p.60)

Description: Trilete spore with rounded triangular to circular amb. The laesurae extend to 2/3 or more of the spore radius. The exine is ornamented by large, rounded verrucae 4 to 12 μm in diameter and 1.5 to 5 μm high.

Dimensions: 24(28)40 μm (10 specimens measured)

Occurrence: nearly 40 specimens randomly distributed throughout the section.

Comments: According to Fensome (1983) L.proxigranulatus and L.plurituberosus are differentiated by the spacing of their distal and equatorial sculptural elements. The elements of L.proxigranulatus are well spaced and their bases tend to be circular to subcircular in outline (Fensome 1983).

L.proxigranulatus tends to be smaller than L.plurituberosus, with respect to both overall dimension and size of ornamentation.

L.proxigranulatus has been encountered in deposits from Middle Jurassic to Lower Cretaceous of the Northern hemisphere.

Genus: Neoraistrickia Potonie 1956

Type species: Neoraistrickia truncata Cookson 1953

Neoraistrickia sp.

Plate: 2 Figure: 6

Description: Trilete spore with triangular to rounded amb, with convex sides and triangular to rounded apices. The straight laesurae; which is often inconspicuous, extends 3/4 of the spore radius: The entire exine (1 μm thick) is covered with long baculate ornamentation, reaching 2-3 μm in height, and 1-1.5 μm in width.

Dimensions: 55 to 70 μm in diameter (3 specimens measured)

Occurrence: Near 10 specimens encountered; randomly distributed throughout the section.

Comments: Wide range in size of specimens. Neoraistrickia is known to have a world wide distribution throughout the Upper Jurassic and Lower Cretaceous.

Genus: Osmundacidites Couper 1953

Type species: Osmundacidites wellmanii Couper 1953

Osmundacidites wellmanii Couper 1953

Plate: 2 Figure: 7

Selected synonymy

1953 Osmundacidites wellmanii Couper, p.20; pl.1, fig.5

1971 Osmundacidites wellmanii Couper; Singh, p.50; pl.4, fig.1

1975 Osmundacidites wellmanii Couper; Filatoff, p.58; pl.9, figs.2-5

1982 Osmundacidites wellmanii Couper; Norris, pl.1, fig.17

1983 Osmundacidites wellmanii Couper; Fensome, p.323; pl.11, figs.4,9,10

Original Diagnosis: "Trilete, laesurae long (at least 3/4 radius); equatorial contour circular but frequently folded; exine around 1 μm thick, with granular-papillate sculpture, projections up to 1.5 μm above general surface" (Couper 1953, p.20).

Description: Spherical trilete miospore often distorted and folded. Exine is thin (0.5 to 1.0 μm thick); covered with irregular spiny granlate ornamentation. Laesurae are straight, length greater than 3/4 spore radius.

Dimensions: 25(40)70 μm (10 specimens measured)

Occurrence: near 30 specimens observed in the section.

Comments: This species is common throughout Jurassic and Cretaceous strata; worldwide distribution.

Genus: Pilosisporites Delcourt and Sprumont 1955

Type species: Pilosisporites trichopapillosus (Thiergart 1949) Delcourt and Sprumont 1955; emend. Doring 1965

Pilosisporites trichopapillosus (Theirgart 1949) Delcourt and Sprumont 1955; emend. Doring 1965

Plate: 2 Figure: 8

Selected Synonymy

1949 Sporites trichopapillosus Theirgart, p.23; pl.4, fig.18

1955 Pilosisporites trichopapillosus (Thiergart) Delcourt and Sprumont, p.34; pl.3, fig.3.

1965 Pilosisporites trichopapillosus (Theirgart) Delcourt and Sprumont; Doring, p.36-37; pl.14, figs.1-3

1986 Pilosisporites trichopapillosus (Theirgart) Delcourt and Sprumont; Ricketts and Sweet, p.21; pl.2, figs.12,13

Emended Diagnosis: "Azonotrilete microspores, amb convexly or concavely triangular with a sculpture of fine, slender spinae or bacula; greatest width of spinae never more than 1/3 of their length (individual elements never joined, neither forming a zona)" (Doring 1965, p.36); English translation from Jansonius and Hills (1986).

Description: See Doring 1965, p.36.

Dimensions: 48(56)72 μm (6 specimens measured)

Occurrence: 15 specimens randomly distributed throughout the section.

Comments: Ricketts and Sweet (1986) have described species with shorter and sparsely distributed spines as co-specific with those having longer and widely distributed spines. Commonly observed in Lower Cretaceous strata; rare records from the Upper Jurassic (Brenner 1963; Doring 1965).

Genus: Polycingulatisporites Simoncsics and Kedves 1961

Type species: Polycingulatisporites circulus Simoncsics and Kedves 1961

Polycingulatisporites reduncus (Bolkhovitina 1956) Playford and Dettmann 1965

Plate: 2 Figure: 9

Selected Synonymy

1953 Chomotriletes reduncus Bolkhovintina, p.35; pl.3, figs.23,24

1964 Taurocusporites reduncus Bolkhovintina; Singh, p.86; pl.11, fig.6

1965 Polycingulatisporites reduncus (Bolkhovintina) Playford and Dettmann, p.144

1971 Polycingulatisporites reduncus (Bolkhovintina) Singh, p.132-133; pl.18, fig.8

1974 Polycingulatisporites reduncus (Bolkhovintina) McIntyre, pl.14, figs.19, 20

1983 Polycingulatisporites reduncus (Bolkhovintina) Fensome, p.120-121; pl.2, fig.12

Original Diagnosis: See Bolkhovintina 1953, p.35 (in Russian). For a description in English see Singh 1964, p.86.

Description: Trilete spore with triangular to subcircular amb. The simple laesurae typically extend to the equator.

The psilate exine is 1 μm thick at the distal pole and near 4 μm thick at the equatorial boundary. The exine appears to consist of three separate concentric bands. The distal pole appears to be lacking exinal thickening.

Dimensions: 28(30)34 μm (8 specimens measured)

Occurrence: 11 specimens randomly distributed throughout the section.

Comments: This species has been recorded in Middle Jurassic to Paleocene strata.

Polycingulatisporites sp.

Plate: 2 Figure: 10

Description: Trilete spore possessing a circular to sub-circular amb with a thickened equatorial band (cingulum). Laesurae are straight extending 2/3 the radius of the spore, and bordered by a margo 1.5-2.0 μm in width. Proximally the exine is psilate; ornamented distally with indeterminite sculpture.

Dimensions: 28-30 μm (2 specimens measured)

Occurrences: Rare; only 2 specimens observed in sample P85058 5/5 at 83.1 m in a subtidal calcareous shale.

Comments: Resembles P.striatus (Filatoff), except this species is slightly larger and lacks the radial striations, which makes P.striatus distinct.

Genus: Reticulisporites Potonie and Kremp 1955

Type species: Reticulisporites parvogranulatus Weyland and Krieger 1953

Reticulisporites semireticulatus (Burger 1966) emend. Norris 1969

Plate: 2 Figure: 11

Selected Synonymy

1966 Lycopodiumsporites semireticulatus Burger, p.247; pl.4, fig.4

1969 Reticulisporites semireticulatus (Burger) Norris, p.589; pl.105, fig.4,5

1982 Reticulisporites semireticulatus (Burger) Norris; Burden, p.253; pl.16, figs.36-40

Original Diagnosis: "Trilete, amb triangular with concave

sides and rounded corners. Trilete mark raised and reaching to the equator. Exine at proximal face minutely rugulate, at distal face ornamented with muri, serpentining and sometimes bifurcating, showing a kind of imperfect reticulum. Muri are 0.8 µm wide and 1-1.5 µm high, the lumina, not closed, may show diameters of around 2 µm" (Burger 1966, p.248).

Description: See Burger (1966, p.248)

Dimensions: 20-22 µm (2 specimens measured)

Occurrence: Rare; only 2 specimens encountered. Restricted to sample P85171 5/5 collected from a subtidal calcareous shale at 22.0 m.

Comments: Although rare in Portugeuse material, this species is known to occur in Upper Jurassic to Lower Cretaceous strata of the Northern hemisphere.

Genus: Retitriletes Pierce 1961

Type species: Retitriletes globosus Pierce 1961

Retitriletes singhii Srivastava 1972

Plate: 2 Figure: 12

Selected Synonymy

1964 Lycopodiumsporites marginatus Singh, p.41; pl.1, figs.7-10

1971 Lycopodiumsporites marginatus Singh; Playford, pl.103, fig.13

1972 Retitriletes singhii Srivastava, p.32; pl.27, fig.10

1980 Lycopodiumsporites marginatus Singh; McIntyre and Brideaux, p.10; pl.1, figs.8,9

1982 Lycopodiumsporites marginatus Singh; Norris, pl.2, figs.6,7

1983 Retitriletes singhii Srivastava; Fensome, p.195-198; pl.6,figs.13,14

Original Diagnosis: "Miçrospores trilete; amb triangular, sides convex, angles rounded; laesurae length longer than 3/4 spore-radius, enclosed within 3 μm wide, elevated lips; exine on proximal face smooth with a few irregular ridges; distal surface convex, reticulate, very large polygonal meshes ranging from 9 to 14 μm in diameter; muri $\pm$ 1 μm wide, raised into membraneous network about 10 μm high, thickened and rod-like at intersections" (Srivastava 1972, p.72).

Description: Trilete spore with a semi-rounded to rounded triangular amb. The laesurae are straight, about 3/4 or

more of the spore radius in length. The reticulate exine is thin, generally less than 1.0 μm thick. The muri of the reticulum contain membranes which are 1 μm thick, and 8 to 12 μm in height. The mesh network (lumina) are polygonal in shape and at the base range from 5 to 10 μm in diameter.

Dimensions: 40(50)60 μm (5 specimens measured)

Occurrence: 11 specimens encountered; distributed throughout the section with apparently greater abundance near the upper part of the section.

Comments: Previously, R.singhii has been recorded from Lower Cretaceous strata. Here, R.singhii occurs sporadically throughout the section.

Genus: Stereisporites Pflug in Thomson and Pflug 1953

Type species: Stereisporites stereoides (Potonie and Venitz 1934) Pflug

Stereisporites antiquasporites (Wilson and Webster 1946) Dettmann 1963

Plate: 2 Figure: 13

Selected Synonymy

1946 Sphagnum antiquasporites Wilson and Webster, p.273; fig.2

1958 Sphagnumsporites psilatus Ross; Couper, p.131; pl.15, figs.1,2

1963 Stereisporites antiquasporites (Wilson and Webster) Dettman, p.25; pl.2, figs.20,21

1964 Sphagnumsporites antiquasporites (Wilson and Webster) Dettmann; Singh, p.38; pl.1, fig.1

1971 Stereisporites antiquasporites (Wilson and Webster) Dettmann; Singh, p.33-34, pl.1, figs.4,5

1976 Stereisporites antiquasporites (Wilson and Webster) Dettmann; Saad and Ghazaly, p.418, pl.2, fig.8

1978 Stereisporites antiquasporites (Wilson and Webster) Dettmann; Wilson, p.108-109, pl.1, figs.7-11

1983 Stereisporites antiquasporites (Wilson and Webster) Dettmann; Fensome,p.88-95; pl.1, figs.1-20

Description (comb.nov.): "Microspores trilete, biconvex; amb subcircular to subtriangular with convex sides and broadly rounded angles. Laesurae straight, simple, length 1/2-3/4 spore radius. Exine smooth, 1-2 μm thick; with slight thickenings in the radial regions at the equator and a low, distal polar thickening which is circular in outline and 6-8 μm in diameter" (Dettmann 1963, p.25).

Discription: Trilete, laesurae commonly simple and comparitively short; about 2/3 to 3/4 of the spore radius. Equatorial outline rounded triangular with strongly convex sides, rounded apices. Exine is smooth, 1.5 μm thick.

Dimensions: 20(28)35 μm (25 specimens measured)

Occurrence: near 50 specimens randomly distributed throughout the section.

Comments: Jurassic and Cretaceous specimens of S.antiquasporites have a diverse variation in their morphology as observed in the material from Fensome (1983, pl.1). Such variation includes forms both with and without a distal polar thickening, and the difference in the shapes of the trilete marks.

S.antiquasporites has been reported from Jurassic to Tertiary strata. It is widespread in various parts of the world, including the Portlandian of Cabo Espichel.

Genus: Todisporites Couper 1958

Type species: Todisporites major Couper 1958

Todisporites major Couper 1958

Plate: 3 Figure: 1

Selected Synonymy

1958 Todisporites major Couper, p.134; pl.16, figs.6-8

1958 Cyclinasporites minutus Nilsson, p.42; pl.2, fig.14

1962 Todisporites major Couper; Groot and Groot, p.143; pl.1,fig.1

1964 Todisporites major Couper; Singh, p.45-46; pl.1, fig.22

1975 Todisporites major Couper; Filatoff, p.57; pl.9, fig.1

1979 Punctatisporites major Couper; Dorhofer, pl.1,fig.15

1983 Todisporites major Couper; Fensome, p.328-332, pl.11, figs.5,7

1984 Todisporites minor Couper; Suneby, p.138, pl.3, fig.14

1984 Todisporites major Couper; Suneby, p.138, pl.3, fig.15

Original Diagnosis: "Trilete, laesurae distinct, long (ratio length laesurae to radius of spore = 0.72 to 0.88, mainly 0.83); equatorial contour circular but frequently folded; exine 1 to 1.5 μm thick and unsculptured" (Couper 1958, p.134).

Description: Trilete spore with equatorial outline, laesurae usually 2/3 or more the radius of spore in length. Exine thin, less than 2 μm thick, psilate.

Dimensions: 48(52)54 μm (10 specimens measured)

Occurrence: 13 specimens randomly distributed throughout the section.

Comments: Couper (1958) found a bimodal size distribution within his specimens of Todisporites and concluded there was two species T.major and T.minor. Couper placed all specimens less than 52 μm in diameter in T.minor, whereas all those larger than 52 μm in diameter were T.major.

Many subsequent authors have had a tendency to use both species; however, differentiation of the Portugeuse material was difficult. Statistical measurements of the Portugeuse material shows a peak at 52 μm. Therefore, based upon Couper's (1958) original descriptions of the genus Todisporites, it makes it difficult to place the Portugeuse specimens in one or the other species. Within this paper the author will use T.major, the type species for this genus.

T.major is a widespread species in Jurassic and Cretaceous strata, and occurs sporadically throughout the Cabo Espichel.

Genus: Tuberositriletes Doring 1964b

Type species: Tuberositriletes montuosus Doring 1964b

Tuberositriletes montuosus Doring 1964b

Plate: 3 Figure: 2

Selected Synonymy

1958 Concavisporites variverrucatus Couper, p.142; pl.22, fig.5

1964b Tuberositriletes montuosus Doring, p.1104; pl.4, figs.4-6

1964b Tuberositriletes major Doring, p.1104, pl.5, figs.1,2

1971 Trilobosporites sphaerulentus Paden Phillips and Felix, p.326; pl.8, figs.4,5

1973 Trilobosporites apiverrucatus Couper; Reyre, pl.11, fig.2

1977 Tuberositriletes grossetuberculatus Bolkhovitina; Dorhofer,p.27-28; pl.4, figs.4,7

1983 Concavissimisporites montuosus Doring; Fensome, p.280; pl.8, fig.3,12; pl.9, fig.3,10; pl.10, fig.4

Original Diagnosis: "Azonotrilete microspores with triangular amb; angles well rounded; sides slightly concave to straight, rarely convex; proximal and distal surfaces graulate, tuberose or verrucate; Y mark distinct" (Doring 1964b, p.1104) (translation from german by Jansonius and Hills 1986).

Description: Triangular amb with slightly concave to convex sides and rounded apices. The simple trilete laesurae are 2/3 or greater than the spore radius in length. The exine is 1 to 2 μm thick and covered by verrucae ornamentation 3 to 4 μm in diameter, 2 to 3 μm in height, and circular to slightly ellipsoidal in plan view. These verrucae are stretched towards some apices to give them an ellipsoidal geometry.

Dimensions: 70 μm (3 specimens measured)

Occurrence: 18 specimens encountered; randomly distributed throughout the section, however material is more concentrated towards the upper portion of the section.

Comments: Doring's (1964b) descriptions of T.major and T.montuosus are so similar that it makes it difficult to differentiate between them. Trilobosporites sphaerulentus is essentially identical to T.montuosus in both size and appearrance.

All previous literature on T.montuosus and its synonyms have been from the Neocomian. However, Fensome (1983) did find specimens in the Upper Jurassic Husky Formation of the Mackenzie Basin, N.W.T. Canada.

Genus: Undulatisporites Pflug in Thomson and Pflug 1953

Type species: Undulatisporites microcutis Pflug in Thomson and Pflug 1953

Undulatisporites undulapolus Brenner 1963

Plate: 3 Figure: 3

Selected Synonymy

1962 Undulatisporites sinuosus Groot and Groot, p.154; pl.6, fig.3

1963 Undulatisporites undulapolus Brenner, p.72; pl.24, fig.1

1971 Undulatisporites undulapolus Brenner; Singh, p.148-149; pl.20, figs.11,12

1979 Undulatisporites undulapolus Brenner; Dorhofer, pl.1, fig.7

1983 Undulatisporites undulapolus Brenner; Fensome, p.444; pl.16,fig.2

Original Diagnosis: "Trilete spore; laesurae reaching the margin, commissure bordered by a narrow lip 1.5 μm wide; outline in polar view triangular with straight to slightly convex sides. The laesurae are strongly undulate for about

1/3 the radius from the proximal pole; exine smooth, 1.5-2 μm thick" (Brenner 1963, p.72).

Description: Trilete spore with triangular amb, moderately concave to convex sides and rounded apices. The laesurae are usually strongly sinuous and reach the equator. Exine is psilate (1.0-2.0 μm thick).

Dimensions: 21(26)33 μm in diameter (4 specimens measured)

Occurrence: 11 specimens randomly distributed through the upper 200 m of the section.

Comments: U.undulapolus occurs in Upper Jurassic through Lower Cretaceous strata of North America and Europe.

3.1.1.2 Monolete

Laevigatosporites haardtii (Potonie and Venitz) Thomas and Pflug

Genus: Laevigatosporites Ibrahim 1933

Type species: Laevigatosporites vulgaris Ibrahim 1933

Laevigatosporites haardtii (Potonie and Venitz) Thomas and Pflug

Plate: 3 Figure: 4

Selected Synonymy

1934 Sporites haardtii Potonie and Venitz p.13; pl.1, fig.13

1946 Laevigatosporites ovatus Wilson and Webster, p.273; fig.5

1953 Laevigatosporites haardtii (Potonie and Venitz) Thomas and Pflug, p.59; pl.3, figs.27-38

1962 Laevigatosporites ovatus Wilson and Webster; Pocock, p.58;pl.8, figs.130-133

1964 Laevigatosporites ovatus Wilson and Webster; Singh p.99; pl.13, fig. 1-3

1969 Laevigatosporites gracilis Wilson and Webster; Norton and Hall, p.19; pl.2, fig.12

1978 Laevigatosporites haardtii (Potonie and Venitz) Thomas and Pflug; Wilson, p.117-118; pl.4, figs.7,8

1981 Laevigatosporites haardtii (Potonie and Venitz) Thomas and Pflug; Srivastava,pl.7,fig.4

Original Diagnosis: (Potonie and Venitz 1934, p.13 in German). See Wilson 1978, p.118 for English description.

Description: Kidney to bean shaped monolete spore; laesura is short (10 μm) approximately half the length, the laesura is frequently ruptured. The exine is psilate and about 1 μm thick.

Dimensions: Length 25-50 μm; Width 15-37 μm; Length:Width 1.3-1.7 (10 specimens measured)

Occurrence: 17 specimens randomly distributed throughout the section.

Comments: The author agrees with Wilson (1978) and Fensome (1983) that the species L.ovatus, L.gracilis, and L.haardtii are indistinguishable. According to Thomas and Pflug (1953) the definition of L.haardtii covers the size range from 20 to 70 μm, L.ovatus from 33-39 μm and L.gracilis from 27 to 30 μm. There is a complete size range in the observed in these samples that fits within the range of L.haardtii and covers the ranges of both the other species.

L.haardtii occurs in the Upper Jurassic and Cretaceous strata. According to Pocock (1962) it is an extremely common spore throughout the Lower Cretaceous.

3.1.1.3 Alete

Chomotriletes minor (Kedves) Pocock

Genus: Chomotriletes Naumova 1939,. emend. 1953; Stover 1962

Type species: Chomotriletes vedugensis Naumova 1939

Chomotriletes minor (Kedves 1961) Pocock 1970

Plate: 3 Figure: 5

Selected Synonymy

1961 Schizaeoisporites minor Kedves, p.129; pl.6 figs.11-16

1962 Chomotriletes fragilis Pocock, p.39; pl.2, figs.30-32

1970 Chomotriletes minor (Kedves) Pocock, p.61; pl.11, 14

1971 Chomotriletes fragilis Pocock; Herngreen, p.288; pl.2, fig.1

1977 Chomotriletes minor (Kedves) Pocock; Dorhofer, p.42; pl.8, fig.11;pl.15, fig.7

1982 Chomotriletes minor (Kedves) Pocock; Burden, pl.23, figs.1-3

Description (comb.nov.): "Alete; circular to subcircular in equatorial outline; exine single-layered, very thin (less

than 1 μm); ornamented with ridges spaced about 1 μm apart separated by furrows; on the proximal face the ridges are distributed in a band running obliquely across the spore and then folding back on themselves to form a type of sulcus which may possibly enclose a germinal opening; the ridges on the distal face are arranged in concentric circles parallel to the equatorial margin, individual ridges do not appear to br interrupted; spore colour pale yellow; equatorial diameter 23-27 microns" (Pocock 1970, p.61).

Description: Alete spore with thin exine 1 μm thick. Concentric canals running parallel to the equator appear as a finger imprint.

Dimensions: 28-29 μm in diameter (2 specimens measured)

Occurrence: 2 specimens restricted to samples P85188 5/5 and P85204 5/5 at 129 m and 152 m; both samples were collected from facies D of a subtidal calcareous shale.

Comments: A very rare spore in the Portlandian sediments of Portugal.

3.1.2 POLLEN

3.1.2.1 Monoporate Pollen

Corollina itunensis (Pocock) Cornet anf Traverse

Corollina simplex Rouse

Corollina torosus Reissinger

Exesipolienites scrabatus (Couper) Pocock

Exesipollenites tumulus Balme

Spheripollenites psilatus Couper

Genus: Corollina (Malyavkina 1949) Cornet and Traverse 1975

Type species: Corollina torosus Reissinger 1950

Corollina itunensis (Pocock 1962) Cornet and Traverse 1975

Plate: 3 Figure: 6

Selected Synonymy

1962 Classopollis itunensis Pocock, p.71-72; pl.11, figs.176-177;pl.12,fig.178

1970 Classopollis itunensis Pocock; Pocock, p.104

1975 Corollina itunensis Pocock; Cornet and Traverse;

p.18-19, pl.5, fig.1

Original Diagnosis: "Pollen grains, sub-circular to oval in polar outline, circular in equatorial section; monoporate with distal pore which is frequently covered by a circular plate "operculum" up to 25 microns in diameter, proximal pole frequently shows a weak trilete mark or, more rarely a weak area in the exine similar to that shown by [Classopollis classoides], scabrate, comprising a series of elongate pits radially arranged with respect to the spore surface; annular bands of exinal thickening surrounded the equator as in [Classopollis classoides], but the thickening is relatively much less than in that species, the exinal thickening averaging 3 to 5 microns; the "Rimula" is not as prominant as in [Classopollis classoides] making the division of the exoexine into proximal and distal hemispheres less obvious. The main difference between the species and[Classopollis classoides] is the larger size of the species; polar diameter 45 (47) 51 microns; equatorial diameter 36 (48) 65 mirons; Holotype 63 microns" (Pocock 1962, p.72).

Description: Spherical to discoidal pollen grain. The distal cryptopore (8-10 μm in diameter) is often covered by tectum, proximal pole often shows a trifid tetrad mark (10-20 μm long) which frequently extends to the equatorial

infrastriae, again covered by tectum. The exine is two layered, with scabrate ornamentation. Equatorial infratectal striate band 2.5 to 3 μm thick, 7 to 10 μm wide consists of 9 to 14 striae running parallel around the equator.

Dimensions: 43(51)64 μm (75 specimens measured)

Occurrence: over 100 specimens observed; restricted to carbonate facies of the subtidal environment. Most abundant in the upper half of the section.

Comments: Pocock (1962) described an abundance of C.itunensis in the Portlandian sediments of Western Canada, and mentioned that they do not appear to persist into the Lower Cretaceous.

In the Portugeuse material C.itunensis only occurs in the carbonate facies (A through D) and appears to be facies controlled.

It is similar to, but quite different from C.torosus being larger (twice the average size), less strongly ornamented, thinner exinal thickening around the equator, lighter in color (pale yellow) and possessing more infrastriae (9 to 14).

In the Portugeuse material C.itunensis occurs predominantly as solitary grains. There are relatively few

tetrads, though diads were encountered.

Although not described in the literature C.itunensis strongly resembles Classopollis major (Groot and Groot). Grains of C.major were observed in significant abundance (70% of total sample) in Lower Cretaceous strata of Portugal (Groot and Groot 1962). Another taxon, Classopollis multistriatus (Burger) has been defined as a separate species based simply upon its 10 to 15 infrastriae. Since C.itunensis often possess such abundant striae, the distinction is based on size; C.itunensis is much larger.

The size of the proximal trifid tetrad mark in C.itunensis extends to the equatorial boundaries, whereas in C.torosus the tetrad mark does not extend further than the boundaries of the distal cryptopore. This morphological observation has not been described in any literature to date and may prove useful in differentiating between species. Cornet and Traverse (1975) described C.itunensis in Lower Jurassic strata of the Northeastern U.S.A..

Corollina simplex (Danze-Corsin and Laevine 1963)
Cornet and Traverse

Plate: 3 Figure: 7 and 10

Selected Synonymy

1963 Classopollenites simplex Danze-Corsin and Laevine,

p.106; pl.11, figs.7,8

1969 Classopollis simplex (Danze-Corsin and Laevine) Reiser and Williams, p.16; pl.6, fig.15

1975 Corollina simplex (Danze-Corsin and Laevine) Cornet and Traverse, p.20; pl.6, fig.10

Diagnosis (comb.nov.): See Reiser and Williams (1969, p.16)

Description: Small spherical to subspherical monoporate pollen grain. The proximal trifid tetrad scar is triangular with concave sides 5-7 μm long. The thin circular distal cryptopore is 2-4 μm in diameter. The psilate exine is thin (1 μm thick) and has a columellate structure. Frequently, equatorial infrastriae (4-6 μm wide) consisting of 4-7 bands are distinct.

Dimensions: 14(17)22 μm (75 specimens measured)

Occurrence: over 900 specimens encountered, restricted to the siliciclastic facies E, F, G and J.

Comments: C.simplex is characterized by a smooth exine with a more or less continuous, massive structure (less ornamentation), narrower equatorial bands with less infrastriae and small size. These characteristics distinguish it from C.torosus. Brenner (1963) only

described faint suggestions of equatorial bands; whereas the Cabo Espichel species possess distinct bands. Brenner also considered that " the small size and smooth exine distinguishes this species from Classopollis classoides (Corollina torosus)". In contrast to C.torosus only a single tetrad of C.simplex was encountered.

According to the description by Herngreen (1971), C.minimus supposedly lacks equatorial striae. Ironically enough, close examination of Herngreen's plates of C.minimus reveal equatorial striae.

With the exception of the "lacking of infrastriae"; which apparently do exist, the descriptions of C.minimus and C.parvus are virtually the same. The use of C.parvus over C.minimus in the above description was based upon seniority of C.simplex.

Previously, C.simplex has been described in strata of Neocomian age from Eastern North America and Western Europe. C.simplex occurs in siliciclastic sediments, and appears to be facies controlled.

Corollina torosus (Reissinger 1950) emend. Cornet and Traverse 1975

Plate: 3 Figure: 8, 9 and 11

Selected Synonymy

1950 Pollenites torsus Reissinger, p.115; pl.14,fig.20

1953 Classopollis classoides Pflug, p.91; pl.16,figs.20-25, 29-37

1953 Classopollis declassis Pflug, p.92; pl.16,figs.16-19

1955 Classopollis classoides Pflug; Krutzsch, p.74; pl.2,fig.23

1958 Classopollis torosus (Reissinger) Couper, p.156-157; pl.28,figs.2-7

1961 Classopollis minor Pocock and Jansonius, p.444; pl.1, figs.21-25

1962 Classopollis torosus (Reissinger) Couper; Chaloner, p.19-20; pl.2,figs.1-2

1962 Classopollis classoides Pflug; Pocock, p.71; pl.11, figs,171-175

1963 Classopollis torosus (Reissinger) Brenner, p.84-85; pl.34,figs.4-6

1964 Classopollis classoides Pflug; Singh, p.125; pl.17, fig.2

1965 Classopollis torosus (Reissinger) Deak, p.35; pl.14, figs.7,9-17

1966 Classopollis torosus (Reissinger) Burger, p.264-265; pl.38,figs.1-5

1971 Classopollis classoides Pflug; Singh, p.176-177; pl.26, figs.5-7

1975 Corollina torosus (Reissinger) Cornet and Traverse, p.17;pl.5, figs. 2,9,14

1975 Classopollis classoides Pflug; Brideaux and McIntyre, pl.4;figs.25,26

1975 Classopollis classoides Pflug; Vigran and Thusu, pl.11, Figs.5,9,10,13,14

1976 Classopollis classoides Pflug; Saad and Ghazaly, p.446; pl.11,figs.11-4

1977 Corollina torosus (Reissinger) Bjaerke, pl.6, fig.31

1977 Corollina torosus (Reissinger) Bujak and Williams, p.326

1978 Classopollis classoides Pflug; Williams, pl.8, fig.8

1982 Classopollis torosus (Reissinger) Norris, pl.8, fig.6

1983 Classopollis classoides Pflug; Fensome, p.523-531; pl.20,figs.1-14,16,17,19,20

1984 Classopollis torosus (Reissinger) Suneby, pl.11, fig.5

Emended Diagnosis: "Isolated pollen grains or occurring as tetrads; spherical to ovoid, or acorn-shaped; diameter in equatorial view (100 grains): 18-41 μm (median 32 μm), 90% of grains between 24 and 37 μm (Couper, 1958, notes range 24-46 μm, mode 32 μm). Diameter in polar view 24-37 μm (diameter of subequatorial furrow 83-88% of overall diameter). Distal pseudopore variable in size, even for grains of same size: 4.3-8.5 μm in diameter, frequently distorted and widened in equatorial view. Proximal triangular area of thinning, which sometimes contains trilete mark, 6.8-13.6 μm high. Exine two layered; ektexine

divisible into outer tegillum, continuous over whole surface of grain, and inner structured layer, which is thickened in equatorial region to form a band or belt. Endexine variably distinct to indistinct, spherical frequently scabrate, occasionally with a small proximal trilete mark. Structure of equatorial band ranges from pseudoreticulate, to vaguely striate with aligned intrastructural columellae (pseudostriations), to distinctly striate, with columellae fused to form more or less parallel bands, the number of striations frequently varying from one part of band to another. Sometimes combinations of grains with all degrees of striation development occur in same tetrad. When striations are well developed, maximum number per grain ranges from 6 to 10. Width of equatorial band, which frequently ranges from 5 to 13 μm at its maximum, usually decreases in one area to 4-10 μm, and striations decrease in number to 4 or 5 through anastomosis or disintegration of more proximal striations into discrete intrastructural elements. Exine thickness varies with grain size, and presumably also with preservation; it is thickest in equatorial band: 1.3-2.4 μm (Couper 1958 records 3.0 μm), decreasing gradually toward the proximal pole: for example, 2.1 μm down to 0.9 μm; thickness on distal side of equatorial furrow (range 0.7-1.7 μm) generally slightly less than that proximal to equatorial band. Intrastructure of ektexine mostly pseudoreticulate, with positive elements

largest on proximal side of equatorial furrow, particularly if equatorial band is pseudoreticulate; pseudoreticulum on distal side of grain usually finer in pattern, occasionally becoming punctate. Sculpture of tegillum variable" (Cornet and Traverse 1975, p.18).

Description: Spherical to subspherical monoporate pollen grain (acorn-like shape); circular in equatorial section. The circular or subcircular distal cryptopore is 8 to 10 μm in diameter, the proximal trifid tetrad mark forms as a triangular opening with straight to concave sides 5-15 μm in length. Seven to nine annular bands of tectum thickening, may form a 3-4 μm thick equatorial infratectal striate band averaging 10 μm in width surrounding the equatorial region. This band of striations may have granulose or in some instances micro-reticulate ornamentation. The psilate or scabrate two layered exine consists of a homogeneous tectate layer, which is thicker on the equatorial band than on the cryptopore and tetrad mark; and a baculate layer which is not present over the cryptopore or the trifid mark. Tetrads are common.

Dimensions: 28(33)40 μm (250 grains measured)

Occurrence: Over 23,000 specimens distributed throughout the entire section.

Comments: From detailed examination of the Portugeuse material it can be observed that Corollina torosus closely resembles Classopollis alexi (Burger 1965), C.intrareticulatus (Volkheimer 1972), C.meyeriana (Klaus 1960), C.klausii (Boltenhagen 1973) and C.chateaunovi (Reyre 1969) that it makes it nearly impossible to distinguish them as separate species, especially based upon their morphology.

Some 45 species have been placed in the genus Corollina (Srivastava 1976). Many of these are difficult to differentiate because of the confusion generated from descriptions in the literature (Fensome 1983).

Statistical investigations of some 475 grains have allowed for the distinction between at least three species based upon grain diameter (Figure 3.1).

Corollina torosus range from 28 to 40 μm in diameter with a mean of 33 μm and consisting of 7-9 infrastriae; C.simplex and C.itunensis range from 14 to 22 μm with a mean of 17 μm, consisting of 4-7 infrasriae and from 43 to 64 μm with a mean of 51 μm, consisting of 9-14 infrastriae respectively.

Corollina torosus is an ubiquitous species in Rhaetic to Eocene strata, and is especially abundant within the Upper Jurassic; including the Portugeuse material. Worldwide distribution.

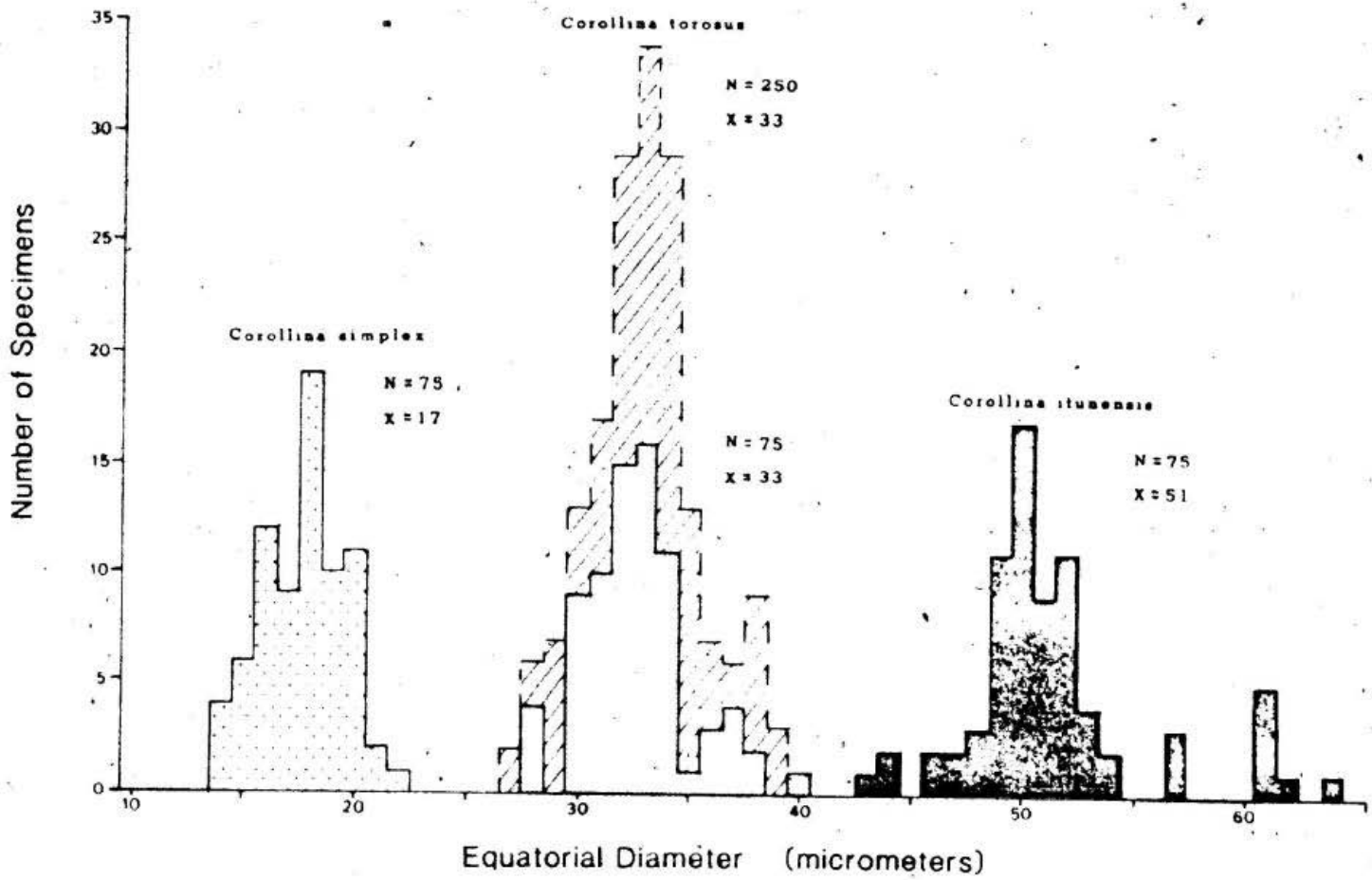


Figure 3.1 Size frequency histograms of Corollina species.

Genus: Exesipollenites Balme 1957

Type species: Exesipollenites tumulus Balme 1957

Exesipollenites scabratus (Couper 1958) Pocock 1970

Plate: 3 Figure: 12

Selected Synonymy

1958 Spheripollenites scabratus Couper, p.158;pl.31, figs.12-14

1962 Spheripollenites scabratus Couper, Pocock, p.74; pl.12, figs.188-189

1970 Exesipollenites scabratus (Couper) Pocock, p.101-102; pl.22,figs.11,12,14,15a-d

1975 Exesipollenites scabratus (Couper) Pocock; Filatoff, p.88; pl.27,figs.22,23(?), pl.28, fig.6

1975 Exesipollenites scabratus (Couper) Pocock; Vigran and Thusu, pl.11,fig.16

1979 Exesipollenites scabratus (Couper) Pocock; Dorhofer, pl.3, fig.45

Original Diagnosis: "Grains monoporate (?) (most specimens appear to have a weak area in the exine which tears readily, suggesting the presence of a poorly developed pore); grains originally spherical but fold readily; exine 1 to 1.5 micron

thick, sculpture scabrate, in optical section edge of grain appears smooth" (Couper 1958, p.158).

Description: Monoporate pollen grain; outline more or less circular in polar view. Exine is 1 to 1.5 μm thick with scabrate to microverrucate ornamentation. Tenuitas when visible is 2 to 8 μm in diameter. Occasionally the distal area lacks exinal thickening making the tenuitas indistinct.

Dimensions: 25(35)46 μm (100 specimens measured)

Occurrence: over 6,000 specimens distributed throughout the entire section.

Comments: E.scabratus ranges from Jurassic to Cretaceous (Albian).

Exesipollenites tumulus Balme 1957

Plate: 4 Figure: 1

Selected Synonymy

1957 Exesipollenites tumulus Balme, p.39; pl.11, figs.123-125

1964 Exesipollenites tumulus Balme; Singh, p.126-127; pl.17, figs.4,5

1969 Exesipollenites scabrosus Norris, p.600-601; pl.III, figs.20-22

1971 Exesipollenites tumulus Balme; Singh, p.178-179; pl.26,fig.11

1971 Exesipollenites tumulus Balme; Playford, pl.107, fig.15

1975 Exesipollenites tumulus Balme; Filatoff, p.88; pl.27, figs.22,23; pl.28, fig.6

1977 Exesipollenites tumulus Balme; Norris, pl.1, figs.24,25

1982 Exesipollenites tumulus Balme; Burden, pl.27, figs.9-12

Original Diagnosis: "Pollen grains with circular or oval amb; no tetrad scar visible; exine differentially thickened in a circular depression about 5 microns in diameter, in which the exine is much thinner than elsewhere; exine smooth or with occasional granules" (Balme 1957, p.39).

Description: Monoporate pollen grain; outline in polar view is more or less spherical to sub-triangular; exine is psilate to scabrate and 1 to 1.5 μm thick. The distal pole is marked by a darker exine in a circular area which is 1/2 or greater the diameter of the grain; containing in the center a circular area of exinal thinning about 5 μm in diameter (tenuitas). The center of the area contains a pore (1 to 2 μm in diameter).

Dimensions: 24(29)37 μm (100 specimens measured)

Occurrence: over 9,000 specimens distributed throughout the entire section.

Comments: Norris (1969) separated E.scabratus, from E.tumulus by its fine clearly defined infrastructure. Some Alberta specimens show a vestigal trilete mark (Singh 1971); trilete marks were not observed on the Portlandian fossils from Cabo Espichel.

The larger grains of this species show better defined tenuitas; this may represent a possible morphological development.

E.tumulus ranges from Jurassic to Cretaceous (Albian). It is very common in the material examined here.

Genus: Spheripollenites Couper 1958

Type species: Spheripollenites psilatus Couper 1958

Spheripollenites psilatus Couper 1958

Plate: 4 Figure: 2 and 3

Selected Synonymy

1958 Spheripollenites psilatus Couper, p.159; pl.31, figs.4-8

1965 Spheripollenites psilatus Couper; McGregor, pl.10,

fig.30

1965 Spheripollenites classopolloides Nilsson; Playford and Dettmann, p.74; pl.7, figs.62,63

1966 Spheripollenites psilatus Couper; Burger, p.263; pl.36, fig.4

1971 Spheripollenites psilatus Couper; Singh, p.179; pl.26, fig.12

1975 Spheripollenites classopolloides Nilsson; Vigran and Thusu,p.36; pl.11, figs.1,6,15

1976 Spheripollenites psilatus Couper; Saad and Ghazaly, p.448;pl.12, figs,6,7

1977 Spheripollenites psilatus Couper; Norris, pl.1, fig.23

1982 Spheripollenites psilatus Couper; Burden, pl.27, figs.13,14

1983 Globiporites psilatus Couper; Fensome, p.541-543; pl.17,figs.15,18; pl.22, fig.18

Original Diagnosis: "Grains monoporate (?); originally spherical but frequently folded in the fossil state; exine smooth, about 1.5 micron thick" (Couper 1958, p.159).

Description: Simple spherical pollen grain, exine thin 0.5 to 1 μm thick, psilate or it may be finely ornamented. A single circular tenuitas (approx. 10 μm in diameter), presumably distal, is frequently present but may be indistinct (weakened or absent).

Dimensions: 21(30)40 μm (100 grains measured)

Occurrence: over 4,600 specimens distributed throughout the entire section.

Comments: Exesipollenites possess a distinct exinal thickening about the tenuitas, which appears absent or indistinct in Spheripollenites. See Fensome (1983) for a detailed critique of morphologic variations in these genera.

Spheripollenites, Exesipollenites and Classopollis are often found in close association with one another, especially in the Portugeuse strata.

This taxon has a known stratigraphic range from Middle Jurassic to Cretaceous (Albian).

3.1.2.2 Bisaccate

Alisporites bilateralis Rouse

Piceapollenites sp.

Pityosporites constrictus Singh

Podocarpidites minisiculus Singh

Podocarpidites multesimus (Bolkhovitina) Pocock

Genus: Alisporites Daugherty 1941; emend.Potonie and Kremp 1956

Type species: Alisporites opii Daugherty 1941

Alisporites bilateralis Rouse 1959

Plate: 4 Figure: 4

Selected Synonymy

1959 Alisporites bilateralis Rouse, p.316; pl.1, figs.10,11

1962 Alisporites thomassi Couper; Pocock, p.62; pl.14, fig.143

1964 Alisporites thomassi Couper; Singh, p.109; pl.14, fig.11

1971 Alisporites bilateralis Rouse; Singh, p.169; pl.24, fig.9

1974 Alisporites sp. Rouse; Riley, pl.1, fig.3

1976 Alisporites bilateralis Rouse; Scott, p.592; pl.9, fig.5

1982 Alisporites bilateralis Rouse; Burden, pl.26, figs.5,6

Original Diagnosis: "Pollen grains bilaterally symmetrical, with two bladders diametrically opposed, united in the region of the proximal furrow, and with little or no constriction into two distinct bladder units. Marginal cap or crest relatively thin, consisting of two concentric or

linear flaps subtending the central furrow, and with well developed margins. Ornamentation of bladders coarsely reticulate in outer regions, grading into fine reticulate or weakly punctate in the area of the proximal furrow. Shape generally oblong, but varying toward circular or elliptical. Overall range of length 40-300 micron; of width 20-150 micron" (Rouse 1959, p.314).

Description: Bisaccate; shape elliptical in polar view; central body transversely elliptical, sacci are well developed and of the same size as the central body. Attached laterally, to give the whole grain an oval shape. Occasionally, a narrow parallel distal furrow is present. Exine is thin, finely reticulate.

Dimensions: Overall breadth 48(59)70 μm
Length of central body 34(42)50 μm
Breadth of central body 28(34)38 μm
Length of sacci 34(42)50 μm
Breadth of sacci 22(27)28 μm (40 specimens measured)

Occurrence: over 1000 specimens distributed throughout the entire section.

Comments: According to Singh (1971) the specimens

erroneously assigned to Alisporites thomassi (Couper) by Pocock (1962), Singh (1964) and McGregor (1965) actually belong to Alisporites bilateralis. There is obvious similarity between A.thomassi and A.bilateralis. A.bilateralis ranges from Late Jurassic to Cenomanian.

Genus: Piceapollenites Potonie 1931

Type species: Piceapollenites alatus Potonie 1931

Piceapollenites sp.

Plate: 4 Figure: 5

Description: Bisaccate pollen grain with sacci equivalent size or greater than that of the central body. Sacci are attached to the equator proximally and has a coarse infrareticulate ornamentation.

Dimensions: Overall breadth 120-140 μm

Length of central body 90-100 μm

Breadth of central body 80-85 μm

Length of sacci 80-90 μm

Breadth 50-60 μm (2 grains measured)

Occurrence: only 3 specimens all observed in sample P85170

5/5 at 16.0 m in a subtidal calcareous shale.

Comments: Rare in the Portugeuse material studied.

Genus: Pityosporites Seward 1914; emend. Manum 1960

Type species: Pityosporites antarcticus Seward 1914

Pityosporites constrictus Singh 1964

Plate: 4 Figure: 6

Selected Synonymy

1964 Pityosporites constrictus Singh, p.122; pl.16, figs.8,9

1971 Pityosporites constrictus Singh; Singh, p.167; pl.25, fig.10

1980 Pinuspollenites constrictus Singh; Wingate, p.40; pl.15,figs.6,7

1982 Pityosporites constrictus Singh; Burden, pl.26, figs.2,3

Original Diagnosis: "Bisaccate; bladders distally pendant, narrowing towards their roots and diverging; the roots reaching slightly beyond the equator; the space separating the two bladders on the distal side about 15 microns wide;

central body oval, broader than long; bladders finely granulate; exine uniformly thick" (Singh 1964, p.122).

Description: Bisaccate, with sacci more than hemispherical and equivalent dimensions or smaller than that of the central body. Overall the central body is oval. The bladders are reticulate with finely granulate body.

Dimensions: Overall breadth 68(76)82 μm
Length of central body 40(42)47 μm
Breadth of central body 45(52)54 μm
Length of sacci 34(38)40 μm
Breadth of sacci 22(28)30 μm (50 specimens measured)

Occurrence: near 800 specimens distributed throughout the entire section.

Comments: Subsequent encounters in Aptian to Maastrichtian strata from North America.

Genus: Podocarpidites Cookson 1947; emend.Couper 1953

Type species: Podocarpidites ellipticus Cookson 1947

Podocarpidites minisculus Singh 1964

Plate: 4 Figure: 7

Selected Synonymy

1964 Podocarpidites minisculus Singh, p.117; pl.15, fig.15, 16

1971 Podocarpidites minisculus Singh, Singh, p.165; pl.24, fig.1

1982 Podocarpidites minisculus Singh, Burden, p.313; pl.25, fig.15

Original Diagnosis: "Bisaccate; central body oval; length of central body more than the breadth; marginal crest present; bladders distally pendant, longer than the central body and very thin walled; proximal cap scabrate; bladders finely reticulate" (Singh 1964, p.117).

Description: Bisaccate pollen grain with sacci length greater than that of the oval central body. Sacci attached proximally to the equator. Bladders are thin with fine reticulate ornamentation.

Dimensions: Overall breadth 38(40)49 μm

Length of central body 26(40)43 μm

Breadth of central body 24(29)35 μm

Length of sacci 34(36)38 μm

Breadth of sacci 16(19)20 μm (6 specimens measured)

Occurrence: 15 specimens; randomly distributed throughout the section.

Comments: Previously observed by Singh (1964, 1971) and Burden (1982) in Lower Cretaceous strata of Western Canada. This taxon is relatively rare in the Portugeuse material.

Podocarpidites multesimus (Bolkhovitina 1956) Pocock 1962

Plate: 4 Figure: 8

Selected Synonymy

1956 Podocarpus multesimus Bolkhovitina, p.127; pl.24, fig.235

1962 Podocarpidites multesimus Bolkhovitina, Pocock, p.67; pls.10-11, figs.161-163

1971 Podocarpidites multesimus (Bolkhovitina) Pocock; Singh, p.166; pl.24, fig.2

1982 Podocarpidites multesimus (Bolkhovitina) Pocock; Burden, p.314; pl.25, fig.16

Diagnosis (comb.nov.): "Bisaccate; central body more or less circular; marginal crest appears to be crenulate in proximal view, but this is not always clear in distal view; ornamentation of central body not clear on Canadian specimens; proximal cap granulose; sacci large, extending well beyond the central body, attached to the distal side of the central body and pendant. The two sacci on any one grain are normally more or less the same, but they may vary slightly and deviant forms are found in which one saccus has become greatly enlarged, sometimes enveloping up to 3/4 of the central body; sacci reticulate, reticulation fine (1 micron to 2.5 microns between muri) with a tendency to radial distribution of sculpture" (Pocock 1962, p.67).

Description: Bisaccate pollen grain with sacci length greater than that of the circular central body. Bladders have fine reticulate ornamentation.

Dimensions: Overall breadth 60(70)80 μm
Length of central body 42(50)52 μm
Breadth of central body 36(43)50 μm
Length of sacci 40(51)60 μm
Breadth of sacci 26(36)38 μm (20 specimens measured)

Occurrence: Near 100 specimens distributed throughout the

section.

Comments: This species has a worldwide distribution in Upper Jurassic and Lower Cretaceous strata.

3.1.2.3 Monosulcate

Cerebropollenites macroverrucosus (Thiergart) Schulz
Cycadopites follicularis Wilson and Webster

Genus: Cerebropollenites Nilsson 1958
Type species: Cerebropollenites macroverrucosus Nilsson 1958

Cerebropollenites macroverrucosus (Thiergart 1949) Schulz 1967

Plate: 4 Figure: 9

Selected Synonymy

1949 Pollenites macroverrucosus Thiergart, p.17; pl.2, fig.19

1958 Tsugaepollenites mesozoicus Couper, p.155; pl.30, figs.8-10

1967 Cerebropollenites macroverrucosus (Thiergart) Schulz, p.603;pl.21, figs.4-6

1983 Cerebropollenites macroverrucosus (Thiergart) Schulz; Fensome, p.564;pl.21, figs.3,18,19; pl.22, figs.1,2

Emended Diagnosis: "42-82 microns; amb oval to circular, exine thickness obscured by heavy sculpture, probably 1 micron; on all sides covered with verrucose to loop-shaped or ribbon-like sinuous sculptural elements; exine on distal side with a sulcoid invagination, sulcus round to oval, 16-20 microns long" (Schulz 1967, p.603 in German) (English translation from Jansonius and Hills 1983).

Description: Pollen grain, monosulcate with equatorial outline circular to sub-circular. The sulcus is circular to elliptical in shape and usually much shorter than the overall length of the pollen grain. The exine of the distal surface is very thin and near psilate over a circular area, the proximal surface is saccate; but saccus is not as well developed as around the equator.

Dimensions: 30(46)70 μm (5 specimens measured)

Occurrence: over 30 specimens randomly distributed throughout the section.

Comments: The size and coarseness of ornamentation is diverse in this species.

This species is widespread in Jurassic and Cretaceous strata in many parts of the world.

Genus: Cycadopites Wodehouse 1933

Type species: Cycadopites follicularis Wilson and Webster 1946

Cycadopites follicularis Wilson and Webster 1946

Plate: 4 Figure: 10

Selected Synonymy

1946 Cycadopites follicularis Wilson and Webster, p.274;. fig.7

1975 Cycadopites follicularis Wilson and Webster; Filatoff, p.75;pl.21, figs.1-4

1983 Cycadopites follicularis Wilson and Webster; Fensome, p.551;pl.21, figs.4,6

Original Diagnosis: "Ellipsoidal; approximately twice as long as wide; length 39-42 microns; width 18-21 microns; furrow extending total length of grain, open at ends, usually closed in the middle by furrow edges overlapping in shrinkage; surface smooth, wall 1.5 microns thick, translucent" (Wilson and Webster 1946, p.274).

Description: Pollen grain, monosulcate with oval amb and rounded apices. The furrow extends for the entire length of the grain. The psilate to scabrate exine is 1 to 2 μm thick.

Dimensions: 18(35)52 μm in length

12(18)26 μm in width (10 specimens measured)

Occurrence: near 20 specimens randomly distributed throughout the section.

Comments: This species ranges in strata from the Carboniferious to the Cenozoic (Recent). Although this species is often quite abundant in Jurassic material, it was scarce in the Portugeuse material.

3.1.2.4 Perinous

Callialasporites dampieri (Balme) Sukh Dev
Callialasporites trilobatus (Balme) Sukh Dev
Callialasporites turbatus (Balme) Schulz
Perinopollenites elatoides Couper

Genus: Callialasporites Sukh Dev 1961

Type species: Callialasporites trilobatus Balme 1957

Callialasporites dampieri (Balme 1957) Sukh Dev 1961

Plate: 4 Figure: 11

Selected Synonymy

1957 Zonalapollenites dampieri Balme, p.32; pl.8, figs.88-90

1961 Callialasporites dampieri (Balme) Sukh Dev, p.48; pl.4, figs.26,27

1966 Applanopsis dampieri (Balme) Burger, p.255-256; pl.27, fig.2

1975 Callialasporites dampieri (Balme) Sukh Dev; Filatoff, p.84, pl.24, figs.6-11; pl.25,figs.1-8

1979 Applanopsis dampieri (Balme) Dorhofer, pl.3, figs.33,44

1980 Callialasporites dampieri (Balme) Sukh Dev; Burger, pl.17, figs.6,7

Diagnosis: "Monosaccate, amb circular to oval, bladder equatorially attached. Exine of central body thin, psilate to minutely granulate, often radially folded near the equator. Sometimes a vague trilete mark can be observed. Bladder psilate with an overall equal width of about 5 micron occasionally slightly constricted at the corners. In most cases the radial foldings continue on to the bladder, giving it a characteristical, undulating outline" (Burger

1966, p.255) (For original diagnosis see Balme 1957, p.32).

Description: Perinous pollen grain with subcircular to sub-triangular amb and proximally positioned non-functional trilete mark. The exine, typically folded, consists of an inner exine 0.5 to 1.5 μm thick and an outer exine is 1 to 3 μm thick; both layers of the exine are scabrate to granulate. A hollow zona exists about the margin of the equator. The inner exine forms a dark circular to rounded triangular corpus.

Dimensions: 42(58)76 μm overall diameter. Corpus diameter 24(45)56 μm (5 specimens measured).

Occurrence: 5 specimens restricted to sample P85206 5/5 at 209.9 m in a subtidal calcareous shale.

Comments: C.dampieri is common in Middle Jurassic to Lower Cretaceous material.

Callialasporites trilobatus (Balme 1957) Sukh Dev 1961

Plate: 5 Figure: 1

Selected Synonymy

1957 Zonalapollenites trilobatus Balme, p.32; pl.8,

figs. 91,92

1961 Callialasporites trilobatus (Balme) Sukh Dev, p.48; pl.4, figs.28-29

1966 Applanopsis trilobatus (Balme) Burger, p.261; pl.27, fig.1

1975 Callialasporites trilobatus (Balme) Sukh Dev; Filatoff, p.85; pl.25,figs.9,10

1979 Applanopsis trilobatus (Balme) Dorhofer, pl.3, fig.29

1983 Callialasporites trilobatus (Balme) Sukh Dev; Fensome, p.488-492, pl.19, figs.1,3,4,6,7,10

Original Diagnosis: "Equator ± circular to oval; body ± circular, subcircular to triangular; grain complex, body encircled by an equatorial bladder, which may be incomplete to appear 3 separate bladders or a position in between; bladders smaller and ± of same breadth unlike Alatisporites; Y-mark absent (or a very vestigal Y-fold present); exine over the body and bladders infra- to extra-granulate" (Balme 1957, p.33).

Description: Trilobate saccus with a distinct dark rounded triangular corpus having straight to convex sides. Corpus diameter nearly 3/4 the size of the body. A proximally positioned trilete mark may be developed. The inner exine is (0.5 to 1.5 μm) thick and the outer exine is (1 to 2 μm) thick; both layers have scabrate to finely granulate

ornamentation. Three separate psilate bladders are attached at the equator to produce a hollow zona with gaps at the apices. Bladders 10 to 15 μm wide, generally become smaller towards each corner.

Dimensions: Total diameter 48(60)76 μm. Corpus diameter 36(40)56 μm (10 specimens measured)

Occurrence: near 20 grains randomly distributed throughout the section.

Comments: This species has a global distribution in Upper Jurassic and Lower Cretaceous strata.

Callialasporites turbatus (Balme 1957) Schulz 1967

Plate: 5 Figure: 2

Selected Synonymy

1957 Inaperturopollenites turbatus Balme, p.31-32; pl.7, figs.85,86; pl.8, fig.87

1967 Callialasporites turbatus (Balme) Schulz, p.593; pl.17, figs.3,4

1975 Callialasporites turbatus (Balme) Schulz; Filatoff, p.84; pl.26,figs.5-9

1979 Callialasporites turbatus (Balme) Schulz; Dorhofer,

pl.3, fig.37

Original Diagnosis: See Balme 1957, p.31.

Description: Perinous pollen grain with a circular to subcircular amb. The inner exine is 0.5 to 1.5 μm thick, the outer exine is 1 to 2 μm thick, both exines being scabrate to granulate. The inner exine produces a circular corpus with a triangular outline.

Dimensions: 40(60)75 μm overall diameter. Corpus diameter 30(36)60 μm (4 specimens measured)

Occurrence: 4 specimens encountered, all specimens restricted to sample P85212 5/5 at 314.0 m in a subtidal calcareous shale.

Comments: Common in Lower Jurassic to Lower Cretaceous sediments.

Genus: Perinopollenites Couper 1958

Type species: Perinopollenites elatoides Couper 1958

Perinopollenites elatoides Couper 1958

Plate: 5 Figure: 3

Selected Synonymy

1958 Perinopollenites elatoides Couper, p.152; pl.27, figs.9-11

1962 Perinopollenites elatoides Couper; Pocock, p.60; pl.9, figs.136-137

1964 Perinopollenites elatoides Couper; Singh, p.107; pl.14, fig.9

1966 Perinopollenites elatoides Couper; Burger, p.264; pl.36,fig.2; pl.37, fig.1

1975 Perinopollenites elatoides Couper; Vigran and Thusu, pl.13,figs.11,16,17

1982 Perinopollenites elatoides Couper; Norris, pl.8, figs.4,5

1982 Perinopollenites elatoides Couper; Burden, pl.24, figs.21,22

1983 Perinopollenites elatoides Couper; Pensome, p.545-547; pl.17, figs.16,17

Original Diagnosis: "Monoporate, pore not always clearly shown; grains originally spherical but fold readily; exine consisting of two distinct layers; the outer is scabrate and very thin (less than 0.5 μm) loosely fitting and wrinkles and tears easily; the inner is around 0.75 to 1.0 μm thick, smooth to finely scabrate" (Couper 1958, p.152).

Description: Perinous pollen grain, with pore 2 μm in diameter, although pore is often invisible. Exine is two layered; the outer transparent layer is 0.5 μm thick and folds readily. The psilate to scabrate inner layer is 0.75 to 1.0 μm thick, and occurs as a central spherical body 20 to 25 μm in diameter.

Dimensions: Outer body, diameter approx. 55 μm; inner body diameter approx. 25 μm (10 specimens measured)

Occurrence: near 15 specimens randomly distributed throughout the section.

Comments: P.elatoides has been observed in Lower Jurassic to Lower Cretaceous strata.

3.1.2.5 Inaperturate Pollen

Araucariacites australis (Cookson) Couper
Taxiodiacepollenites hiatus Potonie

Genus: Araucariacites Cookson 1947; ex. Couper 1953
Type species: Araucariacites australis Cookson 1947

Araucariacites australis Cookson 1947; ex. Couper 1953

Plate: 5 Figure: 4

Selected Synonymy

1947 Granulonapites (Araucariacites) australis Cookson, p.130;pl.13, figs.1,2,3

1953 Araucariacites australis Cookson; ex. Couper, p.39 (designation as type species)

1963 Araucariacites australis Cookson; Dettmann, p.105-106; pl.26, fig.15

1964 Araucariacites australis Cookson; Singh, Srivastava and Roy, p.299; pl.8,fig.113

1966 Araucariacites australis Cookson; Burger, p.262; pl.35, fig.3

1971 Araucariacites australis Cookson; Singh, p.156, pl.22, fig.4

1974 Araucariacites australis Cookson; Riley, pl.2, fig.2

1975 Araucariacites australis Cookson; Filatoff, p.82; pl.23,figs.10-11

1980 Araucariacites australis Cookson; Burger, p.64, pl.17, fig.4

1983 Araucariacites australis Cookson; Fensóme, p.501, pl.19,figs.2,11

Emended Diagnosis: "No germinal aperture (inaperturate); grains originally spherical but frequently folded in the fossil state; exine about 0.5 to 0.75 μm thick, sub-granular sub-papillate or scabrate sculpture, rather variable" (Couper 1953, p.39).

Description: Spherical to subspherical inaperturate pollen. The two layered exine is 0.5 to 1.5 μm thick, frequently folded, and covered with granulate or scabrate ornamentation.

Dimensions: 44(60)90 μm in diameter (15 specimens measured)

Occurrence: near 20 specimens randomly distributed throughout the entire section.

Comments: A.australis has a range extending from middle Jurassic to Tertiary. Worldwide distribution.

Genus: Taxodiaceaepollenites Kremp 1949;
ex. Potonie 1958

Type species: Taxodiaceaepollenites hiatus Potonie 1931; ex. Potonie 1958

Taxodiaceaepollenites hiatus Potonie 1931; ex. Potonie 1958

Plate: 5 Figure: 5

Selected Synonymy

1931 Pollenites hiatus Potonie, p.5; fig.27

1953 Inaperturopollenites hiatus Potonie; Thomson and Pflug, p.65; pl.5, figs.14-20

1958 Taxodiaceaepollenites hiatus Potonie; ex. Potonie, p.78 (Designated as type species)

1962 Taxodium hiatipites Wodehouse; Rouse, p.201; pl.2, fig.4

1965 Taxodiaceaepollenites hiatus Potonie; Stanley, p.273; pl.38,figs.1-3

1971 Taxodiaceaepollenites hiatus Potonie; Singh, p.158; pl.22,fig.7

1977 Taxodiaceaepollenites hiatus Potonie; Norris, p.154

1985 Taxodiaceaepollenites hiatus Potonie; Davies, p.109

Diagnosis: "Equator circular; exine ± infrapunctate; exine has tendency to split open along a ± straight, radial line, resembling a beak; this constitutes an example of the value of preservational condition for the separation of sporomorphs" (Potonie 1958, p.78).

Description: Pollen grain with a thin exine (0.5 μm thick). The exine is scabrate and characteristically split, resembling that of an open mouth.

Dimensions: 25(28)31 μm in diameter (15 grains measured)

Occurrence: over 30 specimens randomly distributed throughout the section.

Comments: According to Singh (1971) this species is more common in Upper Cretaceous and Early Tertiary material. Recent literature from Norris (1977) and Davies (1985) indicate that this species is present in Middle and Upper Jurassic strata of Canada and Portugal.

3.1.3 MARINE MICROPLANKTON

3.1.3.1 Acritarchs

Micrhystridium fragile Deflandre

Genus: Micrhystridium Deflandre 1937; emend. Sarjeant

Cabo Espichel Palynomorph Counts

RANGE CHART OF NUMBER OF SPECIMENS BY LOWEST APPEARANCE

	Corollina torosus	Exesipollenites scabratus	Exesipollenites tumulus	Spheripollenites psilatus	Alisporites bilateralis	Pityosporites constrictus	Corollina simplex	Surculosphaeridium	Taxodiaceaepollenites hiatus	Micrhystridium	Cicatricosisporites striatus	Deltoidospora hallii	Klukisporites foveolatus	Podocarpidites multesimus	Cycadopites follicularis	Stereisporites antiquasporites	Podocarpidites ellipticus	Laevigatosporites haardti	Leptolepidites pityrugosus	Leptolepidites praegranulatus	Osmundacites wellmanii	Cyathidites minor	Cerebrospora mesozoica
332.0	676	56	44	....	....	....	....	....	....	....	1	....	....	....	....	....	....	....	....	....	....	1	1
318.6	1090	34	56	40	....	....	....	23	1	12	....	2	....	....	....	....	....	....	....	....	1	....	1
314.0	1200	115	121	....	2	....	....	20	....	9	1	2	....	....	....	....	....	2	....	....	....	....	....
297.0	4986	1119	1209	785	117	75	....	130	....	32	....	9	....	70	....	....	....	....	....	....	....	....	....
286.25	1100	124	78	33	90	7	....	....	2	....	2	9	1	....	....	....	1	....	1	4	5	2	....
229.0	1278	146	132	....	140	19	....	....	3	....	2	9	1	10	2	....	....	2	1	5	7	1	3
220.0	14	2	3	10	2	....	4	....	....	....	....	....	....	....	....	....	....	....	....	....	....	....	....
212.0	....	1	2	1	21	5	....	39	1	16	....	1	....	....	....	....	....	....	....	....	....	....	....
209.9	453	689	733	30	25	21	....	31	....	15	1	4	1	....	2	1	....	1	3	2	2	2	....
204.0	26	3	2	6	....	....	....	12	....	2	....	....	....	....	....	....	....	....	....	....	....	1	2
152.0	453	321	367	78	46	28	....	12	....	7	....	15	1	9	....	1	1	....	....	....	....	....	....
139.0	543	454	398	131	4	1	....	2	2	2	3	11	2	....	1	5	....	1	2	3	4	3	....
136.45	1486	1390	1214	229	58	26	....	17	....	5	1	2	1	4	....	4	2	....	1	1	1	1	....
130.75	487	212	876	54	4	2	9	....	....	....	2	1	....	....	....	1	....	1	1	2	....	....	....
129.0	578	355	212	53	11	4	....	3	....	1	2	4	3	....	1	2	....	1	3	1	5	1	....
127.0	354	278	290	32	18	5	....	20	....	4	....	2	1	....	....	1	....	....	....	....	....	1	....
123.0	6	2	1	15	4	....	12	....	....	....	....	....	....	....	....	....	....	....	....	....	....	....	....
118.9	58	23	12	39	2	1	2	2	....	....	3	....	....	....	....	....	....	....	....	....	....	....	....
117.0	60	23	21	23	6	....	23	3	....	1	3	1	2	....	....	1	....	....	....	....	....	....	....
114.2	90	11	21	40	24	4	141	....	1	2	5	3	....	3	1	1	....	2	....	1	1	2	....
106.0	108	41	21	32	9	....	142	....	2	....	3	5	....	....	....	1	....	....	....	....	....	....	....
97.0	101	12	21	40	3	....	5	....	....	....	4	6	....	....	....	....	....	....	....	....	....	....	....
90.3	198	35	42	99	5	3	21	....	1	....	2	7	1	....	....	2	....	3	....	1	1	1	....
87.8	165	65	45	71	4	13	35	....	1	....	4	3	1	....	....	2	....	2	....	1	2	1	....
83.1	953	256	563	66	20	5	30	....	....	....	....	3	1	....	....	....	....	....	2	....	....	2	....
76.0	160	198	187	344	14	2	97	....	....	....	3	5	....	....	....	....	....	....	....	....	....	....	....
68.3	137	325	201	141	....	....	11	2	....	....	2	10	....	....	....	3	....	....	2	....	....	1	....
64.1	....	....	....	32	32	27	....	....	....	....	....	....	....	....	....	....	....	....	....	....	1	....	....	....
63.0	....	....	7	2	2	....	....	....	....	....	....	2	....	....	....	....	....	....	....	....	....	3	....
49.5	2067	....	....	....	....	....	....	....	....	....	....	3	....	....	....	....	....	....	....	....	....	1	....
45.5	18	39	94	39	....	....	39	....	....	....	1	....	....	....	....	....	....	....	....	....	....	....	....
43.25	92	21	11	75	12	....	121	....	....	....	1	....	....	....	....	....	....	....	2	....	....	1	....
38.5	202	58	64	48	1	....	49	....	....	....	....	1	....	....	....	....	....	....	....	....	....	....	....
34.7	....	....	....	....	1	....	3	....	....	....	....	....	....	....	....	....	....	....	....	....	....	....	....
34.0	218	....	74	180	....	....	68	15	....	8	2	....	....	....	....	....	....	....	....	....	....	....	....
29.0	179	32	29	49	....	....	....	20	....	4	....	....	....	....	....	....	....	....	....	....	....	....	....
25.0	497	187	221	388	....	....	....	19	....	9	3	....	....	2	....	....	....	....	....	....	....	....	....
22.0	393	554	876	144	6	3	....	....	3	1	7	4	3	....	1	14	....	....	3	....	5	2	....
21.0	145	32	27	92	....	....	48	....	....	....	....	....	....	....	2	....	....	3	....	....	....	....	....	....
17.5	....	....	....	11	....	....	....	....	....	....	....	....	....	....	....	....	....	....	....	....	....	....	....
16.0	266	897	342	23	33	18	....	....	....	4	....	7	1	2	....	....	....	....	3	1	1	1	....
14.0	292	528	453	172	53	27	....	12	....	6	2	12	....	42	....	4	3	....	2	1	....	2	....
11.0	88	120	226	374	62	15	2	....	....	....	....	....	....	....	....	....	....	....	....	....	....	....	....
10.0	90	65	95	200	2	....	....	18	....	2	....	....	....	....	....	....	....	....	....	....	....	....	....
9.0	79	185	195	460	33	4	10	....	3	1	....	5	....	5	....	....	....	....	....	....	....	....	....
8.0	....	....	4	6	1	....	....	....	....	....	....	....	....	....	....	....	....	....	1	2	....	3	....
2.75	495	500	756	389	5	....	35	....	....	....	6	4	6	....	....	....	....	....	1	....	....	6	....
2.3	370	126	200	....	7	2	33	....	1	....	1	1	2	....	....	....	....	....	1	4	1	1	....
1.75	158	....	....	236	12	3	5	....	....	....	7	3	6	....	3	....	....	....	....	....	....	....	....
1.0	112	200	274	725	34	20	10	2	12	1	2	5	2	5	4	1	1	1	....	....	....	....	....

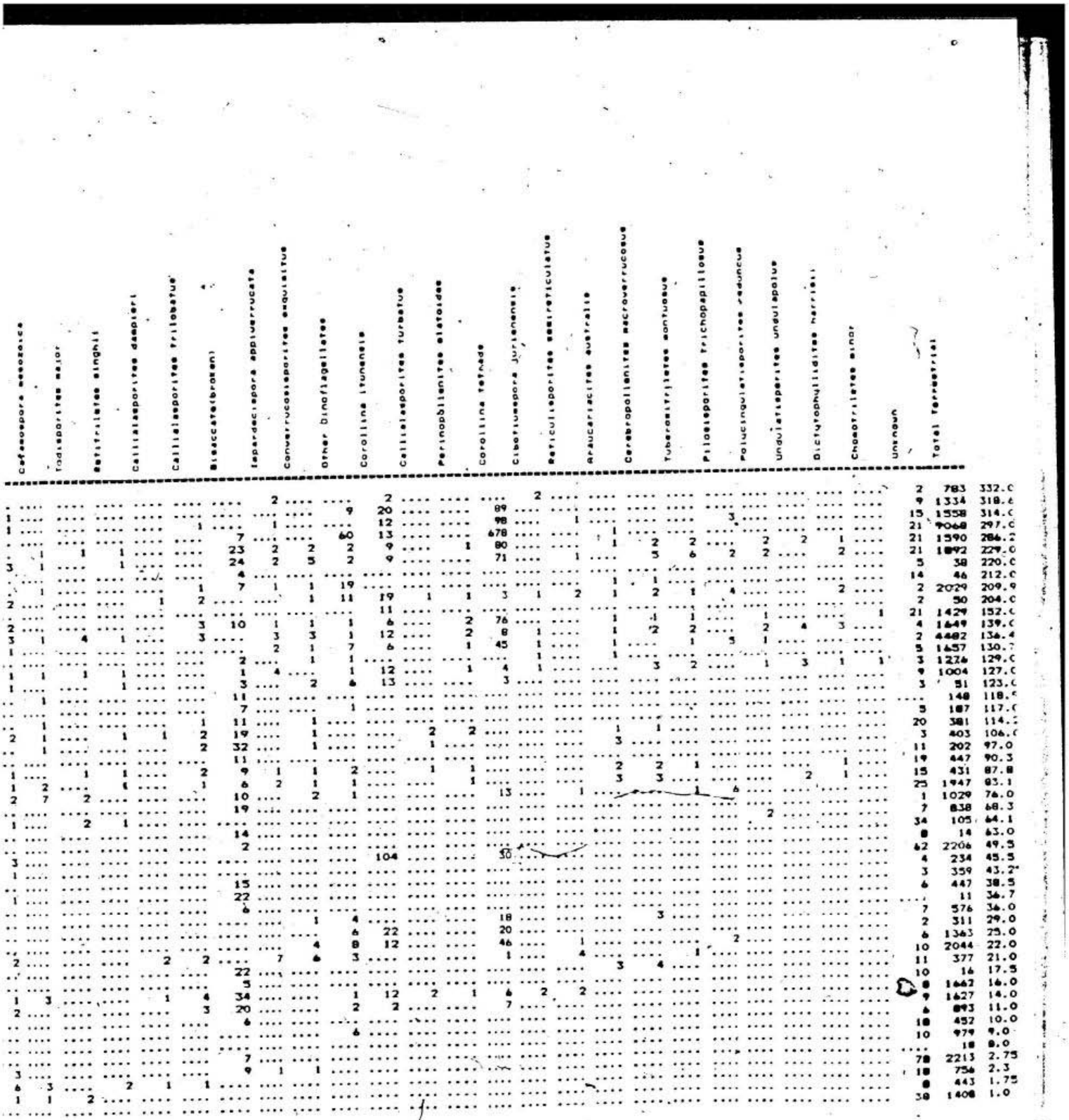
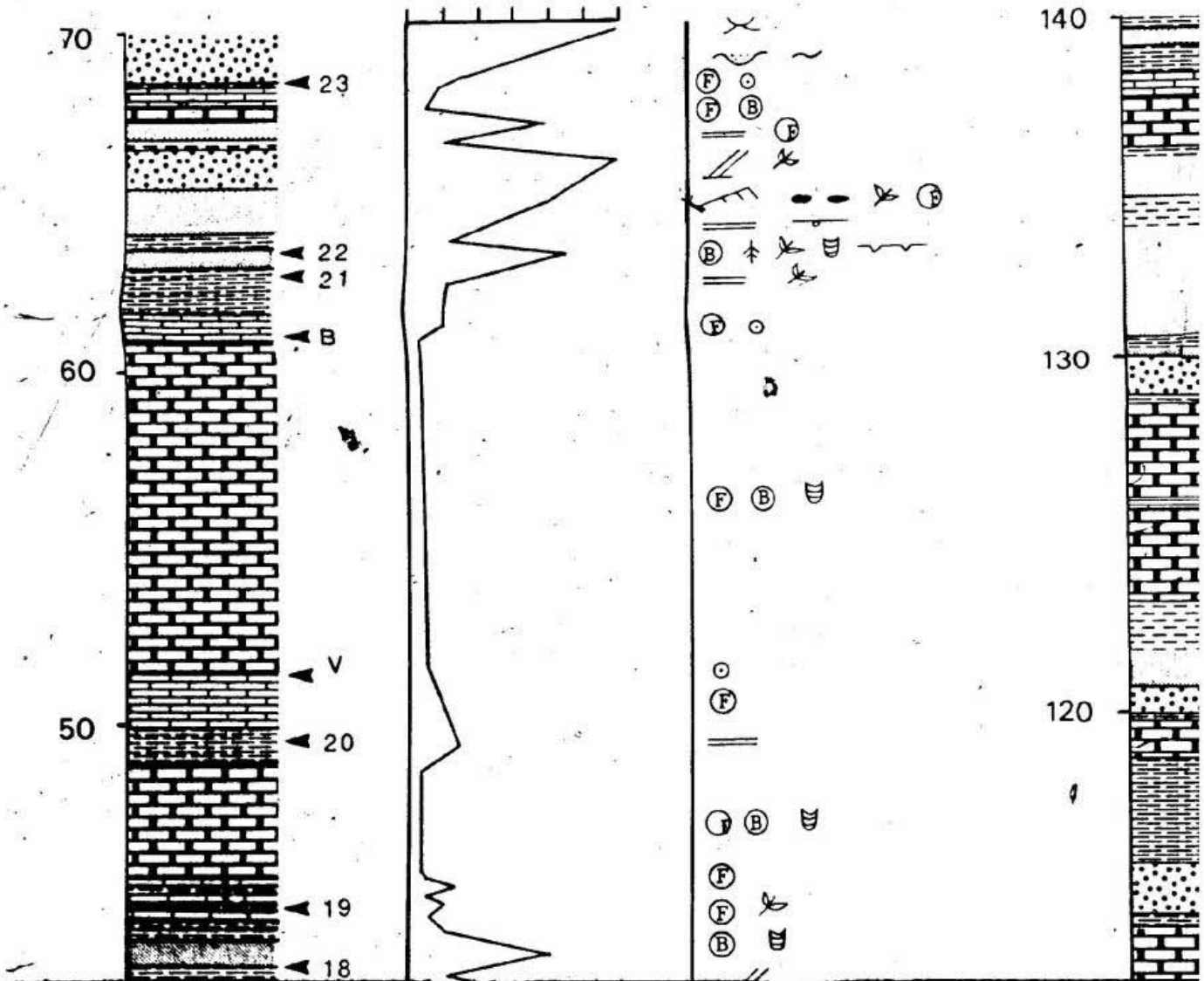
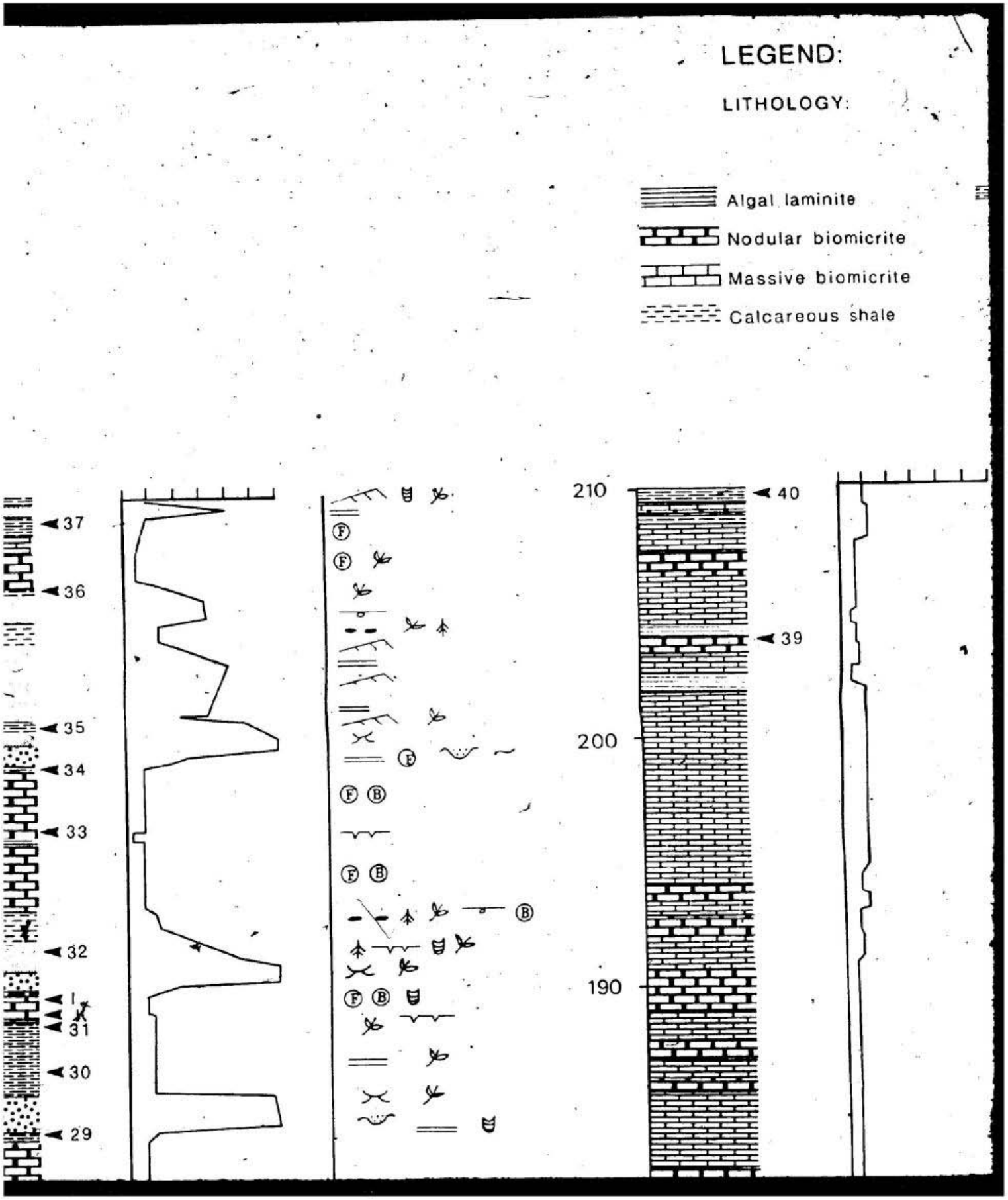


Figure 2.32

Stratigraphic Section of Cabo Espichel, Portugal




LEGEND:
LITHOLOGY:
Algal laminite
Nodular biomicrite
Massive biomicrite
Calcareous shale
37
36
35
34
33
32
31
30
29
210
200
190
40
39
F
B

ND:

OGY:

SEDIMENTARY STRU

aminite

r biomicrite

e biomicrite

eous shale

Non-calcareous shale

Siltstone

Sandstone

Granule conglomerate

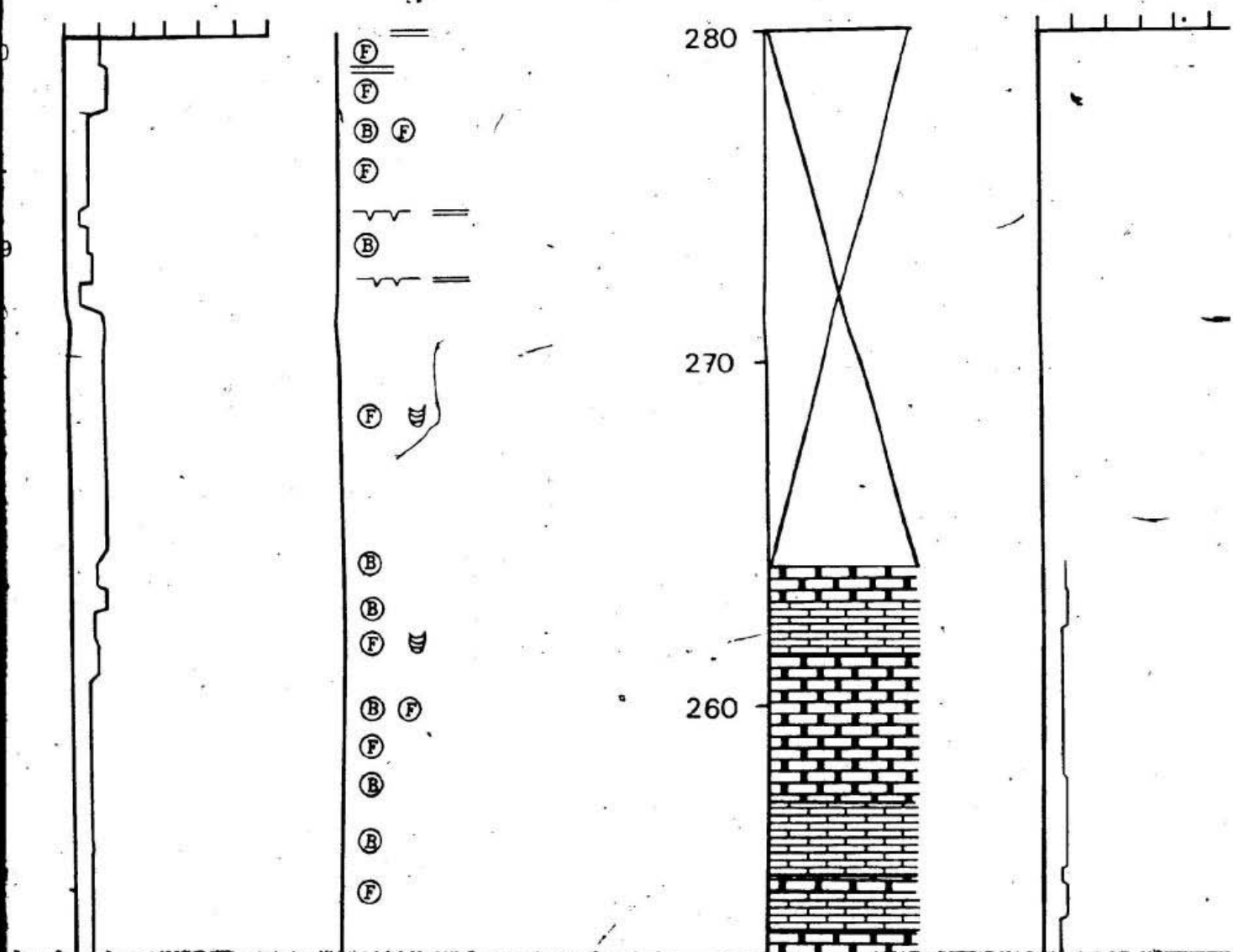
Horizontal parallel la

Trough cross-beddin

Planar cross-bedding

Climbing ripple lamir

Scour surface



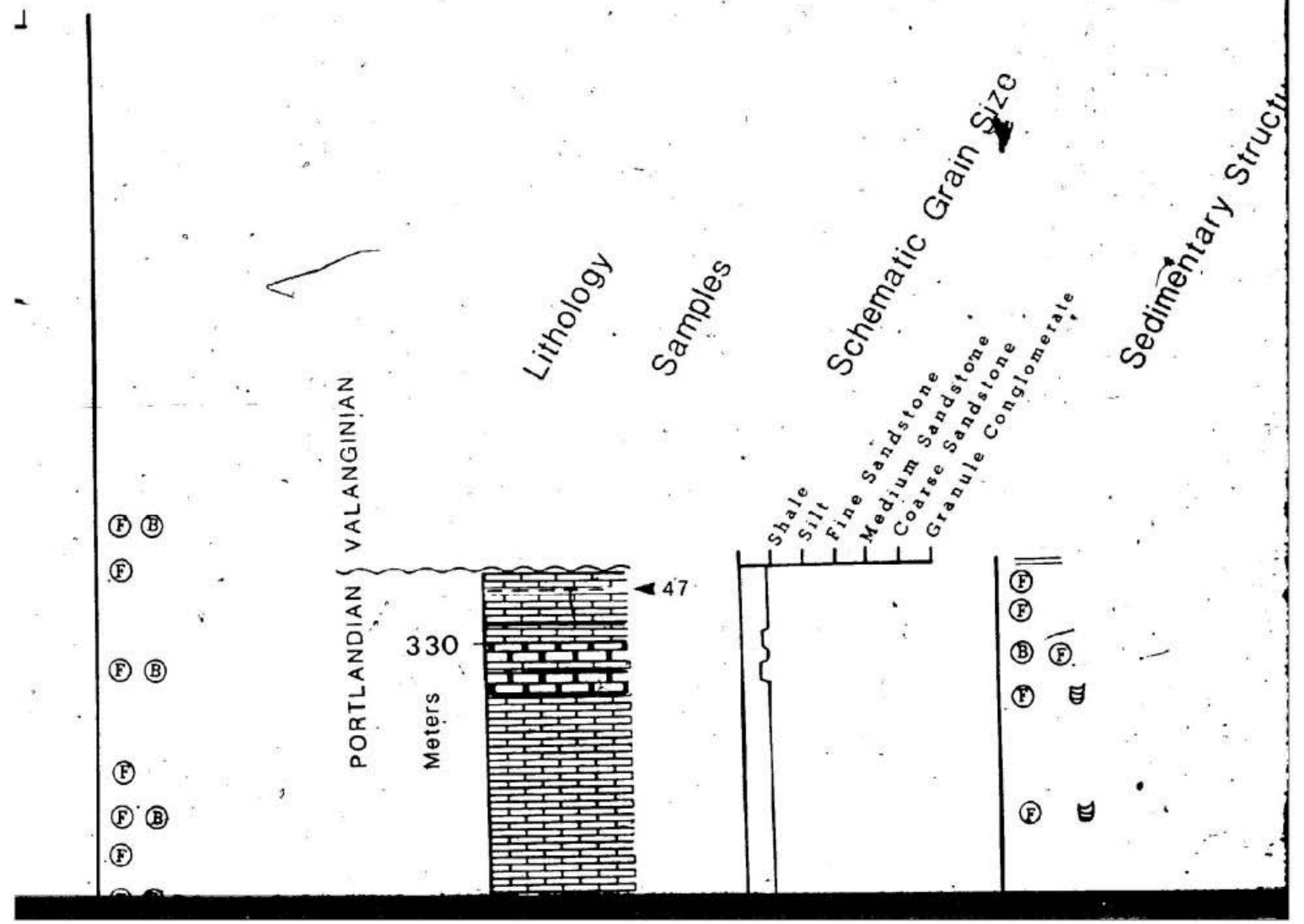
ICTURES AND ACCESSORIES:

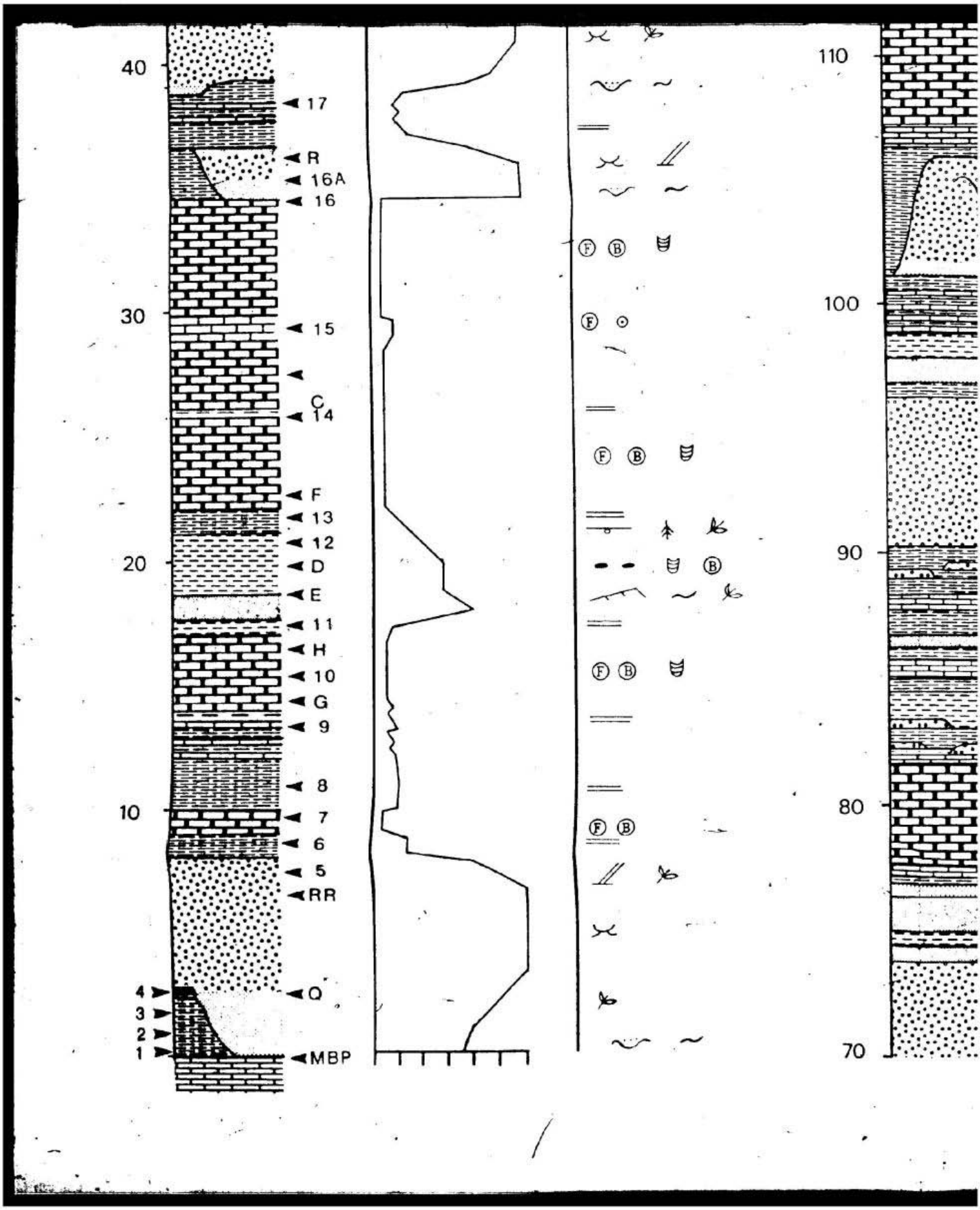
mination
g
ation

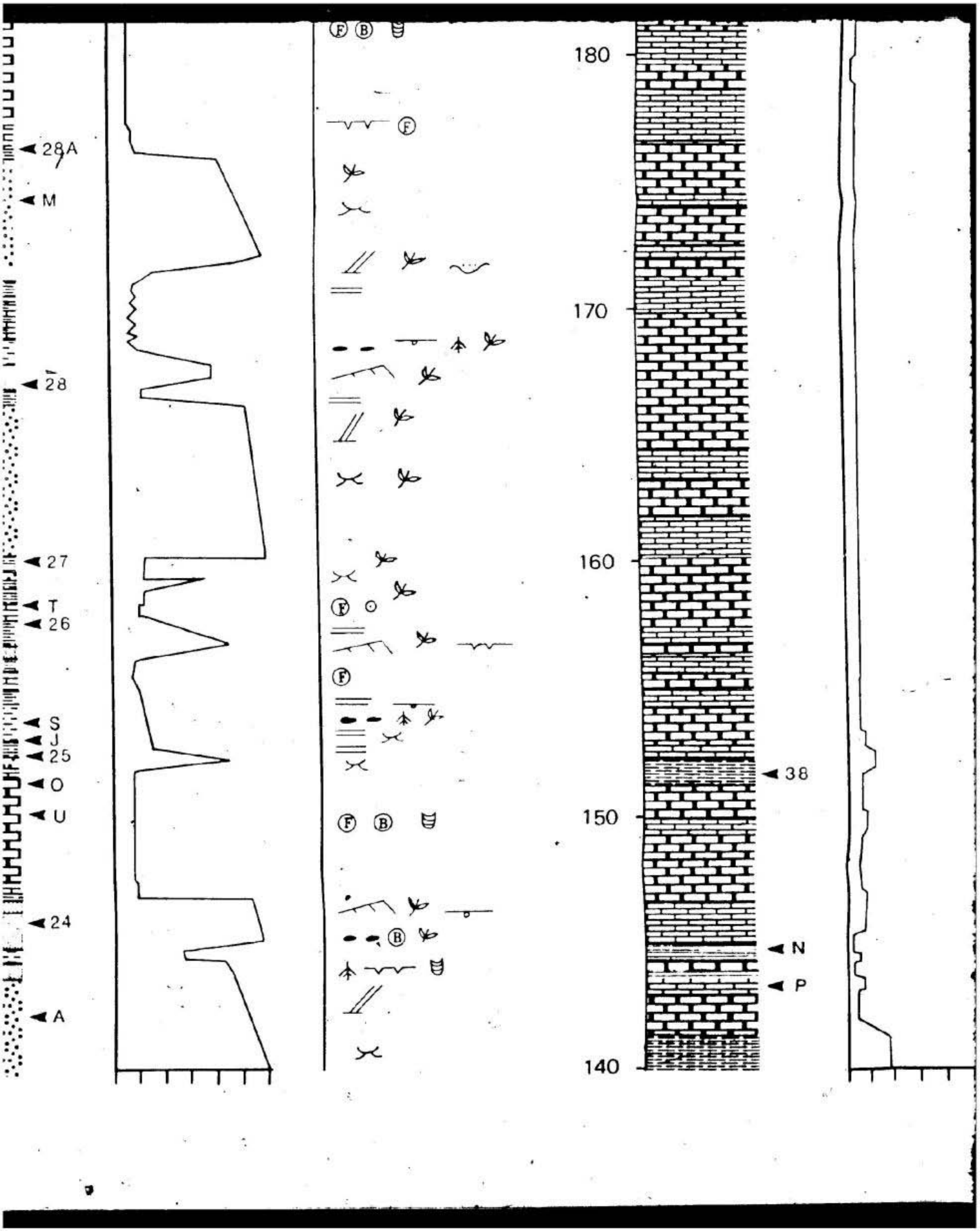
Burrows
Biofurbation
Fossiliferous
Mud cracks
Load casting

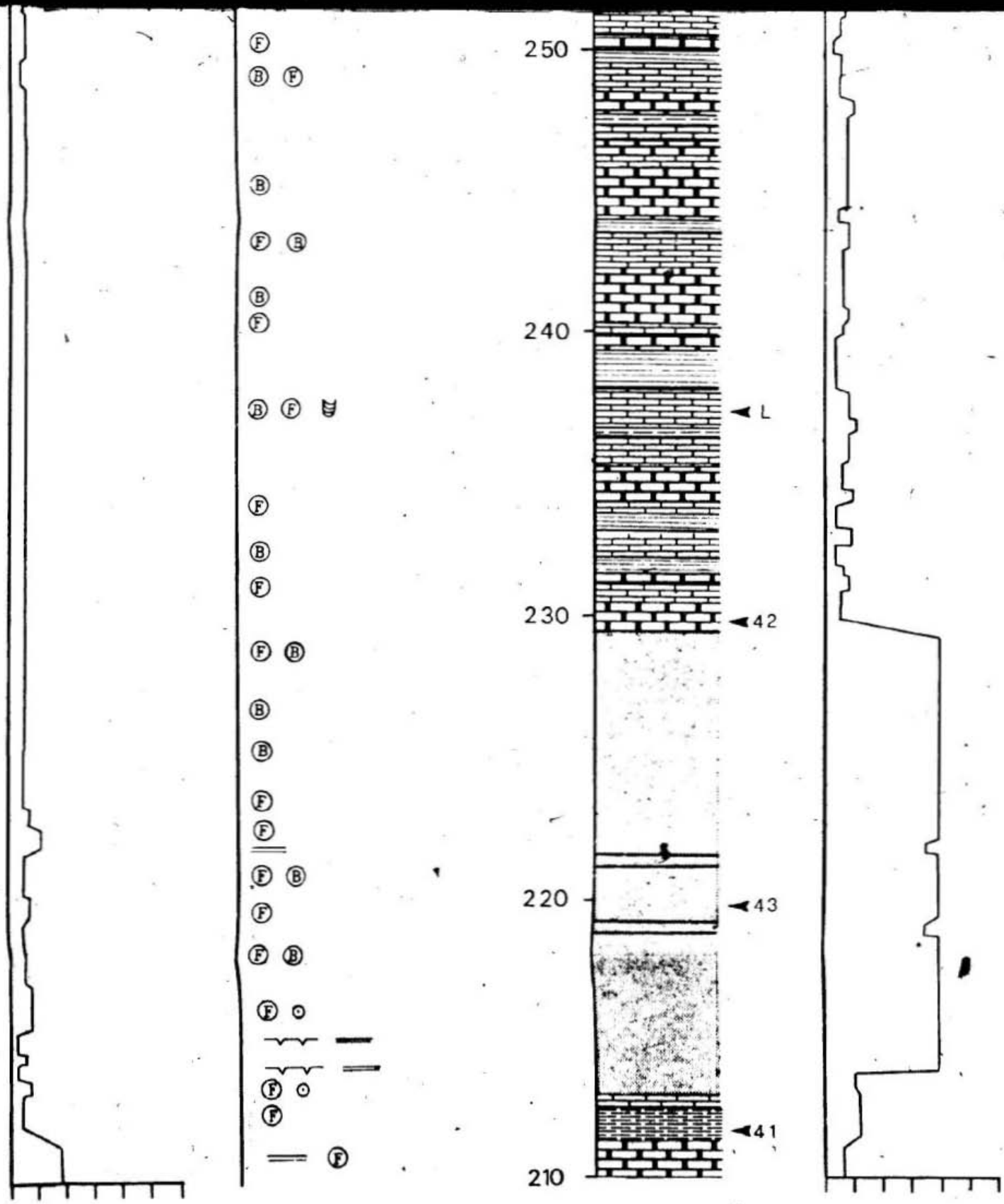
Nodules (calcrete)
Rip-up clasts
Roots in situ
Plant and woody debris
Oolitic

1 ◄ Palynology sample
A ◄ Hand samples




40
30
20
10
17
R
16A
16
15
C
14
F
13
12
D
E
11
H
10
G
9
8
7
6
5
RR
Q
4
3
2
1
MBP
110
100
90
80
70


28A
M
28
27
T
26
S
J
25
O
U
24
A
180
170
160
150
140
38
N
P


250
240
230
220
210
L
42
43
41

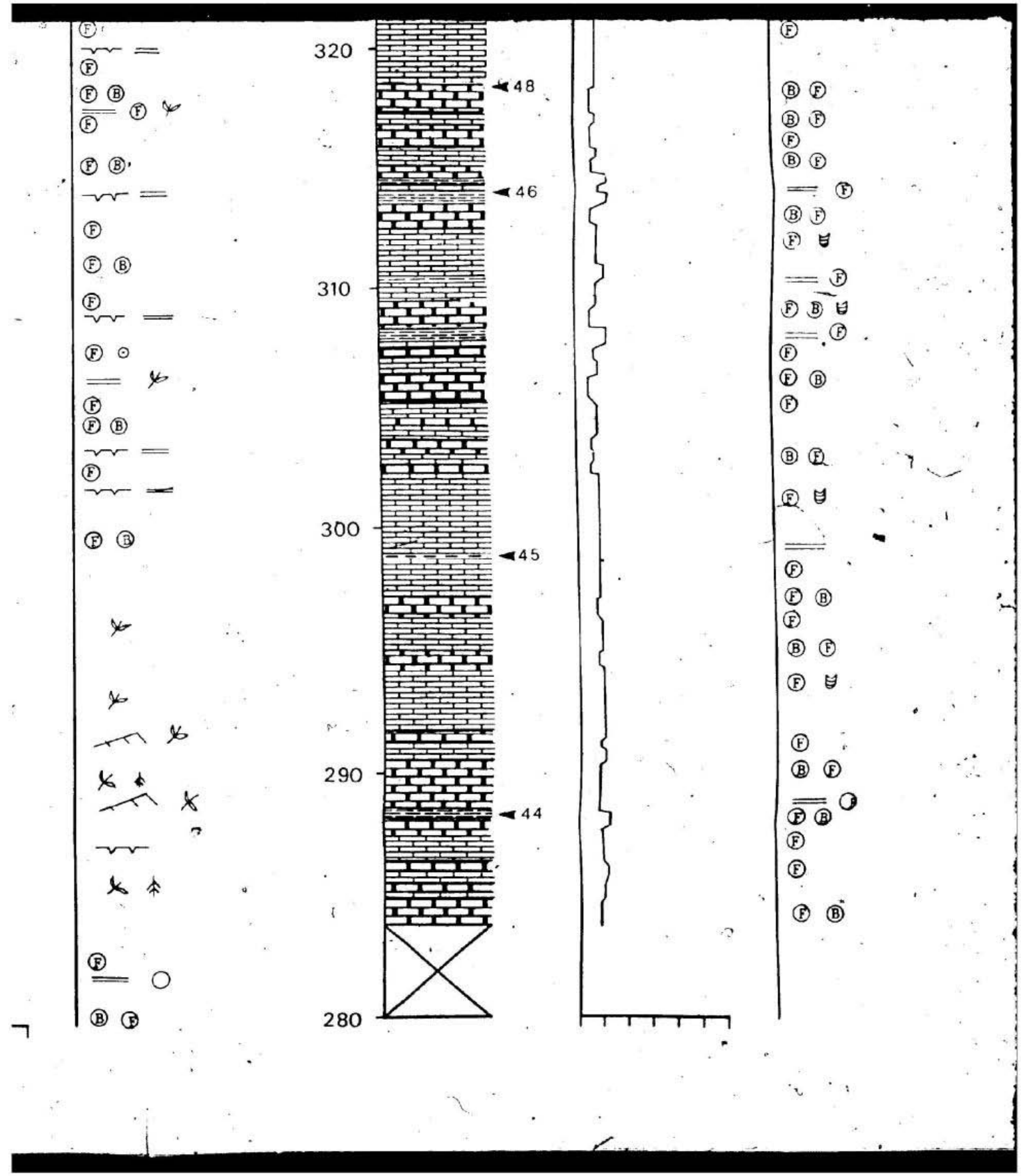
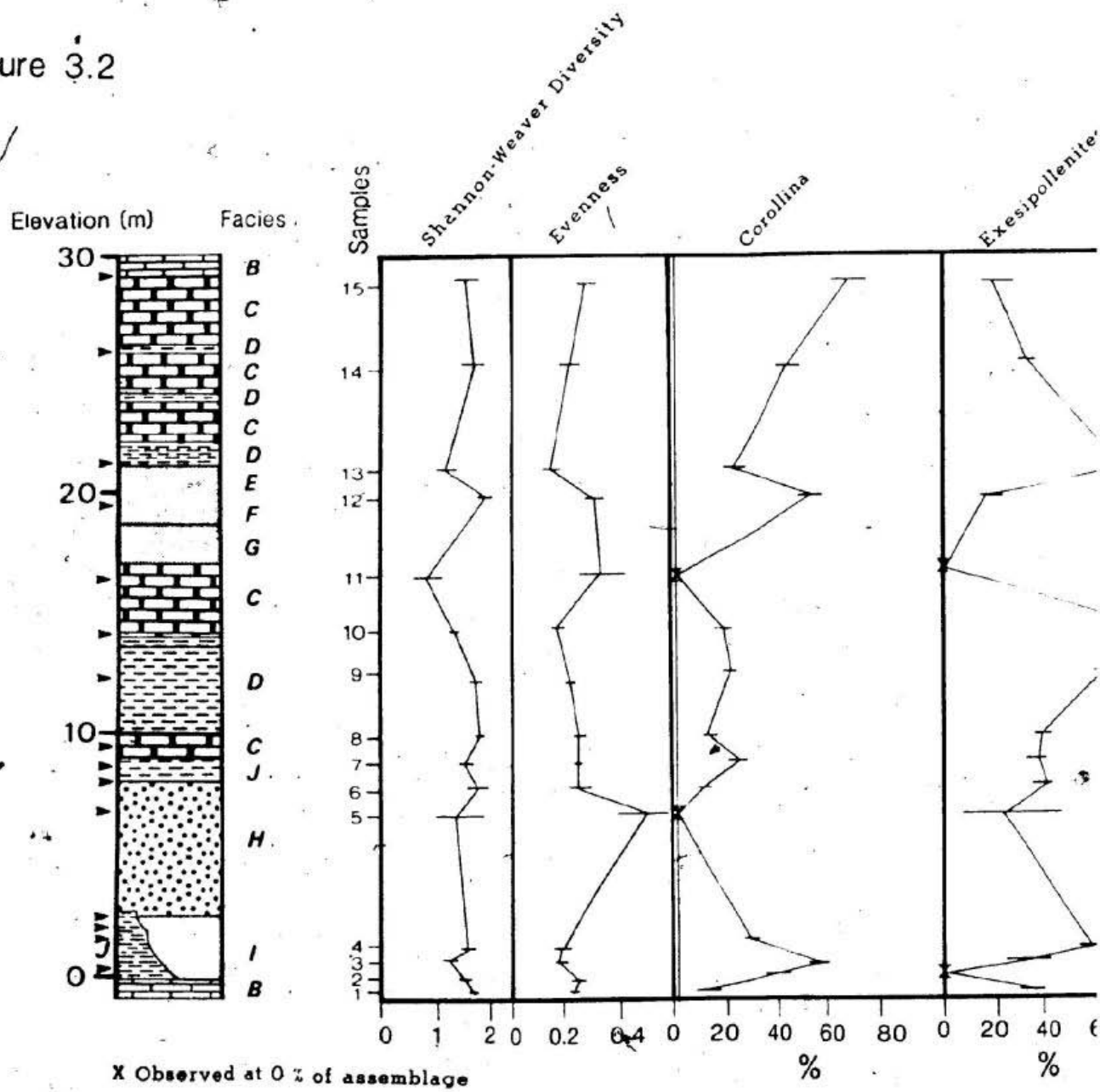
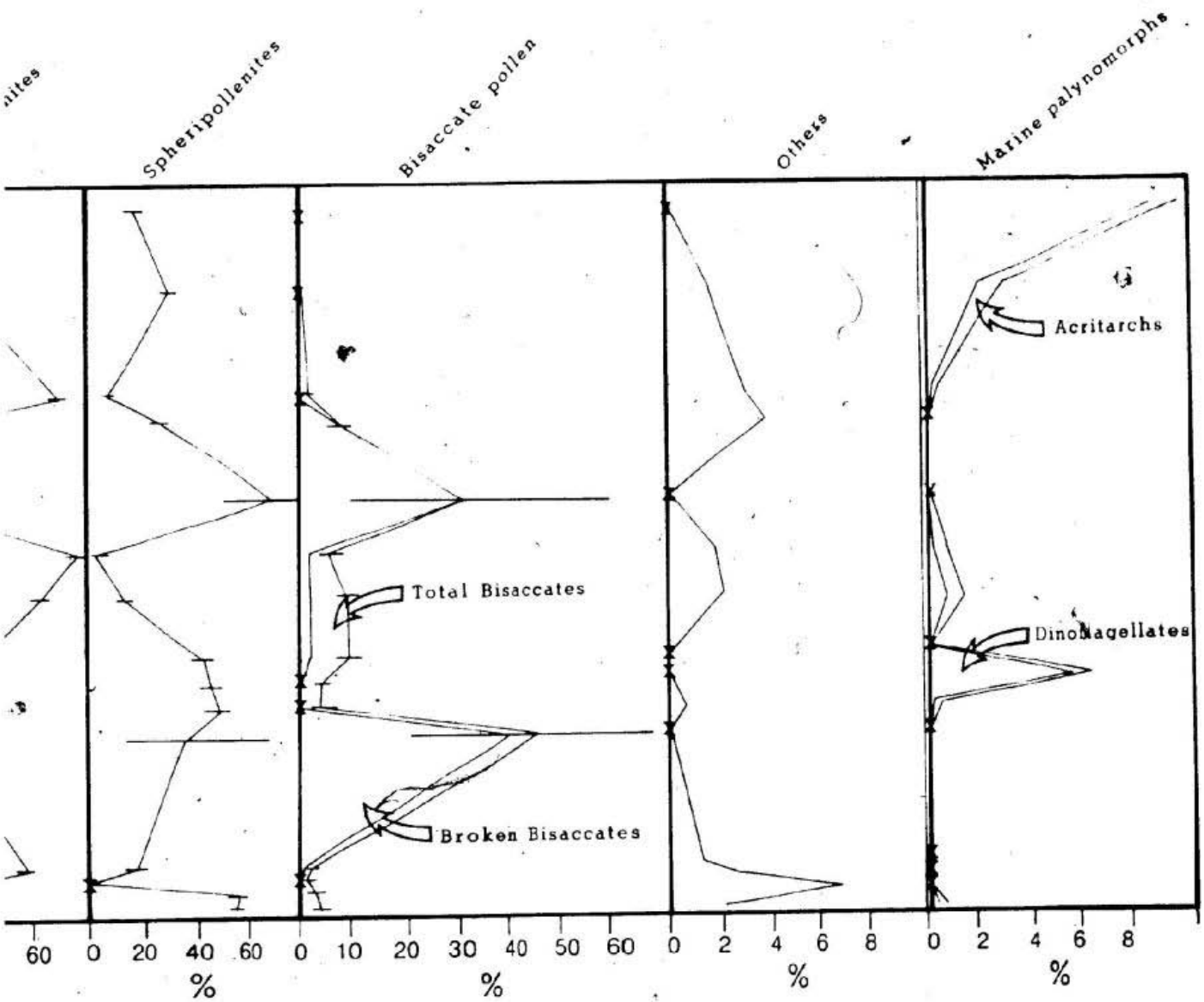

320
310
300
290
280
48
46
45
44

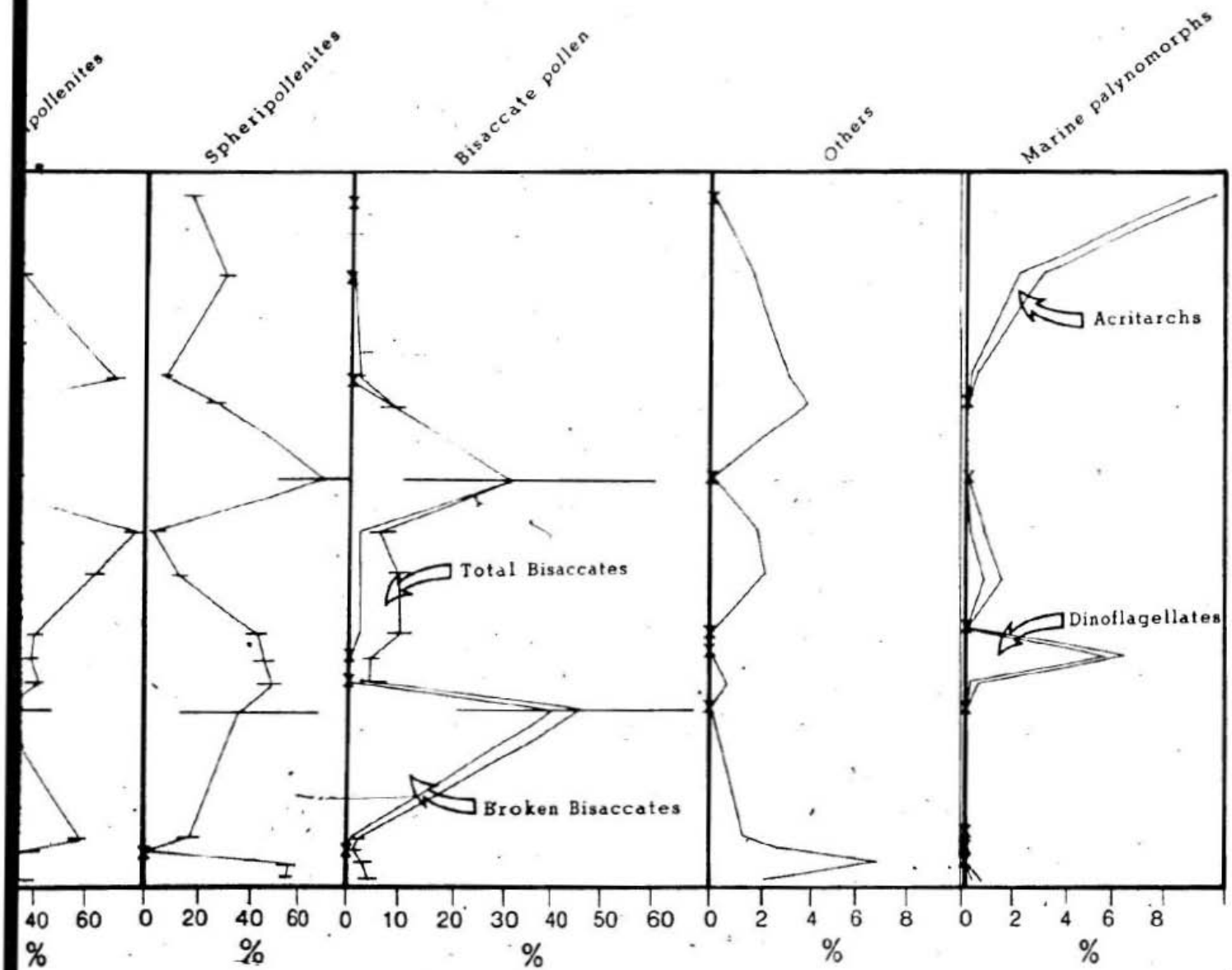
Figure 3.2



X Observed at 0 % of assemblage

Bars illustrate abundance limits


Spheripollenites
Bisaccate pollen
Others
Marine palynomorphs
Total Bisaccates
Broken Bisaccates
Acritarchs
Dinoflagellates
60 0 20 40 60
%
0 10 20 30 40 50 60
%
0 2 4 6 8
%
0 2 4 6 8
%


Spheripollenites
Bisaccate pollen
Others
Marine palynomorphs
Acritarchs
Total Bisaccates
Dinoflagellates
Broken Bisaccates
40 60
0 20 40 60
0 10 20 30 40 50 60
0 2 4 6 8
0 2 4 6 8
%
%
%
%
%

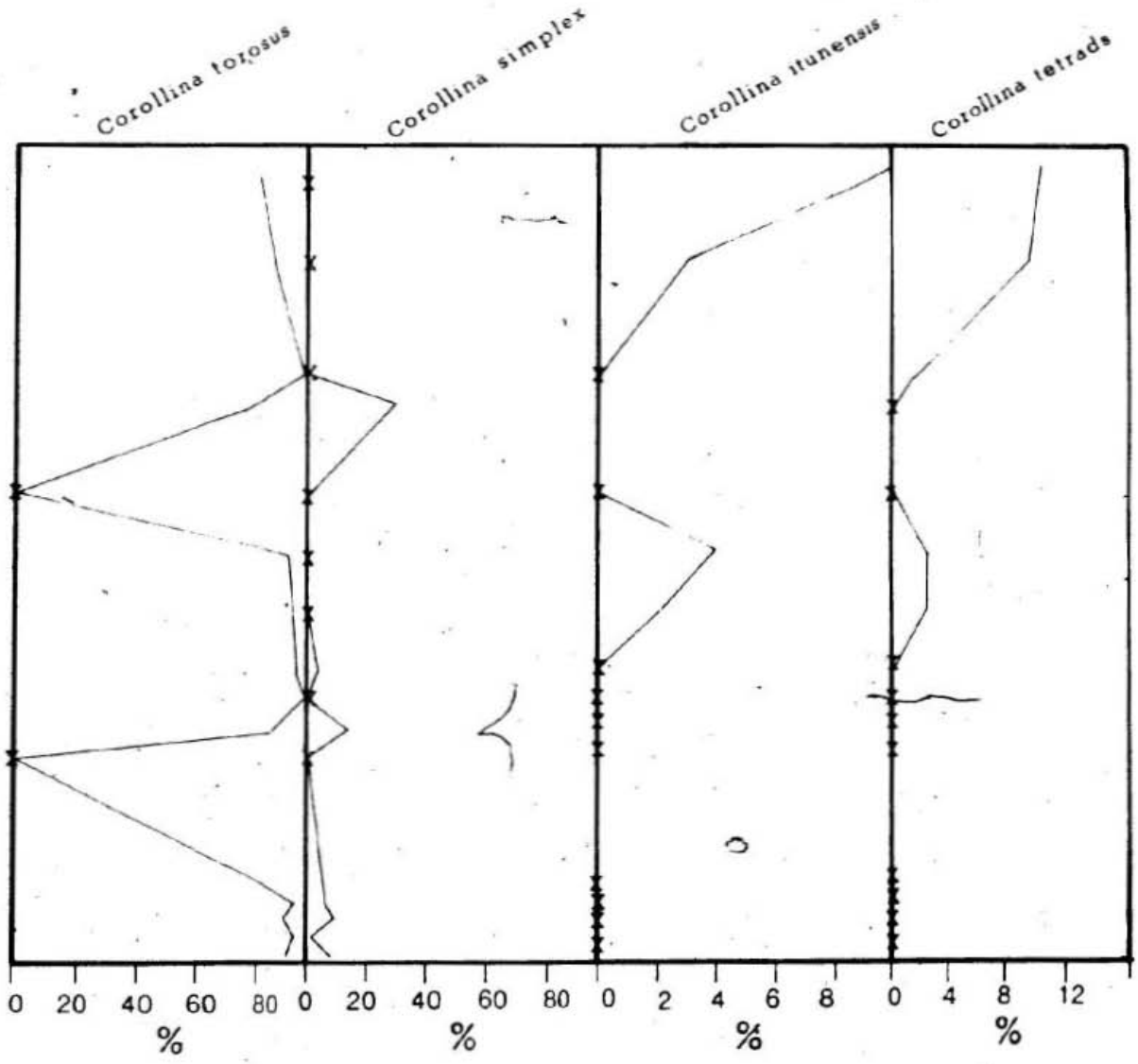
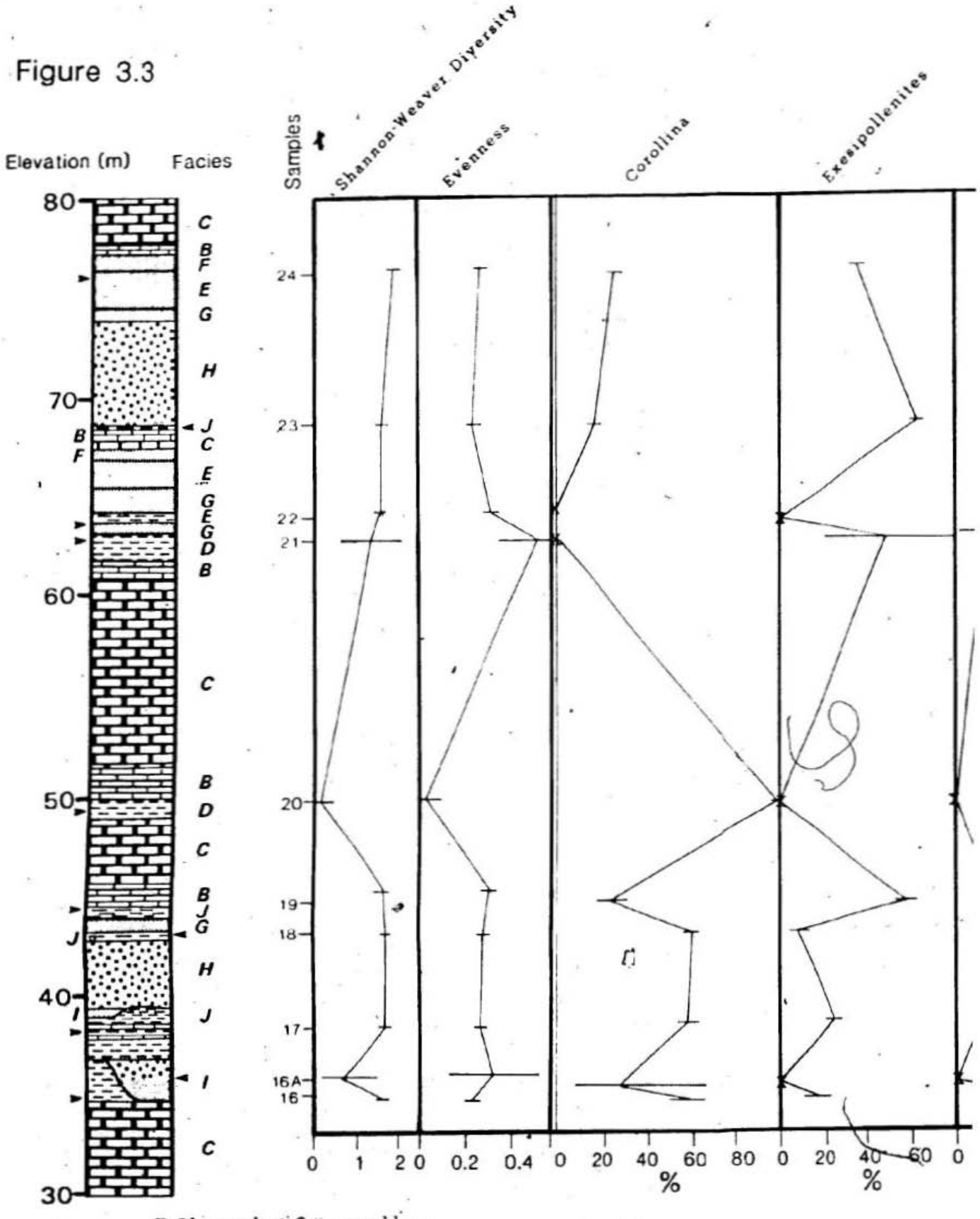
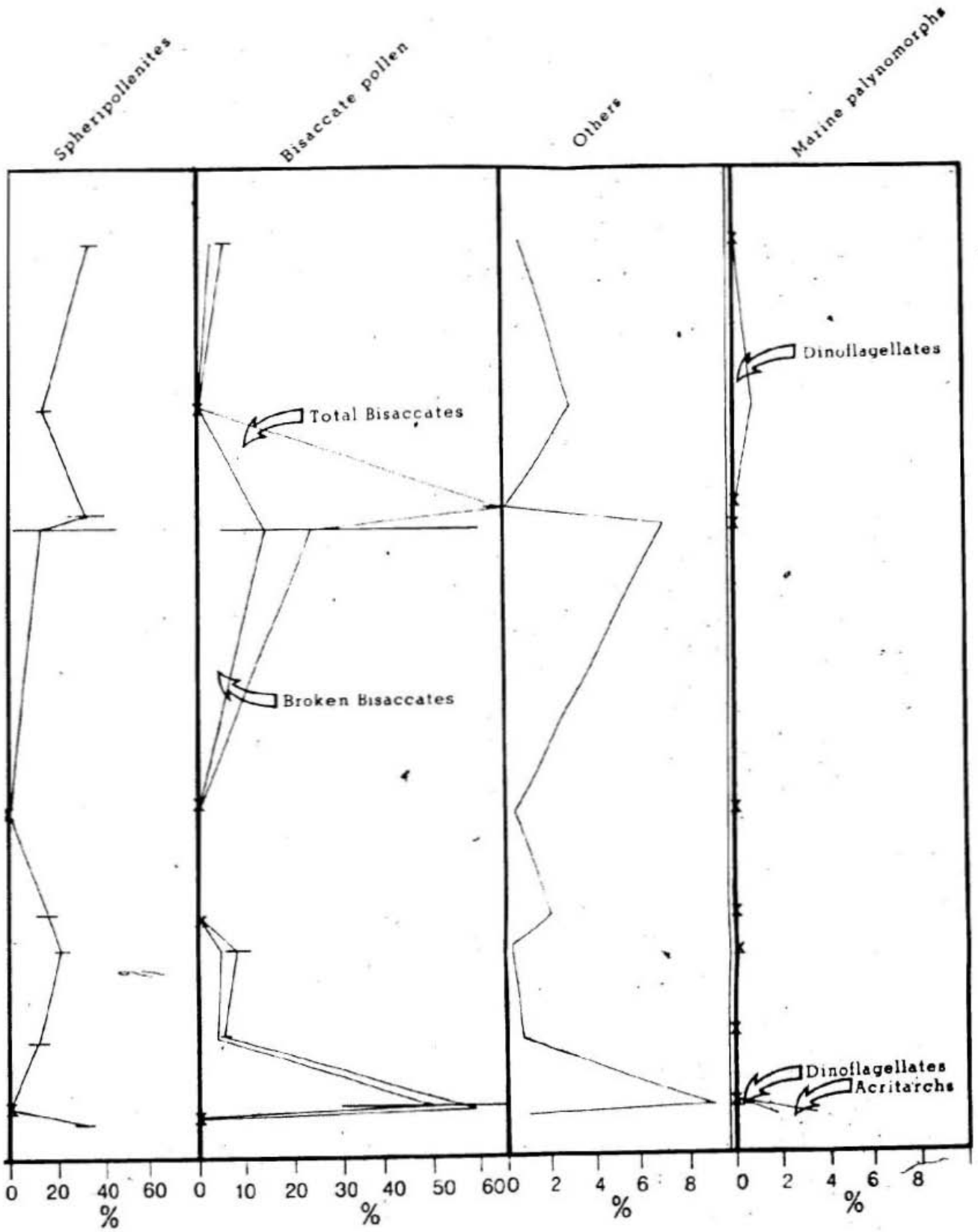

Corollina torosus
Corollina simplex
Corollina itunensis
Corollina tetrads
0 20 40 60 80
%
0 20 40 60 80
%
0 2 4 6 8
%
0 4 8 12
%

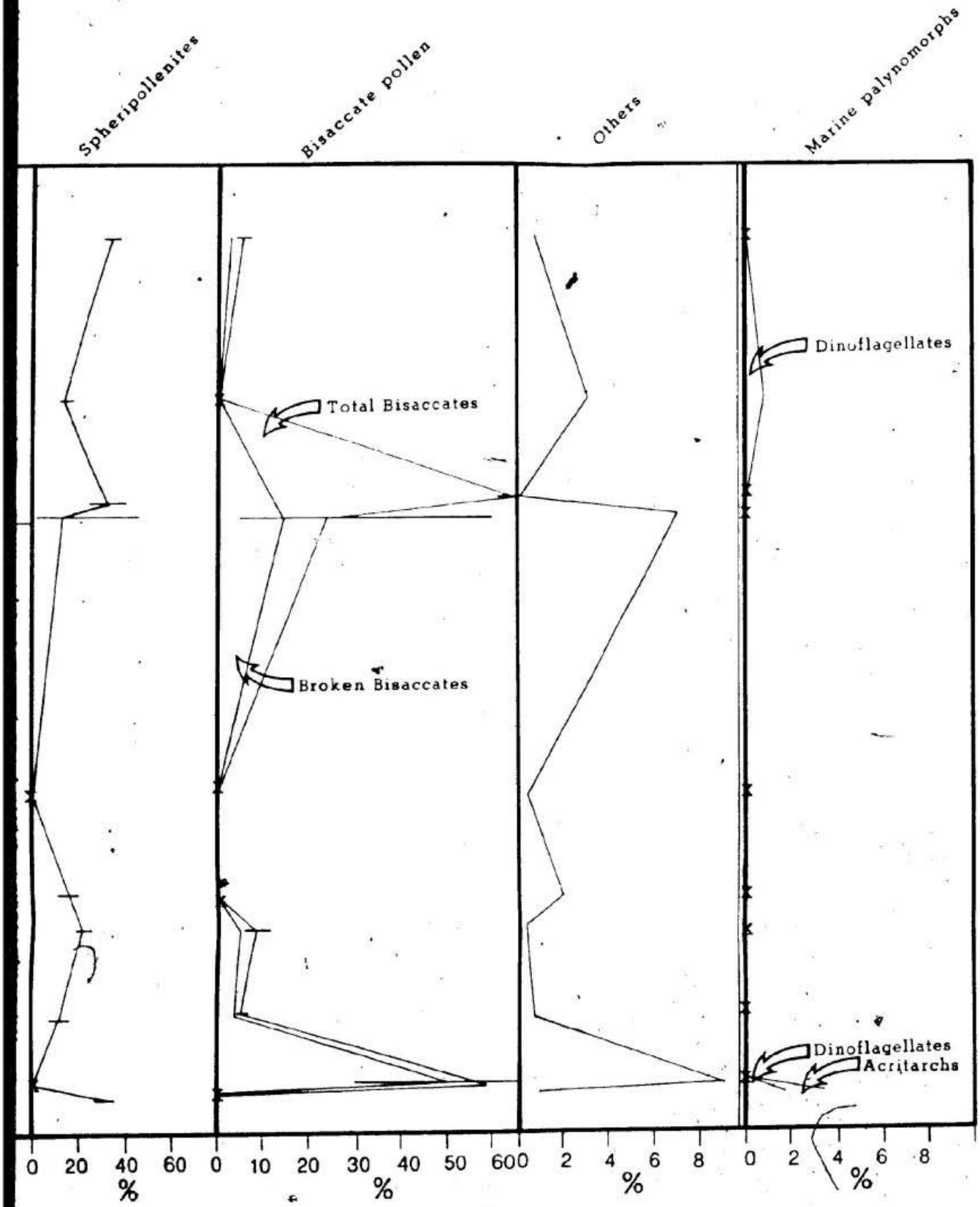
Figure 3.3



X Observed at 0 % assemblage

Bars illustrate abundance limits


Spheripollenites
Bisaccate pollen
Others
Marine palynomorphs
Total Bisaccates
Broken Bisaccates
Dinoflagellates
Dinoflagellates
Acritarchs
0 20 40 60
%
0 10 20 30 40 50 600
%
2 4 6 8
%
0 2 4 6 8
%


Spheripollenites
Bisaccate pollen
Others
Marine palynomorphs
Total Bisaccates
Broken Bisaccates
Dinoflagellates
Dinoflagellates
Acritarchs
0 20 40 60
%
0 10 20 30 40 50 600
%
2 4 6 8
%
0 2 4 6 8
%

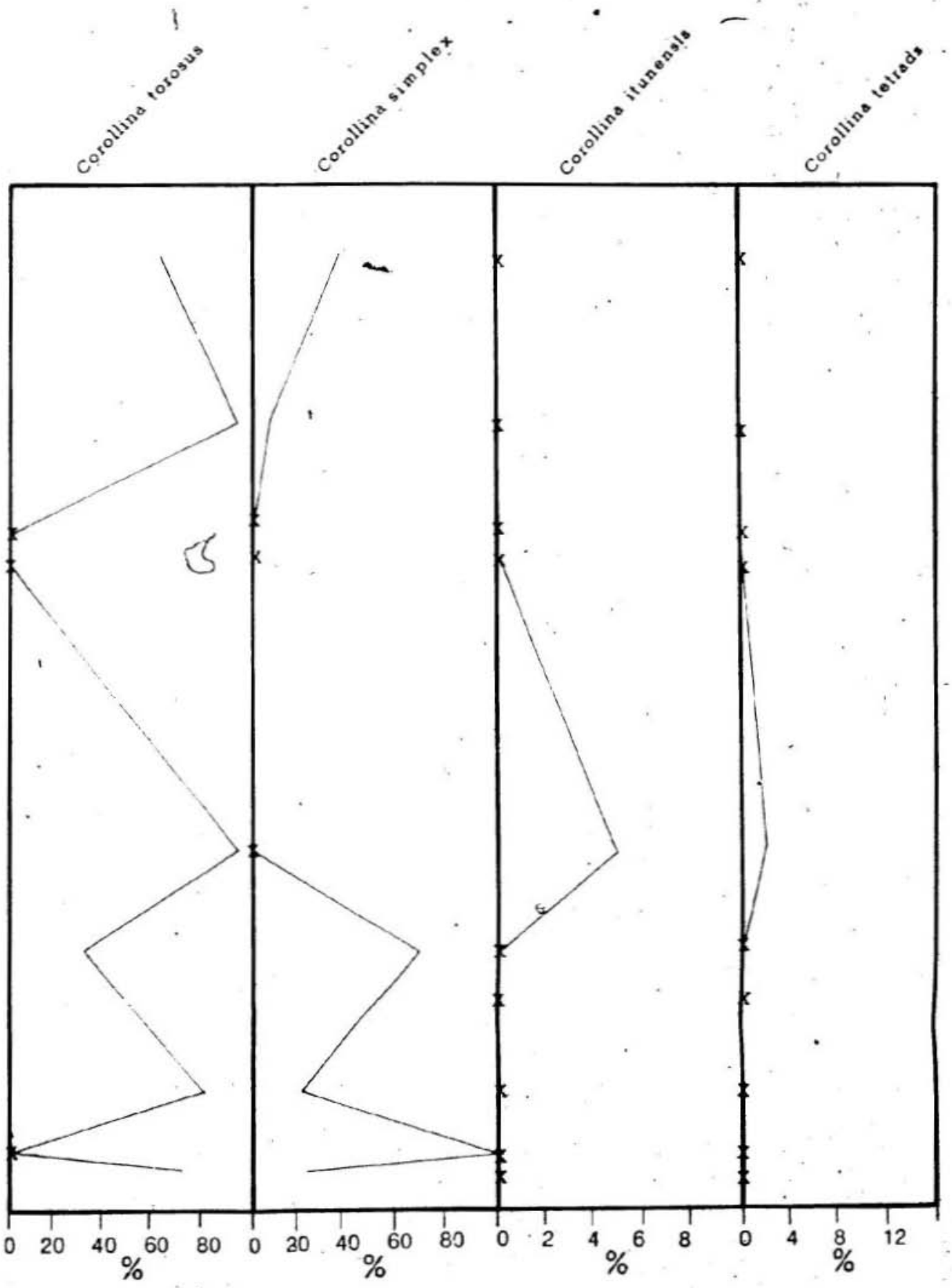
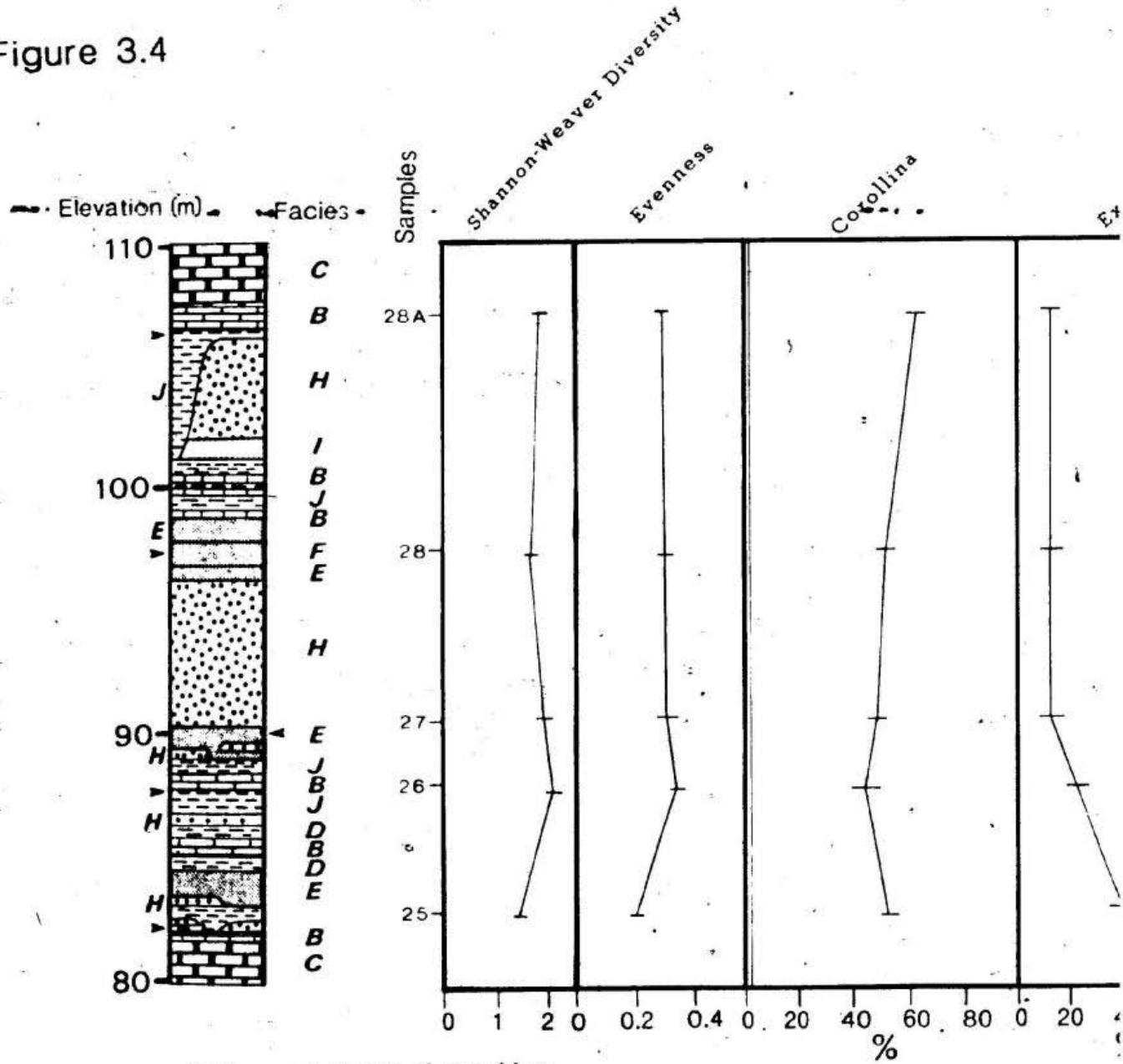
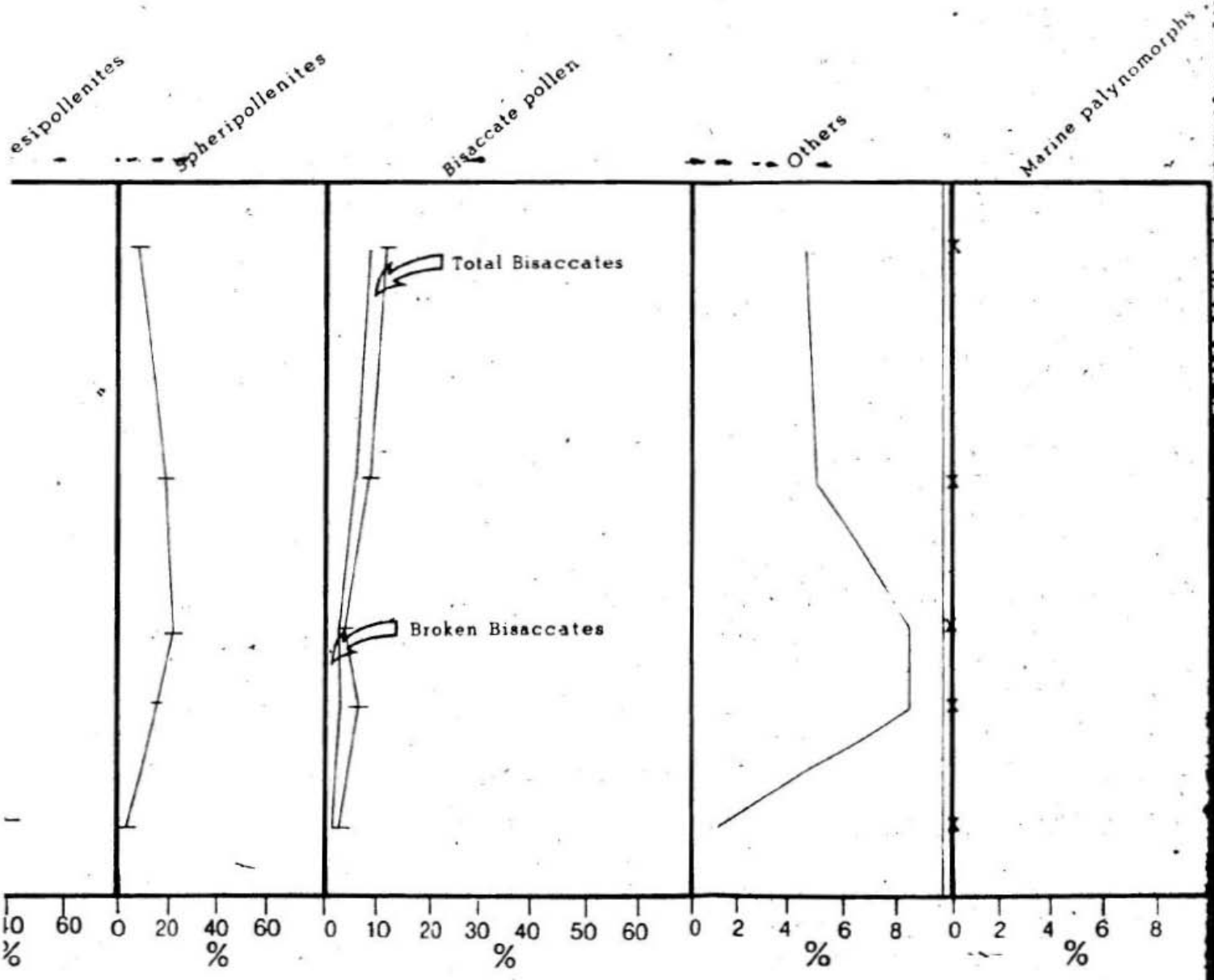

Corollina torosus
Corollina simplex
Corollina itunensis
Corollina telrads
0 20 40 60 80
%
0 20 40 60 80
%
0 2 4 6 8
%
0 4 8 12
%

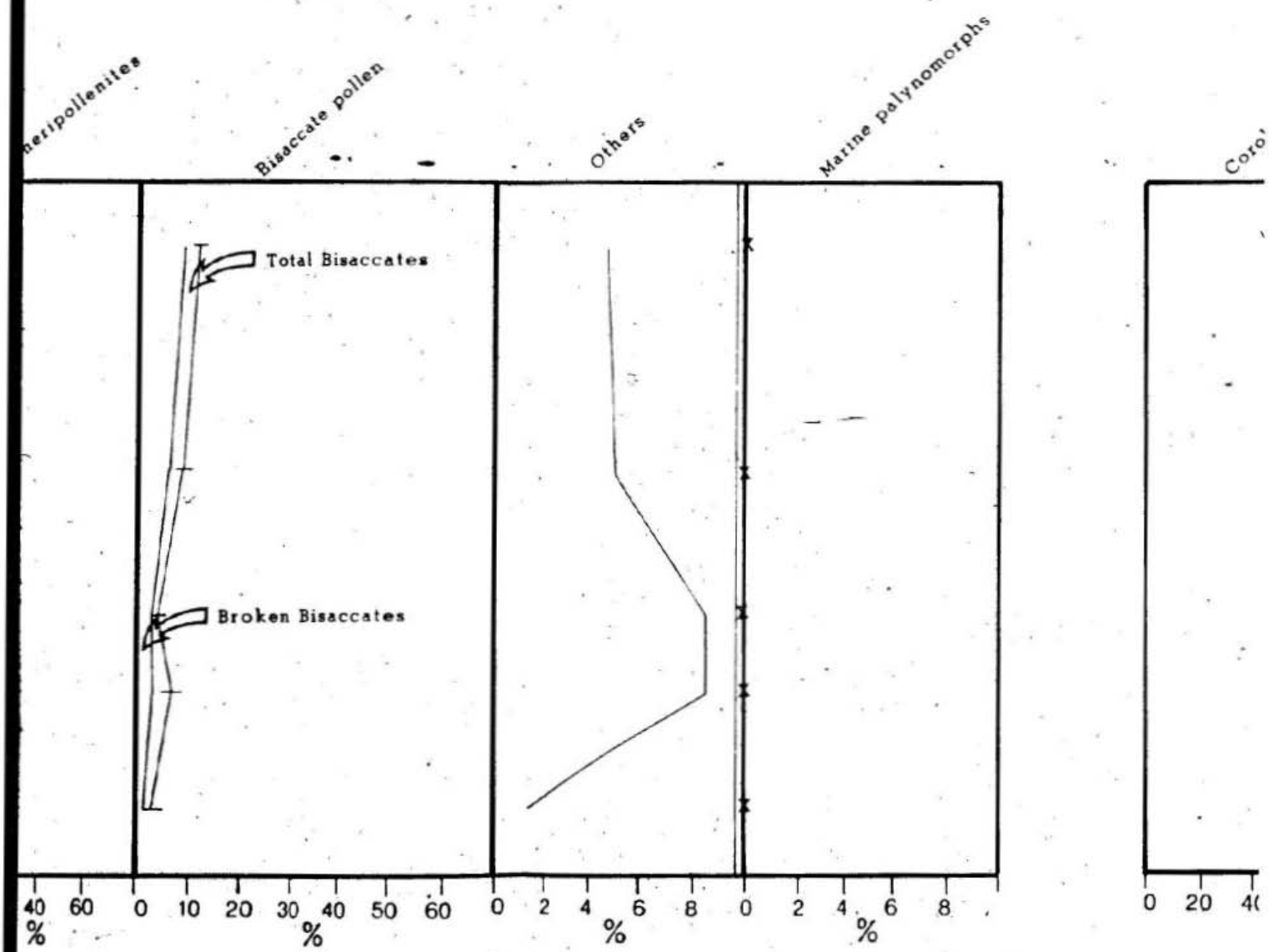
Figure 3.4



X Observed at 0 % of assemblage

Bars illustrate abundance limits


esipollenites
Spheripollenites
Bisaccate pollen
Others
Marine palynomorphs
Total Bisaccates
Broken Bisaccates
60
0 20 40 60
%
0 10 20 30 40 50 60
%
0 2 4 6 8
%
0 2 4 6 8
%


Bisaccate pollen
Others
Marine palynomorphs
Total Bisaccates
Broken Bisaccates
40 60 0 10 20 30 40 50 60
%
0 2 4 6 8
%
0 2 4 6 8
%
0 20

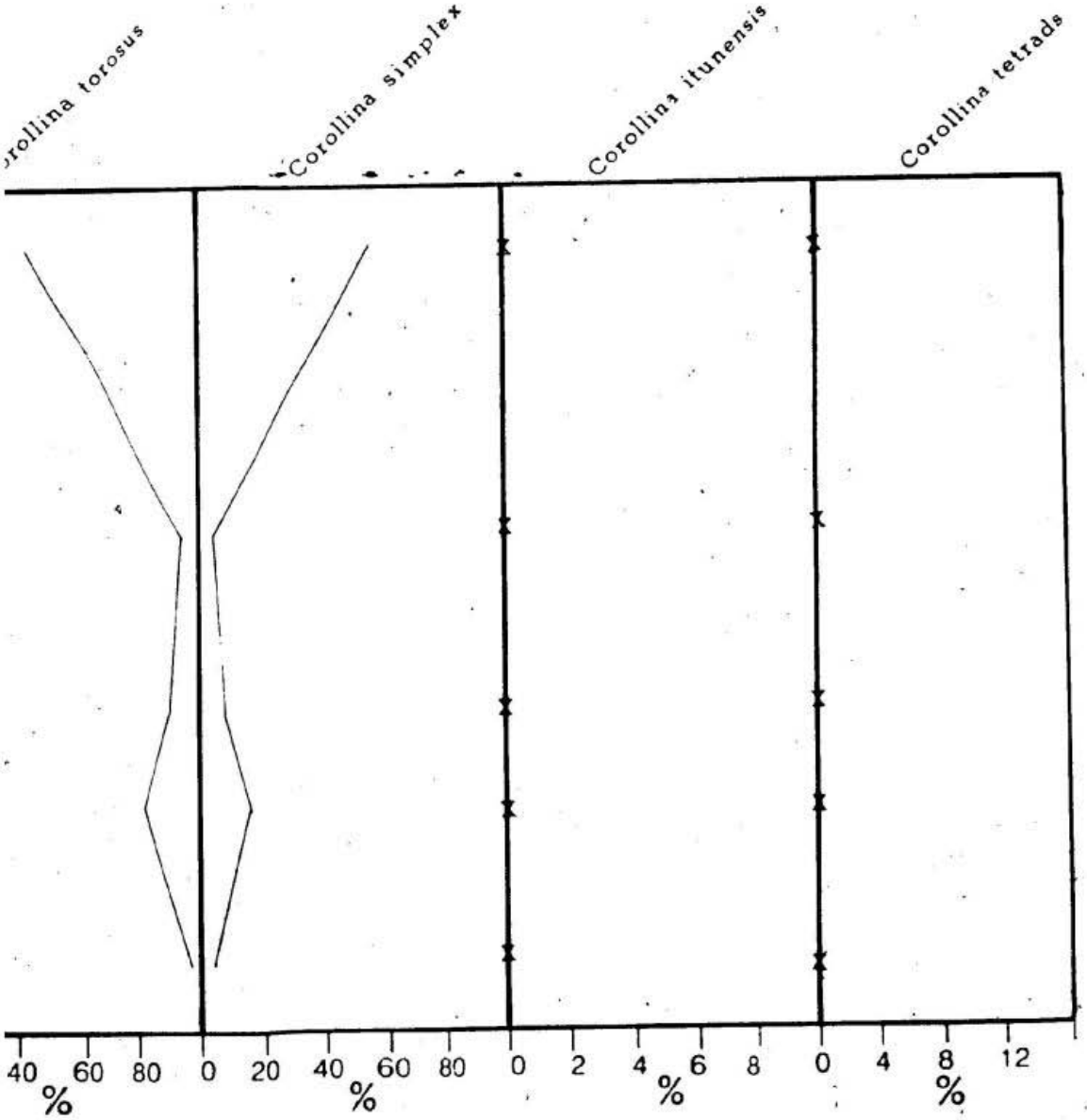
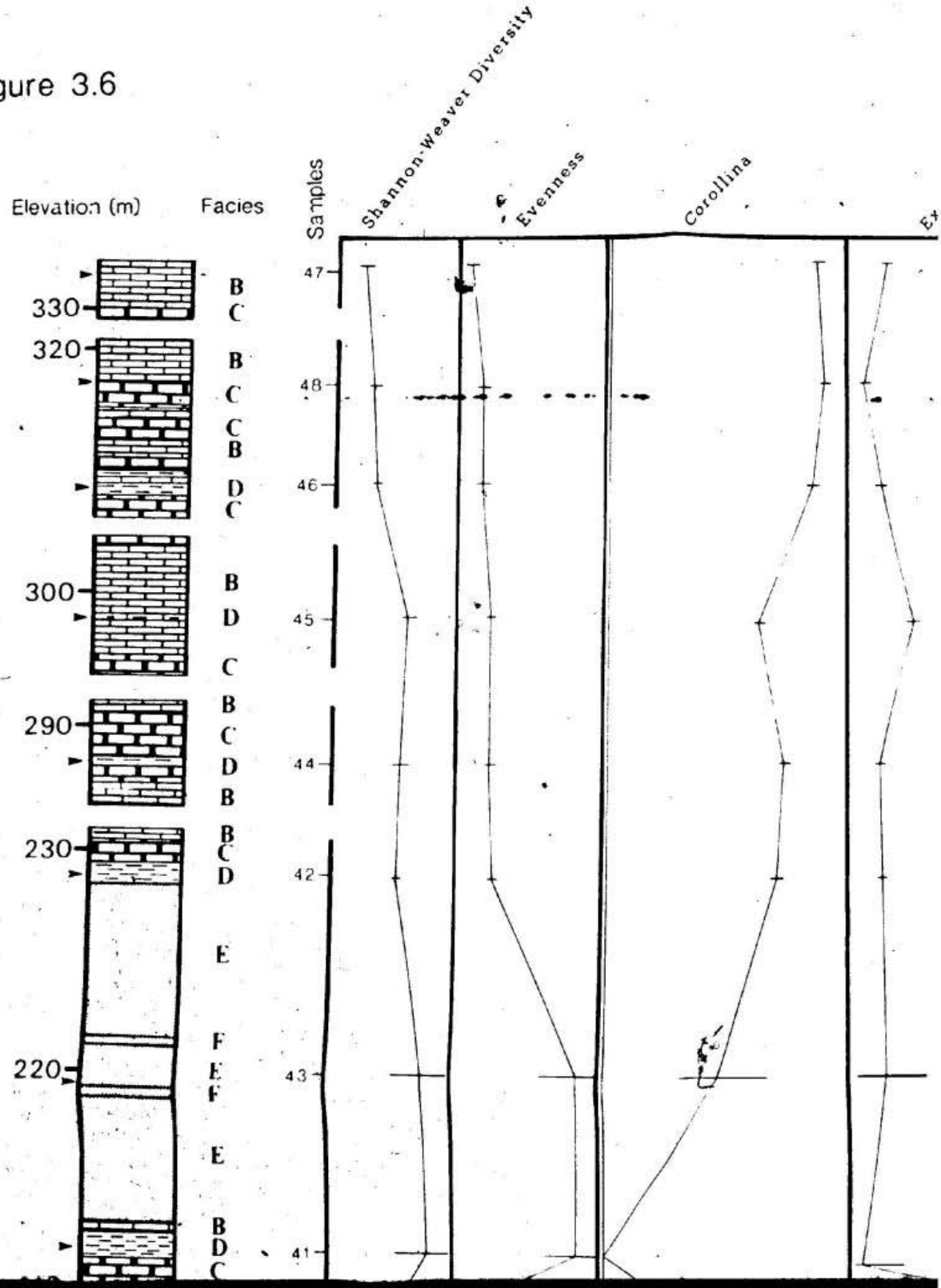
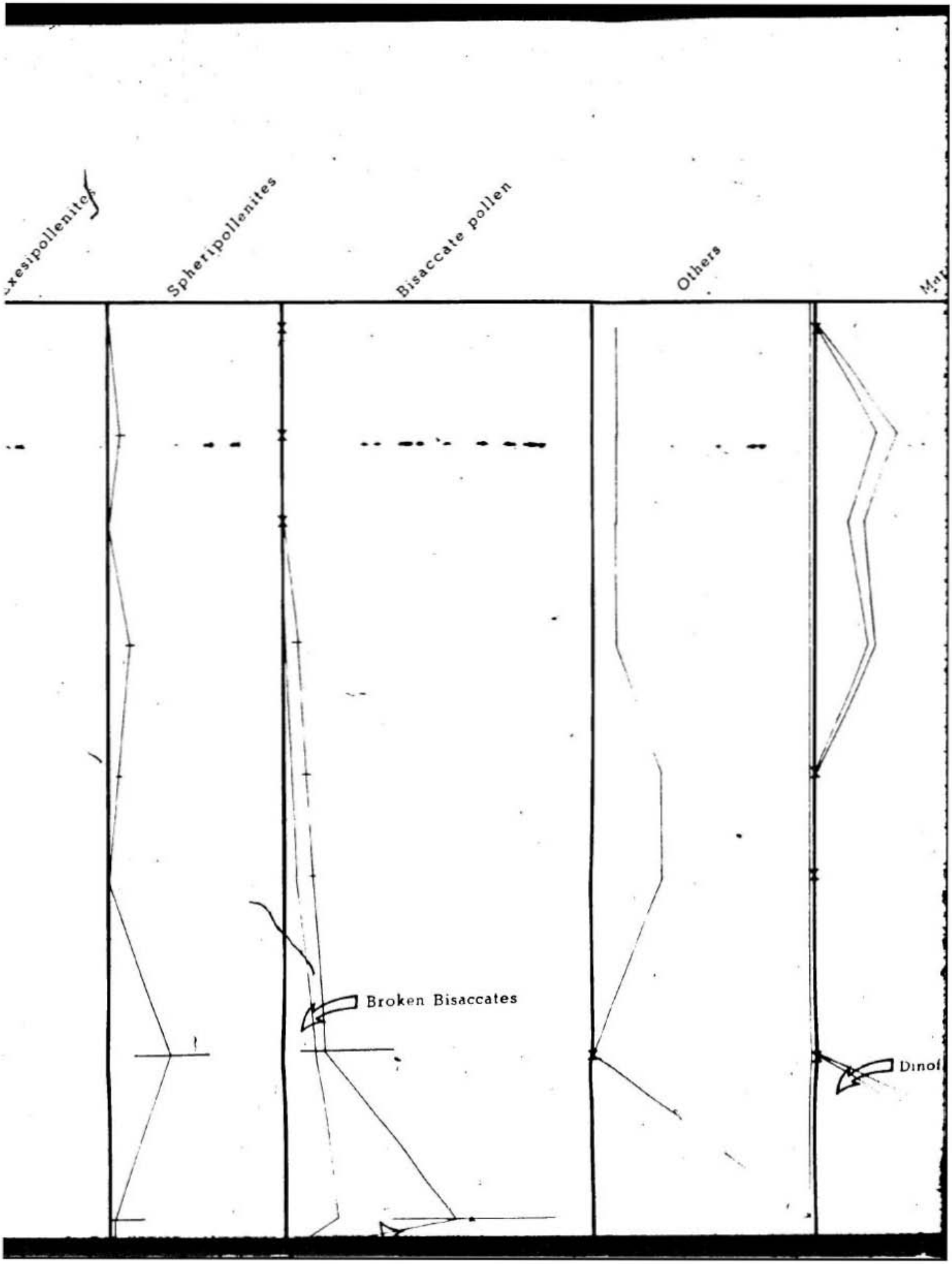
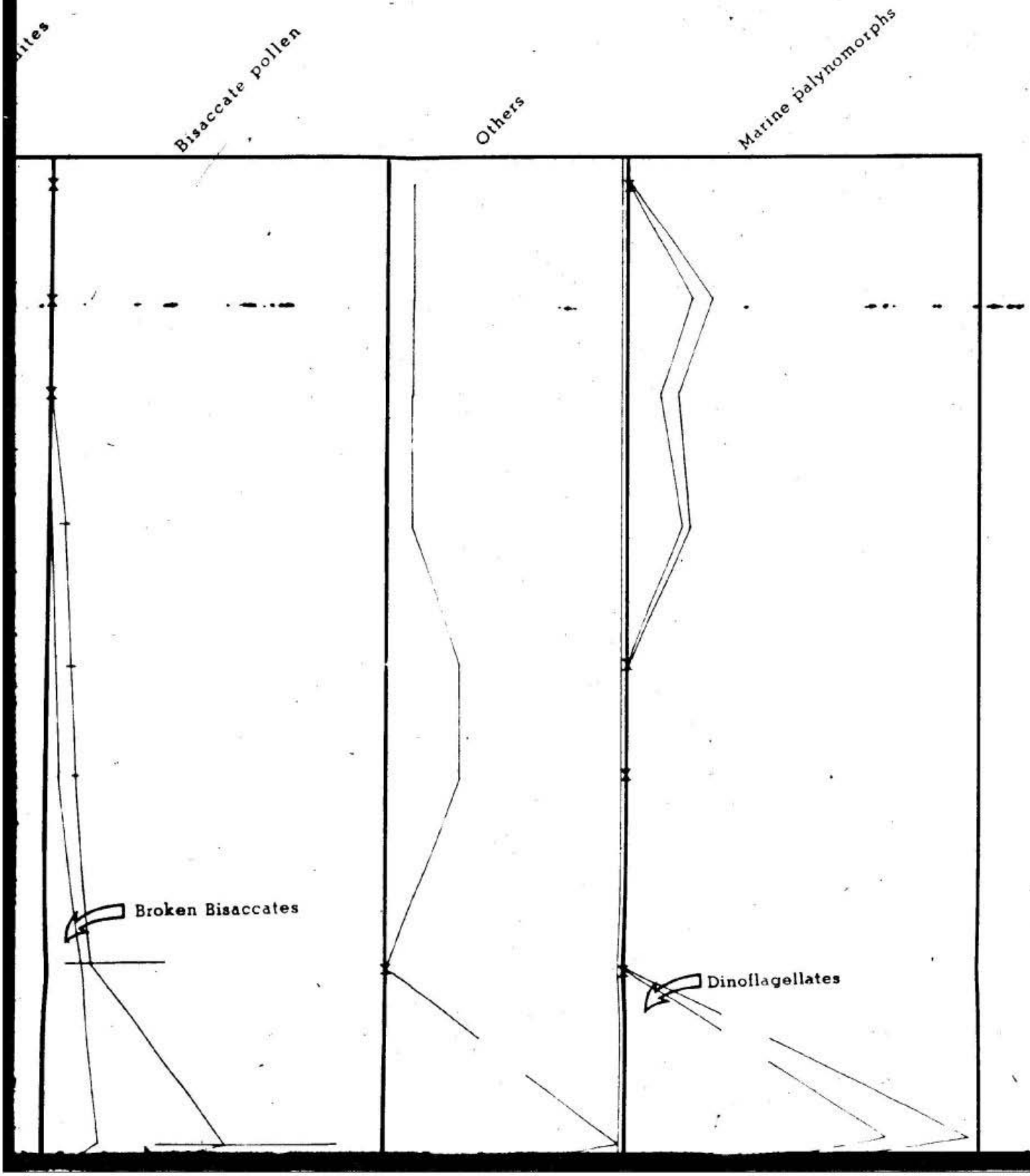
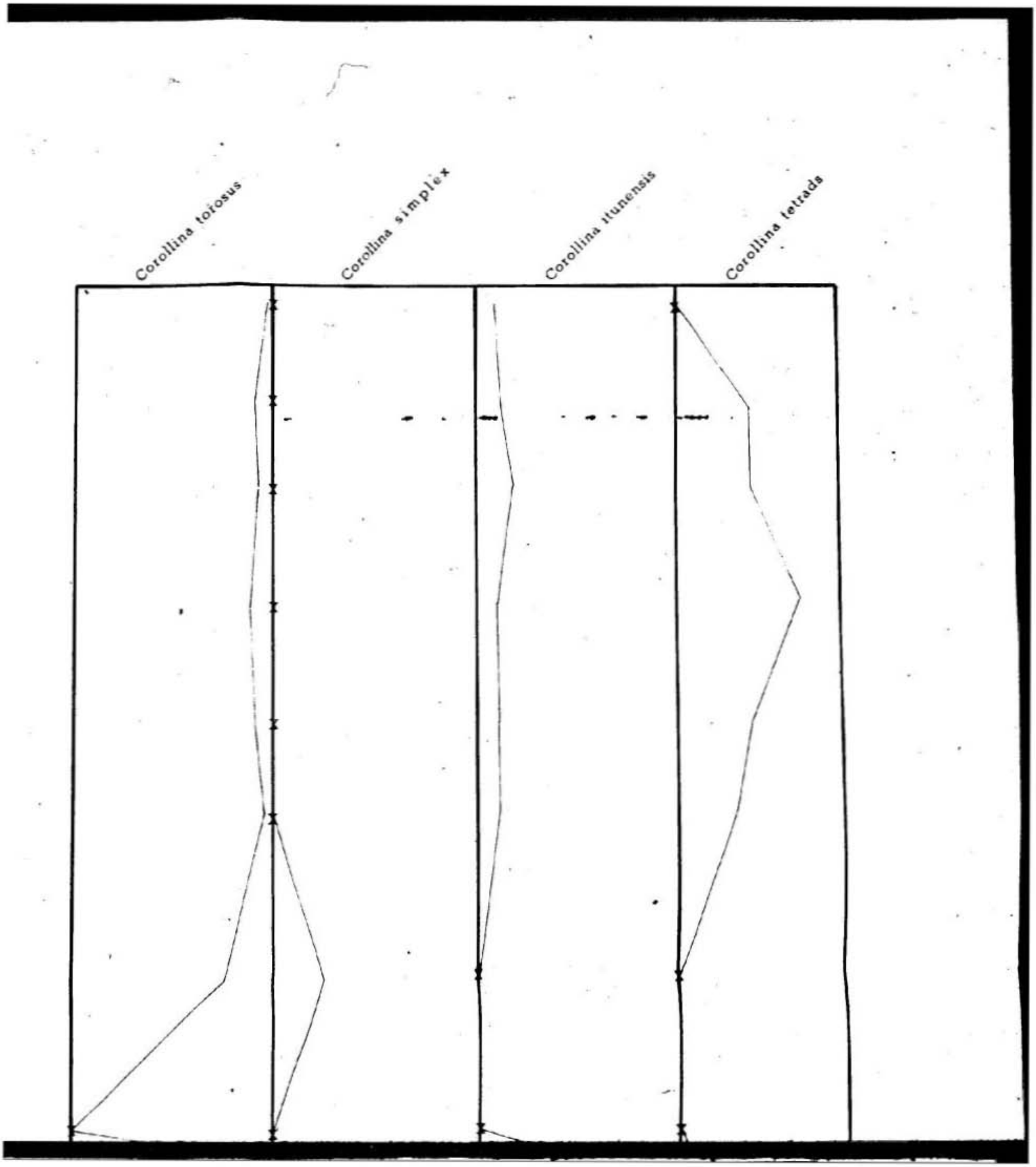

orollina torosus
Corollina simplex
Corollina itunensis
Corollina tetrads
40 60 80 0 20 40 60 80 0 2 4 6 8 0 4 8 12
% % % %

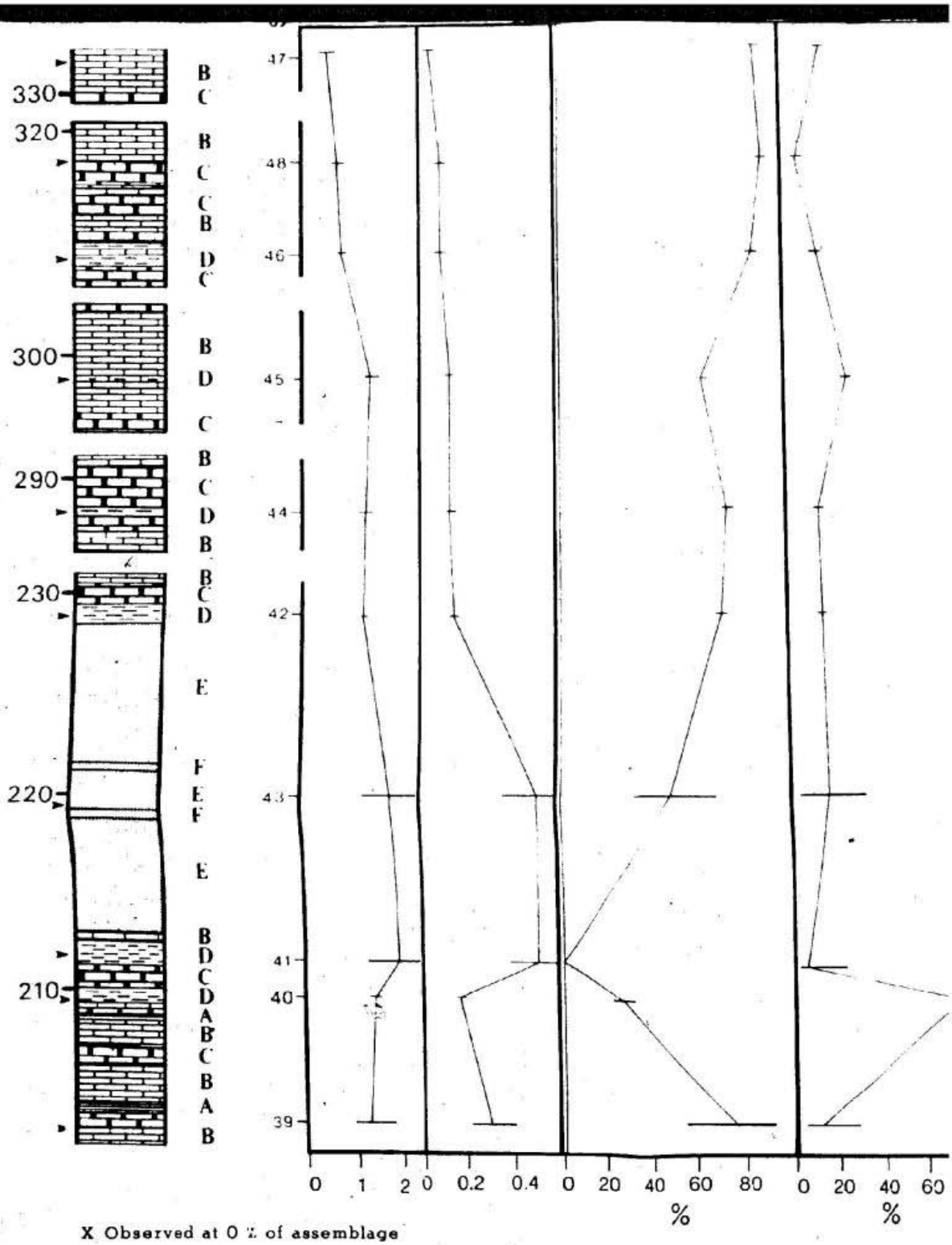
Figure 3.6


Elevation (m)
Facies
Samples
Shannon-Weaver Diversity
Evenness
Corollina
Ex
330
320
300
290
230
220
47
48
46
45
44
42
43
41
B
C
B
C
C
B
D
C
B
D
C
B
C
D
B
B
C
D
E
F
E
F
E
B
D
C


Spheripollenites
Bisaccate pollen
Others
Broken Bisaccates

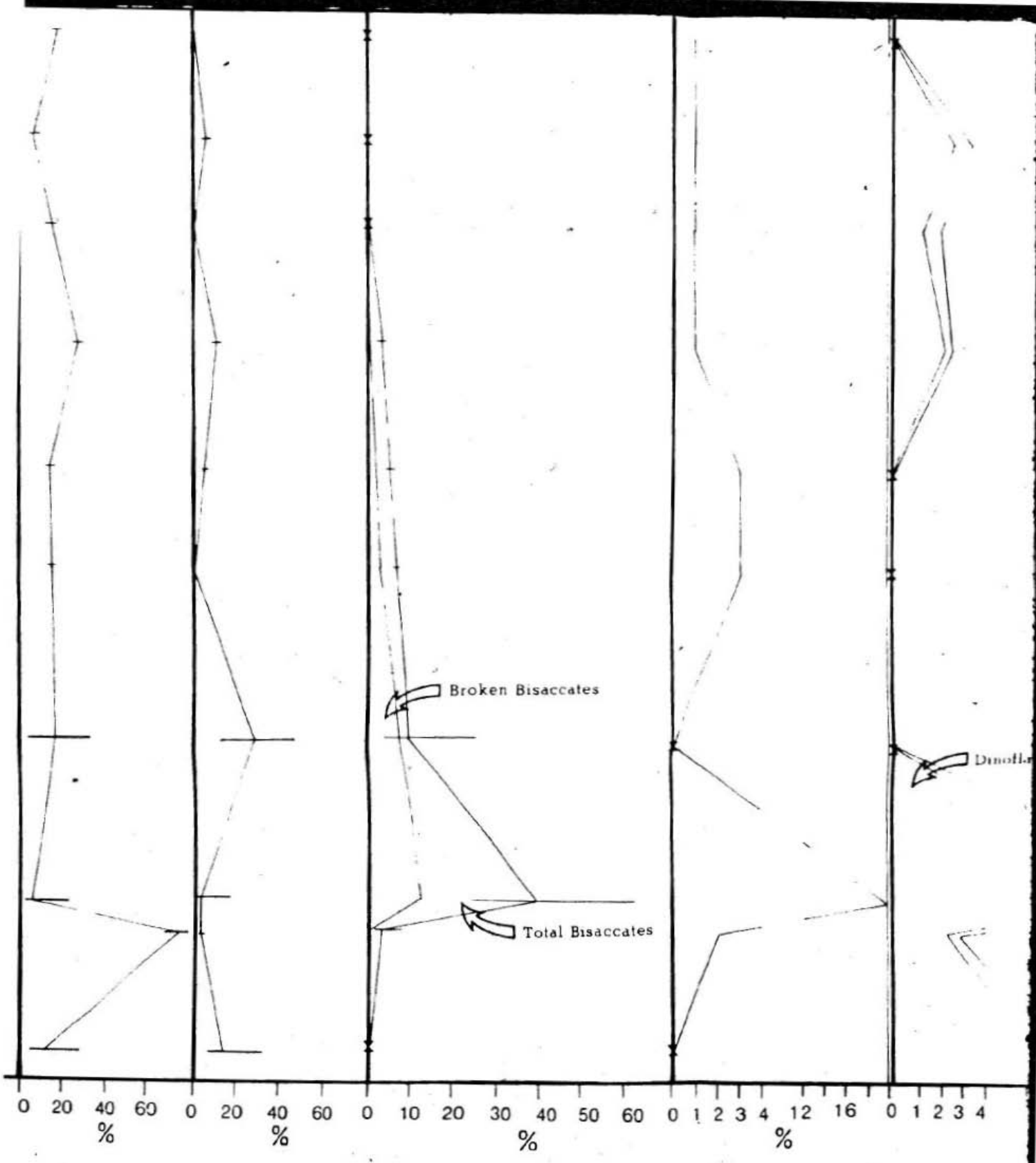

Bisaccate pollen
Others
Marine palynomorphs
Broken Bisaccates
Dinoflagellates

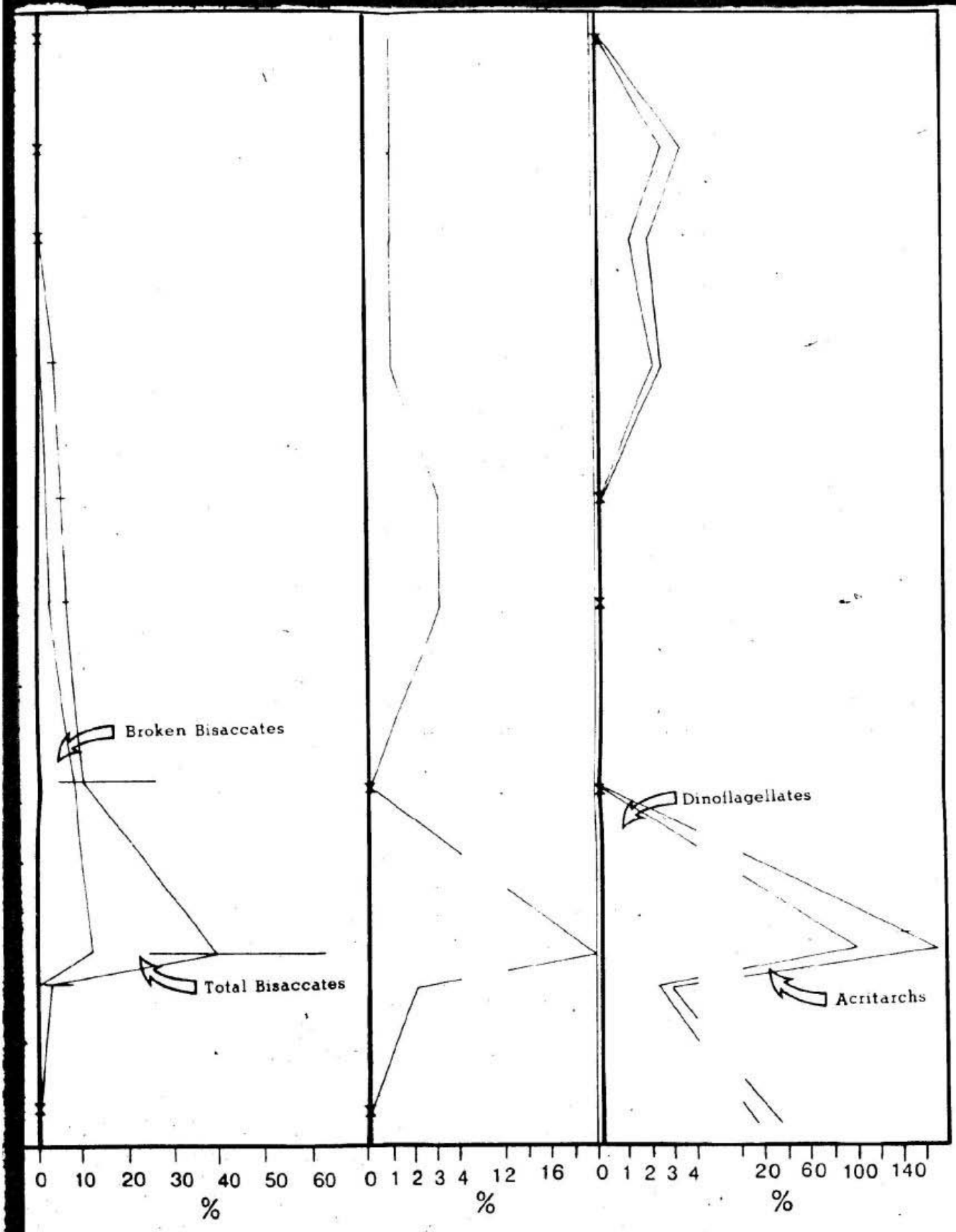

Corollina torosus
Corollina simplex
Corollina itunensis
Corollina tetrads



X Observed at 0 % of assemblage

Bars illustrate abundance limits


Broken Bisaccates
Total Bisaccates
0 20 40 60
%
0 20 40 60
%
0 10 20 30 40 50 60
%
0 1 2 3 4 12 16
%
0 1 2 3 4


Broken Bisaccates
Total Bisaccates
Dinoflagellates
Acritarchs
0 10 20 30 40 50 60
%
0 1 2 3 4 12 16
%
0 1 2 3 4 20 60 100 140
%

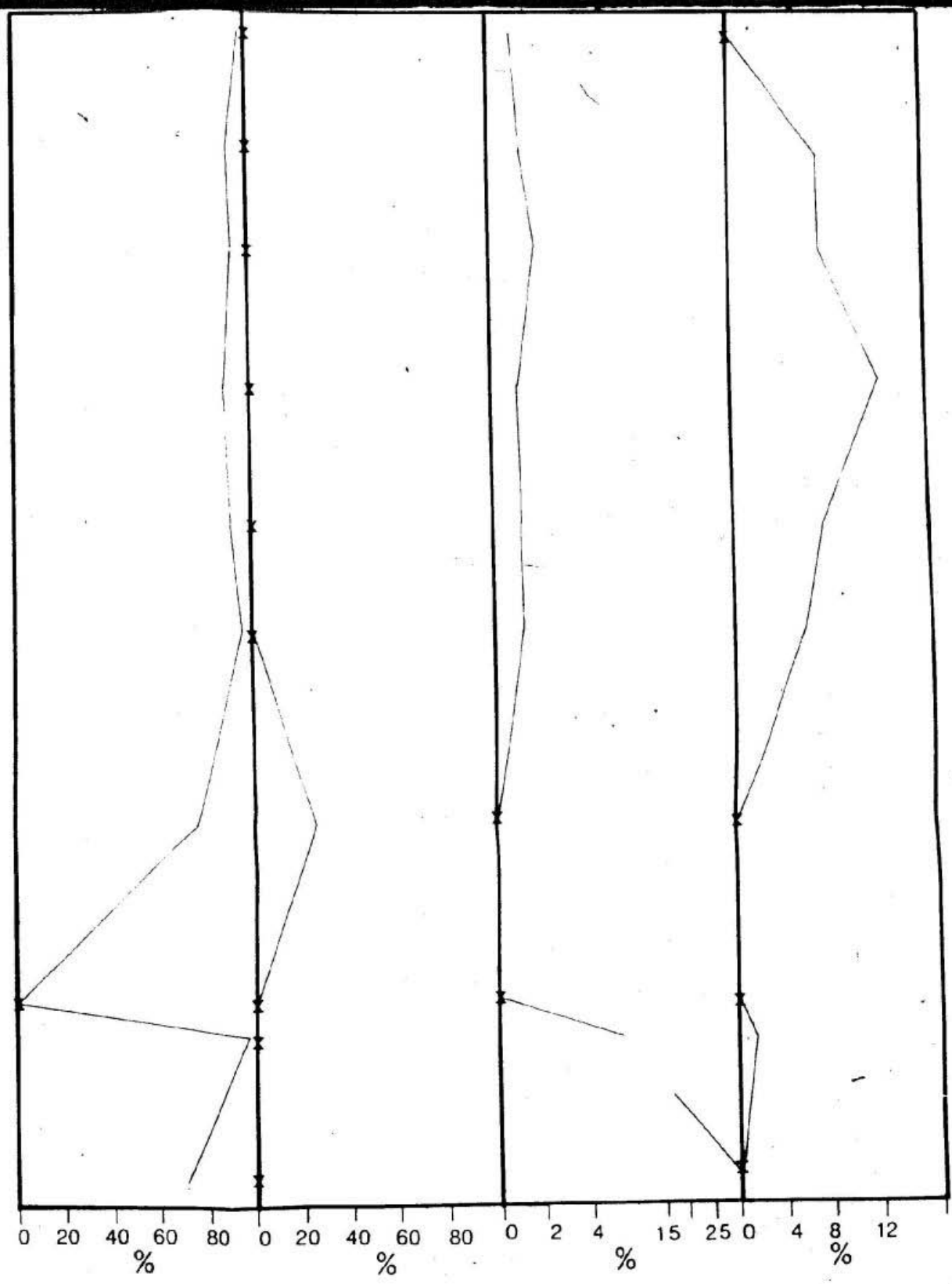
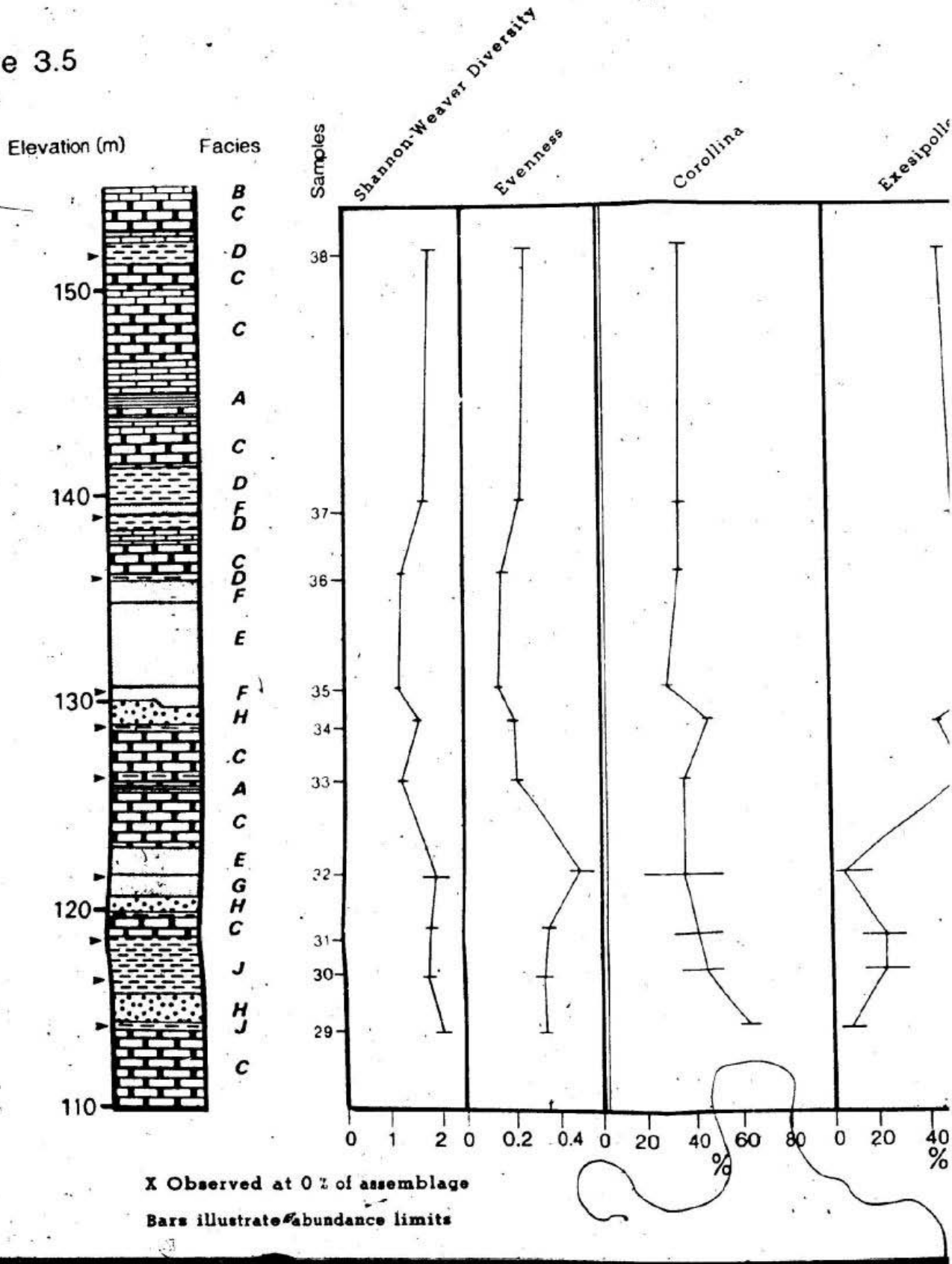
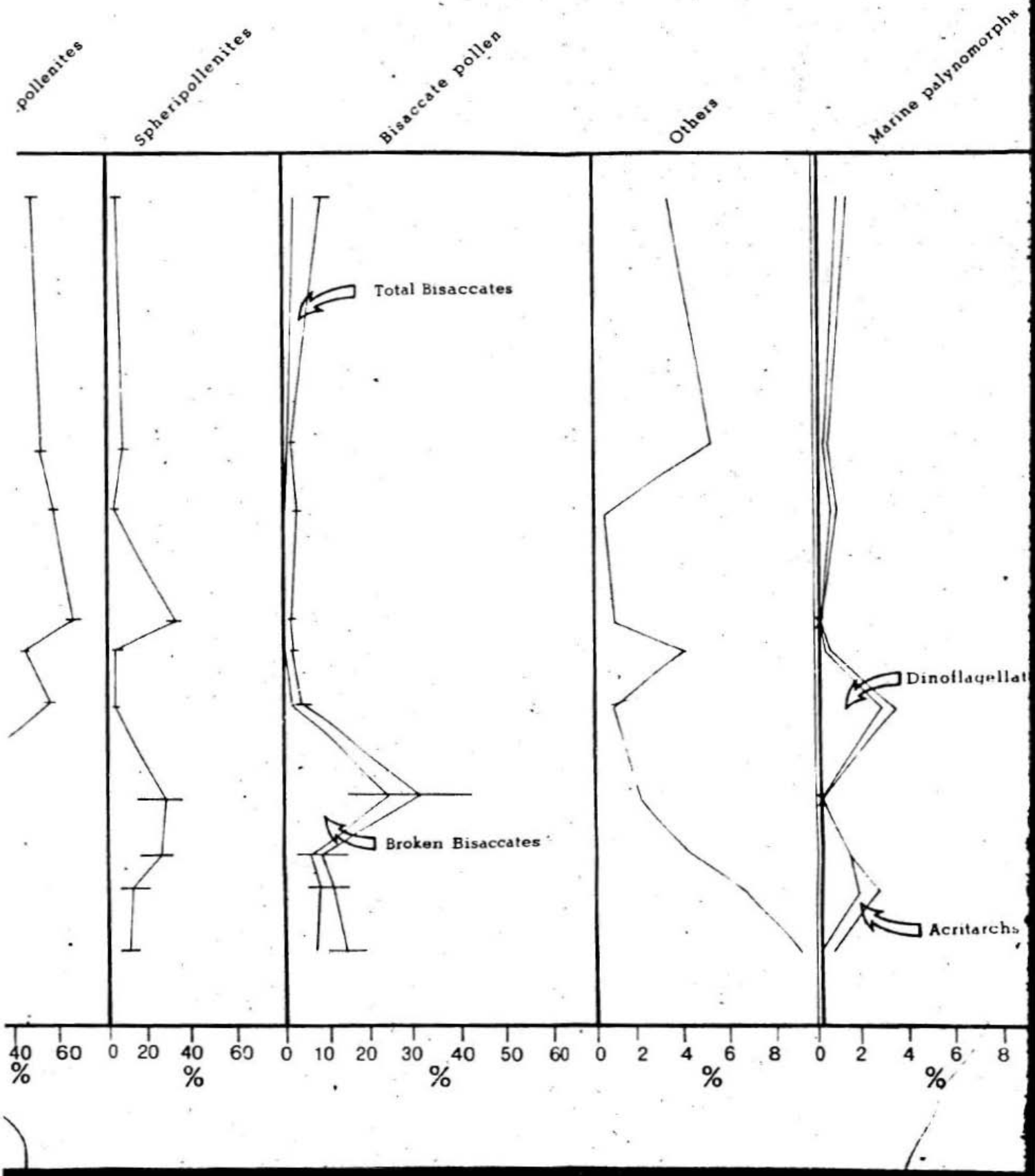
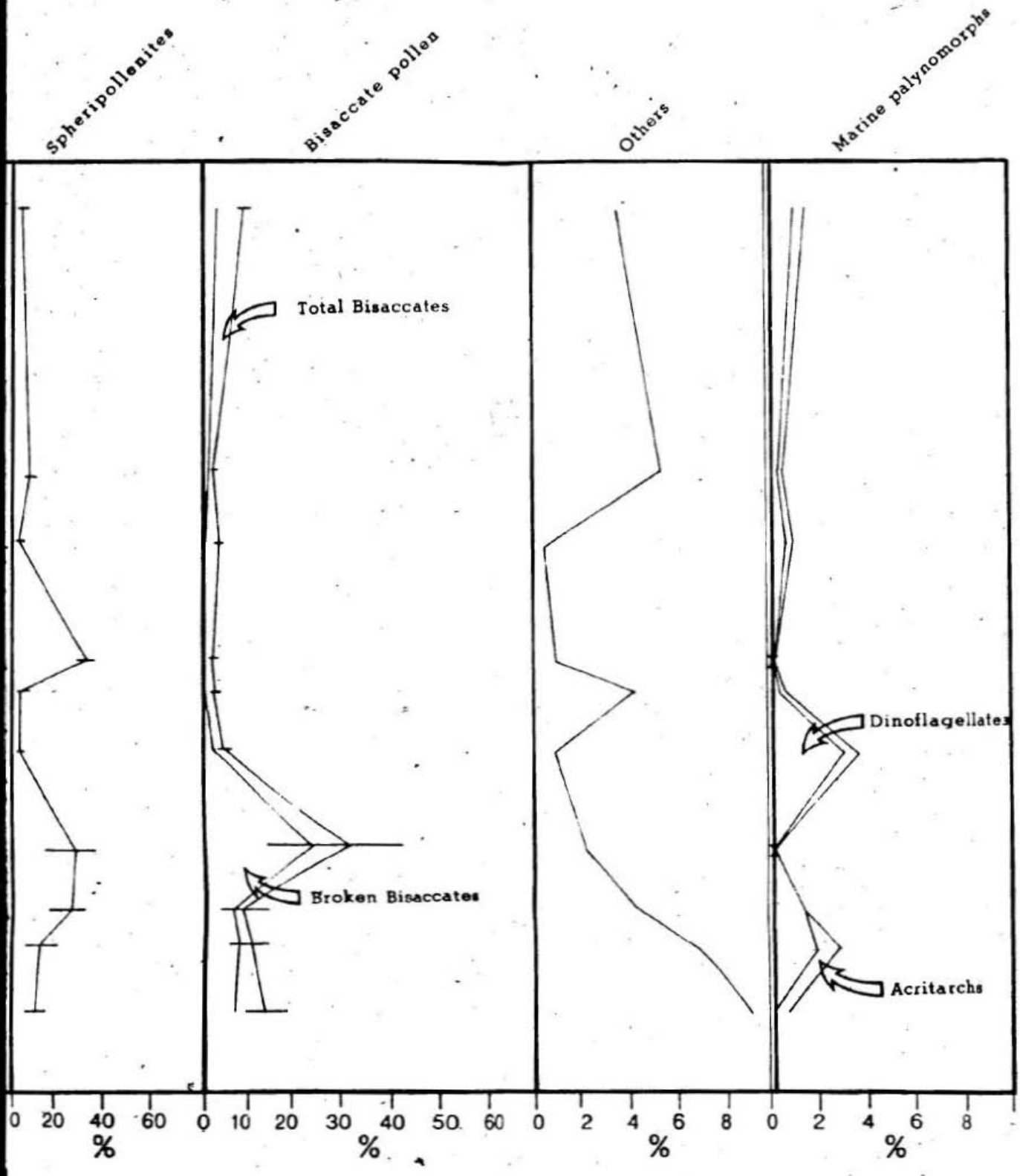
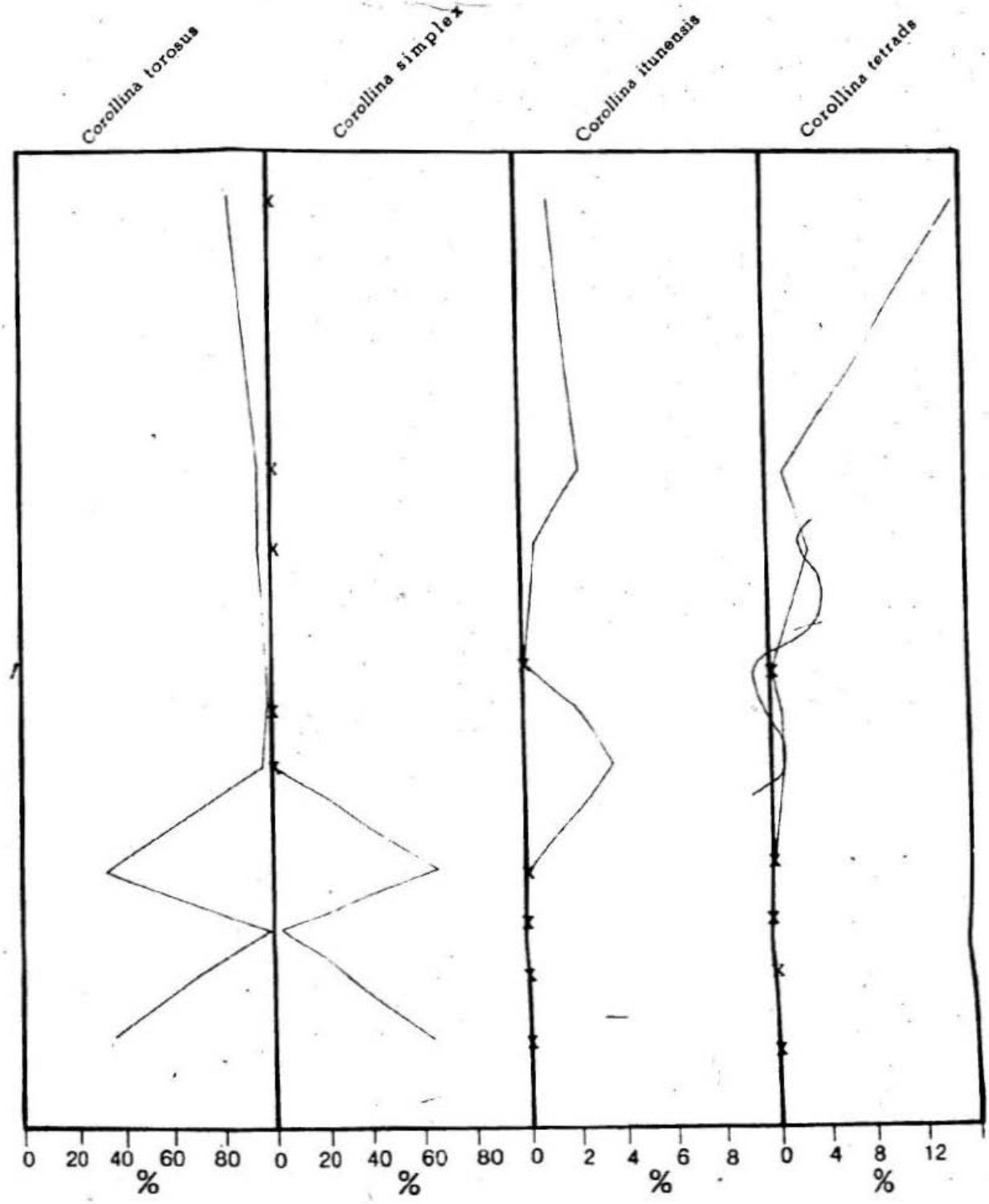

0 20 40 60 80
%
0 20 40 60 80
%
0 2 4
%
15 25 0 4 8 12
%

Figure 3.5


Elevation (m)
Facies
150
140
130
120
110
B C D C C A C D F D C D F E F H C A C E G H C J H J C
Samples
Shannon-Weaver Diversity
Evenness
Corollina
Exesipolle
38
37
36
35
34
33
32
31
30
29
0 1 2
0 0.2 0.4
0 20 40 60 80
%
0 20 40
%
X Observed at 0 % of assemblage
Bars illustrate abundance limits


pollenites
Spheripollenites
Bisaccate pollen
Others
Marine palynomorphs
Total Bisaccates
Broken Bisaccates
Dinoflagellat
Acritarchs
40 60
0 20 40 60
0 10 20 30 40 50 60
0 2 4 6 8
0 2 4 6 8
%
%
%
%
%


Spheripollenites
Bisaccate pollen
Others
Marine palynomorphs
Total Bisaccates
Broken Bisaccates
Dinoflagellates
Acritarchs
0 20 40 60
%
0 10 20 30 40 50 60
%
0 2 4 6 8
%
0 2 4 6 8
%


Corollina torosus
Corollina simplex
Corollina ituaensis
Corollina tetrade
0 20 40 60 80
%
0 20 40 60 80
%
0 2 4 6 8
%
0 4 8 12
%

Cabo Espichel Palynomorph Counts

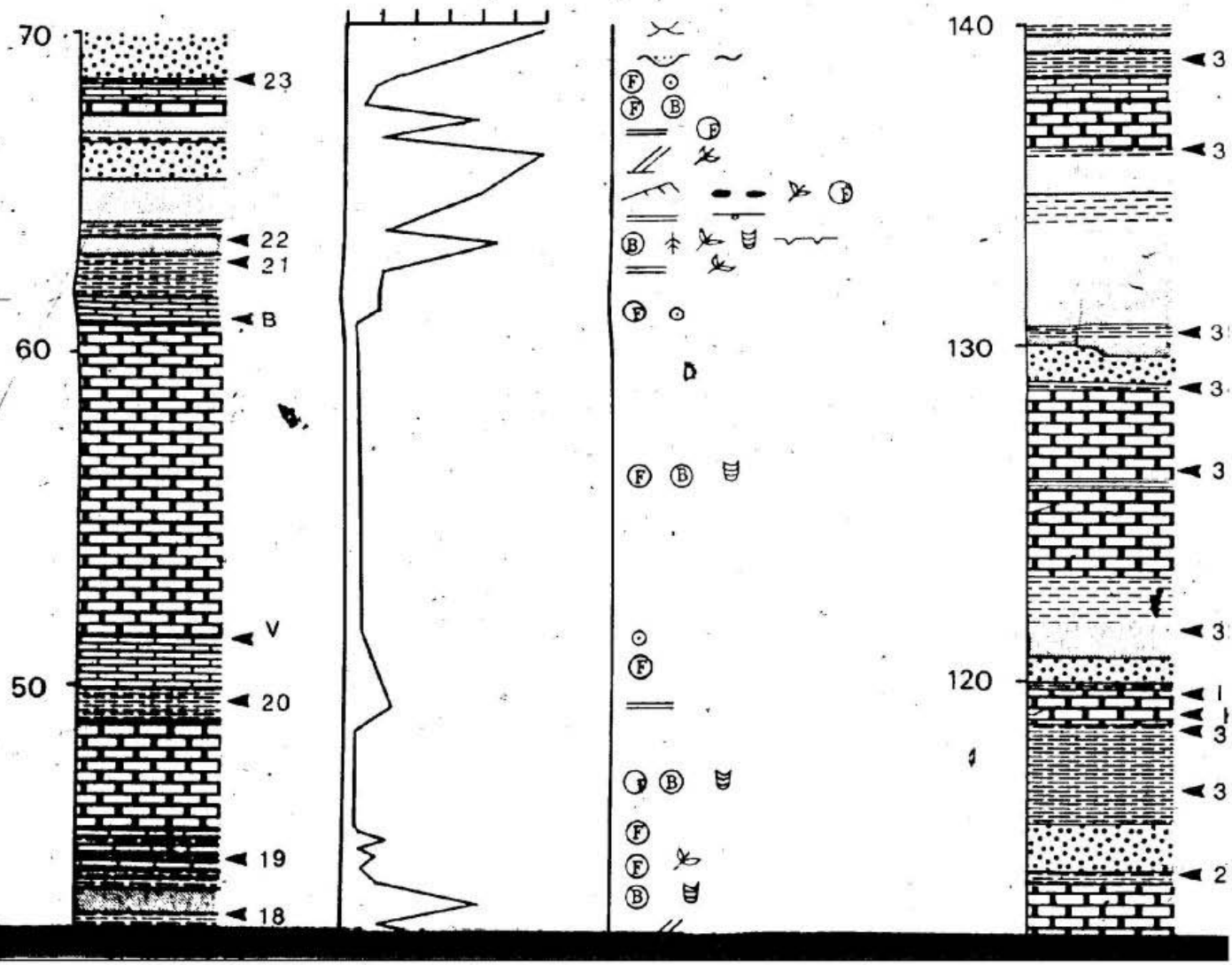
RANGE CHART OF NUMBER OF SPECIMENS BY LOWEST APPEARANCE

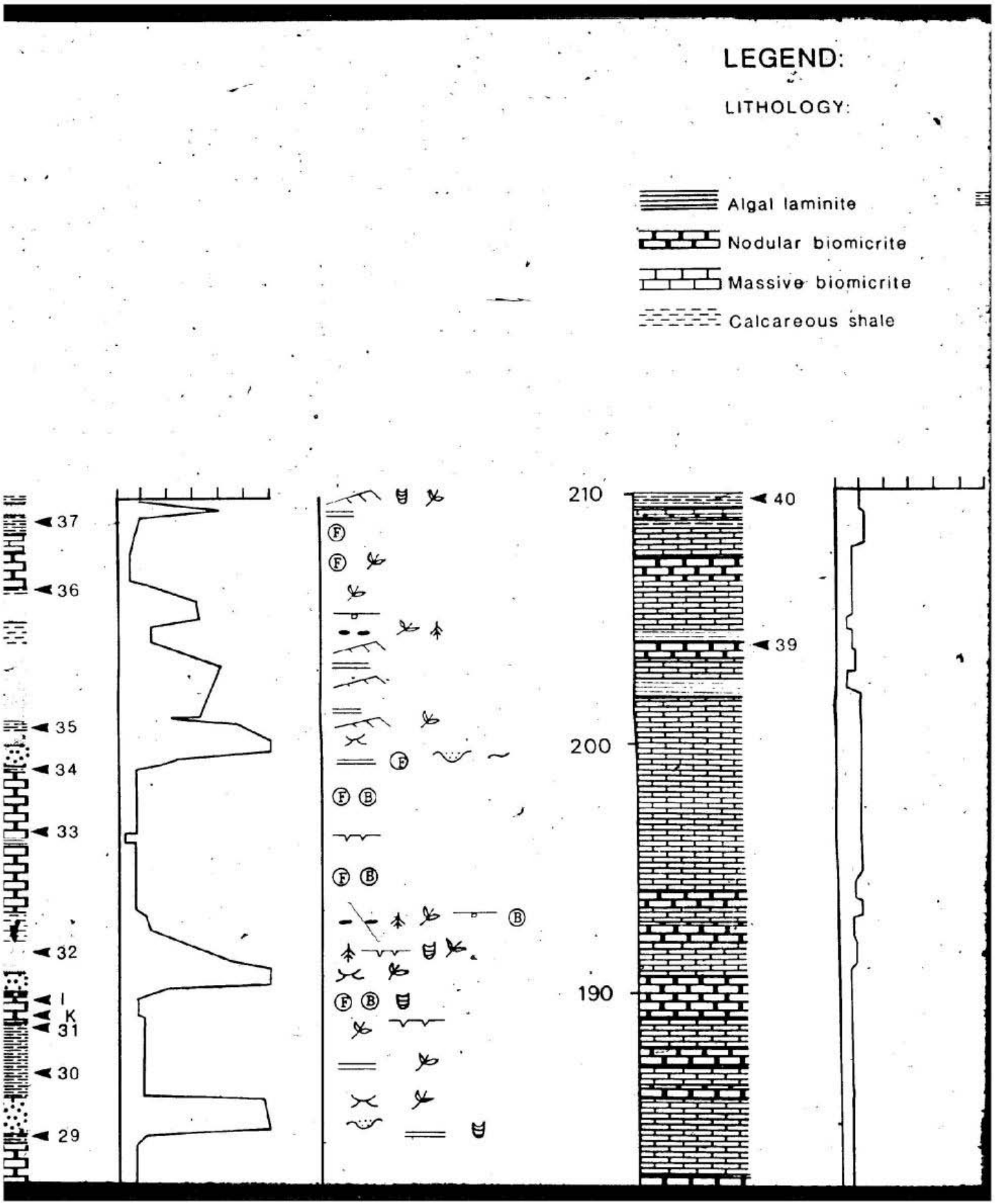
	Cerotilina teresaue	Exesapollenites scabratus	Exesapollenites tuberculus	Spheripollenites psilatus	Alisporites bilateralis	Pityosporites constrictus	Cerotilina elegans	Surculosphaeridium	Taxodiaceaepollenites hiatus	Micrystridium	Cicatricosisporites striatus	Deltoidospora hallii	Klukisporites foveolatus	Podocarpidites multesimus	Cycadopites follicularis	Stereisporites antiquasporites	Podocarpidites ellipticus	Laevigatosporites haardtii	Leptolepidites pilpiruberosus	Leptolepidites proxigranulatus	Osmundacites wellmanii	Cyathidites minor	Cretaceoporia paleozoica	Todisporites major
332.0	674	56	44	....	....	....	....	....	....	....	1	....	....	....	....	....	....	....	....	....	....	1	....	....
318.6	1090	34	56	40	....	....	....	23	1	12	....	2	....	....	....	....	....	....	....	....	....	....	1	....
314.0	1200	115	121	....	2	....	....	20	....	9	1	2	....	....	....	....	....	....	....	1	....	1	....	....
297.0	4986	1119	1209	785	117	75	....	130	....	32	....	9	....	70	....	....	2	....	....	....	....	....	....	....
286.25	1100	124	78	33	90	7	....	....	2	....	2	9	1	....	....	1	....	1	4	5	2	....	1	
229.0	1278	146	132	....	140	19	....	....	3	....	2	9	1	10	2	....	2	1	5	7	1	3	1	....
220.0	14	2	3	10	2	....	4	....	....	....	....	....	....	....	....	....	....	....	....	....	....	....	....	....
212.0	....	1	2	1	21	5	....	39	1	16	....	1	....	....	....	....	....	....	....	1	....	....	....	1
209.9	453	689	753	30	25	21	....	31	....	15	1	4	1	....	2	1	....	1	3	2	2	2	....	....
204.0	26	3	2	6	....	....	....	12	....	2	....	....	....	....	....	....	....	....	....	....	....	....	....	....
152.0	453	321	367	78	46	28	....	12	....	7	....	15	1	9	....	1	1	....	....	....	1	2	....	....
139.0	563	456	398	131	4	1	....	2	2	2	3	11	2	....	1	5	....	1	2	3	4	3	1	
134.45	1486	1390	1214	229	58	26	....	17	....	5	1	2	1	4	....	4	2	....	1	1	1	1	....	....
130.75	487	212	876	54	4	2	9	....	....	....	2	1	....	....	....	1	....	1	1	2	....	....	....	....
129.0	578	355	212	53	11	4	....	3	....	1	2	4	3	....	1	2	....	1	3	1	5	1	1	
127.0	354	278	290	32	18	5	....	20	....	4	....	2	1	....	....	1	....	....	....	....	....	1	....	....
123.0	6	2	1	15	4	....	12	....	....	....	....	....	....	....	....	....	....	....	....	....	....	....	1	
118.9	58	23	12	39	2	1	2	2	....	....	3	....	....	....	....	....	....	....	....	....	....	....	....	....
117.0	60	23	21	23	6	....	23	3	....	1	3	1	2	....	....	1	....	....	....	....	....	....	1	
114.2	90	11	21	40	24	4	141	....	1	2	5	3	....	3	1	1	....	2	....	1	1	2	1	....
106.0	108	41	21	32	9	....	142	....	2	....	3	5	....	....	....	1	....	....	....	....	....	....	1	
97.0	101	12	21	40	3	....	5	....	....	....	4	6	....	....	....	....	....	....	....	....	....	....	....	....
90.3	198	35	42	99	5	3	21	....	1	....	2	7	1	....	....	2	....	3	....	1	1	1	....	
87.8	165	65	45	71	4	13	35	....	1	....	4	3	1	....	....	2	....	2	....	1	2	1	2	....
83.1	953	256	563	66	20	5	30	....	....	....	....	3	1	....	....	....	....	....	....	2	2	2	7	
76.0	160	198	187	344	14	2	97	....	....	....	3	5	....	....	....	....	....	....	....	....	....	....	....	....
68.3	137	325	201	141	....	....	11	2	....	....	2	10	....	....	....	3	....	....	2	....	....	1	....	
64.1	....	....	....	32	32	27	....	....	....	....	....	....	....	....	....	....	....	....	....	1	....	....	....	....
63.0	....	....	7	2	2	....	....	....	....	....	....	....	....	....	....	....	....	....	....	....	....	3	....	....
49.5	2067	....	....	....	....	....	....	....	....	....	....	2	....	....	....	....	....	....	....	....	....	1	....	....
45.5	18	39	94	39	....	....	39	....	....	....	1	3	....	....	....	....	....	....	....	....	....	....	....	....
43.25	92	21	11	75	12	....	121	....	....	....	1	....	....	....	....	....	....	....	....	2	....	1	....	....	....
38.5	202	58	64	48	1	....	49	....	....	....	....	....	....	....	....	....	....	....	....	....	....	....	....	....
36.7	....	....	....	....	1	....	3	....	....	....	1	....	....	....	....	....	....	....	....	....	....	....	....	....
36.0	218	....	76	180	....	....	68	15	....	8	2	....	....	....	....	....	....	....	....	....	....	....	....	....
29.0	179	32	29	49	....	....	....	20	....	4	....	....	....	....	....	....	....	....	....	....	....	....	....	....
25.0	497	187	221	388	....	....	....	19	....	9	3	....	2	....	....	....	....	....	....	....	....	....	....	....
22.0	393	554	876	144	6	3	....	....	3	1	7	4	3	....	1	14	....	....	3	....	5	2	....	....
21.0	145	32	27	92	....	....	48	....	....	....	....	....	....	....	2	....	....	3	....	....	....	....	....	....
17.5	....	....	....	11	....	....	....	....	....	....	....	....	....	....	....	....	....	....	....	....	....	....	....	....
16.0	266	897	342	23	33	18	....	....	....	4	....	7	1	2	....	....	....	....	3	1	1	1	3	
14.0	292	528	453	172	53	27	....	12	....	6	2	12	....	42	....	4	3	....	2	1	....	2	....	....
11.0	88	120	226	374	62	15	2	....	....	....	....	....	....	....	....	....	....	....	....	....	....	....	....	....
10.0	90	65	95	200	2	....	....	18	....	2	....	....	....	....	....	....	....	....	....	....	....	....	....	....
9.0	79	185	195	460	33	4	10	....	3	1	....	5	....	5	....	....	....	....	....	....	....	....	....	....
8.0	....	....	4	6	1	....	....	....	....	....	....	....	....	....	....	....	....	....	....	....	....	....	....	....
2.75	495	500	754	389	5	....	35	....	....	....	6	4	6	....	....	....	....	....	1	2	....	3	....	....
2.3	370	126	200	....	7	2	33	....	1	....	1	1	2	....	....	....	....	....	1	....	....	6	3	
1.75	158	....	....	236	12	3	5	....	....	....	7	3	6	....	3	....	....	....	1	4	1	1	1	....
1.0	112	200	274	725	34	20	10	2	12	1	2	5	2	5	4	1	1	1	....	....	....	....	....	....

Cefamospora assugica	Isolasporites major	Retrisporites singhii	Callialasporites dampieri	Callialasporites triloboatus	Callialasporites trilobatus	Biretisporites eneabbaensis	Impardecaspora apiverrucata	Converrucosisporites exquisitus	Other Dinoflagellates	Coronina ityuneneis	Callialasporites turbatus	Perinopollenites elatoides	Coronina tetrads	Cicatricosporites jurienensis	Reticulatisporites reticulatus	Araucariacites australis	Cerebropollenites macroverrucosus	Tuberculatisporites montagnacus	Pilosisporites trichopapillosus	Polycingulatisporites reduncus	Undulatisporites undulapolus	Dictyophyllidites harrisii	Chasmatosporites minor	Unknown	Total Terrestrial		
.	....	....	....	....	....	....	2	....	....	2	....	....	....	2	....	....	....	....	....	....	....	....	....	2	783	332.0
1	....	....	....	....	....	....	....	....	9	20	....	....	89	....	....	....	....	....	....	....	....	....	....	9	1334	318.6
1	....	....	....	....	....	1	....	....	....	12	....	....	98	....	1	....	....	....	....	3	....	....	....	15	1558	314.0
.	....	....	....	....	....	....	7	....	....	60	13	....	....	478	....	....	1	....	....	....	....	....	....	21	9068	297.0
.	1	1	1	....	....	....	23	2	2	2	9	....	1	80	....	....	1	2	2	....	2	2	1	21	1590	286.2
3	1	....	1	....	....	....	24	2	5	2	9	....	....	71	....	1	....	5	6	2	2	....	2	21	1892	229.0
.	....	....	....	....	....	....	4	....	....	....	....	....	....	....	....	....	....	....	....	....	....	....	....	5	38	220.0
.	1	....	....	....	1	....	7	1	1	19	....	....	....	....	....	....	1	1	....	....	....	....	....	14	46	212.0
2	....	....	....	1	2	....	....	....	1	11	19	1	1	3	1	2	1	2	1	4	....	....	2	2	2029	209.9
.	....	....	....	....	....	....	....	....	....	....	11	....	....	....	....	....	....	....	....	....	....	....	....	2	50	204.0
3	1	4	1	....	3	10	1	1	1	6	....	2	76	....	....	....	1	1	1	....	1	....	1	21	1429	152.0
1	....	....	....	....	3	....	3	3	1	12	....	2	8	1	....	....	1	2	2	....	2	4	3	4	1449	139.0
1	....	....	....	....	....	....	....	2	1	7	6	....	1	45	1	....	1	....	1	5	1	....	....	2	4482	136.4
.	....	....	....	....	....	....	2	....	1	1	....	....	....	....	1	....	1	....	....	....	....	....	....	5	1657	130.7
1	1	1	1	....	....	....	1	4	....	1	12	....	1	4	1	....	....	3	2	....	1	3	1	3	1224	129.0
1	....	....	1	....	....	....	3	....	2	6	13	....	....	3	....	....	....	....	....	....	....	....	....	9	1004	127.0
.	1	....	....	....	....	....	11	....	....	....	....	....	....	....	....	....	....	....	....	....	....	....	....	3	51	123.0
.	....	....	....	....	....	....	7	....	....	1	....	....	....	....	....	....	....	....	....	....	....	....	....	....	148	118.4
.	1	....	....	....	1	....	11	....	....	....	1	....	....	....	....	....	....	....	....	....	....	....	....	5	187	117.0
2	1	....	1	1	2	....	19	....	....	1	....	....	2	2	....	....	....	1	1	....	....	....	....	20	381	114.3
.	1	....	....	....	2	....	32	....	....	1	....	....	1	....	....	....	....	3	....	....	....	....	....	3	403	104.6
.	....	....	....	....	....	....	11	....	....	....	....	....	....	....	....	....	....	....	....	....	....	....	....	11	202	97.0
1	....	1	1	....	2	....	9	1	1	2	....	....	1	1	....	....	....	2	2	1	....	....	1	19	447	90.3
1	2	....	1	....	1	....	6	2	1	1	....	....	....	1	....	....	....	3	3	....	....	2	1	15	431	87.8
2	7	2	....	....	....	....	10	....	2	1	....	....	....	13	....	1	....	....	....	1	6	....	....	25	1947	83.1
.	....	....	....	....	....	....	19	....	....	....	....	....	....	....	....	....	....	....	....	....	....	....	....	1	1029	76.0
1	....	2	1	....	....	....	....	....	....	....	....	....	....	....	....	....	....	....	....	....	2	....	....	7	838	68.3
.	....	....	....	....	....	....	14	....	....	....	....	....	....	....	....	....	....	....	....	....	....	....	....	34	105	64.1
.	....	....	....	....	....	....	2	....	....	....	....	....	....	....	....	....	....	....	....	....	....	....	....	8	14	63.0
3	....	....	....	....	....	....	....	....	....	....	104	....	....	30	....	....	....	....	....	....	....	....	....	62	2206	49.5
1	....	....	....	....	....	....	....	....	....	....	....	....	....	....	....	....	....	....	....	....	....	....	....	4	234	45.5
.	....	....	....	....	....	....	15	....	....	....	....	....	....	....	....	....	....	....	....	....	....	....	....	3	359	43.2
1	....	....	....	....	....	....	22	....	....	....	....	....	....	....	....	....	....	....	....	....	....	....	....	6	447	38.5
.	....	....	....	....	....	....	6	....	....	....	....	....	....	....	....	....	....	....	....	....	....	....	....	....	11	34.7
.	....	....	....	....	....	....	....	....	1	4	....	....	....	18	....	....	....	3	....	....	....	....	....	7	576	34.0
.	....	....	....	....	....	....	....	....	6	22	....	....	....	20	....	....	....	....	....	....	....	....	....	2	311	29.0
.	....	....	....	....	....	....	....	4	8	12	....	....	....	46	....	1	....	....	....	2	....	....	....	6	1363	25.0
2	....	....	....	2	2	....	7	6	3	....	....	....	....	1	....	4	....	....	1	....	....	....	....	10	2044	22.0
.	....	....	....	....	....	....	22	....	....	....	....	....	....	....	....	....	3	4	....	....	....	....	....	11	377	21.0
.	....	....	....	....	....	....	5	....	....	....	....	....	....	....	....	....	....	....	....	....	....	....	....	10	14	17.5
1	3	....	....	1	4	....	34	....	....	1	12	2	1	6	2	2	....	....	....	....	....	....	....	8	1442	14.0
2	....	....	....	....	3	....	20	....	....	2	2	....	....	7	....	....	....	....	....	....	....	....	....	9	1427	14.0
.	....	....	....	....	....	....	6	....	....	....	....	....	....	....	....	....	....	....	....	....	....	....	....	6	893	11.0
.	....	....	....	....	....	....	....	....	....	4	....	....	....	....	....	....	....	....	....	....	....	....	....	18	452	10.0
.	....	....	....	....	....	....	....	....	....	....	....	....	....	....	....	....	....	....	....	....	....	....	....	10	979	9.0
.	....	....	....	....	....	....	7	....	....	....	....	....	....	....	....	....	....	....	....	....	....	....	....	....	18	8.0
3	....	....	....	....	....	....	9	1	1	....	....	....	....	....	....	....	....	....	....	....	....	....	....	78	2213	2.75
6	3	....	2	1	1	....	....	....	....	....	....	....	....	....	....	....	....	....	....	....	....	....	....	18	754	2.3
1	1	2	....	....	....	....	....	....	....	....	....	....	....	....	....	....	....	....	....	....	....	....	....	8	443	1.75
.	....	....	....	....	....	....	....	....	....	....	....	....	....	....	....	....	....	....	....	....	....	....	....	38	1408	1.0

Figure 2.32

Stratigraphic Section of Cabo Espichel, Portugal




LEGEND:
LITHOLOGY:
Algal laminite
Nodular biomicrite
Massive biomicrite
Calcareous shale
37
36
35
34
33
32
I
K
31
30
29
210
200
190
40
39
F
B

ND:

OGY:

SEDIMENTARY STRU

aminite

r biomicrite

e biomicrite

eous shale

Non-calcareous shale

Siltstone

Sandstone

Granule conglomerate

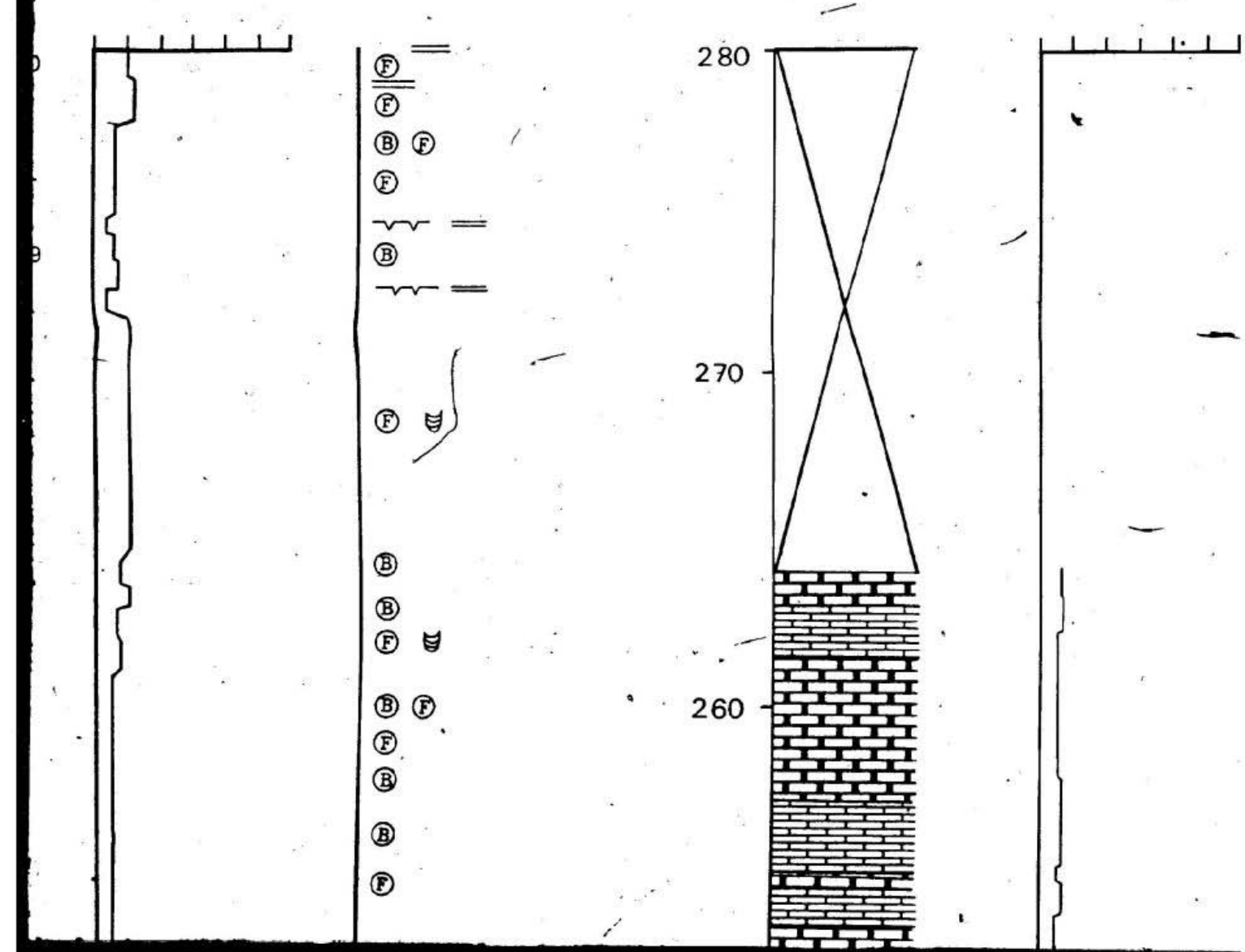
Horizontal parallel la

Trough cross-bedding

Planar cross-bedding

Climbing ripple lamina

Scour surface



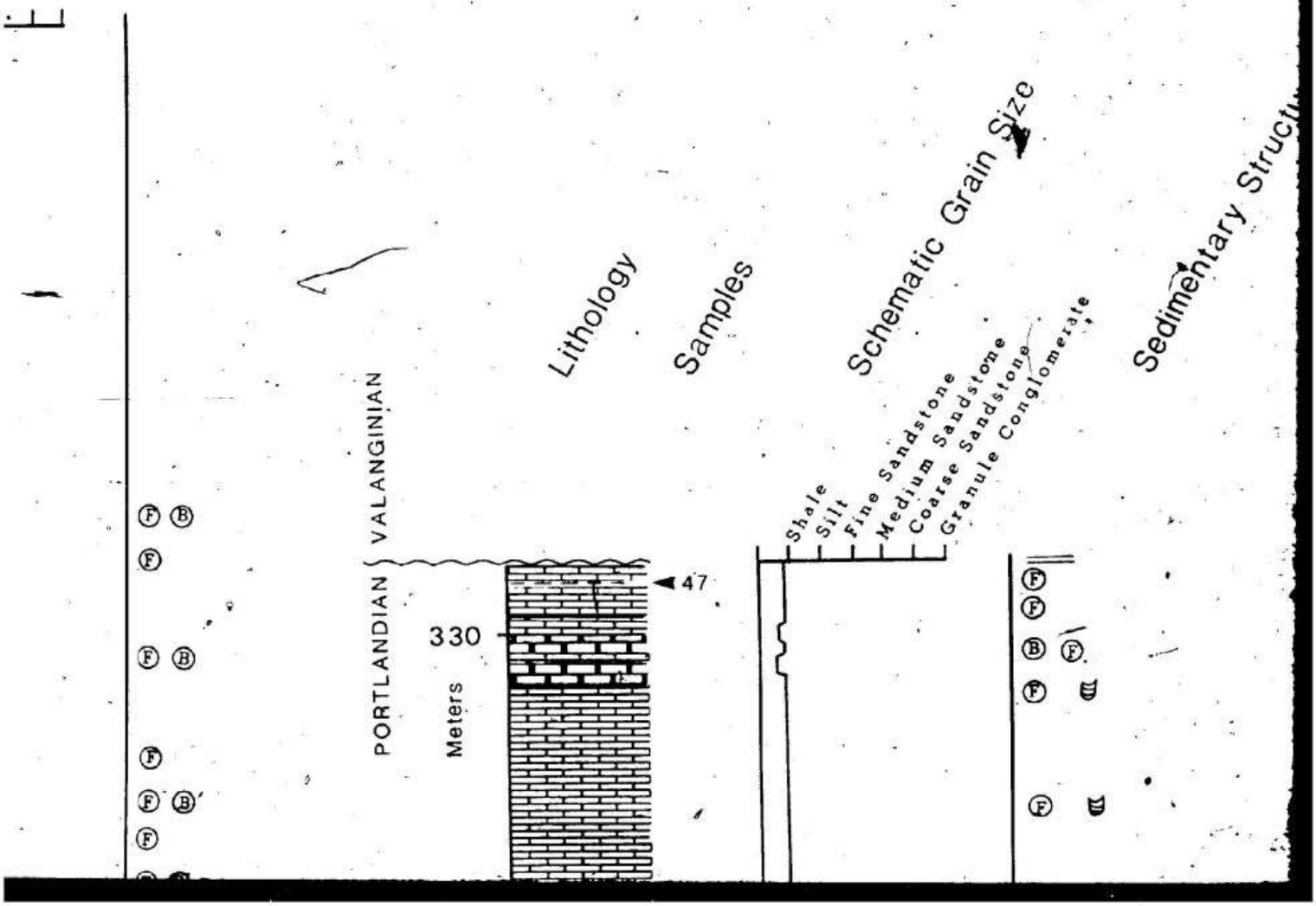
STRUCTURES AND ACCESSORIES:

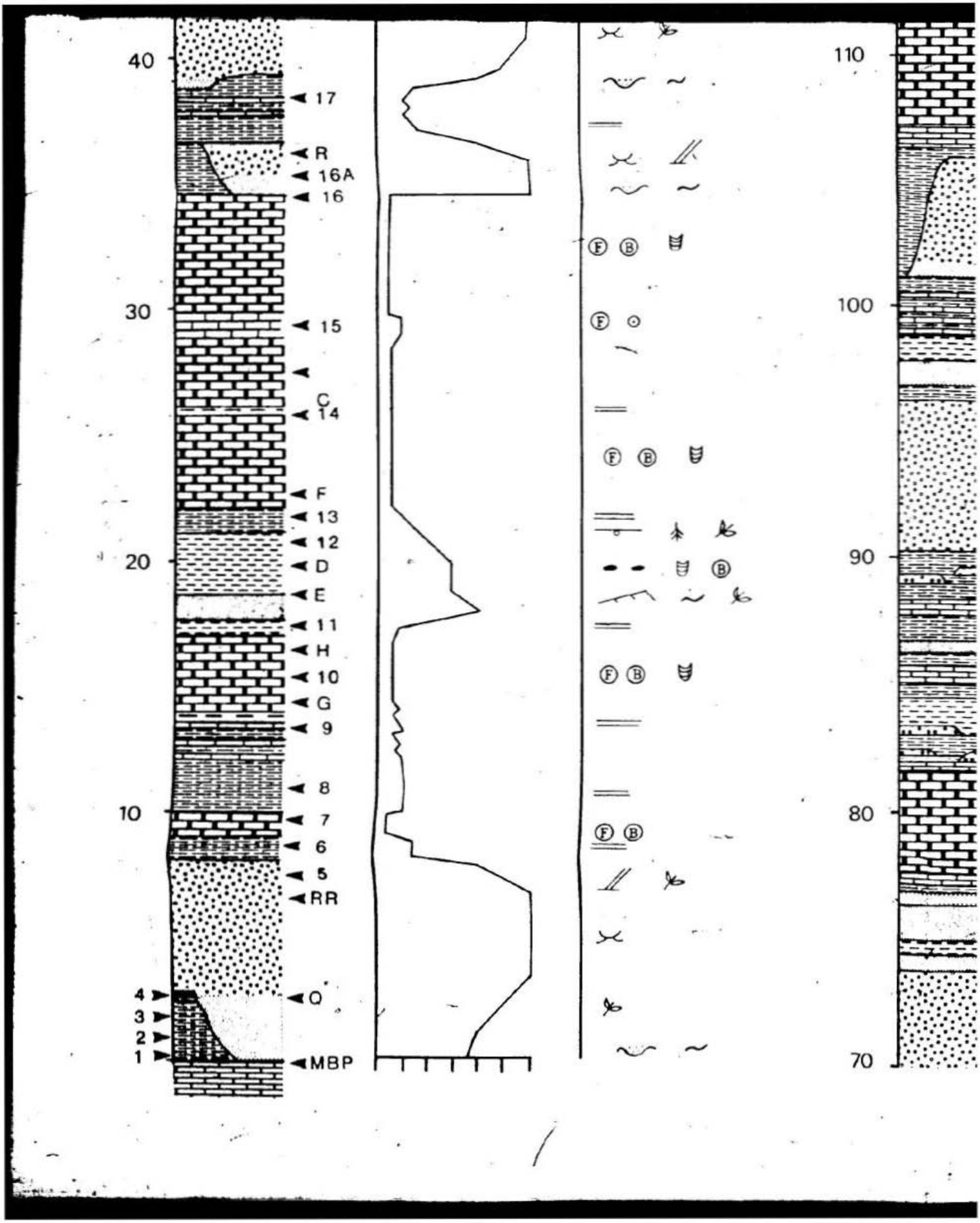
el lamination
dding
lding
amination

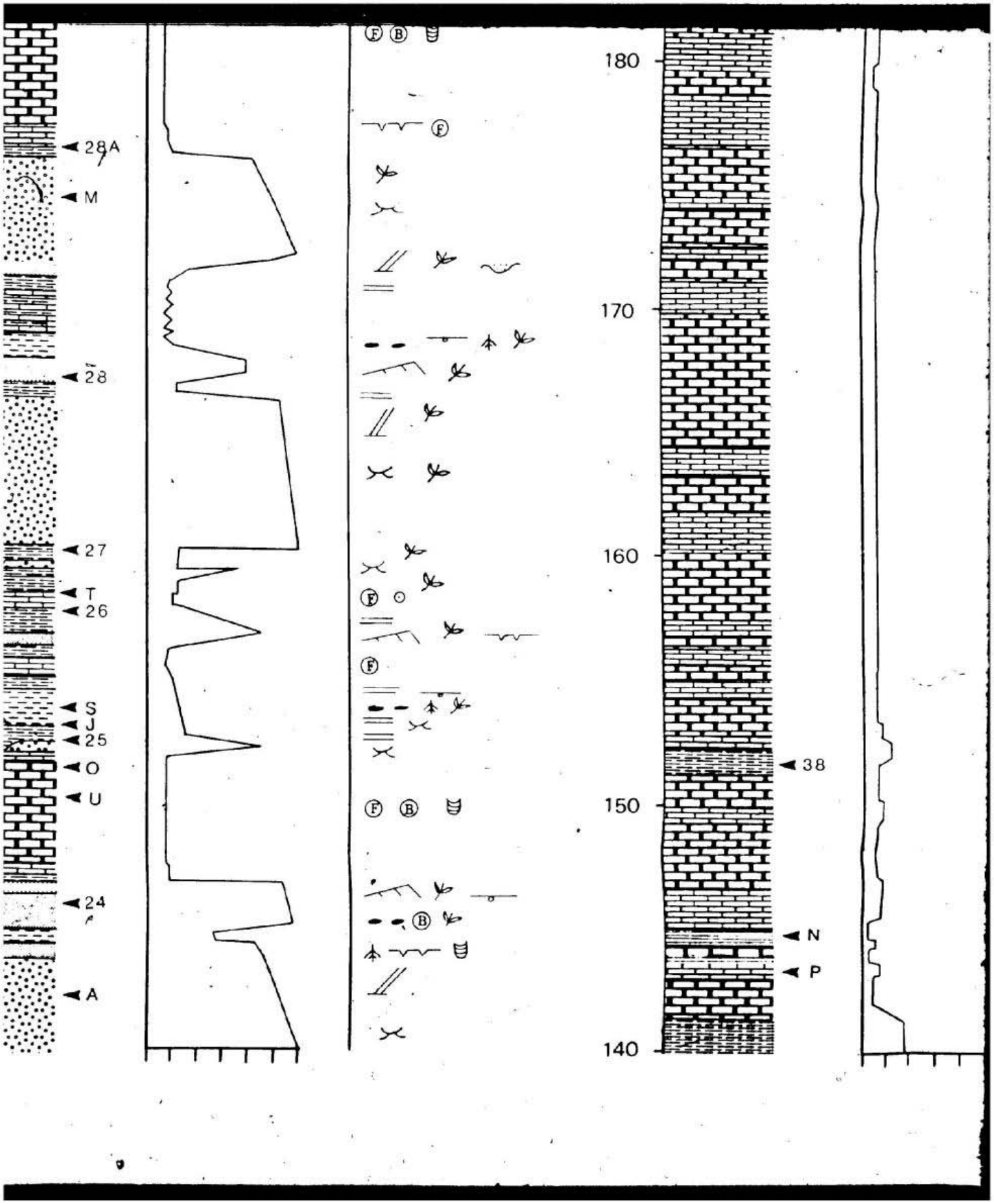
Burrows
Biofurbation
Fossiliferous
Mud cracks
Load casting

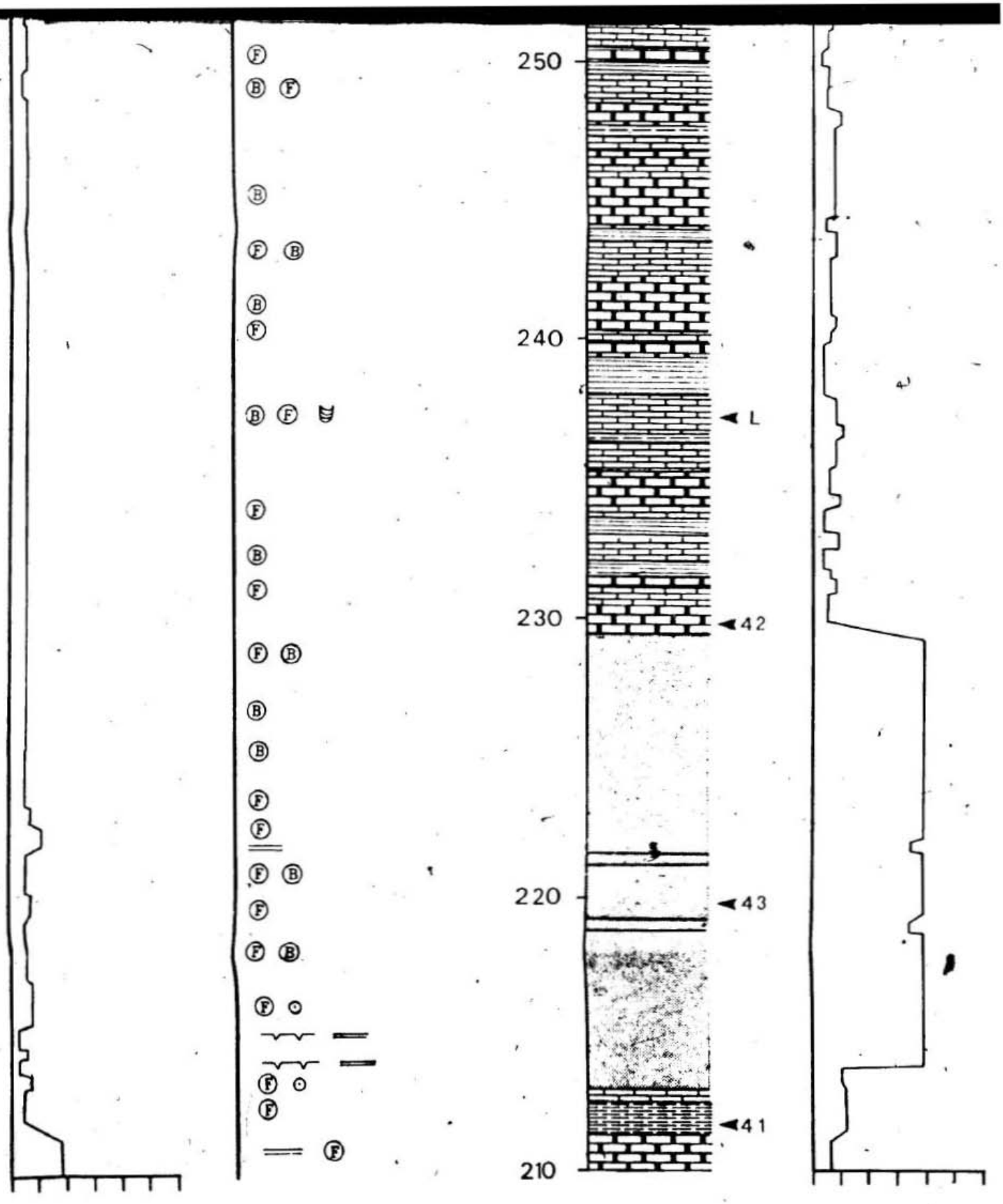
Nodules (calcrete)
Rip-up clasts
Roots in situ
Plant and woody debris
Oolitic

1 ◄ Palynology sample
A ◄ Hand samples




40
30
20
10
17
R
16A
16
15
C
14
F
13
12
D
E
11
H
10
G
9
8
7
6
5
RR
4
3
2
1
Q
MBP
110
100
90
80
70
F
B


28A
M
28
27
T
26
S
J
25
O
U
24
A
38
N
P
180
170
160
150
140


250
240
230
220
210
L
42
43
41

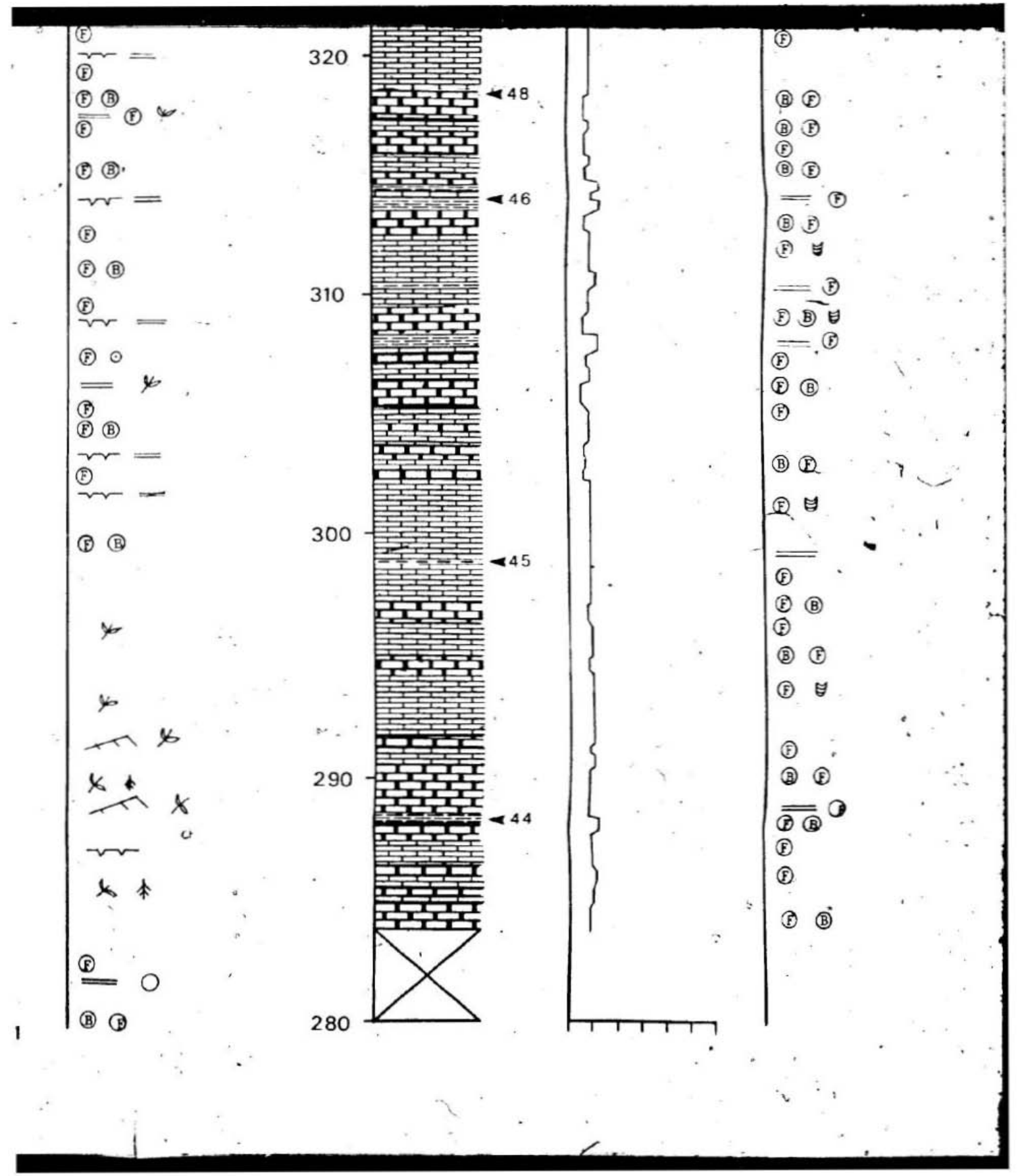
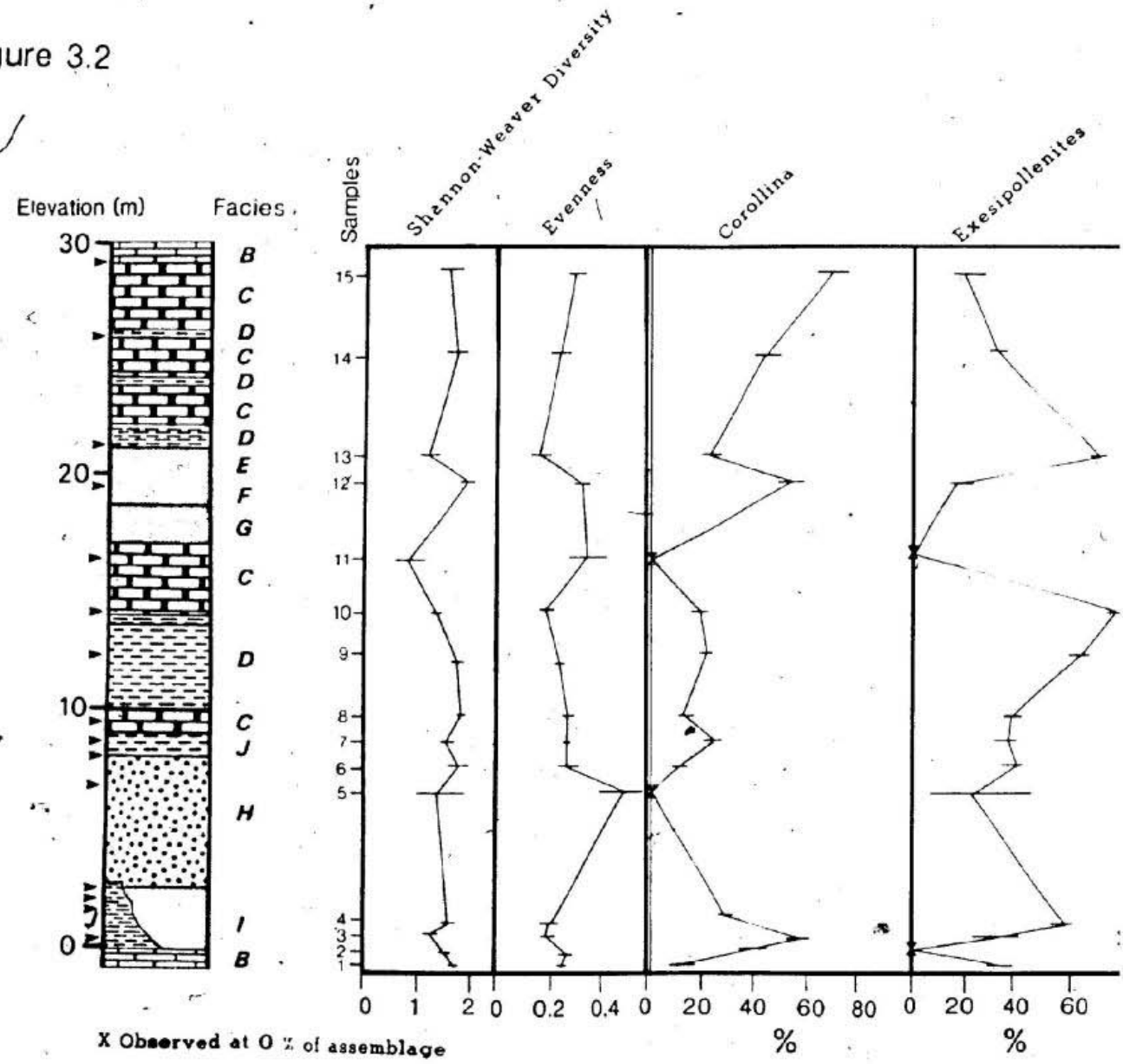
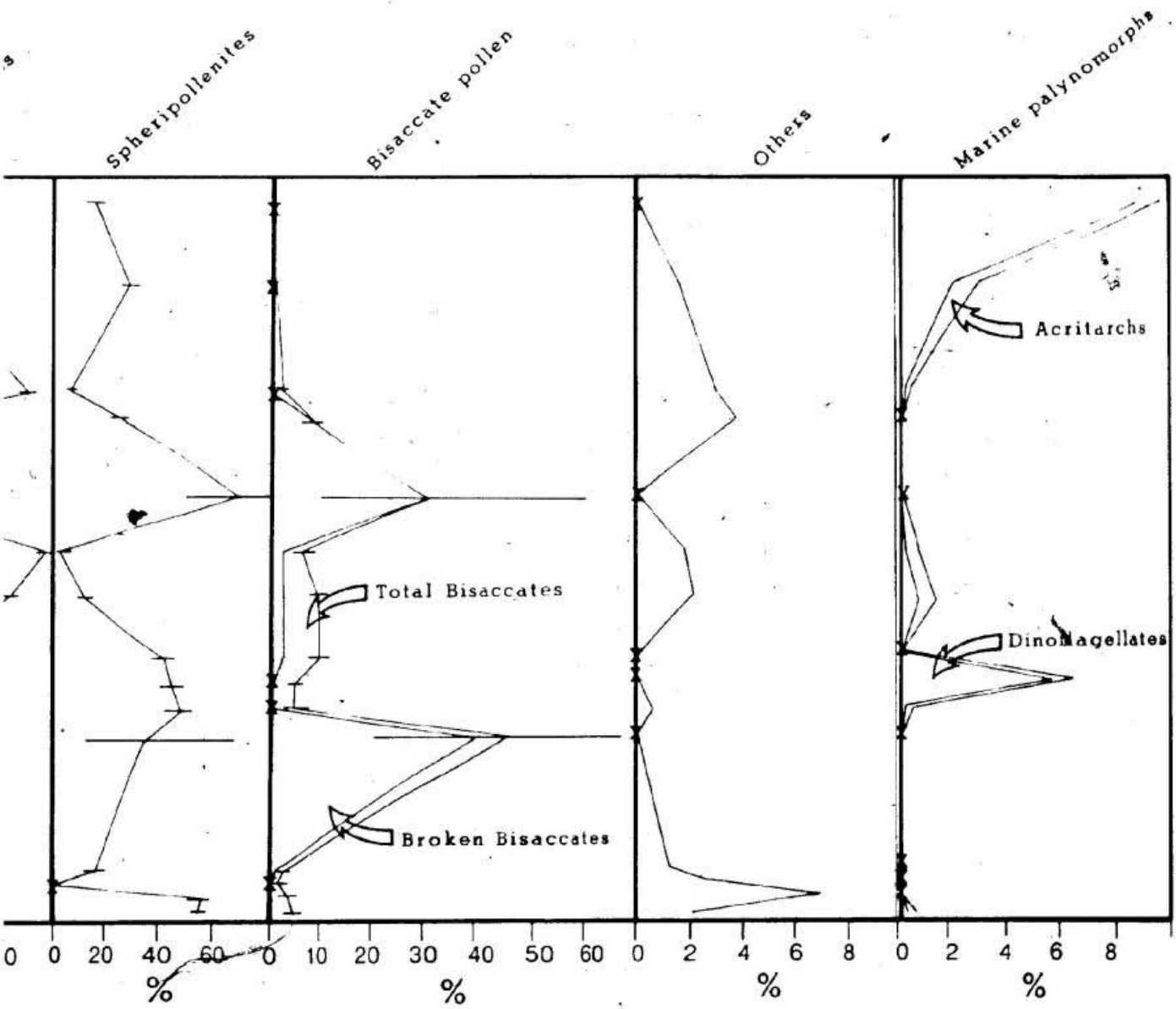

320
310
300
290
280
48
46
45
44

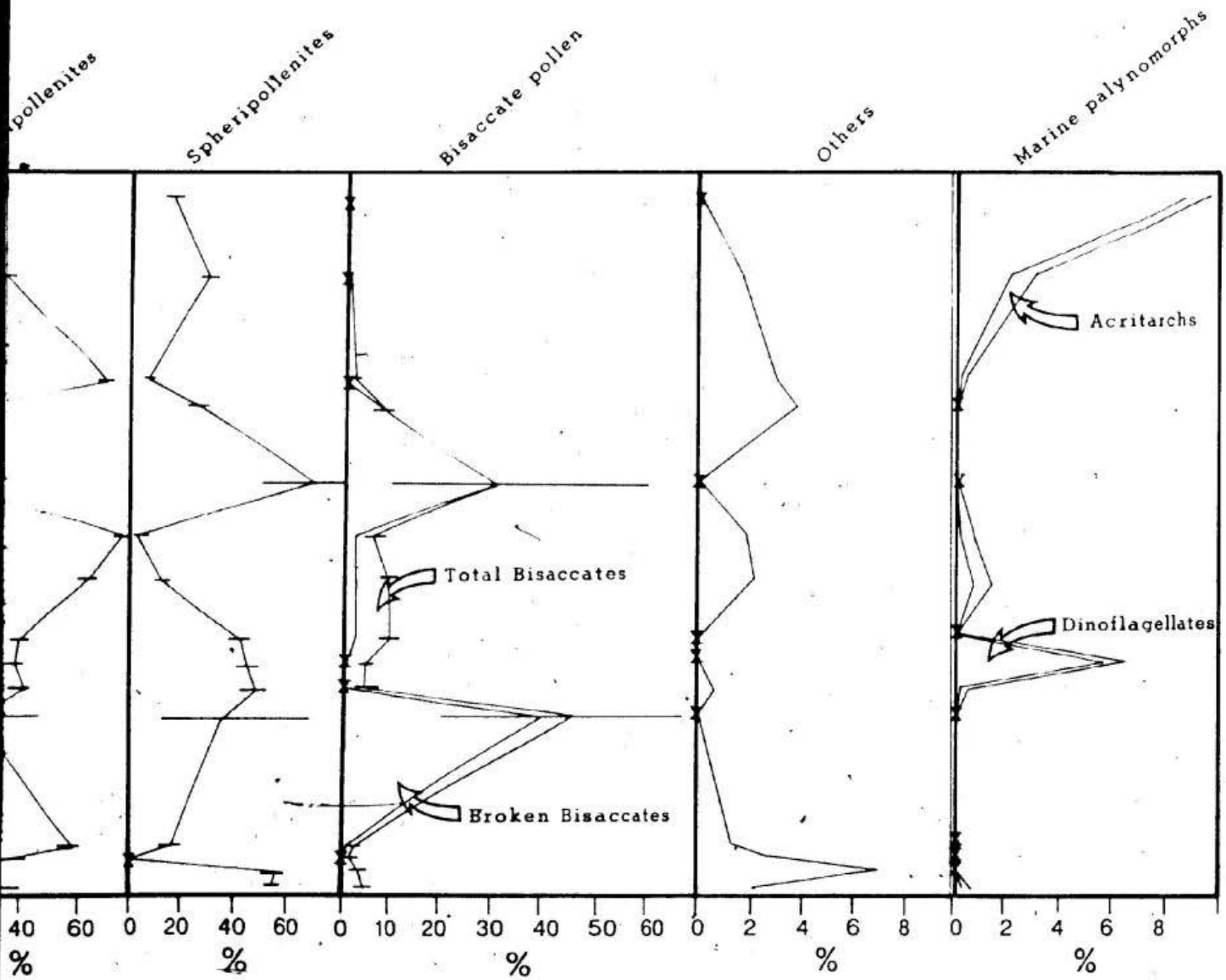
Figure 3.2



X Observed at 0 % of assemblage

Bars illustrate abundance limits


Spheripollenites
Bisaccate pollen
Others
Marine palynomorphs
Total Bisaccates
Broken Bisaccates
Acritarchs
Dinoflagellates
0 0 20 40 60
%
0 10 20 30 40 50 60
%
0 2 4 6 8
%
0 2 4 6 8
%


pollenites
Spheripollenites
Bisaccate pollen
Others
Marine palynomorphs
Total Bisaccates
Broken Bisaccates
Acritarchs
Dinoflagellates
40 60
0 20 40 60
0 10 20 30 40 50 60
0 2 4 6 8
0 2 4 6 8
% % % % %

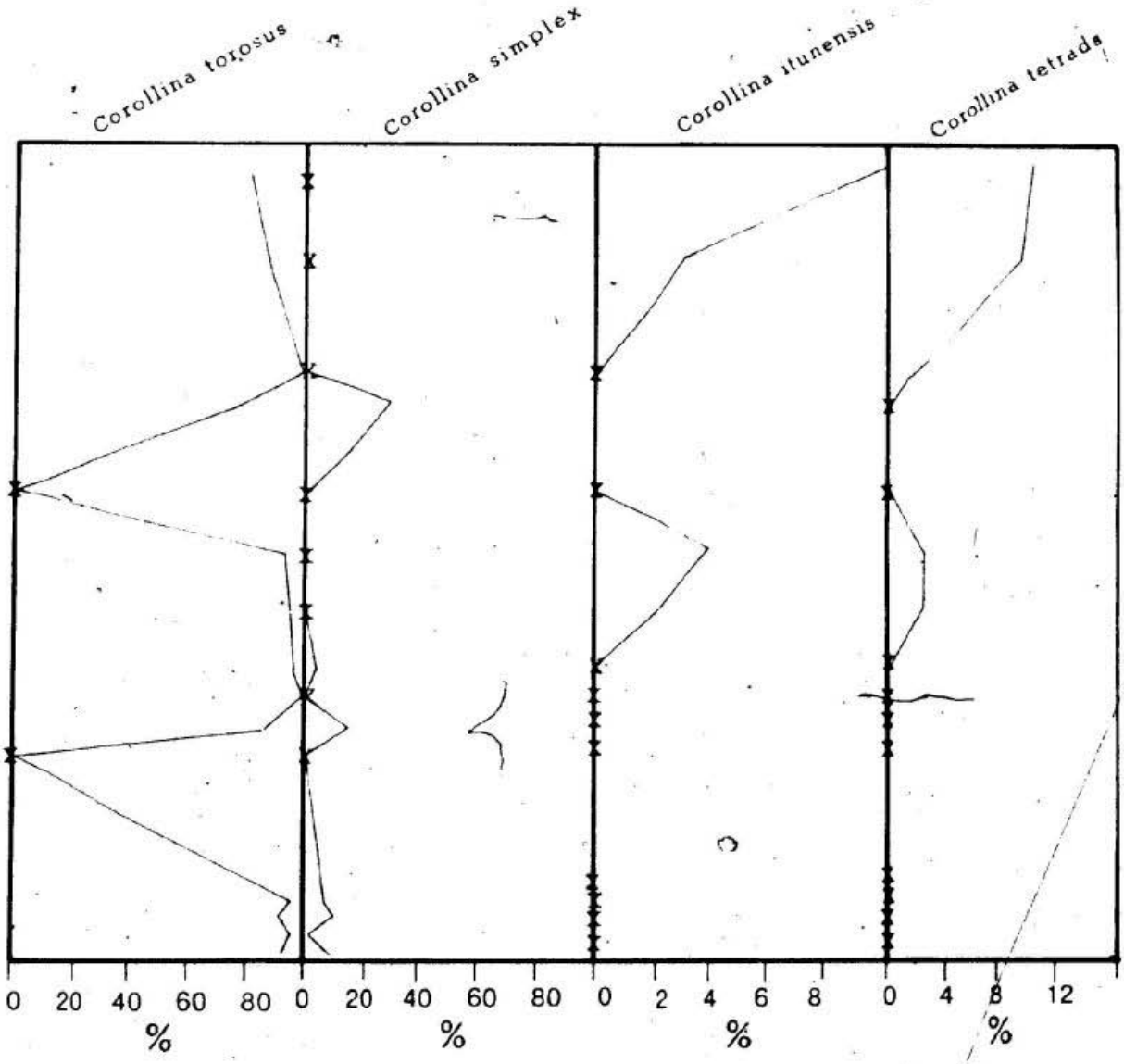
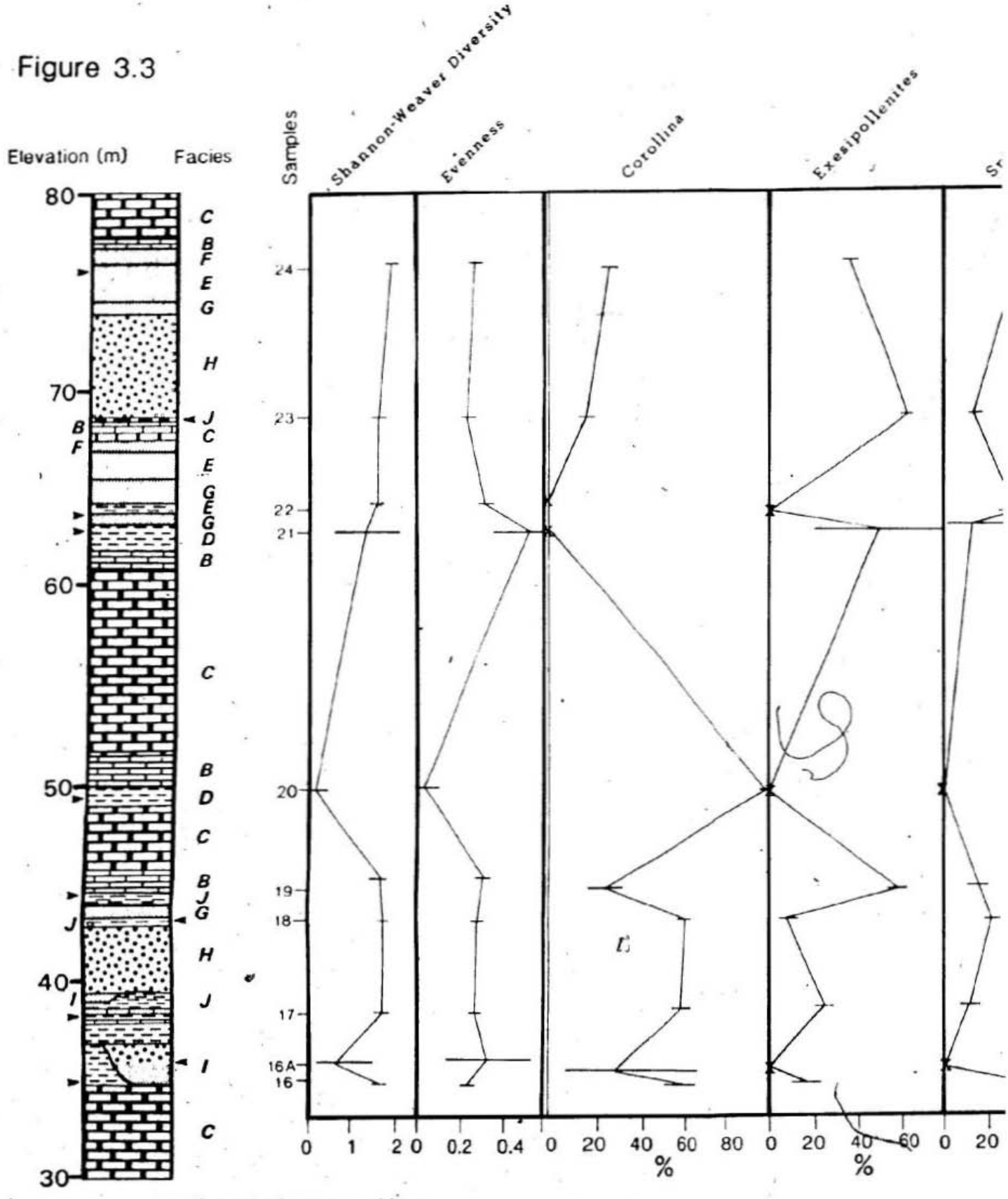
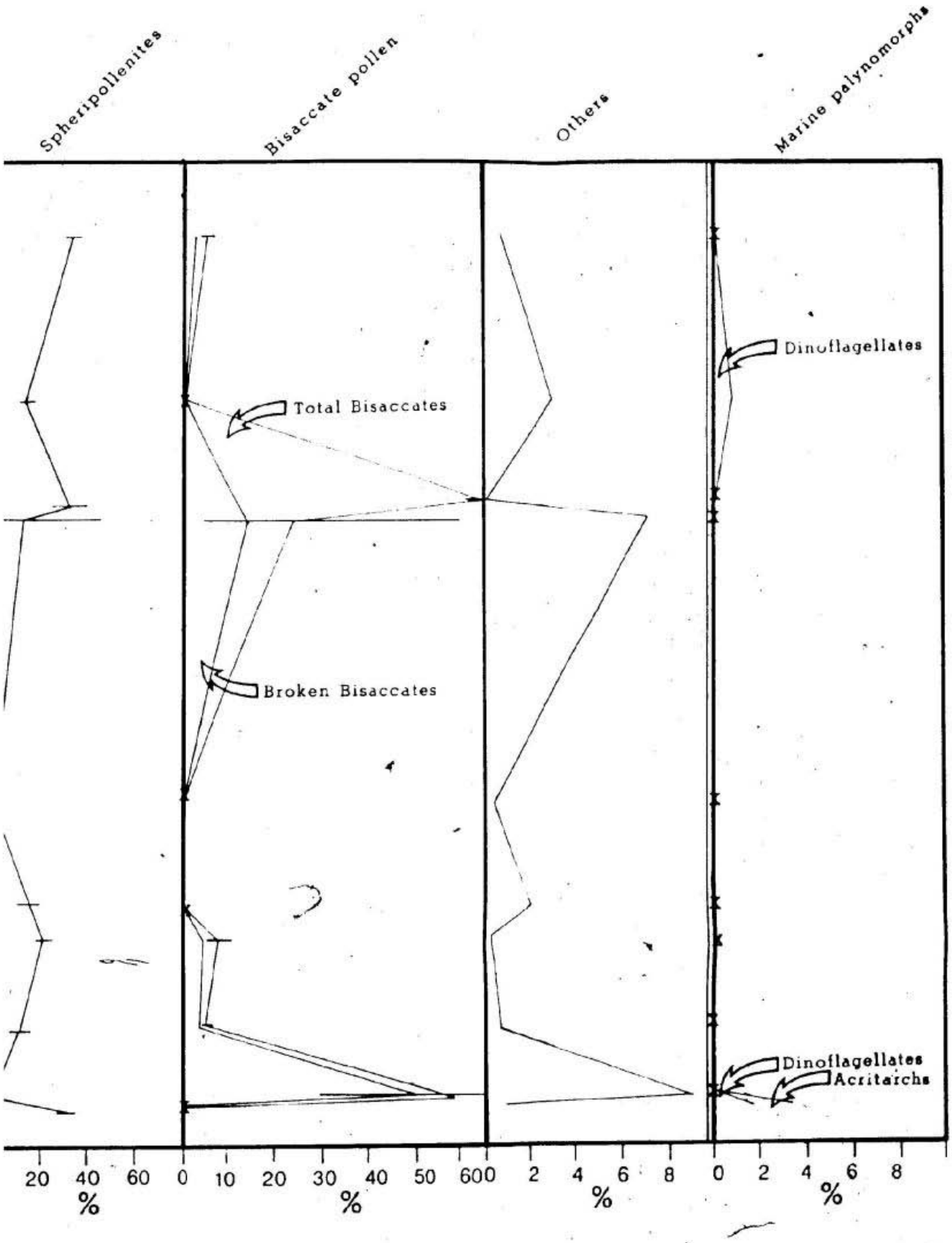

Corollina torosus
Corollina simplex
Corollina itunensis
Corollina tetrads
0 20 40 60 80
%
0 20 40 60 80
%
0 2 4 6 8
%
0 4 8 12
%

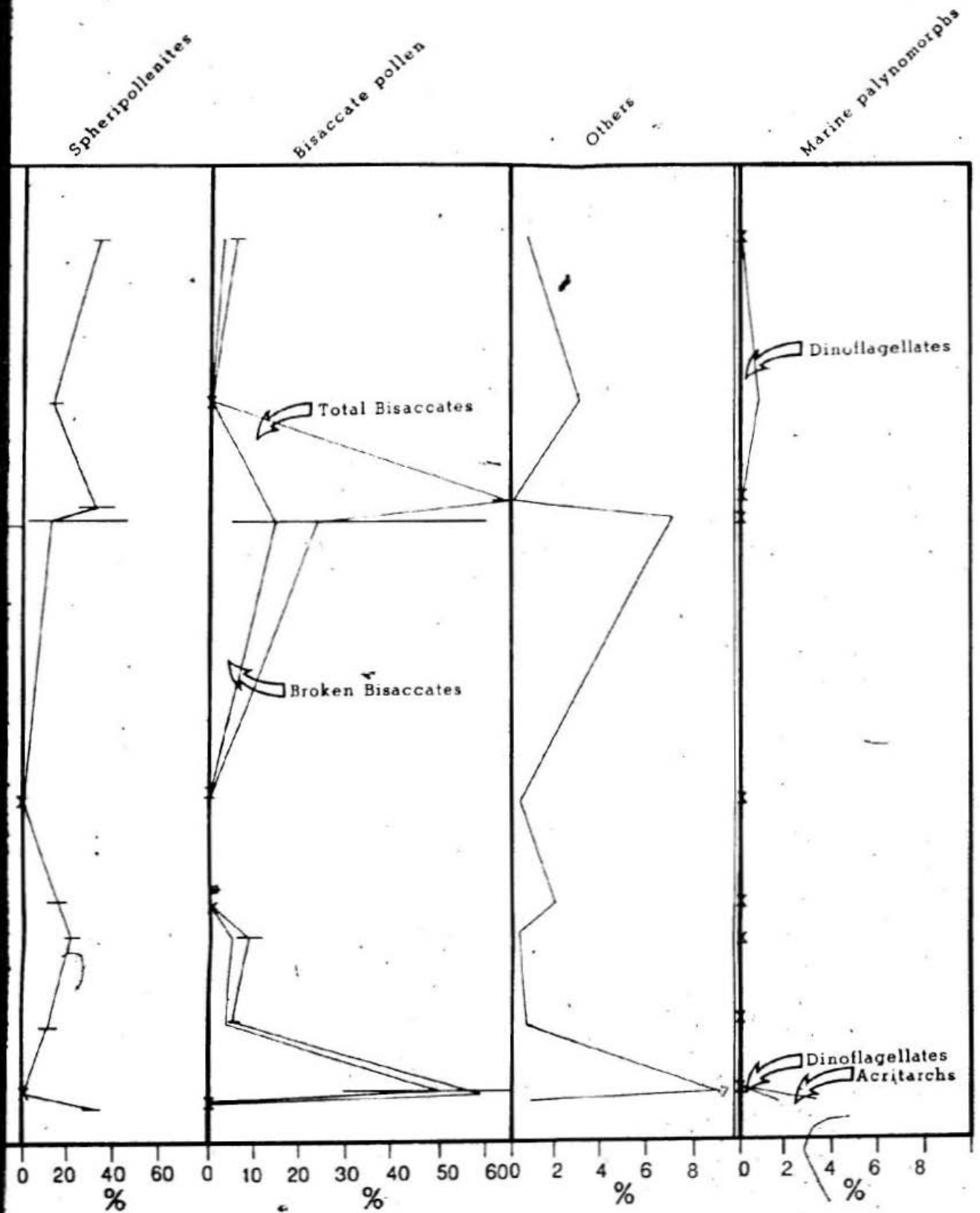
Figure 3.3



X Observed at 0 % assemblage

Bars illustrate abundance limits


Spheripollenites
Bisaccate pollen
Others
Marine palynomorphs
Total Bisaccates
Broken Bisaccates
Dinoflagellates
Dinoflagellates
Acritarchs
20 40 60
%
0 10 20 30 40 50 600
%
2 4 6 8
%
0 2 4 6 8
%


Spheripollenites
Bisaccate pollen
Others
Marine palynomorphs
Total Bisaccates
Broken Bisaccates
Dinoflagellates
Dinoflagellates
Acritarchs
0 20 40 60
%
0 10 20 30 40 50 600
%
2 4 6 8
%
0 2 4 6 8
%

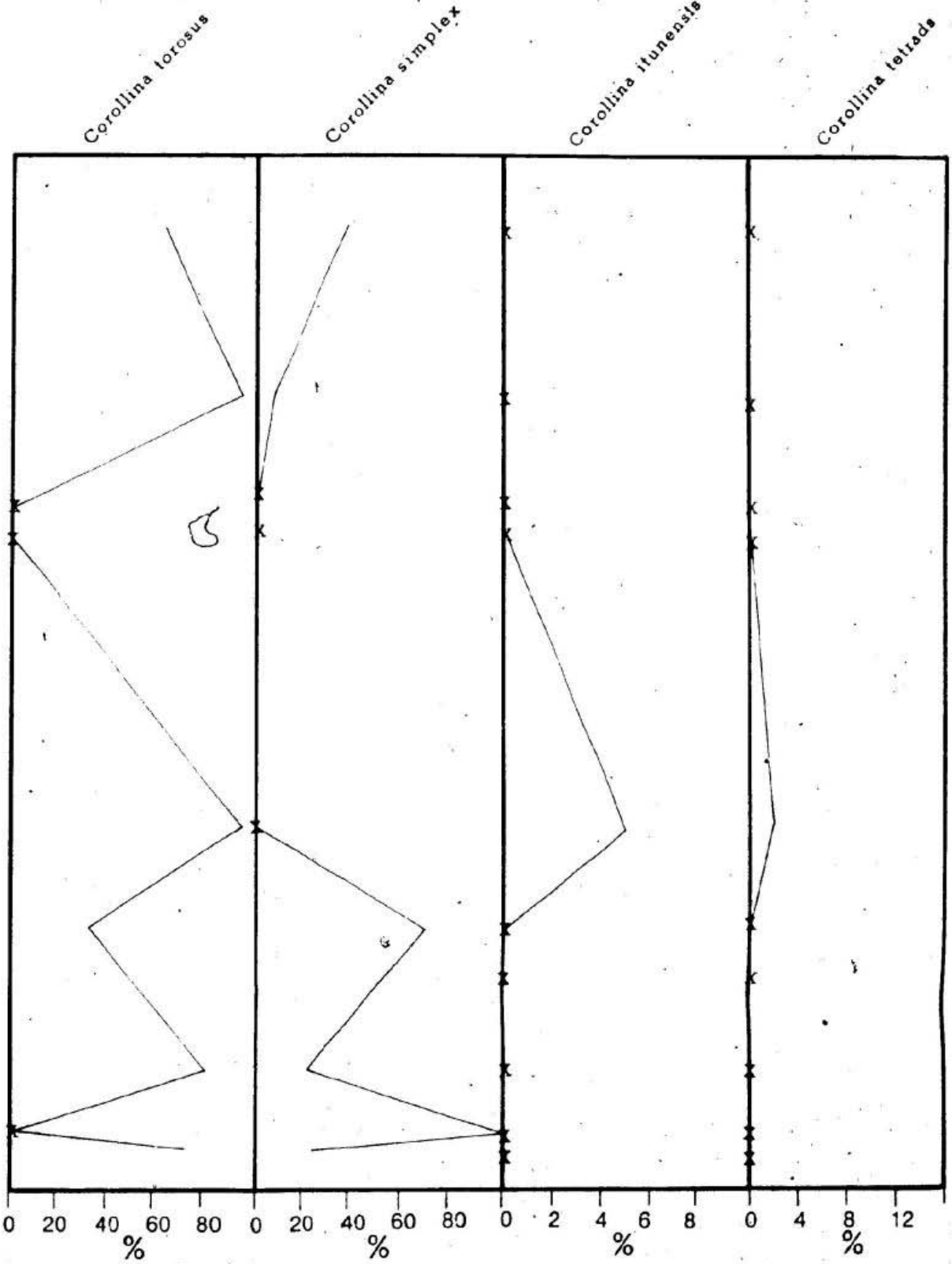
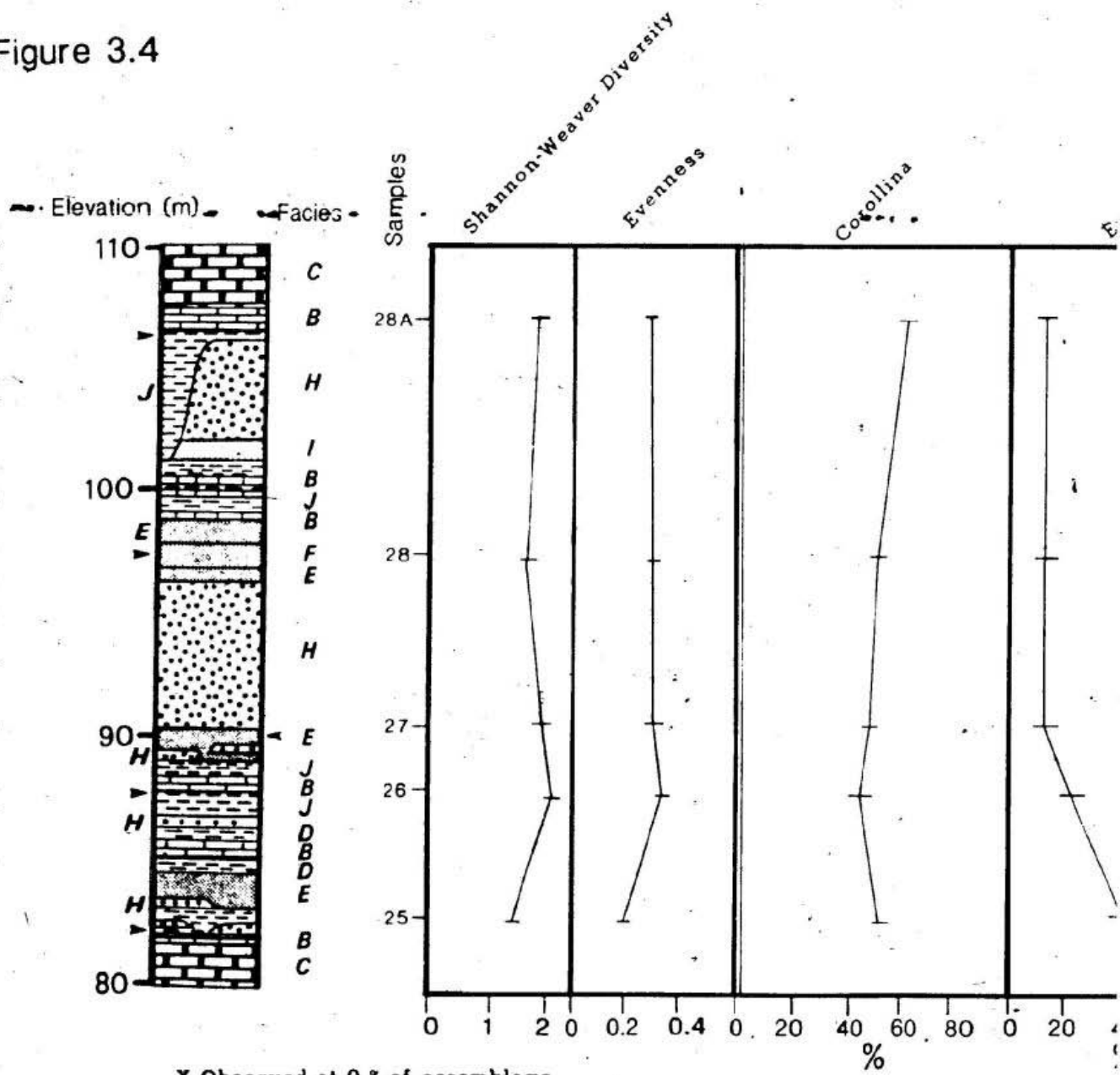
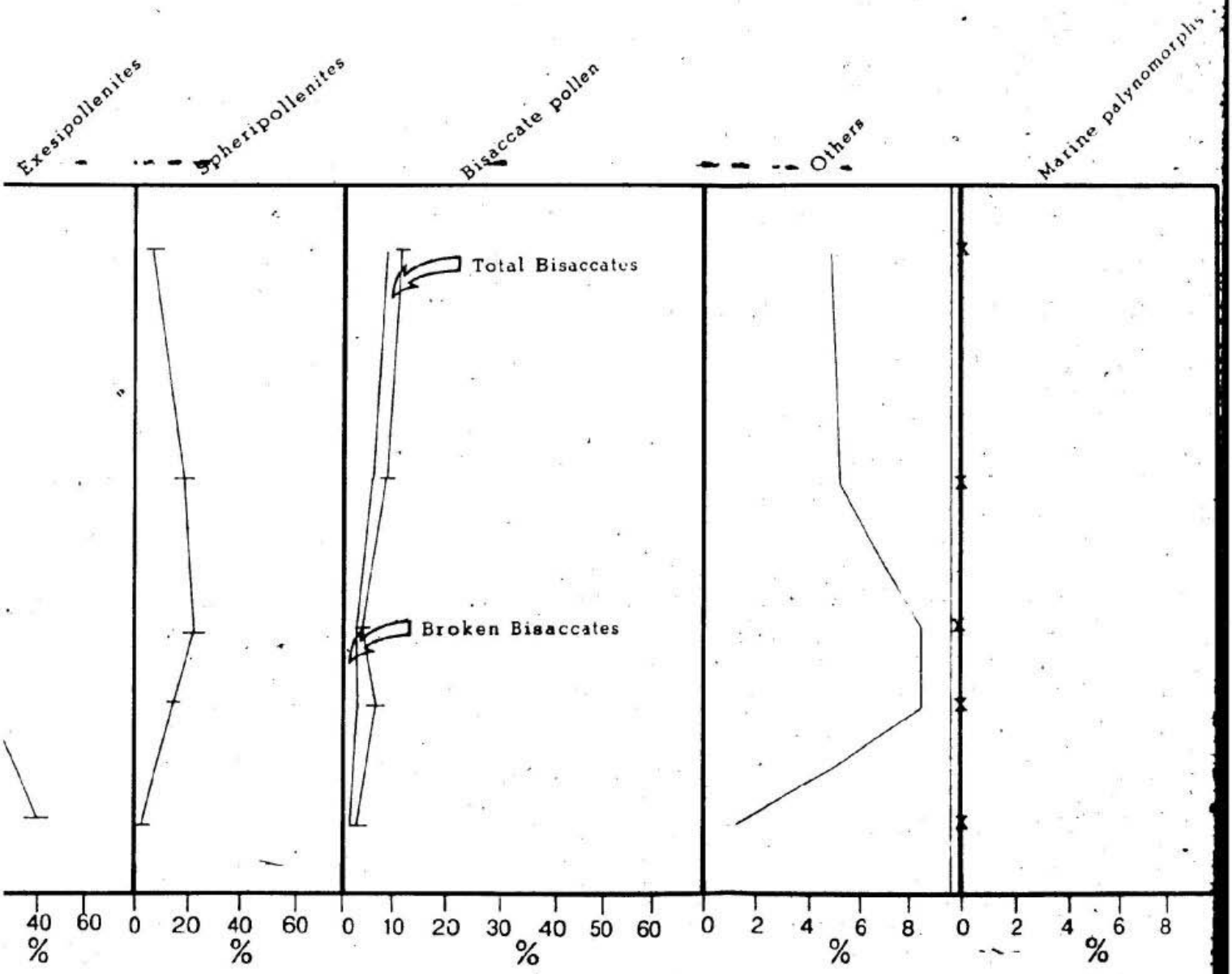

Corollina torosus
Corollina simplex
Corollina itunensis
Corollina tetrads
0 20 40 60 80
%
0 20 40 60 80
%
0 2 4 6 8
%
0 4 8 12
%

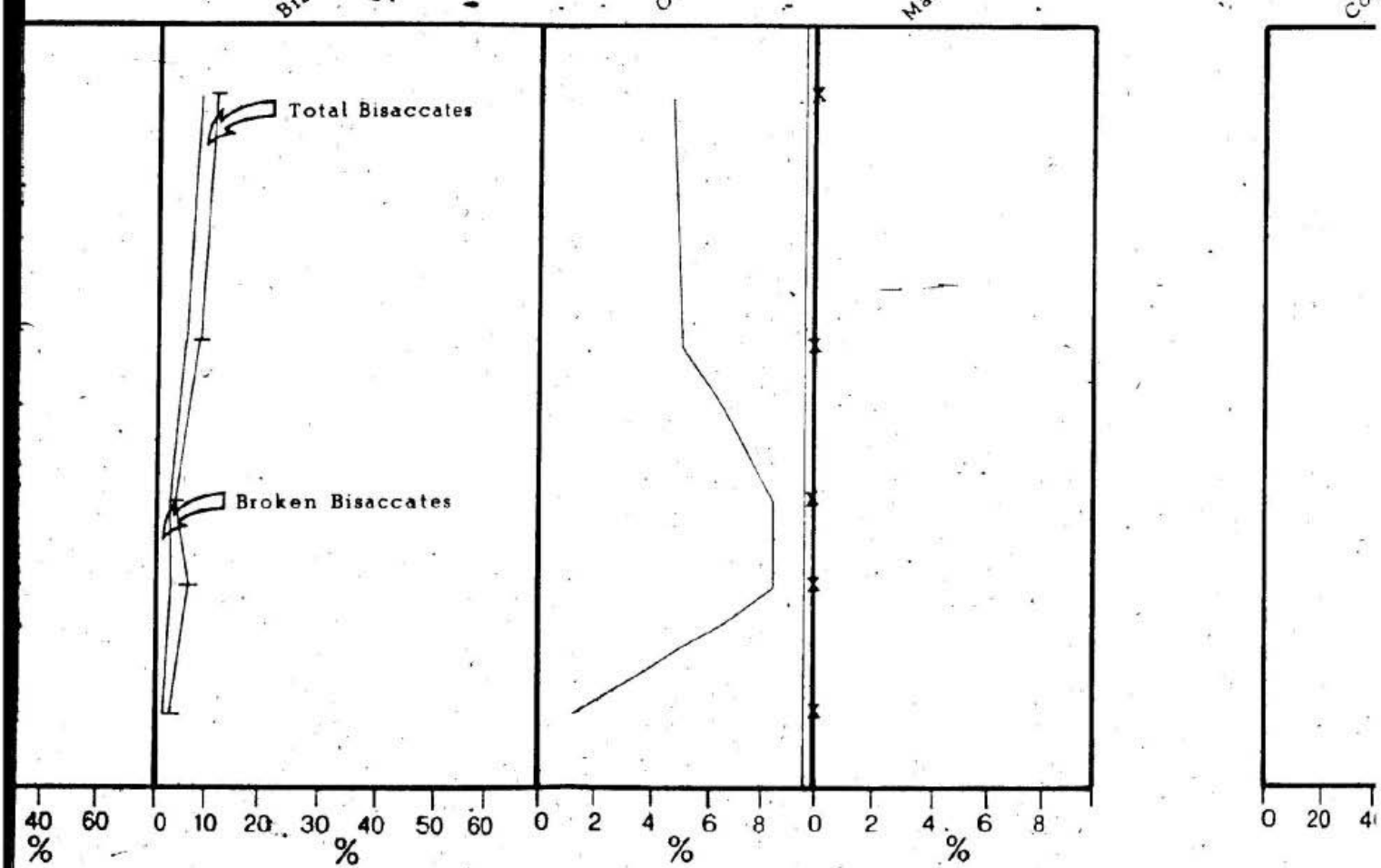
Figure 3.4



X Observed at 0 % of assemblage

Bars illustrate abundance limits


Exesipollenites
Spheripollenites
Bisaccate pollen
Others
Marine palynomorphs
Total Bisaccates
Broken Bisaccates
40 60 0 20 40 60 %
0 10 20 30 40 50 60 %
0 2 4 6 8 %
0 2 4 6 8 %


heripollenites
Bisaccate pollen
Others
Marine palynomorphs
Total Bisaccates
Broken Bisaccates
40 60
%
0 10 20 30 40 50 60
%
0 2 4 6 8
%
0 2 4 6 8
%
0 20

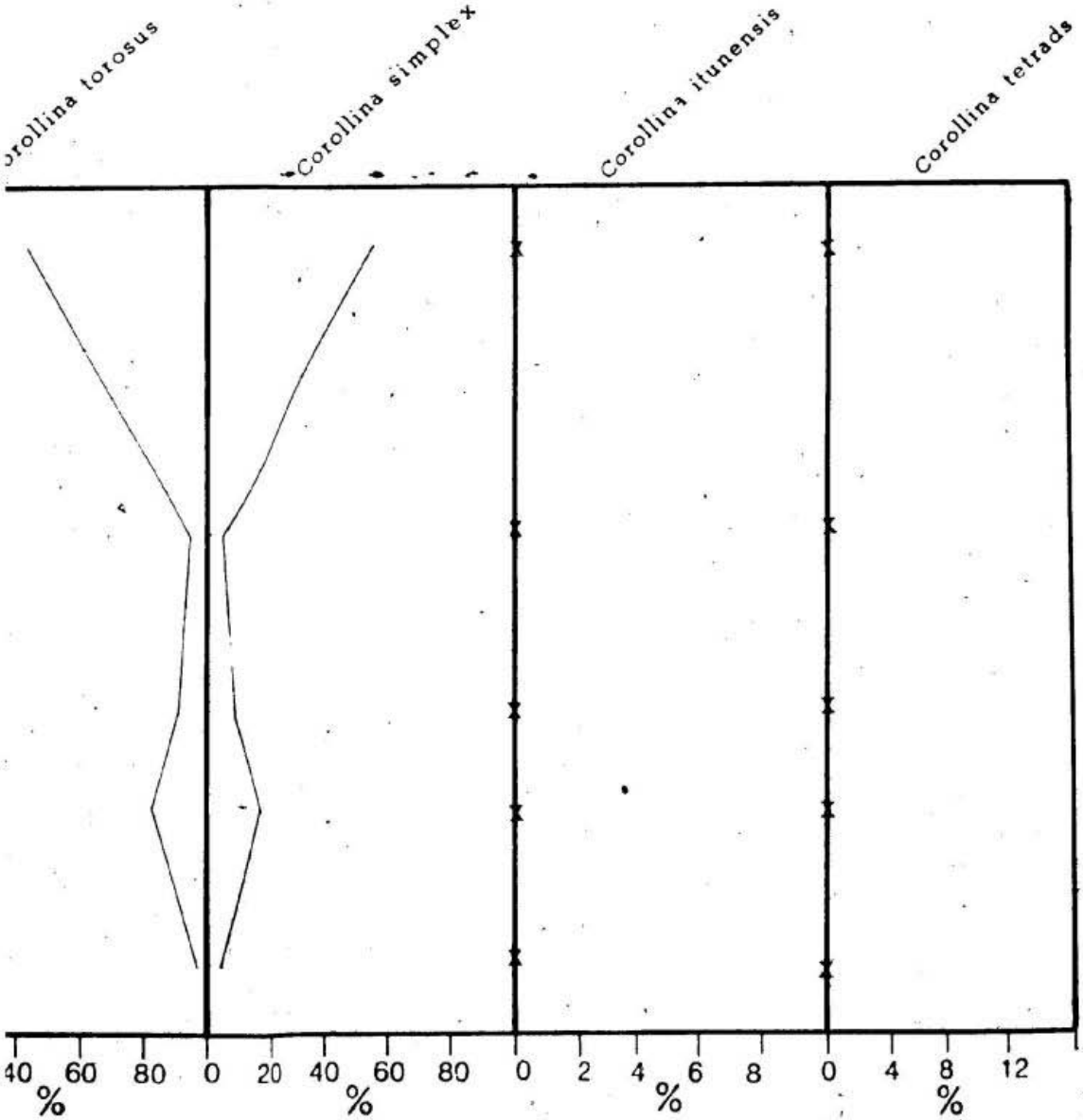
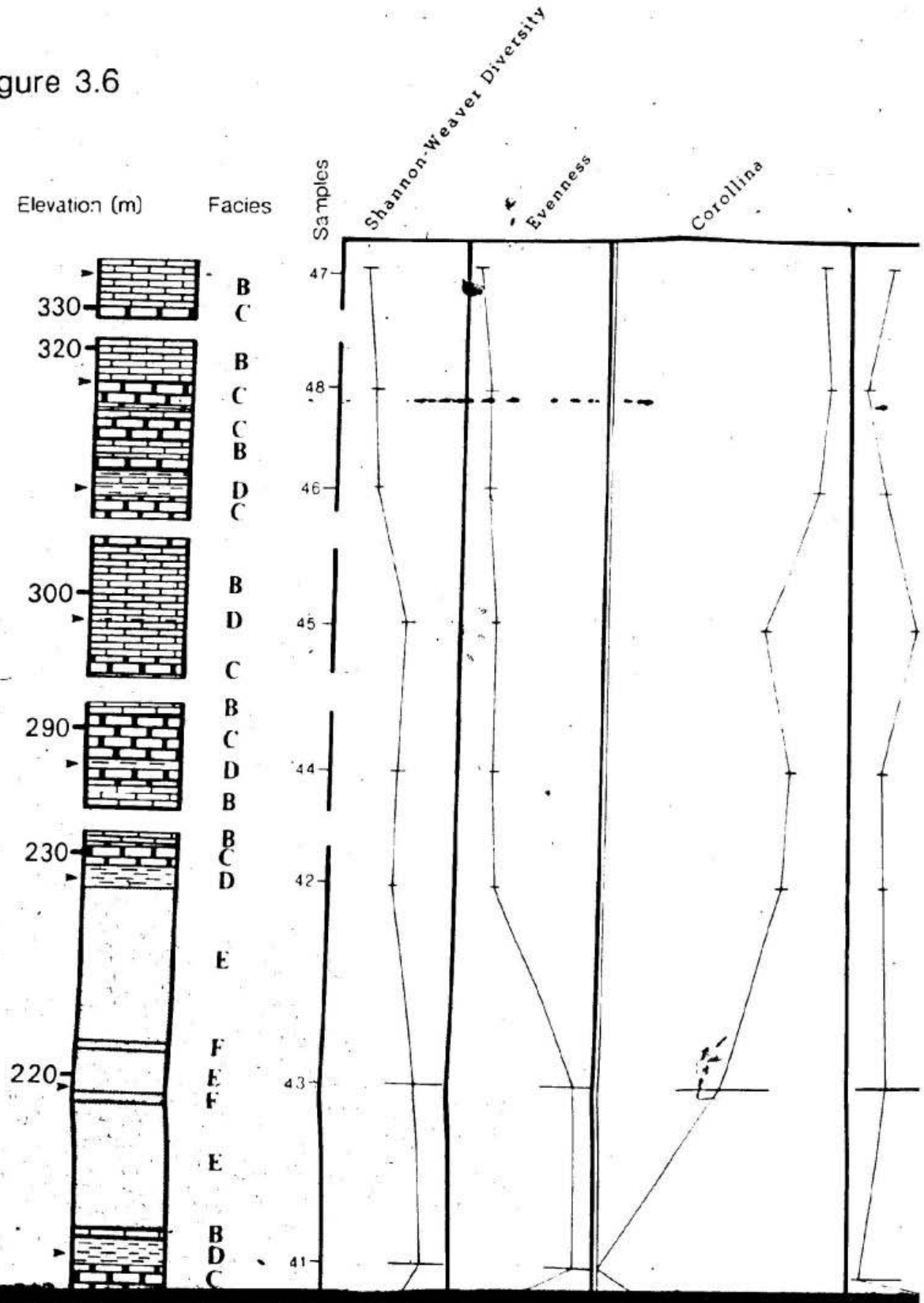
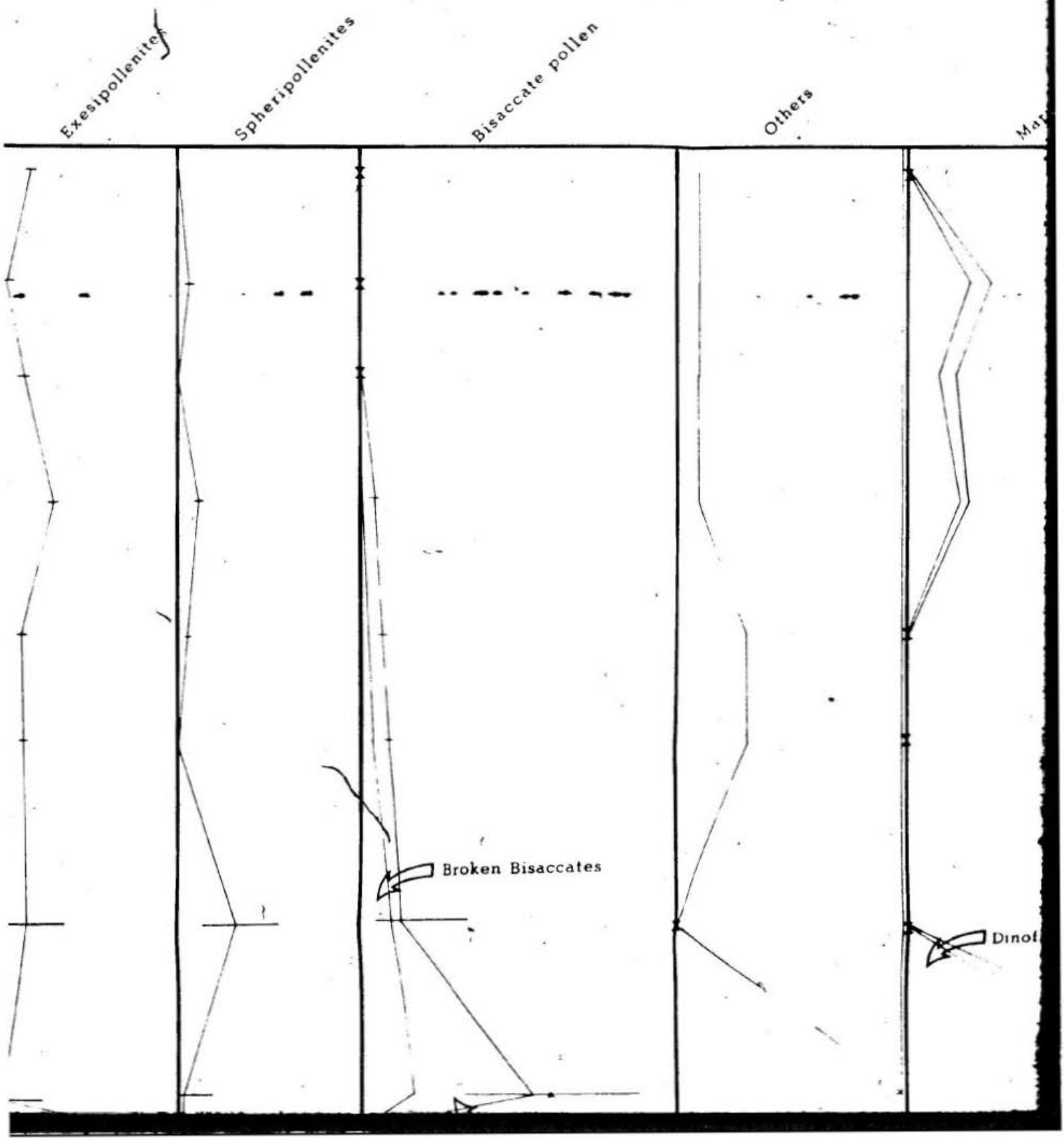
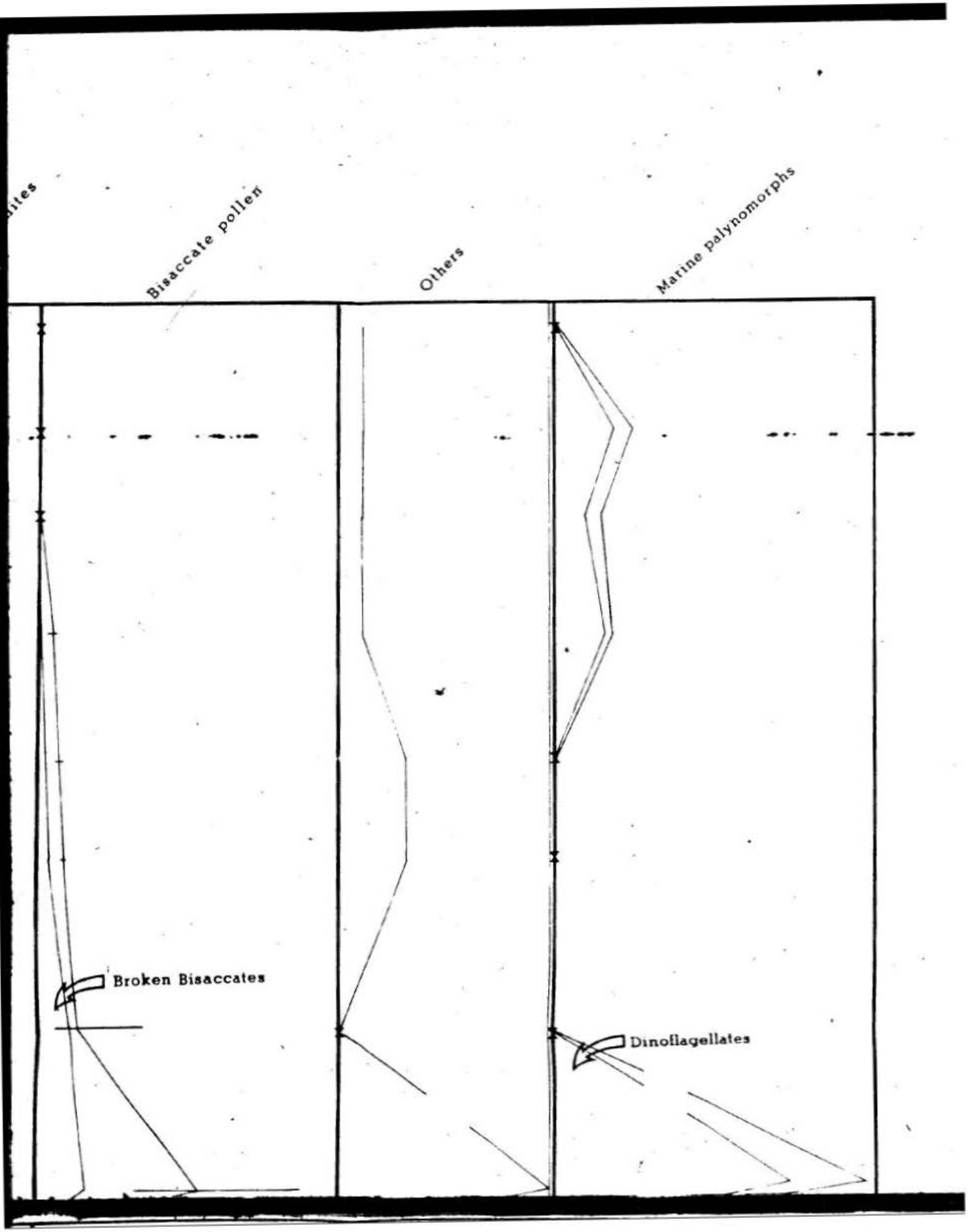
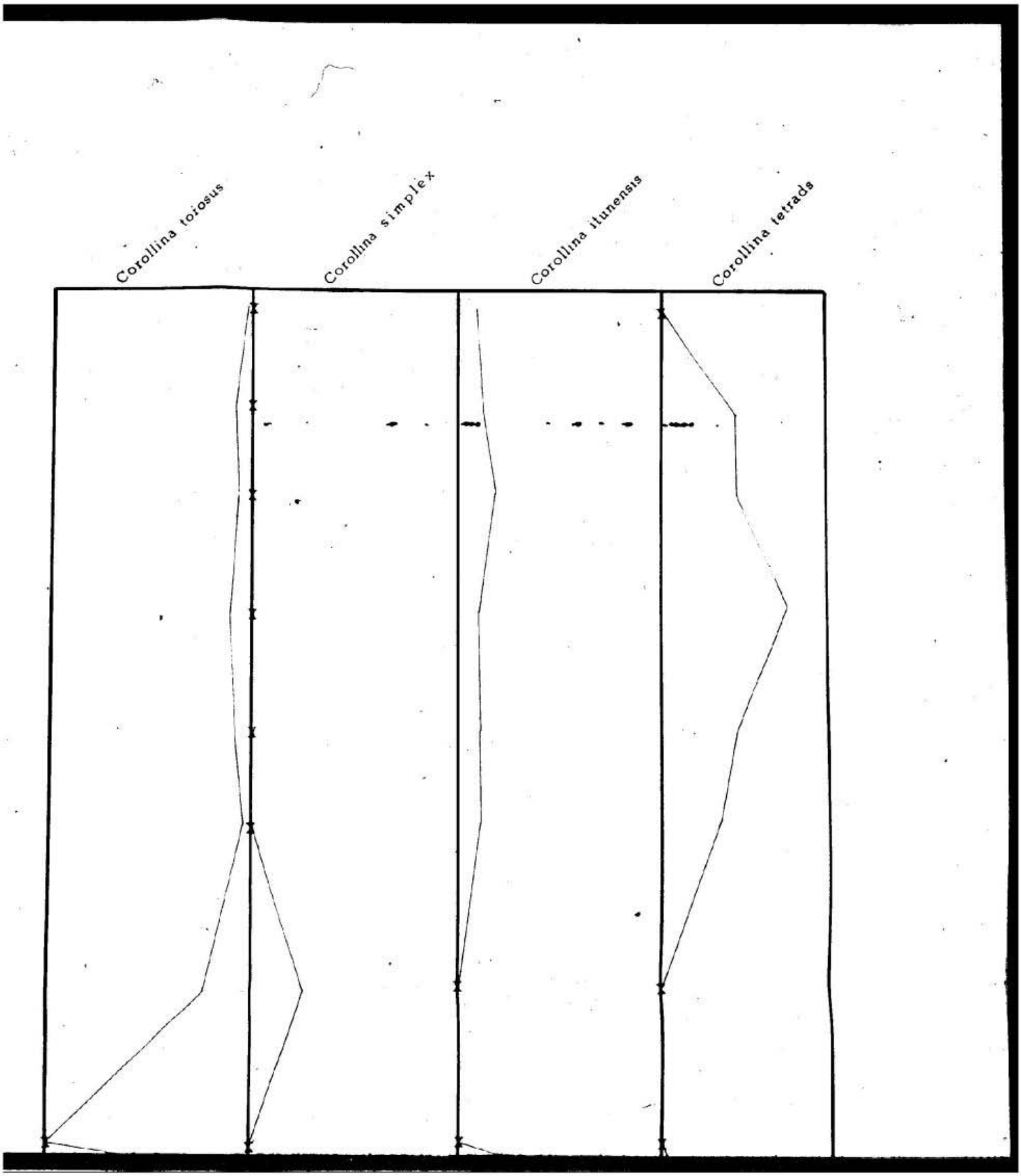

orollina torosus
Corollina simplex
Corollina itunensis
Corollina tetrads
40 60 80 0 20 40 60 80 0 2 4 6 8 0 4 8 12
% % % %

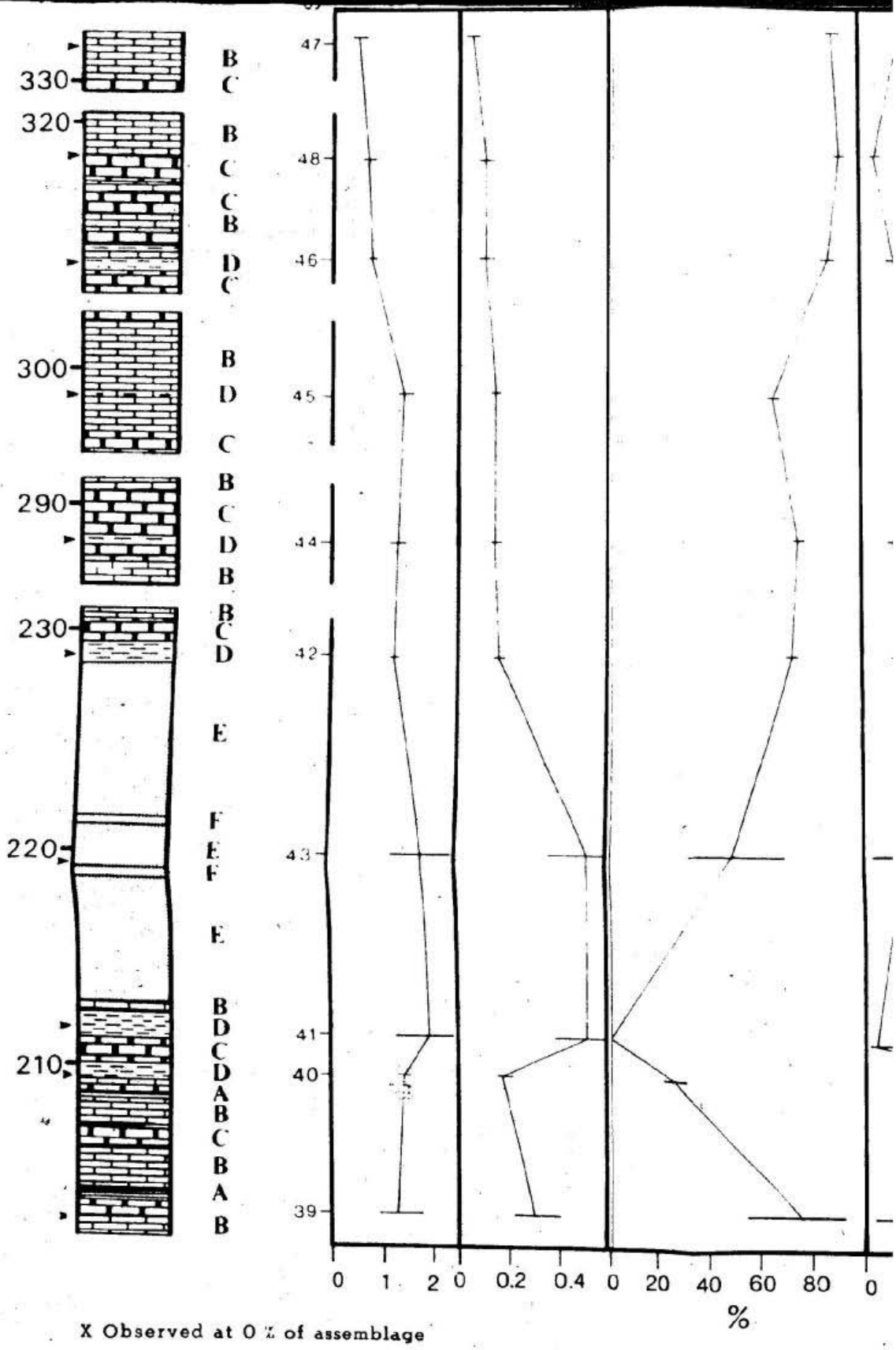
Figure 3.6


Elevation (m)
Facies
Samples
Shannon-Weaver Diversity
Evenness
Corollina
330
320
300
290
230
220
47
48
46
45
44
42
43
41
B C
B C C B D C
B D C
B C D B
B C D E
F E F E
B D C


Exesipollenites
Spheripollenites
Bisaccate pollen
Others
Broken Bisaccates

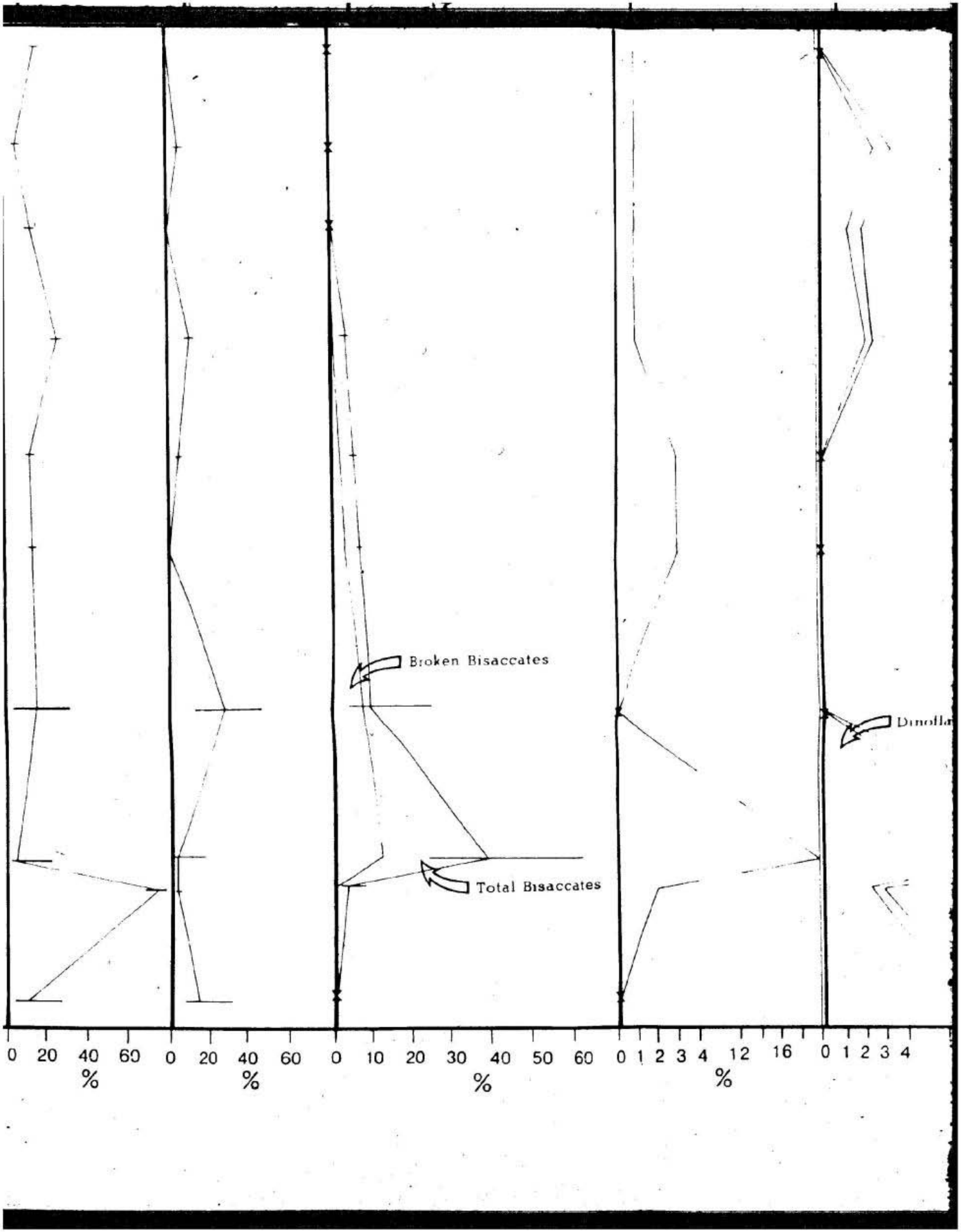

Bisaccate pollen
Others
Marine palynomorphs
Broken Bisaccates
Dinoflagellates

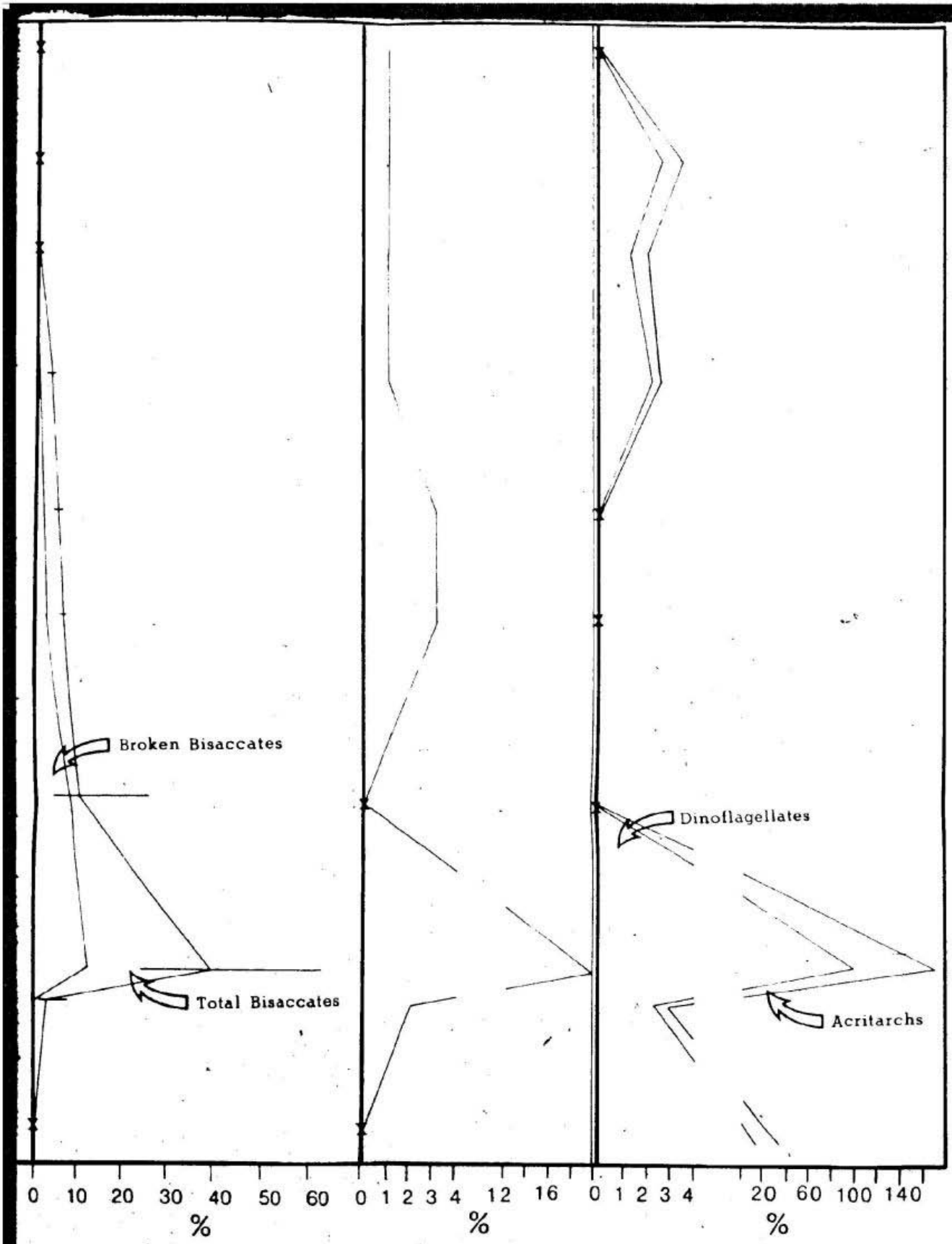

Corollina torosus
Corollina simplex
Corollina ilunensis
Corollina tetrads



X Observed at 0 % of assemblage

Bars illustrate abundance limits


Broken Bisaccates
Total Bisaccates
Dinofla
0 20 40 60
%
0 20 40 60
%
0 10 20 30 40 50 60
%
0 1 2 3 4 12 16
%
0 1 2 3 4


Broken Bisaccates
Total Bisaccates
Dinoflagellates
Acritarchs
0 10 20 30 40 50 60
%
0 1 2 3 4 12 16
%
0 1 2 3 4
20 60 100 140
%

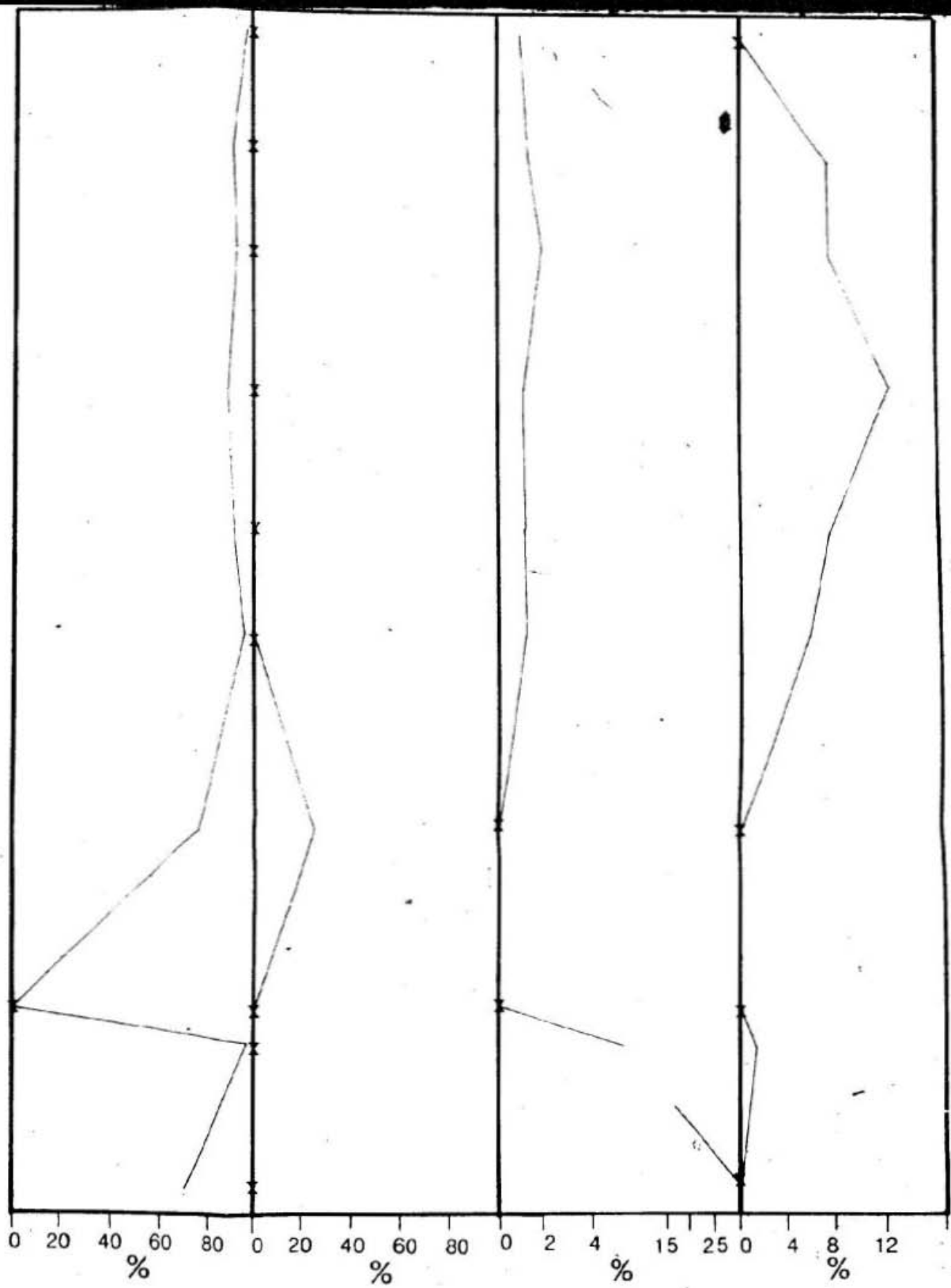
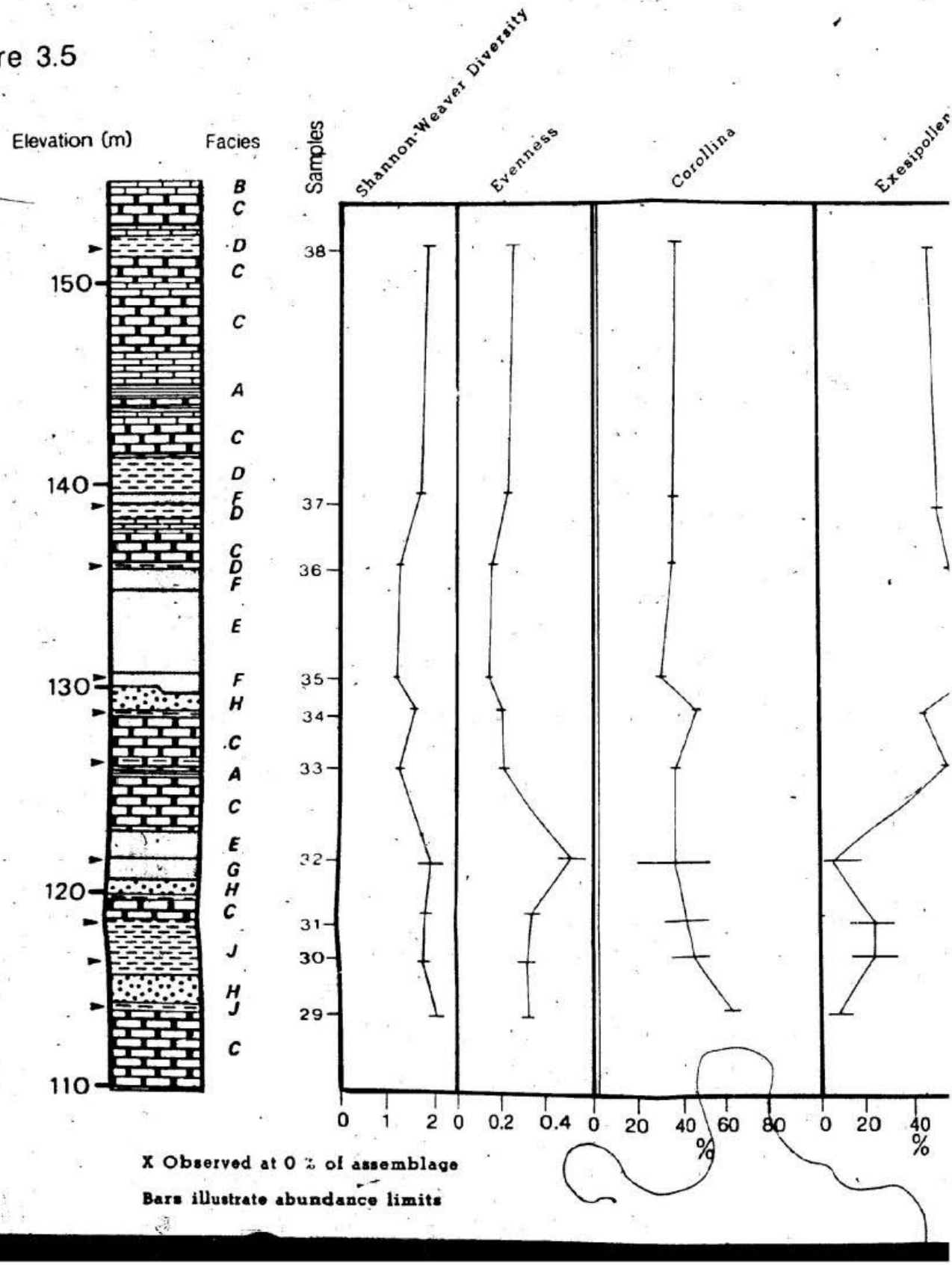
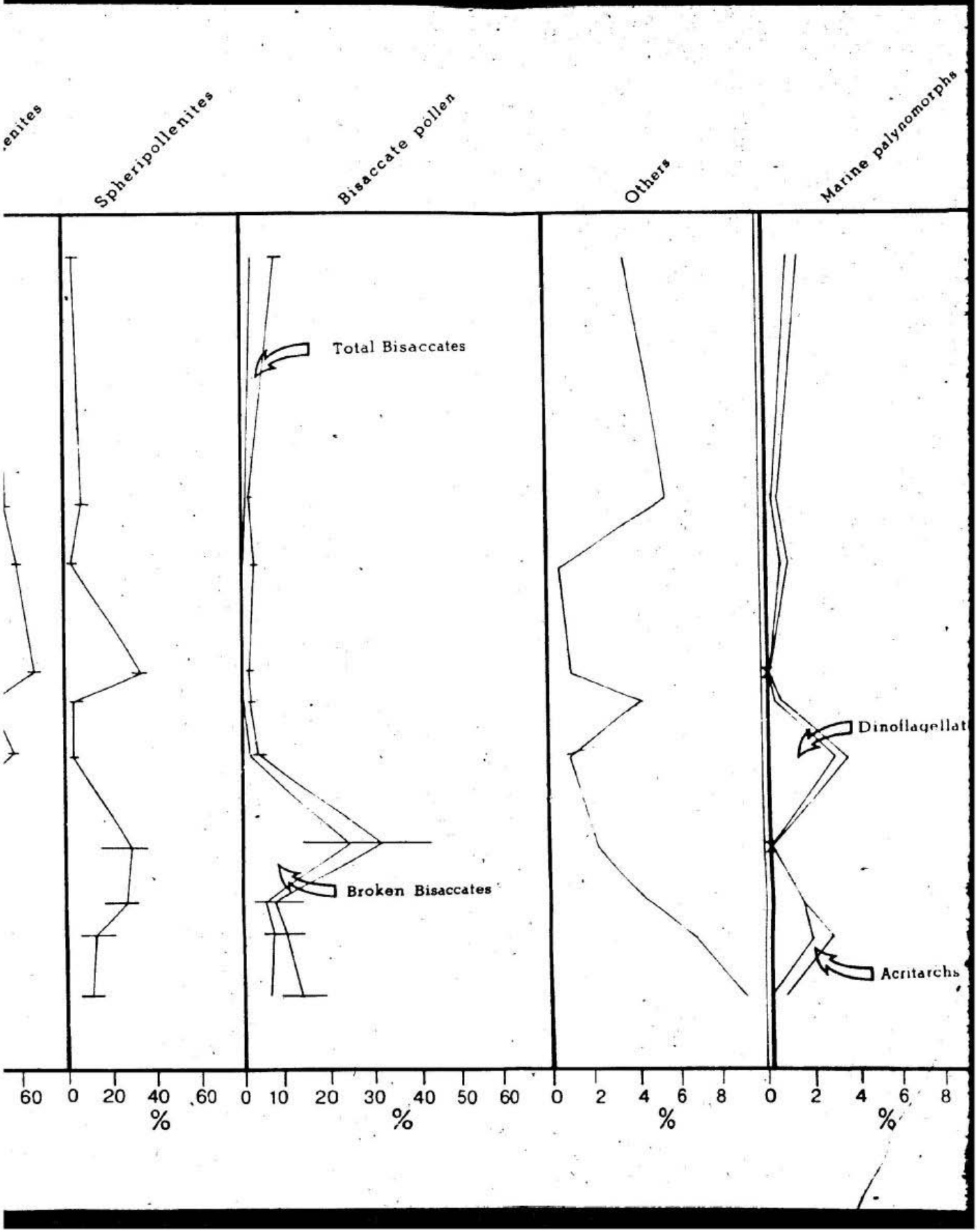
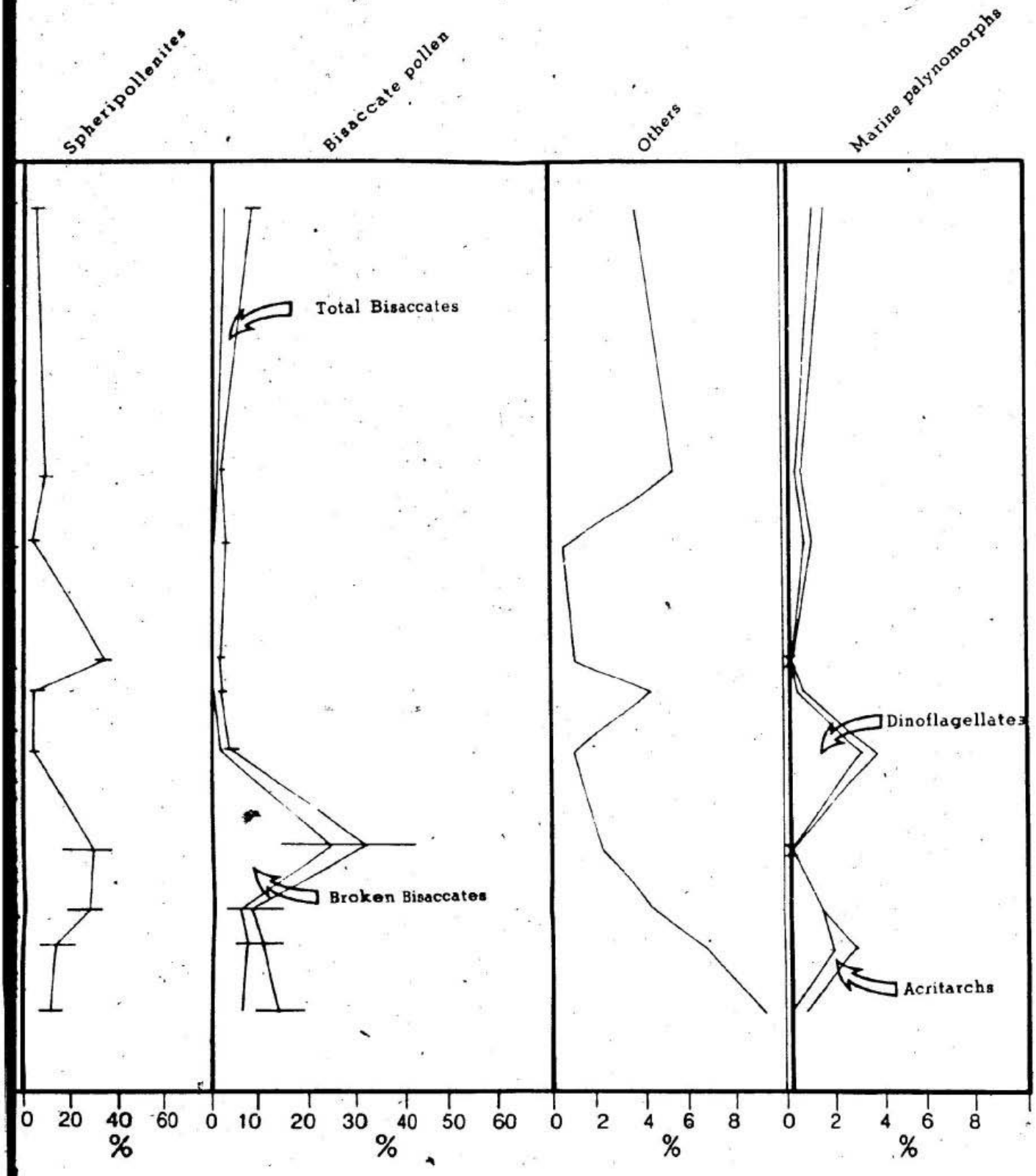
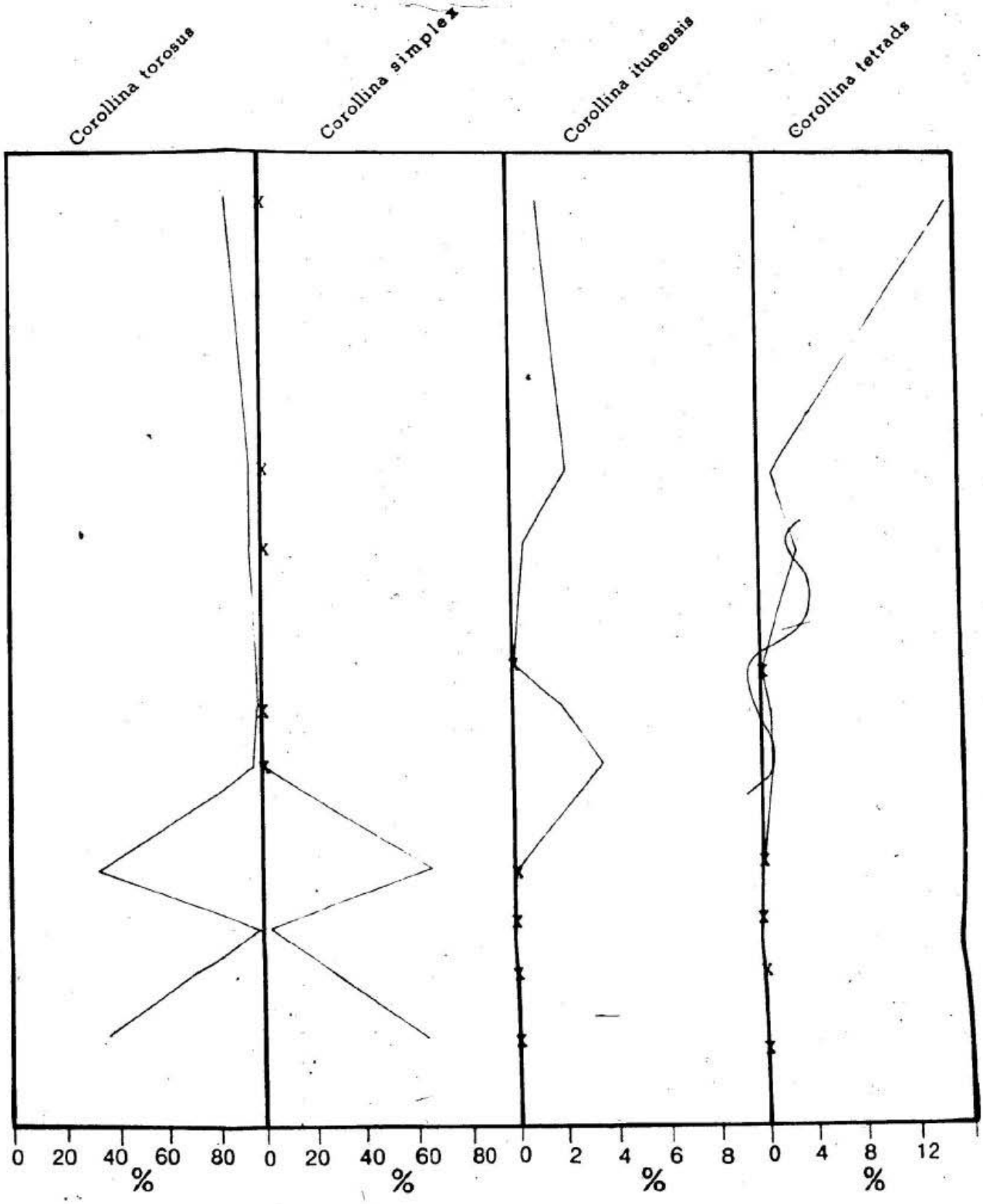

0 20 40 60 80
%
0 20 40 60 80
%
0 2 4 15 25
%
0 4 8 12
%

Figure 3.5


Elevation (m)
Facies
Samples
Shannon-Weaver Diversity
Evenness
Corollina
Exesipollen
150
140
130
120
110
38
37
36
35
34
33
32
31
30
29
0 1 2
0 0.2 0.4
0 20 40 60 80
0 20 40
%
%
X Observed at 0 % of assemblage
Bars illustrate abundance limits


enites
Spheripollenites
Bisaccate pollen
Others
Marine palynomorphs
Total Bisaccates
Broken Bisaccates
Dinoflagellat
Acritarchs
60 0 20 40 60
%
0 10 20 30 40 50 60
%
0 2 4 6 8
%
0 2 4 6 8
%


Spheripollenites
Bisaccate pollen
Others
Marine palynomorphs
Total Bisaccates
Broken Bisaccates
Dinoflagellates
Acritarchs
0 20 40 60
%
0 10 20 30 40 50 60
%
0 2 4 6 8
%
0 2 4 6 8
%


Corollina torosus
Corollina simplex
Corollina itunensis
Corollina tetrads
0 20 40 60 80
%
0 20 40 60 80
%
0 2 4 6 8
%
0 4 8 12
%